ARGININE DECARBOXYLASE (ADC): PREPARATION, EXPRESSION, PURIFICATION AND TEST OF ANTI-CANCER PROPERTIES

WEI XINLEI

Ph.D

The Hong Kong Polytechnic University

2015

The Hong Kong Polytechnic University

Department of Applied Biology and Chemical Technology

Arginine Decarboxylase (ADC): Preparation, Expression, Purification and Test of Anti-Cancer Properties

WEI Xinlei

A thesis submitted in partial fulfilment of the requirements for the degree of Doctor of Philosophy

August 2014

Certificate of Originality

I hereby declare that this thesis is my own work and that, to the best of my knowledge and belief, it reproduces no material previously published or written, nor material that has been accepted for the award of any other degree or diploma, except where due acknowledgement has been made in the text.

WEI Xinlei

August 2014

Abstract

Arginine metabolic enzymes are being investigated worldwide as agents for cancer treatment, because many tumor cells are auxotrophic for arginine. Biosynthetic arginine decarboxylase (ADC), an enzyme that catalyzes the conversion of arginine to agmatine and carbon dioxide, possesses anti-tumor activity yet has received much less attention than the other two arginine-depleting enzymes – arginine deiminase (ADI) and arginase. In order to gain a better understanding of ADC, the expression, purification and anti-cancer properties of this enzyme originates from *Escherichia coli* were explored in this project.

ADC tagged with 6 histidine residues was expressed in *E. coli* grown in shake flask and had undergone a single-step affinity chromatographic purification. Typically, around 110 mg of ADC can be purified from *E. coli* grown in 1 L culture medium. Purified ADC is of around 28.9 ± 2.7 units/mg at 37 ℃ and pH 8.0, and remains relatively stable for at least 6 months when stored at 4 ℃ in darkness.

When tested *in vitro*, ADC inhibits the proliferation of ten cell lines of different human cancer types, with IC_{50} values ranging from 3.8 to 38.1 μg/ml, yet is relatively safer in a non-tumorous cell line. Further *in vitro* studies focusing on HCT116 and LoVo colorectal cancer cells indicates that ADC induces S and/or G_2/M phase arrest as well as intensive apoptosis in these cells. The ADC-induced apoptosis follows the mitochondrial apoptotic

pathway and is caspase-3-dependent in HCT116 cells but not in LoVo cells. Autophagy, surprisingly, is not observed in either cell lines. In fact, the anti-proliferation effect of ADC in HCT116 cells is antagonized by the autophagy inhibitor hydroxychloroquine (HCQ). Related to these effects, multiple pathways in HCT116 cells may have been altered by the treatment of ADC, including the inhibition of extracellular regulated protein kinase (ERK) activity and the activation of Akt through phosphorylation. Further drug combination studies suggest that ADC is synergistic with doxorubicin and LY204002 at high doses, while antagonistic to verapamil at all doses.

To proceed to *in vivo* studies, a major challenge for a protein drug is the extension of its blood circulation half-life. To tackle this problem, ADC fused with an albumin binding domain (ABD) has been tested in this project. Having the specific activity of ADC almost fully retained, ADC-ABD is even more potent than ADC *in vitro* but fails to prolong the arginine-depletion effect *in vivo*. The *Bacillus caldovelox* arginase (BCA)-ABD fusion protein (BHA), however, decreases serum arginine to an undetectable level for a much longer period (24 h) than that when using native BCA (2 h), thus proves the feasibility of the ABD fusion strategy.

With all results obtained, we suggest that ADC has the potential to be a competent drug material due to its simple production process, satisfactory stability, as well as the broad anti-cancer spectrum with high efficacy. Therefore, ADC is worthy to be more deeply investigated in the future.

List of publications

1. **Wei, X. L.**, Chow, H. Y., Chong, H. C., Chu, S. L., Yap, H. K., Tsui, S. M., Lo, W. H., & Leung, Y. C. (2011, March). *Starving breast cancer cells through depletion of arginine – a key nutrient for cancer cells.* Poster session presented at the 5th Functional Food Symposium (FFS), Hong Kong.
2. **Wei, X. L.**, Chow, H. Y., Chong, H. C., Chu, S. L., Tsui, S. M., Wong, K. Y., Siu, Y. S., Yap, H. K., Lo, W. H., & Leung, Y. C. (2012, November). *Arginine decarboxylase inhibits human colorectal cancer cells by inducing cell cycle arrest and apoptosis.* Poster session presented at the 8th National Cancer Research Institute (NCRI) Cancer Conference, Liverpool, UK.
3. **Wei, X.**, & Leung, Y. (2012). Arginine decarboxylase inhibits human colorectal cancer cells by inducing cell cycle arrest and apoptosis. Abstract of the 24th European Organisation for Research and Treatment of Cancer (EORTC)-American Association for Cancer Research (AACR)-National Cancer Institute (NCI) Symposium on Molecular Targets and Cancer Therapeutics, *European Journal of Cancer, 48(Suppl.* 6*)*, 25-26.

Acknowledgements

There are a number of people without whom this thesis might not have been written, and to whom I am greatly indebted.

First and foremost, I offer my sincerest appreciation to my supervisor, Professor Thomas Y. C. Leung, for his patience, motivation, enthusiasm, and immense knowledge. He has been a source of encouragement and inspiration to me throughout my study.

I am also very grateful to all the former and present members as well as the collaborators of this research group, including but not limited to Dr. Carrie Kong, Dr. Emily M. W. Tsang, Dr. Gabriel K. Y. Wong, Mr. Godfrey Y. M. Lam, Dr. H. K. Yap, Dr. Joyce Q. F. Li, Dr. Ryan H. Y. Chow, Ms. Sammi S. M. Tsui, Ms. Sandra Y. S. Siu, Ms. Sharon S. Y. Liu, Ms. Shirley S. L. Chu, Dr. Stephen C. F. Kim, Mr. Steve H. C. Chong, and Dr. Waiting W. T. Wong. I would like to thank all of them for their selfless help and kind support, and I will always cherish the great times we shared. Special thanks go to Dr. Ryan H. Y. Chow and Mr. Steve H. C. Chong who have not only taught me various kinds of experimental techniques but also provided valuable suggestions for my research ever since I was an undergraduate project student.

In addition, I would like to express my gratitude to the technicians of the Department of Applied Biology and Chemical Technology as well as the

staff of the Centralised Animal Facilities in the Hong Kong Polytechnic University for their technical assistance.

Furthermore, I would like to acknowledge the Research Grants Council of Hong Kong for offering me a fellowship in 2010-2013, as well as the Research Committee of the Hong Kong Polytechnic University for offering me a tuition scholarship in 2010-2013 and a studentship in 2013-2014.

Last but not least, heartfelt appreciation is extended to my family, especially my parents, for their love and support throughout my life.

Table of Contents

Chapter 6 Discussion

List of figures

List of Tables

List of abbreviations

5-FU	Fluorouracil
µg	Microgram
µL	Microliter
µM	Micromolar
ALL	Acute lymphoblastic leukemia
ABD	Albumin binding domain
ADA	Adenosine deaminase
ADC	Arginine decarboxylase
ADI	Arginine deiminase
AFM	Arginine-free medium
AGAT	Arginine-glycine amidinotransferase
AML	Acute myeloid leukemia
AMPK	AMP-activated kinase
APS	Ammonium persulfate
ASL	Argininosuccinate lyase
ASS	Argininosuccinate synthetase
ATCC	American Type Culture Collection
BAH	*Bacillus caldovelox* arginase-albumin binding domain-6x histidine fusion
BCA	*Bacillus caldovelox* arginase

BHA	
Bacillus caldovelox arginase-6x histidine-albumin binding domain fusion	
BHBN	N-butyl-N-(4-hydroxybutyl) nitrosamine
BSA	Bovine serum albumin
CAD	Caspase-activated DNAse
CDK	Cyclin-dependent kinases
CI	Combination index
CO_2	Carbon dioxide
Co-hArg	Co^{2+}-substituted human arginase I
CQ	Chloroquine
Da	Dalton
DAMO	Diacetyl monoxime
DI water	Deionized water
DMSO	Dimethyl sulfoxide
DMEM	Dulbecco's Modified Eagle's medium
E. coli	*Escherichia coli*
EDTA	Ethylenediaminetetraacetic acid
EGCG	Epigallocatechin gallate
EGFR	Epidermal growth factor receptor
ERK	Extracellular signal-regulated kinase
EU	Endotoxin unit
FBS	Fetal bovine serum

FDA	Food and Drug Administration
g	Gram
GFP	Green fluorescent protein
GLUT1	Glucose transporter 1
h	Hour
hArg	Human arginase
HCC	Hepatocellular carcinoma
HCQ	Hydroxychloroquine
HRP	Horseradish peroxidase
HSA	Human serum albumin
i.p. injection	Intraperitoneal injection
IPTG	Isopropyl β-D-1-thiogalactopyranoside
i.v. injection	Intravenous injection
JAK	Janus kinase
kDa	Kilodalton
K_m	Michaelis-Menten constant
L	Liter
LAL	Limulus amebocyte lysate
LB medium	Luria-Bertani medium
LC3	Microtubule-associated protein 1A/1B-light chain 3
LDH	Lactate dehydrogenase
M	Molar

mAb	Monoclonal antibody
MAPK	Mitogen-activated protein kinase
MEK	MAPK/ERK kinase
mg	Milligram
min	Minute
mL	Milliliter
mM	Millimolar
MOM	Mitochondrial outer membrane
MOMP	Mitochondrial outer membrane permeabilization
mPEG-MAL	Methoxypolyethylene glycol-maleimide
mPEG-SPA	Methoxypolyethylene glycol-succinimidyl propionate
mTOR	Mammalian target of rapamycin
mTORC1	Mammalian target of rapamycin complex 1
MTT	3-(4,5-dimethylthiazol-2-yl)-2,5-diphenyltetrazolium bromide
MW	Molecular weight
NCCR	National Central Cancer Registry
NCI	National Cancer Institute
ng	Nanogram
nm	Nanometer
NOS	Nitric oxide synthase
ODC	Ornithine decarboxylase
One-way ANOVA	One-way analysis of variance

OTC	Ornithine transcarbamylase
PARP	Poly (ADP-ribose) polymerase
PBS	Phosphate buffered saline
PD-1	Programmed cell death protein 1
PEG	Polyethylene glycol
PI	Propidium iodide
PI3K	Phosphatidylinositol-4,5-bisphosphate 3-kinase
PLP	Pyridoxal-5'-phosphate
PS	Phosphatidylserine
rhArg	Recombinant human arginase I
rhArg-PEG	Pegylated recombinant human arginase I
ROS	Reactive oxygen species
RPMI	Roswell Park Memorial Institute medium
R point	Restriction point
s	Second
sCR1	Soluble complement receptor type 1
SDS	Sodium dodecyl sulfate
SDS-PAGE	Sodium dodecyl sulfate polyacrylamide gel electrophoresis
SQSTM1	Sequestosome 1
SSA	5'-sulfosalicylic acid
STAT	Signal transducer and activator of transcription
TCA	Trichloroacetic acid

TCEP	Tris(2-carboxyethyl) phosphine
U	Unit

Chapter 1

Introduction

1.1 An overview of cancer

1.1.1 Cancer statistics

As a leading cause of death, cancer occurred in 12.7 million people and resulted in 7.6 million deaths worldwide in 2008 (Jemal *et al.*, 2011). Although earlier prognosis and advanced treatment methods have helped to improve survival from cancer in recent years, the number of cancer patients continues to increase mainly as a result of the growing and aging population (DeSantis *et al.*, 2014; Jemal *et al.*, 2011). According to National Central Cancer Registry (NCCR) of China, in the registration areas in 2009, age-standardized incidence of all cancers was 146.87/100,000, and the age-standardized mortality was 85.06/100,000 (Chen *et al.*, 2013). In the United States, there were around 14.5 million Americans living with cancer up to January, 2014, and this number was predicted to rise to around 19 million in the next ten years (DeSantis *et al.*, 2014).

The patterns in cancer incidence are gender- and region-dependent, and usually change with time. In mainland China in 2009, the top three cancer sites in males were lung, stomach, and liver, while the top three in females were breast, lung and colorectum (Chen *et al.*, 2013). In Hong Kong in

2011, the three most frequently diagnosed cancer types were lung, colorectal, and prostate cancer for males while breast, colorectal, and lung cancer for females (Hong Kong Cancer Registry, Hospital Authority, 2013). In the United States in early 2014, the top three cancer types among males were prostate cancer, colorectal cancer, and melanoma, while the top three among females were cancers in breast, uterine corpus, and colorectum (DeSantis *et al.*, 2014). The differences in environment, demography, cultural and genetic backgrounds among different regions may contribute to such variations.

The increasing cases of cancer have not only brought huge pains to millions of people and their families but also exerted serious impacts on global economy and social development. In 2003, cancer cost more than 86 billion RMB in China which accounted for 7.23% of the total national economic cost of diseases (Zhao *et al.*, 2010). The exact global economic cost of cancer, although hard to measure, is sure to be tremendous, and is likely to grow with time due to the increasing trend in cancer incidence and mortality. Therefore, the prevention and control of cancer has long been, and will continue to be one of the main issues for humans.

1.1.2 Therapeutic methods of cancer

1.1.2.1 Surgery

Surgery is one of the main treatments of cancer, especially for cancers at an early stage. The surgical removal of the primary tumor typically provides a great chance of disease-free survival. Other methods such as radiation therapy and chemotherapy are often used prior to or subsequent to surgery to enhance the effectiveness of the treatment.

For surgeons, a main challenge is to differentiate the tumorous tissue from healthy ones. This problem is likely to be tackled in the near future by the rapid development of imaging technologies. For example, invisible near-infrared fluorescence imaging may assist surgeons by providing real-time images of the tumorous region (Gioux *et al.*, 2010). In 2013, a group of researchers demonstrated that with the use of ratiometric activatable cell-penetrating peptides, not only primary but also metastatic tumors could be easily identified in mice model in real time (Savariar *et al.*, 2013).

Although surgery is a necessary treatment for most cancers, the surgical trauma and recovering processes can increase the risk of metastasis through mechanisms including immune suppression, production of angiogenic factors, loss of inhibitory factors generated by the primary tumor, and enhanced tumor cell adhesion (DeLisser *et al.*, 2009; van der Bij *et al.*, 2009).

1.1.2.2 Radiation therapy

Radiation therapy destroys diseased cells with ionizing radiation, and is another cornerstone of cancer treatment at present. Among all cancer patients with solid tumors, around 50% have received radiation therapy (Ringborg *et al.*, 2003). While being a non-invasive method, radiation therapy is able to be accurately manipulated, and is often used along with other therapeutic methods. Despite its effectiveness, radiation therapy is associated with various side effects. Early side effects include skin erythema, dry or moist desquamation of the skin, mucositis, nausea and diarrhea which can occur within weeks after treatment; late side effects such as radiation-induced fibrosis, atrophy, vascular and neural damage usually appear after months or even years posterior to treatment (Bentzen, 2006).

Similar to surgery, a major attempt on the improvement of radiotherapeutic effect is to enhance the preciseness of the treatment while minimizing the impact on adjacent normal tissues. As a result, various techniques such as three-dimensional conformal radiotherapy, stereotactic radiotherapy, intensity-modulated radiotherapy and image-guided radiotherapy have been developed in recent years (Nakamura *et al.*, 2014). As a method to increase the therapeutic ratio, targeted radiotherapy with gold nanoparticles is also being investigated in recent years (Ngwa *et al.*, 2014).

1.1.2.3 Conventional chemotherapy

The earliest application of chemicals on the treatment of cancer dates back to 1940s when nitrogen mustard gas was used on patients with lymphoma (Gilman and Philips, 1946; Goodman and Wintrobe, 1946). In 1958, antifolate was reported to have successfully cured choriocarcinoma which was the first solid tumor cured by chemotherapy (Li *et al.*, 1958).

Standard chemotherapeutic drugs primarily aim at interfering with the integrity of DNA or blocking cell division (Dobbelstein and Moll, 2014). Examples include paclitaxel, irinotecan, fluorouracil (5-FU), platinum compounds (such as cisplatin), anthracyclines (such as doxorubicin), and epipodophyllotoxins. While still playing a major role in clinical uses nowadays, chemotherapeutic agents, with limited effectiveness, can cause substantial side effects as they also damage normal cells. Moreover, secondary neoplasms are sometimes observed in long-term survivors that have been treated by chemotherapy (Armstrong *et al.*, 2011).

1.1.2.4 Targeted therapy

As advanced molecular and genetic technologies have revealed a tremendous amount of information on signaling networks related to cellular activities, various drugs targeting at more diverse signaling intermediates and focusing on molecular defects particularly in cancer cells have been developed, marking the beginning of the "era of targeted therapy". Small molecule drugs and monoclonal antibodies (mAbs) are currently the two major approaches available for clinical use (Imai and Takaoka, 2006).

One of the representative small molecule drugs is imatinib mesylate (Glivec or Gleevec; Novartis) that inhibits the BCR-ABL, a fusion protein responsible for the pathogenesis of chronic myeloid leukemia (Capdeville *et al.*, 2002; Weisberg *et al.*, 2007). Another famous small molecule drug, gefitinib (Iressa; AstraZeneca), inhibits the function of epidermal growth factor receptor (EGFR), and is more effective on non-small-cell lung cancer with EGFR mutation compared to traditional chemotherapy (Maemondo *et al.*, 2010). Other key signaling pathways that are frequently mutated in cancer cells, such as the RAS/RAF/MEK (MAPK/ERK kinase)/ERK (extracellular signal-regulated kinase) pathway, the Hedgehog signaling pathway, JAK (Janus kinase)/STAT (signal transducer and activator of transcription) pathway, mTOR (mammalian target of rapamycin) pathway, and the Wnt pathway, have all become targets for certain small molecule drugs (Chen *et al.*, 2010; Dobbelstein and Moll, 2014; Faivre *et al.*, 2006; Zhou and Huang, 2012).

Another promising aspect of small molecule inhibitors is that they may be used against cancer by blocking the supplementation of nutrients. In mammalian cells, the constant cellular uptake of glucose is facilitated by the glucose transporter (Olson and Pessin, 1996). A subtype of this transporter, glucose transporter 1 (GLUT1), is frequently upregulated in tumor cells to meet their increased demand for nutrients (Ganapathy *et al.*, 2009). In 2014, the solution of crystal structure of GLUT1 marked another breakthrough in cancer treatment as it will certainly provide abundant information for the design of new small molecule inhibitors of GLUT1 (Deng *et al.*, 2014).

As mentioned, nutrient starvation is a promising strategy for cancer therapy. This strategy is based on the differences in metabolism between cancer cells and normal cells, and hence can also be categorized as a type of targeted therapy. Unlike small molecule inhibitors that usually target a specific cell signaling intermediate, nutrient starvation can affect multiple cellular machineries, making it relatively more difficult for cancer cells to develop resistance, and hence may be an advantageous cancer therapeutic method. An example of nutrient starvation in cancer therapy is the selective killing effect of arginine deiminase (ADI) on cancer cells that lack the enzyme argininosuccinate synthetase (ASS) (Ensor *et al.*, 2002; Gong *et al.*, 2000; Kelly *et al.*, 2012; Sugimura *et al.*, 1992). The details of amino acid starvation and its application in cancer therapy will be introduced in Section 1.3.

mAbs that recognize pathogenic antigens represent another prominent type of targeted cancer therapy. One of the earliest clinically approved mAb,

trastuzumab (Herceptin; Genentech/Roche), interferes with the receptor tyrosine kinase HER2 and has become the first-line therapy for HER2-overexpressing metastatic breast cancer patients (Carter *et al.*, 1992; Vogel *et al.*, 2002). In conjugation with other therapeutic agents such as toxins, radioisotopes, cytokines, or small molecule drugs, mAbs can help to deliver these therapeutic agents effectively to tumor cells (Brekke and Sandlie, 2003; Imai and Takaoka, 2006). In addition, mAbs can act on the immune system as indirect agents against cancer. Antibodies against programmed cell death protein 1 (PD-1), such as BMS-936558 (Nivolumab; Bristol-Myers Squibb), can enhance T-cell activities and has resulted in promising responses in cancer patients with mild adverse effect, making their development as a breakthrough in cancer therapy (Topalian *et al.*, 2012).

The side effects of targeted therapeutic agents are generally lower than conventional chemotherapeutic drugs. On the other hand, targeted therapy is still facing some challenges. Relapse has been frequently reported after treatment as a result of the acquired resistance of cancer cells (Dobbelstein and Moll, 2014). Another consideration is the high price of targeted therapy, especially mAbs. For colorectal cancer patients receiving an eight-week treatment, a conventional chemotherapy of 5-FU plus leucovorin costs less than $100, whilst treatment containing bevacizumab or cetuximab can cost up to $30,790 (Gerber, 2008). Such an enormous cost of mAbs restrains their popularization. It is unfortunate that a great number of people with low income may not be benefited from this modern cancer therapeutic method.

1.1.2.5 Combination therapy

Cancer is usually treated by a combination of surgery, radiation therapy, and drugs (Al-Lazikani *et al.*, 2012). For anti-cancer drugs, it has also been observed that their effects can be enhanced through combination (DeVita *et al.*, 1975). Successful combination therapies allow for the reduction of drug doses, and hence may lower the side effects (Chou, 2010). Besides, tumor cells are genetically heterogeneous and often develop resistance to a certain targeting drug through the activation of alternative oncogenic routes, thus it is believed that the combination of drugs with distinct anti-cancer mechanisms is a promising strategy to overcome such plasticity of cancer (Al-Lazikani *et al.*, 2012; Dobbelstein and Moll, 2014).

The first reported cancer cure by combination therapy dates back to 1960s when a quadruple combination of the Vinca alkaloid tubulin inhibitor vincristine, the antifolate methotrexate, the purine nucleotide synthesis inhibitor 6-mercaptopurine and the steroidal agent prednisone was used against acute lymphoblastic leukemia (ALL) (Al-Lazikani *et al.*, 2012; Dobbelstein and Moll, 2014). Modern drug combination strategies usually involve the administration of conventional chemotherapeutic drugs together with targeted drugs. Examples include the combination of paclitaxel and trastuzumab for breast cancer (Slamon *et al.*, 2001), the administration of cyclophosphamide/doxorubicin/vincristine/dexamethasone in combination with rituximab for non-Hodgkin's lymphoma (Coiffier *et al.*, 2002), and the usage of irinotecan in combination with cetuximab for colon cancer

(Sobrero *et al.*, 2008). In addition, nutrient starvation strategy may also be a choice of drug combination studies. In 2006, the United States Food and Drug Administration (FDA) approved a first-line treatment of children with ALL which involved the usage of the asparagine-depleting enzyme, asparaginase, as a component of a multiagent chemotherapy regimen (Dinndorf *et al.*, 2007).

Although there are numeous mathematically possible drug combinations, not all of them make mechanistic sense, and only a few of them may actually be effective. Therefore, strategies for the prediction and evaluation of potential combinations still remain as a great challenge for the future drug combination studies.

1.2 Cell death pathways

1.2.1 An overview of different modalities of cell death

Cells may die in different ways, uncontrollably or in a more programmed manner. Oncosis is a term first proposed by von Reckling-hause in 1910 to describe the phenomenon of accidental cell death with swelling (Majno and Joris, 1995). This type of cell death is usually caused by insufficient energy supply or direct damage to the cell membrane (Elmore, 2007). Being a passive, uncontrolled, irreversible process, oncosis results in necrosis with karyolysis, and the cellular contents are released into the surrounding interstitial tissue (Elmore, 2007; Majno and Joris, 1995). The term necrosis originally refers to the degradative process after cell death, but is now more widely used instead of the term oncosis (Elmore, 2007). In contrast, programmed cell death, including apoptosis and macroautophagy (hereafter referred to as autophagy), are highly regulated self-destructive processes essential for development and survival (Elmore, 2007; Maiuri *et al.*, 2007).

Another relevant term, senescence, refers to the irreversible cell-cycle arrest under the condition in which the cells are stimulated to grow yet the cell cycle is blocked (Blagosklonny, 2011; Schmitt, 2003). Although there have been examples that senescent cancer cells are rapidly eliminated by phagocytic cells (Xue *et al.*, 2007), it has also been reported that some

senescent cells are able to reside in the organism for years (Michaloglou *et al.*, 2005). Therefore, senescence, to be precise, is not a mode of cell death.

Apoptosis, autophagy, and necrosis are also named as type I, II, and III cell death (Kroemer *et al.*, 2009). Together with senescence, they are all possible goals of anti-cancer therapeutic approaches (Amaravadi and Thompson, 2007; Nardella *et al.*, 2011; Schmitt, 2003). Apoptosis, autophagy and senescence will be introduced with more details in the following sections, and will also be investigated in this project.

1.2.2 Apoptosis

The term apoptosis was first brought up in 1972 to describe a type of active, programmed cell death mechanism with unique morphological features (Kerr *et al.*, 1972). The process of apoptosis, from initiation to completion, may take only around 2-3 h (Elmore, 2007), and can be summarized into two stages (Kerr *et al.*, 1972). During the early stage of apoptosis, the cell rounds up, shrinks, starts to have blebs on cellular membrane, and subsequently fragments into a number of membranous vesicles (apoptotic bodies) which can be visualized under a light microscope (Kerr *et al.*, 1972; Kroemer *et al.*, 2009). Apoptotic bodies consist of cytoplasm, intact cell organelles, and sometimes the nuclear fragments (Elmore, 2007). In the late stage of apoptosis, apoptotic bodies are engulfed by other cells and degraded by lysosomal enzymes within phagosomes of the ingesting cells (Kerr *et al.*, 1972).

The early stage of apoptosis can be further divided into two phases. The first phase is mainly the initiation of apoptosis, and can be classified into three pathways: the extrinsic pathway triggered by the binding of death ligands to the receptors on cell surface; the intrinsic pathway which involves changes in mitochondria as a result of non-receptor-mediated stimuli such as absence of nutrients or growth factors, presence of toxins, hypoxia, or radiation; and the perforin/granzyme pathway which involves T-cell mediated killing of the cell (Figure 1.1) (Elmore, 2007). All these three pathways are followed by the execution pathway which involves the

degradation of chromosomal DNA, the condensation of nucleus, the reorganization of cytoskeletons, and the disintegration of the cell into apoptotic bodies (Figure 1.1) (Elmore, 2007).

In the late stage of apoptosis, apoptotic cells are removed by phagocytosis. The recognition of apoptotic cells requires the involvement of phosphatidylserine (PS), a component of the cell membrane. PS normally faces the cytosolic side of the cell membrane, but will translocate to the outer layer of cell membrane during apoptosis which resembles the hallmark of this stage (Bratton *et al.*, 1997).

Depletion of nutrients is likely to trigger the intrinsic pathway of apoptosis which involves the participation of mitochondria. Apoptotic mitochondrial events are under the control of the Bcl-2 family of proteins which are regulated by the tumor suppressor protein *p53* (Cory and Adams, 2002; Schuler and Green, 2001). As a result of apoptotic stimuli, the mitochondrial transition pores on the inner mitochondrial membrane opens, the mitochondrial transmembrane potential therefore decreases, and some mitochondrial proteins are released into cytosol (Saelens *et al.*, 2004). Some of these mitochondrial proteins, such as cytochrome *c*, function at an earlier phase of the intrinsic pathway by activating procaspase-9, one of the main initiator caspases in the cell (Chinnaiyan, 1999). Caspase-9 then triggers the activation of caspase-3, and hence initiates a protease cascade which finally results in rapid cell death (Elmore, 2007). Some other mitochondrial proteins, on the other hand, participate in the later phase of the intrinsic pathway. For example, caspase-activated DNAse (CAD), when released

from mitochondria, enters the nucleus where it is cleaved by caspase-3, and leads to the fragmentation of oligonucleosomal DNA as well as the further condensation of chromatin (Enari *et al.*, 1998).

Apoptosis is an indispensable mechanism for growth and development as it helps to remove undesired contents in human bodies. Apoptosis at a normal level is necessary to maintain homeostasis (Renehan *et al.*, 2001), while increased level of apoptosis has been observed during development, aging, inflammation and disease processes (Greenhalgh, 1998; Nijhawan *et al.*, 2000; Renehan *et al.*, 2001). Dysregulation of apoptosis can lead to diseases such as cancer (Elmore, 2007). In human cancers, the tumor suppressor protein *p53* is frequently mutated (Wang and Harris, 1997). The malfunction of *p53* results in suppressed apoptosis, and hence promotes the development and progression of cancer (Kerr *et al.*, 1994).

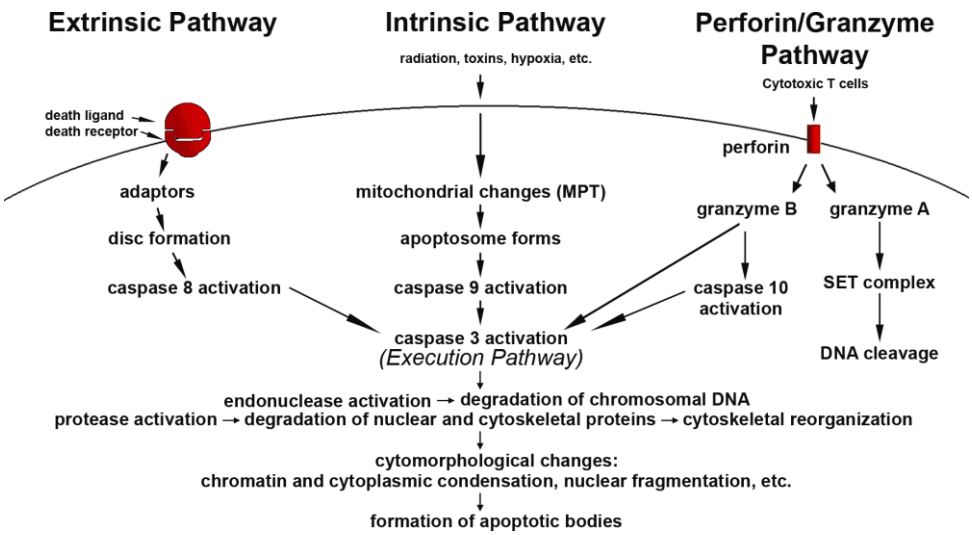

Figure 1.1: A schematic representation of apoptosis (Elmore, 2007).

1.2.3 Autophagy

Autophagy (macroautophagy) refers to the self-degradation process during which the cellular components are delivered to lysosome and degraded there (He and Klionsky, 2009). It is a term first defined in 1963 by C de Duve whom also discovered the lysosome (Ohsumi, 2014). Autophagy enables the cells to remove damaged and harmful contents as well as to recycle nutrients (Kroemer *et al.*, 2010), and hence allows the cells to survive during metabolic stress (Levine and Kroemer, 2008; Mizushima *et al.*, 2008).

The process of autophagy can be divided into multiple steps, as shown in Figure 1.2. The first step is the induction of the generation of a double-membrane structure named phagophore, followed by the expansion of phagophore around intracellular contents (autophagic cargos) which are targeted for degradation (Mari *et al.*, 2011). The phagophore then closes to form an intact double-membrane vesicle named autophagosome which later fuses with lysosome to generate autophagolysosome (Mari *et al.*, 2011). In the final step, lysosomal hydrolases degrade the autophagic cargos to produce metabolites which can be used by the cell as building blocks for new cellular contents or energy source (Mari *et al.*, 2011).

Autophagy can be induced by multiple signals including deprivation of nutrients, withdrawn of growth factors, shortage of cellular energy, bacterial or viral infection, and stresses such as reactive oxigen species (ROS) and

hypoxia (low levels of oxygen) (He and Klionsky, 2009). Figure 1.3 summarizes the pathways involved in autophagy regulation related with the levels of amino acids, growth factors, and energy.

mTOR is the main negative regulator of autophagy in response to amino acid levels (He and Klionsky, 2009). The inhibition of mTOR complex 1 (mTORC1) results in the formation of phagophore which requires the interaction between vacuolar sorting protein 34 (vps34) and Beclin 1 and the participation of autophagy-related proteins (Atg) (Pattingre *et al.*, 2008). The Atg proteins also promotes the conversion of the cytosolic form of microtubule-associated protein 1A/1B-light chain 3 (LC3), namely LC3-I, to its lipidated form, LC3-II (Tanida *et al.*, 2008). LC3-II incorporates into the membrane of autophagosome and is then degraded by autophagolysosomal enzymes (Tanida *et al.*, 2008). Therefore, the level of LC3-II is an excellent reflection of autophagic activity (Tanida *et al.*, 2008). LC3-II also interacts with p62 (sequestosome1, SQSTM1), an autophagy receptor which recognizes the proteins to be degraded (Janku *et al.*, 2011).

Apart from mTOR pathway, autophagy induced by amino acid deprivation is also regulated through the activation of Ras/Raf-1/ERK pathway (Pattingre *et al.*, 2003).

Basal level of autophagy is essential for homeostasis as it removes dysfunctional cellular components (Levine and Klionsky, 2004; Mizushima, 2007). During metabolic stress, upregulated autophagy promotes cell survival by providing nutrients and energy through its recycling process and is considered as a mechanism for the resistance of cancer cells to therapies

(Apel *et al.*, 2008; Degenhardt *et al.*, 2006; Sui *et al.*, 2013; Vazquez-Martin *et al.*, 2009). Therefore, autophagy inhibitors can be developed as anti-cancer drugs. Examples of autophagy inhibitors include chloroquine (CQ) and hydroxychloroquine (HCQ) which are registered antimalarials (Cufi *et al.*, 2013; Goldberg *et al.*, 2012).

On the contrary, unrestricted autophagy leads to cell death due to increased consumption of cellular components (Baehrecke, 2005). Compared to autophagy inhibitors, a great more number of anti-cancer agents are found to have autophagy-inducing effect (Janku *et al.*, 2011). For example, temsirolimus (or CCI-779; Torisel; Wyeth) and everolimus (or RAD-001; Afinitor; Norvatis) are registered drugs for the treatment of renal cancer through the inhibition of mTOR; sorafenib (Nexavar; Bayer and Onyx) which inhibits tyrosine kinases has been approved by FDA for the treatment of renal cancer and hepatocellular carcinoma (HCC); tamoxifen, an estrogen receptor antagonist, is a drug for breast cancer therapy (Janku *et al.*, 2011).

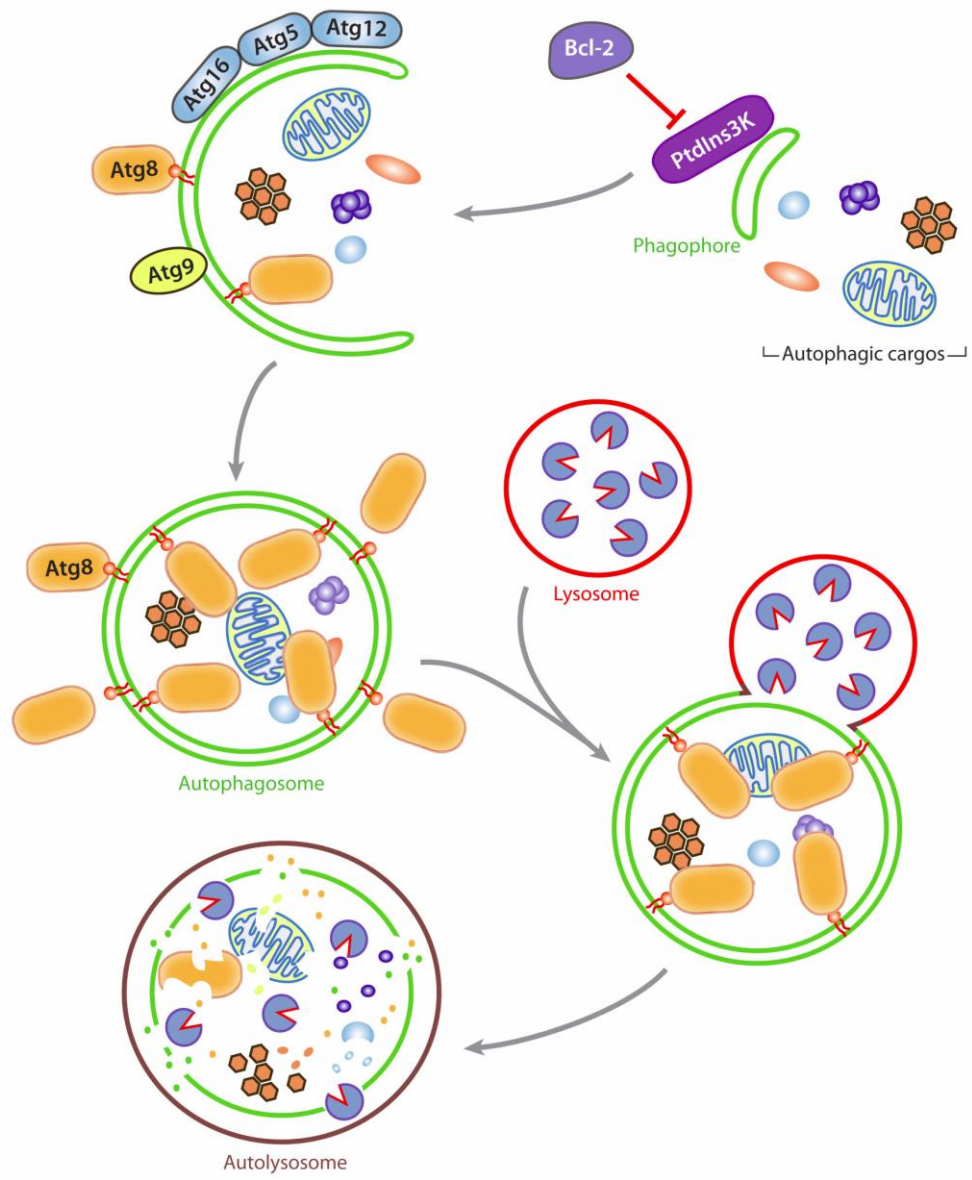

Figure 1.2: The general scheme of autophagic process (He and Klionsky, 2009). The five steps of autophagy are: induction, expansion, vesicle completion, fusion and cargo degradation (Mari *et al.*, 2011).

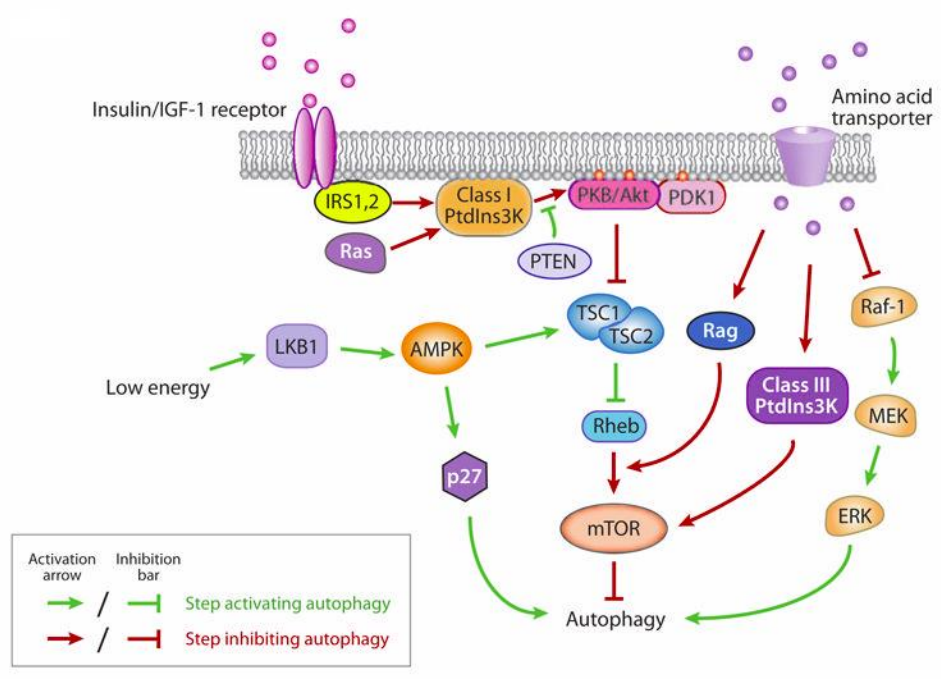

Figure 1.3: The regulatory pathways of autophagy by amino acids, growth factors, and energy in mammals (He and Klionsky, 2009).

1.2.4 Senescence

The cell cycle is composed of four phases: the gap phase before DNA replication (G_1 phase), the phase for DNA synthesis (S phase), the gap phase after DNA replication (G_2 phase), and the mitotic phase during which cell division happens (M phase) (Hartwell and Weinert, 1989). Cell cycle processes are monitored by multiple checkpoints regulated by proteins cyclins and cyclin-dependent kinases (CDKs) to ensure an upstream event be completed before the initiation of a subsequent one (Hartwell and Weinert, 1989; Poon *et al.*, 1996). For example, the restriction point (R point) is a checkpoint in G_1 phase for the commitment of the subsequent cell cycle processes in which extracellular stimulations such as growth factors are no longer required (Pardee, 1974). The withdrawal of growth factors causes normal cells to arrest in early G_1 phase before the R point, a status called G_0 arrest or quiescence (Blagosklonny, 2006). Quiescence is associated with low levels of metabolism, RNA, and protein synthesis (Blagosklonny, 2006). Quiescence, however, is not a stable status, as it can either be reversed when growth factors are re-supplemented or proceed to apoptosis upon prolonged, complete deprivation of growth factors (Blagosklonny, 2006).

Non-G_0 phase arrest happens under the conditions when growth factors are present yet some downstream cell cycle processes are blocked by CDK inhibitors (Blagosklonny, 2006, 2011). As a result, the cells arrest beyond the R point which is a phenomenon named senescence (Blagosklonny,

2006). Senescent cells may arrest in late G_1, S, or G_2/M phase (Blagosklonny, 2011; DiPaola, 2002; Pietenpol and Stewart, 2002). While the cell cycle is arrested, the presence of upstream signals such as growth factors continues to promote cell growth, and hence results in large cell morphology as well as active metabolism (Blagosklonny, 2006). Elimination of the impact brought by CDK inhibitors may overcome senescence yet it has been reported that most re-activated cells undergo abnormal cell cycle processes or die during mitosis (Chang *et al.*, 2000). The bypass of cell cycle blocks upon the effect of oncogenes such as c-Myc may also lead to cell cycle restoration but will in turn result in cancer (Hanahan and Weinberg, 2000).

Senescence, as a detrimental state for the cells, contributes to the process of aging as well as the suppression of oncogenesis (Dimri *et al.*, 1995; Serrano *et al.*, 1997). In fact, as senescence is triggered both *in vitro* and *in vivo* by many chemotherapeutic agents, it is likely to be a possible anti-cancer mechanism of these drugs and may deserve further investigations (Collado *et al.*, 2007; te Poele *et al.*, 2002).

1.2.5 Crosstalk among apoptosis, autophagy, and senescence

Apoptosis, autophagy, and senescence are not unrelated events but instead share multiple signaling pathways such as the mTOR pathway and the Ras/Raf/ERK pathway (Cagnol and Chambard, 2010; Meric-Bernstam and Gonzalez-Angulo, 2009).

The complex relationship among different modalities of cell death, especially apoptosis and autophagy, has been widely studied. Inhibition of apoptosis can switch the cells to autophagy (which is usually cytodestructive in this situation) (Maiuri *et al.*, 2007), and vice versa (Boya *et al.*, 2005). Besides, autophagy, as a relatively transient process, is sometimes observed prior to senescence and/or apoptosis as a death-facilitating process (Maiuri *et al.*, 2007). In addition, autophagy may serve as a cytoprotective mechanism to avoid apoptosis (Maiuri *et al.*, 2007). The proposed relationships among apoptosis, autophagy, and senescence are summarized in Figure 1.4.

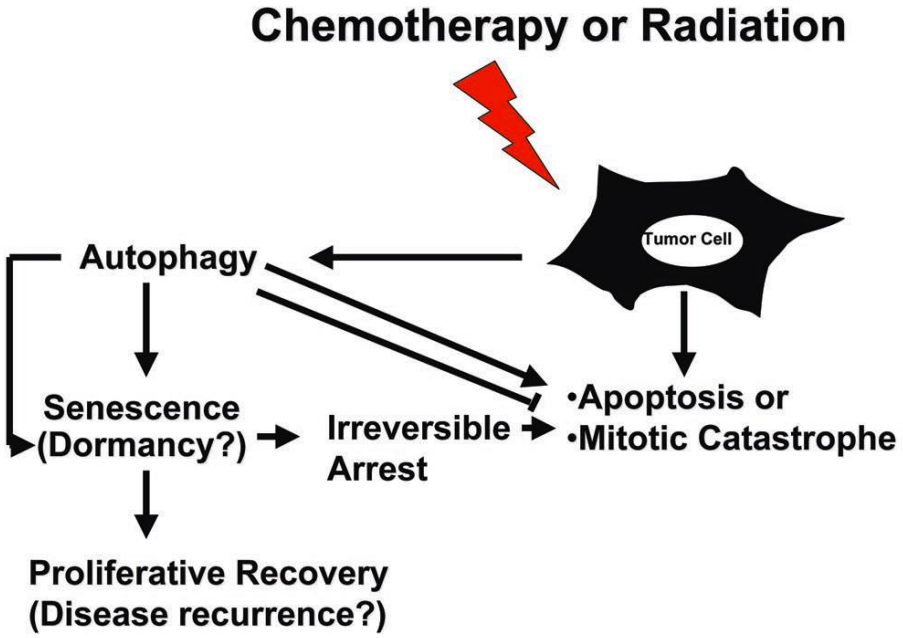

Figure 1.4: The proposed relationships among apoptosis, autophagy, and senescence (Gewirtz, 2009).

1.3 Amino acid-depletion as an anti-cancer method

1.3.1 Principle of amino acid-depletion against cancer

Cancer cells have several characteristics that distinguish them from their normal counterparts. First, normal cells usually cease proliferation after dividing a limited number of times, while most cancer cells are theoretically immortal with limitless replicative potential due to their ability of telomere maintenance (Hanahan and Weinberg, 2000). Besides, unlike normal cells, cancer cells do not exhibit contact inhibition, therefore these cells will keep growing when their cell membranes come into contact (Abercrombie, 1979). In addition, cancer cells may have a different requirement of nutrients due to their rapid speed of growth and altered genetic contents. Moreover, many cancer cells do not have stringent G_1 control, and hence lack the ability of entering quiescence when nutrients or growth factors are depleted (Scott *et al.*, 2000). The resulting continuous cell cycle process in an unfavorable environment may cause the cancer cells to reach an imbalanced state of growth and die eventually (Scott *et al.*, 2000).

Due to their specific genetic contents and metabolic properties, cancer cells may be more liable to the deficiency of nutrient such as glucose or amino acids. So far, multiple researches have been conducted to examine the impact of amino acid deprivation on cancer cells.

1.3.2 The depletion of asparagine by asparaginase

Asparagine is a non-essential amino acid for human since it can be synthesized by asparagine synthetase in normal cells. In leukemic cells, the activity of asparagine synthetase is much lowered so that these cells are auxotrophic for asparagine (Prager and Bachynsky, 1968b). This metabolic difference between leukemic cells and normal cells has inspired the idea of using asparaginase (EC 3.5.1.1), an asparagine-depleting enzyme, to selectively kill the leukemic cells.

L-Asparaginase catalyzes the hydrolysis of asparagine to aspartate and ammonia. Currently in the United States, clinically available asparaginase are derived from *Escherichia coli* and *Erwinia* species (Masetti and Pession, 2009). *E. coli* aspraginase is a homo-tetramer in the form of two intimate pairs of dimers (Swain *et al.*, 1993). Its structure is shown in Figure 1.5. Although each subunit contains one active site, it is only the tetrameric asparaginase that is catalytically functional as the active sites are all located between subunits (Swain *et al.*, 1993). *E. coli* asparaginase functions optimally at 50 ℃, pH 7.0, and its Michaelis-Menten constant (K_m) for L-asparagine is 7 μM (Wada *et al.*, 1990). Under standard conditions, the specific activity of asparaginase is ~300-400 μmol asparagine per min per mg of protein (Masetti and Pession, 2009).

Preclinical studies examining the effect of asparaginase on tumor cells dates back to the late 1950s and the early 1960s (Pasut *et al.*, 2008). After

then, positive results were obtained from several clinical trials using native asparaginase originates from *E. coli* and *Erwinia chrysanthemi,* giving the proof that this enzyme is effective against leukemia (Pasut *et al.*, 2008). Modification of asparaginase was conducted later to eliminate the problem of immunogenicity caused by the native enzyme through the random covalent conjugation of several polyethylene glycol (PEG) molecules with the enzyme. Pegylation, while retaining the catalytic properties of asparaginase, has also significantly enhanced the circulating half-life of this enzyme from ~30 h to ~140 h (Asselin *et al.*, 1993). The pegylated form of asparaginase, named as pegaspargase (Oncaspar; Enzon), has been approved by FDA for the first-line treatment of children with ALL (Masetti and Pession, 2009; Pasut *et al.*, 2008).

Although asparaginase and pegaspargase are both effective anti-leukemia drugs, resistance to these agents has been discovered. A major reason for resistance is the development of anti-asparaginase and anti-PEG antibodies in patients that have previously received the corresponding treatments (Armstrong *et al.*, 2007; Asselin *et al.*, 1993; Cheung *et al.*, 1986; Panosyan *et al.*, 2004). Another possible reason is the increased activity of asparaginase synthetase in cancer cells after treatment with asparaginase (Kiriyama *et al.*, 1989; Prager and Bachynsky, 1968a). Asparaginase is also of limited use as it is only effective against a few types of cancer. Despite these defects, asparaginase is still a powerful tool for the treatment of leukemia at present.

A

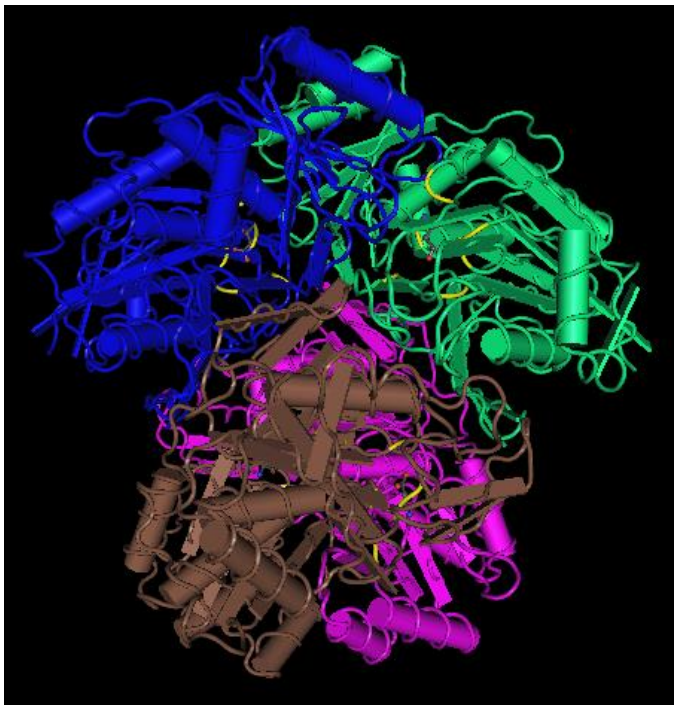

B

Figure 1.5: Crystal structure of *E. coli* L-asparaginase (PDB number: 3ECA) viewed by Cn3D 4.3. (A) *E. coli* L-asparaginase tetramer contains four identical subunits; (B) The interaction between subunits of *E. coli* L-asparaginase. Amino acid residues located at active sites are highlighted in yellow. The catalytic product aspartic acid is shown in ball-and-stick representation.

1.3.3 The depletion of methionine and the application of methioninase

The growth of a few solid tumor cell lines has been found to be methionine-dependent. *In vitro* studies have shown the replacement of methionine with its metabolic precursor homocysteine leads to S/G_2 cell cycle arrest in several tumor cell lines as well as in fresh patient tumors while having no impact on human foreskin fibroblast cells (Guo, Herrera *et al.*, 1993). Methionine-free diet for sarcoma-bearing nude mice has also resulted in an increase of DNA content specifically in tumor cells, indicating a methionine-dependent cell cycle block (Guo, Lishko *et al.*, 1993). Methionine-free diet has significantly extended the survival of tumor-bearing mice while having no significant impact on their body weight and performance (Guo, Lishko *et al.*, 1993; Kudou *et al.*, 2007). In addition, methionine-free diet in combination with standard regimen for colorectal cancer has received satisfactory response rate with minimal toxicity in patients (Durando *et al.*, 2010).

L-Methionine γ-lyase (EC 4.4.1.11), or methioninase, catalyzes the hydrolysis of L-methionine to methanethiol, 2-oxobutanoate and ammonia. Methioninase has been found in many microorganisms such as *Pseudomonas putida*. As shown in Figure 1.6, *P. putida* methioninase is a homo-tetramer built up as a dimer of active dimers (Kudou *et al.*, 2007). Each active dimer consists of two monomers held tightly through hydrogen bonds, hydrophobic interactions and intermolecular active-site interactions

(Kudou *et al.*, 2007). A dimer structure is essential for the binding of the cofactor pyridoxal-5'-phosphate (PLP) as well as the catalytic activity of the enzyme, whilst a tetramer configuration is thought to help make the enzyme more stable (Kudou *et al.*, 2007).

According to the assay method established by Takakura *et al.* (2004), the specific activity of recombinant *P. putida* methioninase is 57 U/mg and the K_m for L-methionine is 1.7 mM at 37 ℃, pH 8.0. The protocols for the large-scale production of recombinant methioninase has been established, and hence enables the application of methioninase as a therapeutic agent (Tan, Xu *et al.*, 1997).

In vitro studies have shown that methioninase has tumor-specific inhibitory effect on many types of human cancer cells including lung, colon, head and neck cancer, and firosarcoma (Yoshioka *et al.*, 1998). Methioninase is also found to be safe and effective on nude mice implanted with human colon cancer cells HCT15 (Tan, Xu *et al.*, 1997). Apart from being active alone, methioninase is synergistic with 5-FU in murine Lewis lung carcinoma model, and its toxicity is negligible (Yoshioka *et al.*, 1998). In a pilot phase I clinical trial, i.v. fusion of recombinant methioninase effectively lowered the serum methionine level in patients while no toxic effects were observed (Tan, Zavala *et al.*, 1997).

In order to solve the problem of immunogenicity and instability, pegylated form of methioninase has been developed (Yang, Wang *et al.*, 2004). Pegylation has been reported to significantly reduce the immnunogenicity of methioninase *in vivo*, and extend the enzyme half-life

from 2 to 38 h (Sun *et al.*, 2003). Although some antibodies against pegylated methioninase were detected in primate model that has received multiple treatments of this enzyme, the level of these antibodies was too low to result in drug resistance (Pasut *et al.*, 2008).

The results so far indicate that methioninase may be a promising anti-cancer enzyme drug. However, the development of methioninase for cancer therapy seems to have obscurely ceased in recent years, and no related clinical trials have been reported. Since methionine is an essential amino acid, the stagnation of studies on methioninase may due to its long-term cytotoxic effect in not only tumors but also normal cells and tissues upon the deprivation of methionine.

A

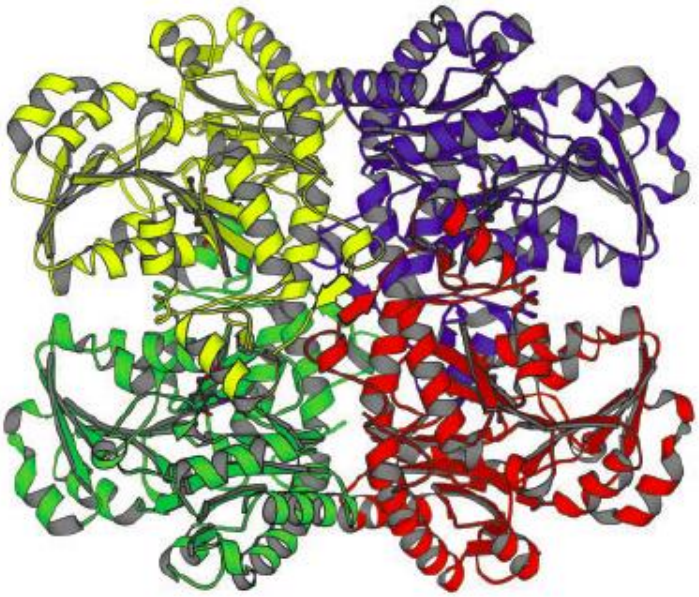

B

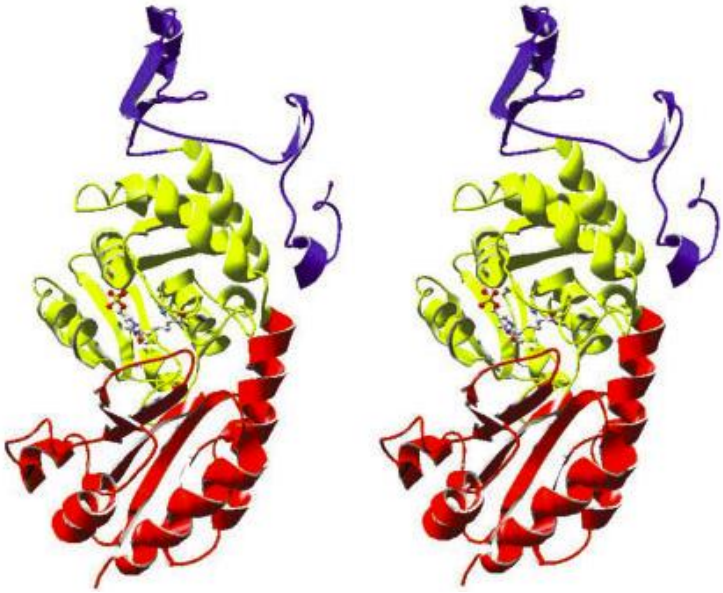

Figure 1.6: Structure of *P. putida* methioninase (Kudou *et al.*, 2007). (A) The homo-tetramer of *P. putida* methioninase is built-up as a dimer of active dimers; (B) Monomer of the enzyme contains an N-terminal domain (blue), a PLP-binding domain (yellow), and a C-terminal domain (red). PLP and PLP-binding Lys211 are shown in ball-and-stick representation.

1.3.4 The absence of leucine and its effect on cancer cells

Leucine is a branched-chain amino acid. It is an essential amino acid that cannot be synthesized by human body. Leucine is the only dietary amino acid that is able to stimulate the synthesis of muscle proteins, its catabolism happens not in liver but primarily in skeletal muscle (Etzel, 2004).

The association between dietary leucine and tumorigenesis is intricate and seems to be tumor type-dependent. For example, leucine is suspected to trigger bladder cancer in rats according to Nishio *et al.* (1986). From their studies, rats given a diet supplemented with a bladder carcinogen BHBN (N-butyl-N-(4-hydroxybutyl) nitrosamine) and additional leucine was found to be more prone to bladder tumorigenesis compared to the rats given a diet supplemented with BHBN only (Nishio *et al.*, 1986). Another *in vivo* study indicates leucine-free diet can lead to significant decrease in food intake and body weight of nude mice bearing human breast cancer xenograft (Singh *et al.*, 2011). In contrast, a study conducted in melanoma cell lines has demonstrated that a cease of proliferation and a decrease in cyclin D1 co-occur in these cells when leucine is depleted (Sheen *et al.*, 2011). Leucine triggers caspase-3-dependent apoptosis in melanoma cells while exerting no such effect on their normal counterparts (Sheen *et al.*, 2011). Unlike asparagine and methionine, studies on leucine related to cancer therapy mainly focus on leucine-free diet instead of any leucine-depleting enzyme.

1.3.5 The depletion of arginine and its anti-cancer effects

1.3.5.1 Arginine and urea cycle

Arginine is a semi-essential amino acid for human because it can be sufficiently synthesized by healthy adults but is required from dietary intake by specific groups of people such as children and patients (Bewley *et al.*, 1999). Arginine plays an important role in various metabolic processes. Despite of being an important material for protein biosynthesis, arginine is also a precursor for a variety of compounds including nitric oxide, urea, ornithine, citrulline, agmatine, putrescine, creatine, and glutamate. Among these compounds, both ornithine and citrulline are intermediates of the urea cycle (Figure 1.7), a cyclic metabolic pathway occurs in animals that produce urea. In brief, arginine is converted to ornithine and urea by arginase in cytosol. While urea is excreted, ornithine is transported into mitochondria where it is converted to citrulline by ornithine transcarbamylase (OTC; EC 2.1.3.2). Citrulline is then transported back to cytosol and is utilized for arginine re-synthesis by two enzymes located close to mitochondria - argininosuccinate synthetase (ASS; EC 6.3.4.5) and argininosuccinate lyase (ASL; EC 4.3.2.1). The urea cycle takes place mainly in liver, and also in kidney to a small extent.

The depletion of arginine has greater impact on tumor cells than on normal cells due to two main reasons. First, most somatic cells have complete urea cycle pathways while many cancer cells do not. Somatic cells can use orithinine, the product of arginine hydrolysis, to resynthesize

arginine and ensure their nutrient supply; in contrast, many tumor cells are ASS- and/or OTC-negative thus are more likely to encounter the problem of arginine deficiency (Cheng *et al.*, 2007; Wheatley *et al.*, 2005). Second, *in vitro* studies have found that in arginine-free medium (AFM), normal cells including human fibroblasts, rat kidney epithelial cells, and mink lung epithelial cells, enter a quiescent state (G_0 phase) that can last for several weeks, and are able to recover when arginine is added back to the medium (Scott *et al.*, 2000). On the other hand, a wide range of cancer cell lines, due to their defective cell checkpoints, continue the cell cycle processes till imbalance and finally die (Scott *et al.*, 2000). These evidences provide the theoretical basis that arginine-depleting enzymes can be used as potential targeting therapeutic agents for cancer.

There are five types of enzymes that can catabolize arginine: nitric oxide synthase (NOS; EC 1.14.13.39), arginine-glycine amidinotransferase (AGAT; EC 2.1.4.1), arginase (EC 3.5.3.1), arginine decarboxylase (ADC; EC 4.1.1.19), and arginine deiminase (ADI; EC 3.5.3.6). All of these enzymes are found to be expressed in mammalian cells except ADI. At present, ADI and arginase are under development as potential anti-cancer drugs due to their arginine-depleting effect, while ADC is much less characterized and so far has received little attention in terms of its anti-cancer potential.

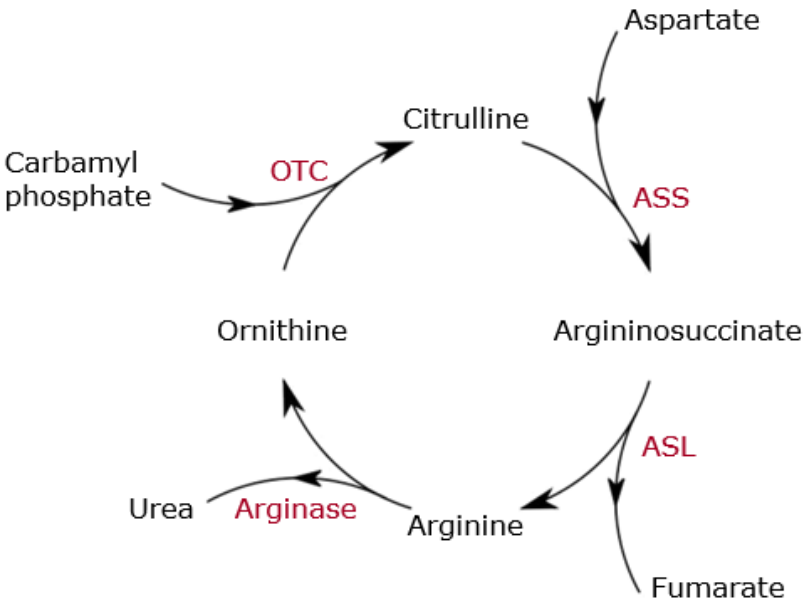

Figure 1.7: Major steps of urea cycle and enzymes involved. OTC, ornithine transcarbamylase; ASS, argininosuccinate synthetase; ASL, argininosuccinate lyase.

1.3.5.2 Arginine deiminase (ADI) and its anti-cancer properties

ADI is a microbial enzyme first identified in *Bacillus pyocyaneus* in 1933 (Ni *et al.*, 2008). In microorganisms, ADI plays an energy-providing role by hydrolyzing arginine to citrulline and ammonia, and generating ATP at the same time. The type of ADI that has been most widely studied is that from *Mycoplasma*. ADI from *Mycoplasma arginini* is a homo-dimer with a subunit MW of ~45 kDa (Takaku *et al.*, 1992), as shown in Figure 1.8. Native *M. arginini* ADI functions optimally at 50 ℃ and pH 6.0-7.5, and its K_m for L-arginine is 0.2 mM (Takaku *et al.*, 1992). Similarly, recombinant *M. arginini* ADI (Asn244Ser) expressed in *E. coli* has optimal reaction conditions of 41 ℃, pH 6.4-7.4, and its K_m for L-arginine is ~0.37 mM (Noh *et al.*, 2002). The measured specific activity of *M. arginini* ADI varies among different research groups, probably due to the differences in protein sequences, reaction conditions and assay methods. According to Misawa *et al.* (1994), the specific activity of recombinant *M. arginini* ADI is around 33.6 μmol L-citrulline per min per mg protein at 37 ℃, pH 6.5, while Noh *et al.* (2002) has reported a much higher specific activity value of recombinant *M. arginini* ADI of 72.3 μmol L-citrulline per min per mg protein under the same conditions.

ASS was first identified in liver where it is highly expressed, and was later found to be a ubiquitous enzyme in mammalian tissues. ASS is the rate-limiting enzyme in the re-synthesis process of arginine (Haines *et al.*,

2011). Its expression is mainly regulated by dietary protein intake and hormones (Morris, 2002). The ASS and ASL pathways are strongly coupled (Wheatley *et al.*, 2005). So far, the complete loss of ASL enzyme activity has not been found in any situation (Wheatley *et al.*, 2005). In contrast, many tumor cells have been characterized as ASS-negative. Due to the lack of ASS, the pathway for arginine re-synthesis from citrulline in these tumor cells is cut off (Figure 1.9), leading to arginine-depletion and resulting in cell death.

ADI is a potent anti-cancer drug candidate, and has been found to have inhibitory effects on the growth of many types of malignant cells that do not express the enzyme ASS (Ensor *et al.*, 2002; Gong *et al.*, 2000; Kelly *et al.*, 2012; Sugimura *et al.*, 1992). A three-day treatment with medium containing 50 ng/ml ADI can cause cell cycle arrest at G_1 and/or S phase in osteosarcoma, neuroblastoma, and retinoblastoma cells (Gong *et al.*, 1999). When the dose of ADI is increased to 200 ng/ml, apoptosis is triggered in these cells (Gong *et al.*, 1999). The inhibitory effect of ADI is found to be around 100-fold stronger than asparaginase in human lymphatic leukemia cell lines (Gong *et al.*, 2000).

Native ADI is thought to be strongly immunogenic since it is of microbial origin. Besides, ADI has a short half-life of only 4 to 5 h in mice (Takaku *et al.*, 1992). These problems have been solved by conjugating ADI with PEG molecules. Conjugation with PEG of 20,000 MW has no impact on the pharmacokinetics and pharmacodynamics of ADI, and is considered as the optimal method for formulating ADI (Holtsberg *et al.*, 2002).

Compared to native ADI which reduces serum arginine to below detectable levels for less than 1 day, the effect of ADI-SS $PEG_{20,000\ mw}$ of the same dose lasts for around 7 days (Ensor *et al.*, 2002). In phase I/II studies on unresectable HCC, 19 patients have received ADI-SS $PEG_{20,000\ mw}$ treatment for three months, two of them gave complete response to the treatment, seven patients showed partial response, another seven showed stable disease, while only three patients had progressive disease (Izzo *et al.*, 2004). No allergic symptom has been developed during the treatment period (Izzo *et al.*, 2004). Phase I and II clinical trials of ADI-SS $PEG_{20,000\ mw}$ on patients with metastatic melanoma have also yielded exciting results (Ascierto *et al.*, 2005). Pegylated ADI has resulted in 25% response rate in 24 patients with metastatic melanoma and has extended the survival period of these patients (Ascierto *et al.*, 2005).

Despite the problem of anti-PEG antibodies, another major problem of ADI left unsolved is that it has only been proved effective on ASS-negative tumor types. The relationship between ASS expression and sensitivity to ADI has been confirmed by transfecting ASS gene into ADI-sensitive tumor cells, as the results showed that these transfected tumors became ADI-resistant (Ensor *et al.*, 2002). Treatment of ADI has resulted in resistance in melanoma cell lines through the c-Myc-mediated induction of ASS expression (Tsai *et al.*, 2009; Tsai *et al.*, 2012). Such findings indicate an obstacle for the long-term application of ADI, and suggest the urgent need to discover proper combination drugs for ADI to combat the drug resistance. In addition, ADI has a limited anti-cancer spectrum as many tumor types are

of high ASS level (Figure 1.10), and are found to be ADI-resistant (Shen *et al.*, 2003).

A

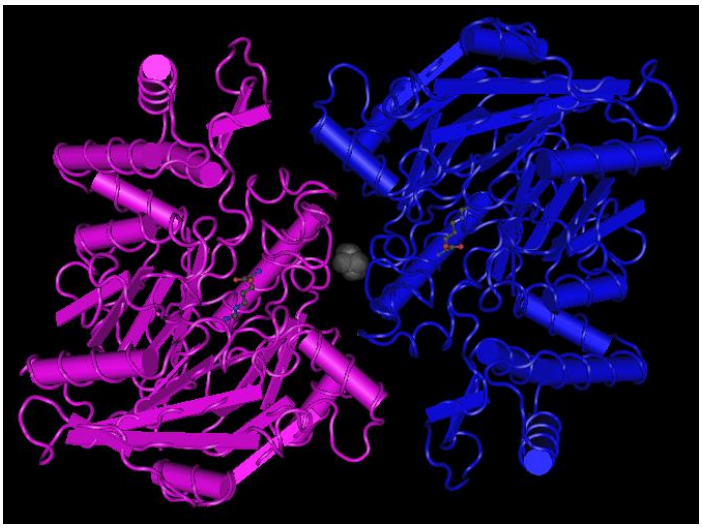

B

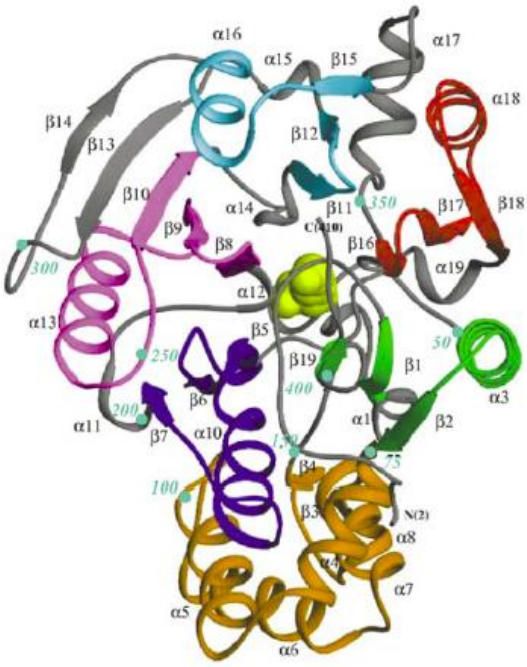

Figure 1.8: Structure of *M. arginini* ADI. (A) Crystal structure of *M. arginini* ADI homo-dimer (PDB number: 1S9R) viewed by Cn3D 4.3. Arginine is shown in ball-and-stick representation, and the amidino reaction intermediate is shown in a spherical representation (Das *et al.*, 2004); (B) Structure of *M. arginini* ADI monomer. The substrate binding site is located at the center of the molecule as marked in cyan (Das *et al.*, 2004).

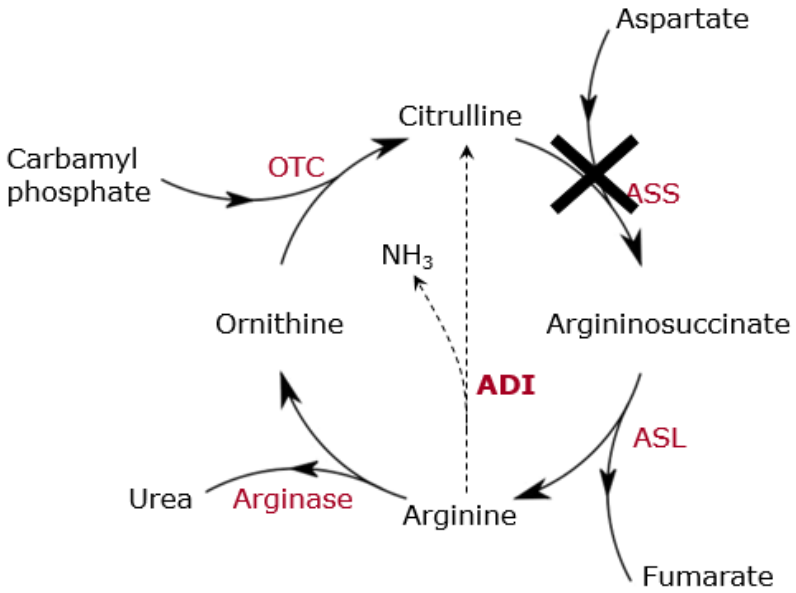

Figure 1.9: The anti-cancer mechanism of ADI. ADI catabolizes arginine and the product citrulline cannot be recycled for the *de novo* synthesis of arginine in ASS-negative tumor cells.

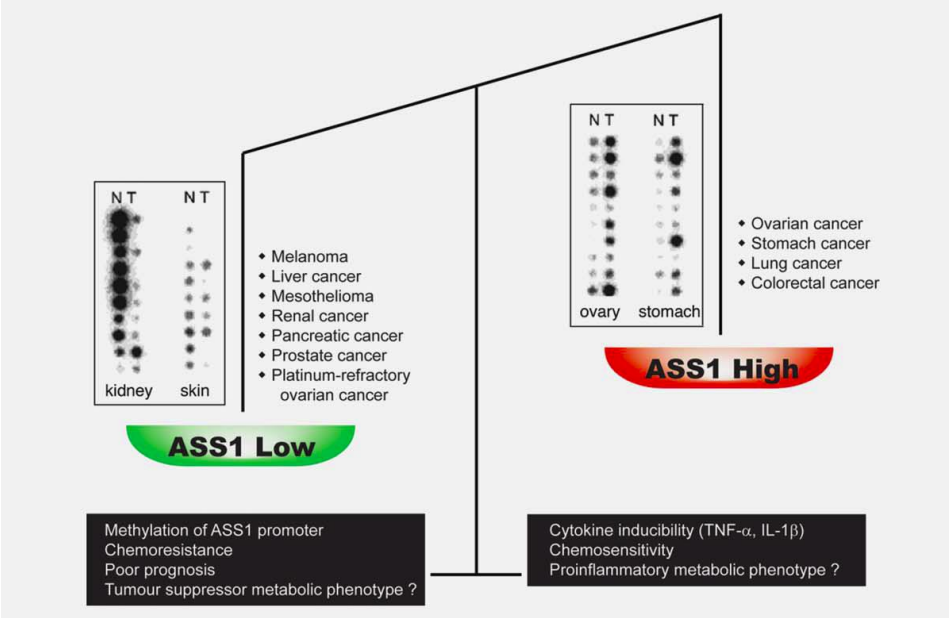

Figure 1.10: Levels of ASS in different types of cancer, according to cDNA profiling arrays (Delage *et al.*, 2010).

1.3.5.3 Arginase and its anti-cancer properties

Arginase catalyzes the hydrolysis of arginine to ornithine and urea. The finding that arginase has inhibitory effect on tumor cells dates back to 1950s (Bach and Simon-Reuss, 1953). According to this study, arginase purified from bovine liver is found to strongly inhibit the mitosis of cultured fibroblast and Jensen sarcoma cells (Bach and Simon-Reuss, 1953). However, bovine liver arginase is considered unsuitable for anti-cancer therapy because of its low affinity for arginine (K_m for L-arginine is 6 mM for native enzyme at a physiological pH) (Savoca *et al.*, 1984), short blood half-life (a few minutes) as well as a non-physiological optimum pH value of 9.6 (Tsui *et al.*, 2009).

Later, as the recombinant protein technology develops, recombinant human liver arginase I (rhArg) has been studied. Human arginase I (hArg) is a homo-trimer and the MW of each subunit is ~35 kDa (Stone *et al.*, 2012). Each monomer of this enzyme is catalytically active, and contains two manganese ions as cofactors (Stone *et al.*, 2010), as shown in Figure 1.11 (A). Compared to its bovine counterpart, rhArg expressed in *Bacillus subtilis* has higher affinity for its substrate arginine (K_m for L-arginine is 1.9 ± 0.7 mM for the native enzyme) (Tsui *et al.*, 2009). At 30 ℃, pH 8.5, the specific activity of rhArg is ~400 μmol urea per min per mg protein (Cheng *et al.*, 2007). Stone *et al.* (2010) have demonstrated a significant improvement of overall catalytic activity as well as serum stability of rhArg when the two Mn^{2+} ions are replaced with Co^{2+} (Co-hArg).

Compared to ADI, arginase has a wider anti-cancer spectrum. Both rhArg and Co-hArg are effective in cells lines of liver cancer, cervical cancer, melanoma, and leukemia (Agrawal *et al.*, 2012; Cheng *et al.*, 2007; Lam *et al.*, 2011; Morrow *et al.*, 2013). Some extra types of cancer cells lines, including those of melanoma, lung cancer, osteosarcoma, pancreatic cancer, prostate cancer, colon cancer, thyroid cancer, and breast cancer, are also found to be sensitive to Co-hArg (Agrawal *et al.*, 2012). Cytotoxicity of Co-hArg against normal human tissues, however, has also been reported (Agrawal *et al.*, 2012). Moreover, 6 mg/kg pegylated Co-hArg can result in transient weight loss in mice model while a doubled dose is harmful (Agrawal *et al.*, 2012). The toxic effect of Co-hArg is probably due to its enhanced catalytic effect compared to normal human arginase containing Mn^{2+}. Some researchers therefore suggest that Co-hArg be used in combination with citrulline against cancers with low ASS level to avoid high toxicity (Agrawal *et al.*, 2012). Such suggestion, even if feasible, will limit the application of Co-hArg to ASS-low cancers only.

By conjugating rhArg with mPEG-SPA (methoxypolyethylene glycol-succinimidyl propionate) of MW 5,000 Da, the resulting rhArg-peg$_{5,000mw}$ has not only retained most of its catalytic activity (K_m for L-arginine ≈ 2.9 mM) but also retained its tumor inhibitory effect at a physiological pH (Tsui *et al.*, 2009). The part of enzyme activity lost through pegylation may be compensated by a prolonged plasma half-life of around 3 days (Cheng *et al.*, 2007). Studies have shown that pegylated rhArg can dramatically inhibit the growth of several HCC and melanoma xenografts in mice (Cheng *et al.*,

2007; Lam *et al.*, 2009; Lam *et al.*, 2011). The pegylated rhArg, PEG-BCT-100, has entered phase I and II trials for patients with liver cancer (Bio-Cancer Treatment International Limited, 2014a, 2014b).

Another arginase which originates from *Bacillus caldovelox*, BCA, has also been studied by our group members. Unlike human arginase, BCA is a homo-hexamer (Figure 1.11 B) (Bewley *et al.*, 1999). Each monomer of BCA is of 31 ± 2 kDa (Patchett *et al.*, 1991) and is thought to have a full set of active-site residues (Bewley *et al.*, 1999). The protein sequence alignment of hArg and BCA is shown in Figure 1.12. As can be seen, these two proteins share moderate similarities with some conserved amino acid sequences.

Since *B. caldovelox* is an extreme thermophile, BCA is quite thermostable and has optimal activity at 60 ℃, pH 9 (Patchett *et al.*, 1991). The heat-resistant property is a great advantage of BCA over its human counterpart as it allows BCA to be easily purified by heat treatment. In addition, the advanced recombinant protein technology allows a 6x histidine tag to be attached to BCA so that the enzyme can be further purified by an affinity column. The anti-cancer properties of BCA is being studied both *in vitro* and *in vivo* which will be discussed in the following chapters.

As introduced previously, the main advantage of arginase over ADI is that it is effective against several tumor cell types that have previously been found to be ADI-resistant (Cheng *et al.*, 2007). Therefore, it is predicted that arginase is effective in both ASS-negative and ASS-positive tumors, as long as OTC is not expressed in these cells. Since the absence of OTC activity is

more frequently observed in tumor cells, it is believed that arginase has a much wider range of uses on cancer therapy than ADI. Another advantage of arginase lies in the fact that urea, the catalytic product of arginase, is less toxic than ammonia produced by the ADI-catalyzed reaction. Therefore, arginase may be a much safer choice for the treatment of cancer patients compared to ADI.

A

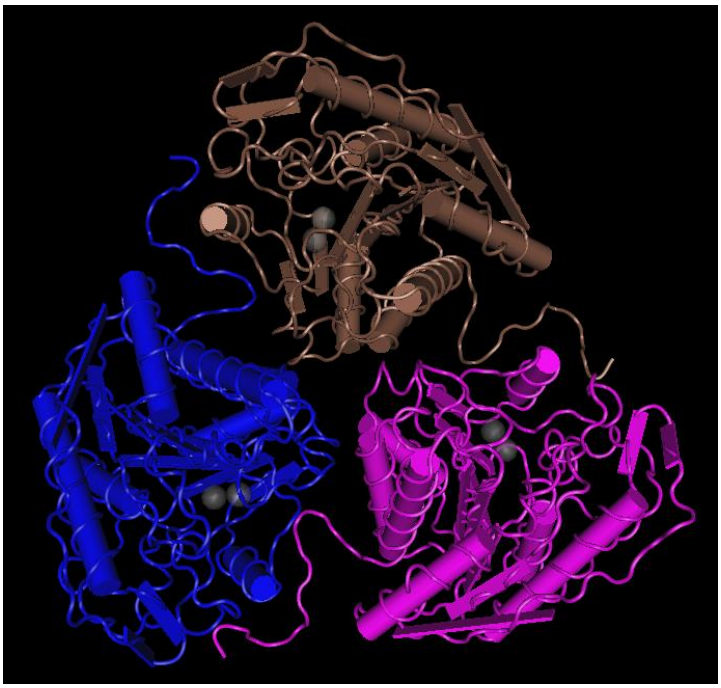

B

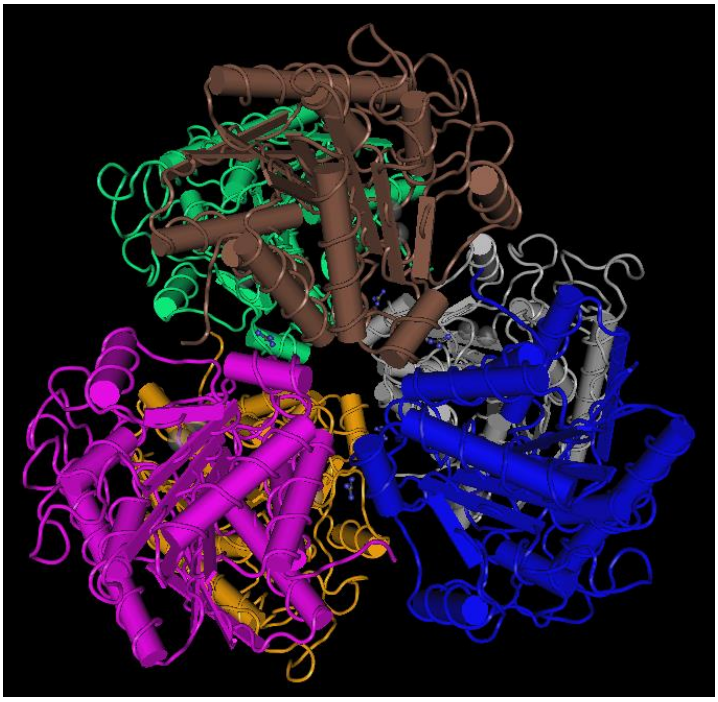

Figure 1.11: Structure of arginase viewed by Cn3D 4.3. (A) Structure of human arginase (PDB number: 2ZAV); (B) Structure of BCA (PDB number: 2CEV). Manganese ions are shown as spheres in gray.

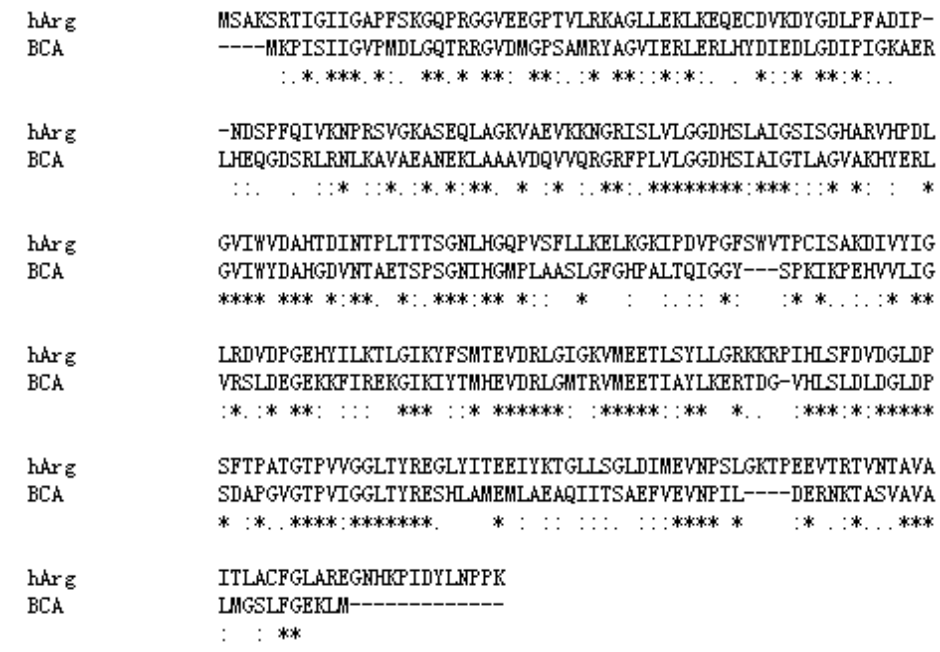

Figure 1.12: Protein sequence alignment of hArg and BCA by CLUSTALW. Protein sequences are corresponding to the crystal structures shown in Figure 1.11. Alignment score: 39.1304.

1.4 Arginine decarboxylase (ADC)

1.4.1 ADC in general

ADC catalyzes the conversion of L-arginine to agmatine and carbon dioxide (CO_2). It has been found in various types of organisms, including bacteria, fungi, parasites, plants, marine animals, and mammals.

In bacteria and plants, ADC, together with ornithine decarboxylase (ODC) which catalyzes the decarboxylation of ornithine to form putrescine, serves in two alternative pathways for the biosynthesis of polyamines (Bouchereau *et al.*, 1999; Morris and Pardee, 1966; Tabor and Tabor, 1985; Watson *et al.*, 1998). Polyamines are organic cations essential for cell growth and proliferation (Gerner and Meyskens, 2004). The ADC pathway of polyamine biosynthesis also involves the enzyme agmatinase which hydrolyzes agmatine to urea and putrescine (Bouchereau *et al.*, 1999; Tabor and Tabor, 1985). Putrescine, while being one of the three main polyamines in living organisms, can be further metabolized to the other two main polyamines – spermidine and spermine (Gerner and Meyskens, 2004).

Unlike bacteria and plants, in mammals, the biosynthesis of polyamines is merely through the enzyme ODC (Zhu *et al.*, 2004). In early days, ADC was not believed to be expressed in mammals (Tabor and Tabor, 1984). It was only till 1994 when ADC activity was first detected in bovine and rat brain (Li *et al.*, 1994). Human ADC, a protein of 460 amino acid residues, is selectively expressed in brain and is of negligible level in some other tissues

including heart, kidney, lung, skeletal muscles, and peripheral leukocytes (Zhu *et al.*, 2004). The catalytic product of ADC, agmatine, can cross the blood-brain barrier (Piletz *et al.*, 2003), and is widely distributed in mammalian tissues (Raasch *et al.*, 1995). While the activity of human ADC is quite low to generate much agmatine (Molderings and Haenisch, 2012), gastrointestinal uptake is also an important source of agmatine (Molderings *et al.*, 2003). Agmatine serves multiple physiological roles such as a neurotransmitter (Reis and Regunathan, 1998) and a suppressor of cell proliferation (Isome *et al.*, 2007; Satriano *et al.*, 1998). It has been reported that in kidney cells, agmatine can suppress the production of polyamines through the inhibition of ODC (Satriano *et al.*, 1998).

Compared to its bacterial and plant counterparts, mammalian ADCs are of a distinct type because: they are membrane-associated (Zhu *et al.*, 2004); their substrates include not only L-arginine but also L-ornithine (Zhu *et al.*, 2004); it is reported that rat (Regunathan and Reis, 2000) and human ADCs can be inhibited by calcium ions, which is also an unique feature of mammalian ADCs (Zhu *et al.*, 2004). The relationships among ADCs of bacteria, plants, and mammals are summarized in Figure 1.13 (Zhu *et al.*, 2004).

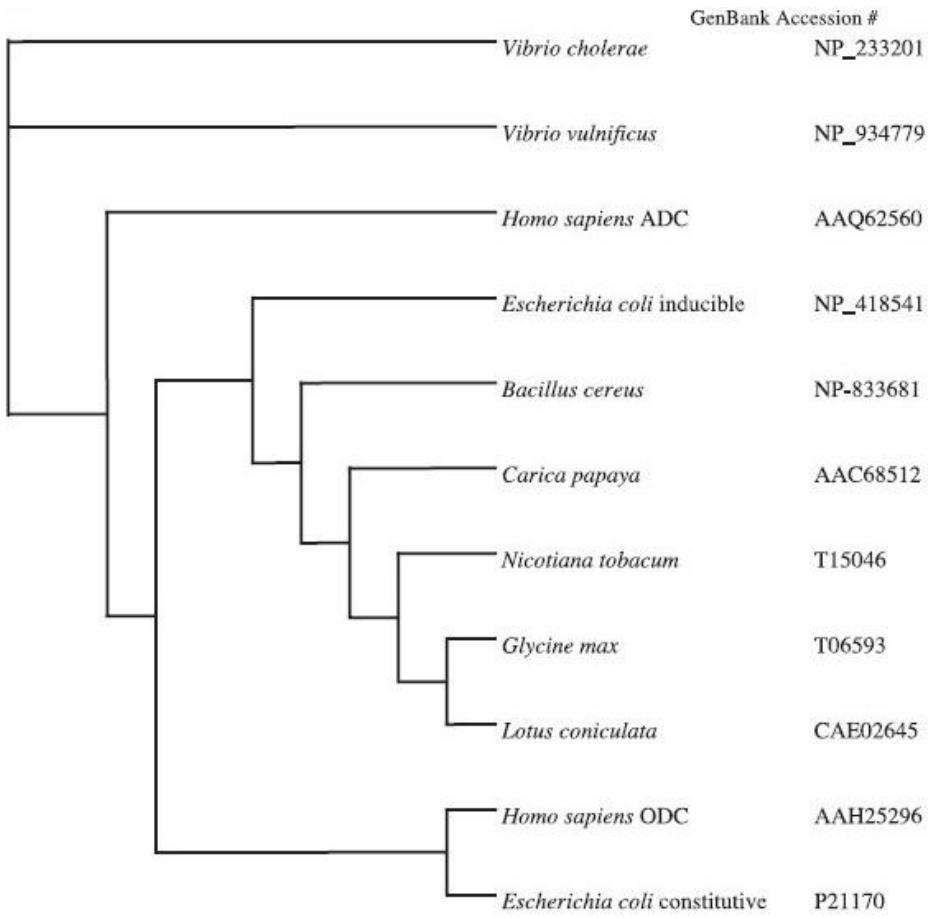

Figure 1.13: Phylogenetic tree based on amino acid sequences showing the relationships among ADCs of different origins (Zhu *et al.*, 2004).

1.4.2 Biodegradative ADC from *E. coli*

In *E. coli*, two isoforms of ADC have been identified: biodegradative (or inducible) ADC, and biosynthetic (or constitutive) ADC. Biodegradative ADC was first studied in 1940 (Gale, 1940). The gene that encodes this type of ADC, *adiA*, is only expressed under anaerobic, acidic conditions (Blethen *et al.*, 1968; Gale, 1940). Therefore, this type of ADC is also named as inducible ADC, or acid-induced ADC.

Characterization studies in early days have shown that biodegradative ADC requires PLP as a cofactor (Baddiley and Gale, 1945). The enzyme has optimal activity at pH 5.2, 37-40 ℃, with its K_m for L-arginine of 0.65 mM (Blethen *et al.*, 1968). Structural studies propose that biodegradative ADC is an 850 kDa-homo-decamer composed of five homo-dimers (Figure 1.14) (Andrell *et al.*, 2009; Blethen *et al.*, 1968).

Similar to other PLP-dependent enzymes, the basic unit of biodegradative ADC is a dimer rather than a monomer (Andrell *et al.*, 2009). The dimer is composed of two identical subunits, one from each pentameric rings (Andrell *et al.*, 2009). These two subunits are packed tightly so that the two active sites are well-buried from the dimer interface (Andrell *et al.*, 2009). The PLP cofactor binds to the lysine residue of one of the subunits, and is further coordinated by several other residues from both subunits of a dimer (Andrell *et al.*, 2009). Salt bridges and hydrogen bonds

are responsible for connecting neighbouring dimers to form the pentameric ring (Andrell *et al.*, 2009).

Biodegradative ADC plays an important role in the acid resistance system of bacteria. Under acidic conditions, the enzyme becomes activated and catalyzes the decarboxylation of arginine to agmatine. This process requires the consumption of proton, therefore prevents the accumulation of protons inside the bacterial cell (Andrell *et al.*, 2009). Due to such a defense mechanism, bacteria, such as *E. coli*, are able to survive in acidic environments such as the digestive tract of a host organism.

A

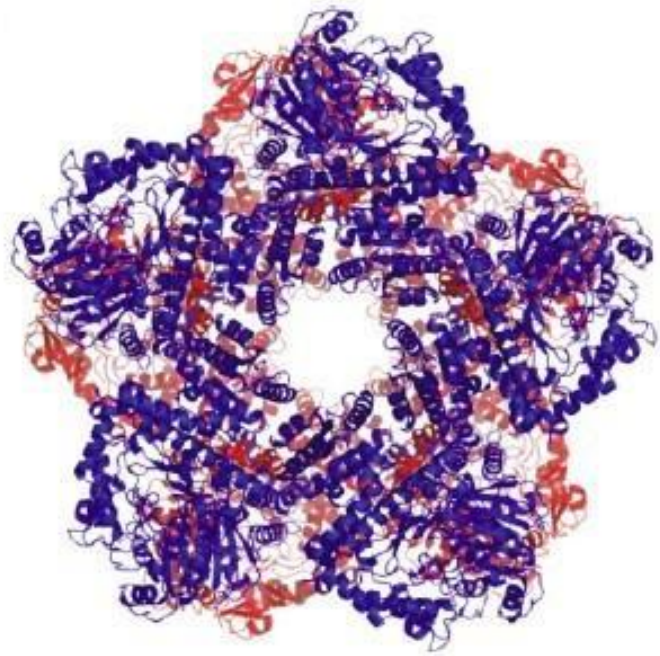

B

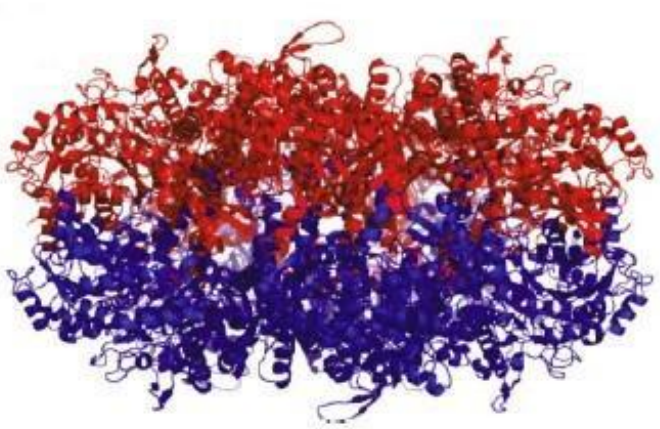

Figure 1.14: Structure of *E. coli* biodegredative ADC homo-decamer (Andrell *et al.*, 2009). (A) Bottom view; (B) Side view.

1.4.3 Biosynthetic ADC from *E. coli*

More than twenty years later after the first observation of biodegradative ADC, scientists pointed out that apart from the decarboxylation of ornithine by ODC, there was actually an alternate pathway for the biosynthesis of putrescine in *E. coli* involving a distinct form of ADC which functions optimally at around pH 8 and requires not only PLP but also magnesium ions as cofactors (Morris and Pardee, 1966). This enzyme, being constitutively expressed, is named as constitutive or biosynthetic ADC.

In 1973, biosynthetic ADC was successfully purified from *E. coli* and was further characterized (Wu and Morris, 1973a). The purified biosynthetic ADC is a tetramer of around 296 kDa (Wu and Morris, 1973a). This enzyme functions optimally at pH 8.4, and its K_m value for L-arginine is 0.03 mM (Wu and Morris, 1973a). Later studies have shown that encoded by gene *speA*, biosynthetic ADC from *E.coli* is a 280 kDa-homo-tetramer (Moore and Boyle, 1990), as depicted in Figure 1.15. The mininal functional unit of biosynthetic ADC is a homo-dimer which contains two active sites that lie at the interface between the two interacting monomers (Forouhar *et al.*, 2010). Each monomer consists of 658 amino acid residues. As shown in Figure 1.16, *E. coli* biosynthetic ADC shares little sequence homology with the biodegradative ADC, and this may account for their different reaction properties. In addition, unlike its biodegradative counterpart which is located in cytoplasm, biosynthetic ADC exists in the periplasmic space

(Buch and Boyle, 1985). It had been reported that many bacterial secreted proteins contain certain hydrophobic signal sequences at their N-termini which help to transport the proteins through the cell membrane (Inouye and Halegoua, 1980). Because of the existence of such a signal peptide sequence, the monomer of biosynthetic ADC is first synthesized as a precursor polypeptide of 74 kDa, then transported into the inner periplasmic space of *E. coli*, where the signal sequence is removed so that the matured enzyme of ADC with a size of 70 kDa can be settled there (Buch and Boyle, 1985). This mechanism is evolved probably to result in a readily conversion of the exogenous arginine to putrescine while having minimum disturbance to the intracellular environment (Buch and Boyle, 1985).

A

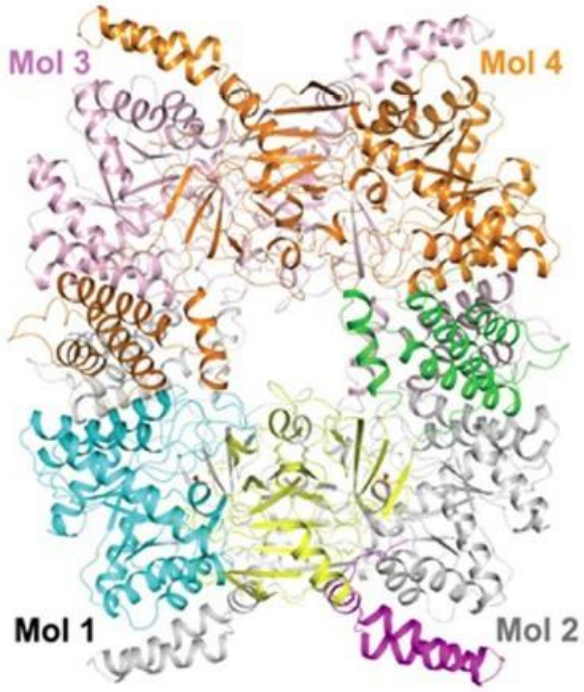

B

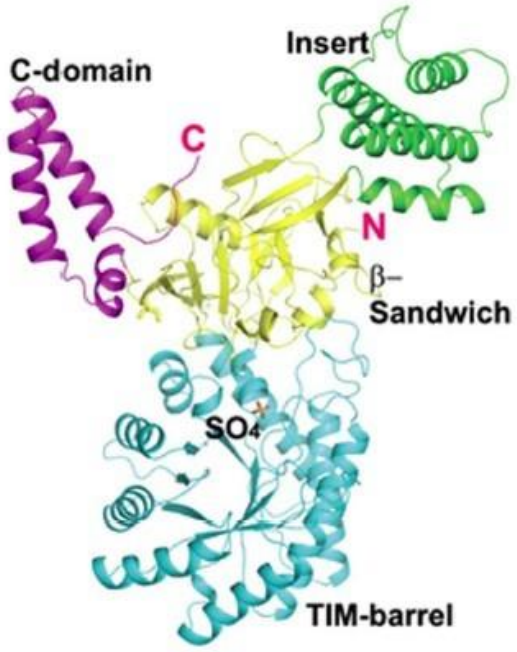

Figure 1.15: Structure of *E. coli* biosynthetic ADC (Forouhar *et al.*, 2010). (A) Tetramer, and (B) monomer of *E. coli* biosynthetic ADC. A sulfate ion is located at the phosphate binding site of PLP.

Figure 1.16: Protein sequence alignment of biodegradative and biosynthetic ADCs from *E. coli* by CLUSTALW. Protein sequences are corresponding to the crystal structures shown in Figures 1.14 and 1.15. Alignment score: 9.15916.

1.4.4 Previous studies on the anti-cancer effects of ADC

As an arginine-depleting enzyme, ADC is expected to have inhibitory effects on tumor growth. Around 7-20 μg/ml *E. coli* biosynthetic ADC has demonstrated obvious inhibitory effect on the growth of HeLa cells cultured *in vitro* starting from the second day of the treatment (Philip *et al.*, 2003). When the dose of ADC is increased to around 330-1000 μg/ml and the treatment period is extended to four days, the growth inhibitory effect of ADC is almost the same as that of using AFM (Philip *et al.*, 2003).

Apart from its arginine-depleting function, ADC may also inhibit tumor growth through it catalytic product, agmatine. This idea is supported by multiple studies which have demonstrated the *in vitro* inhibitory effect of agmatine on cell growth (Molderings *et al.*, 2004; Philip *et al.*, 2003; Wang *et al.*, 2005; Wolf *et al.*, 2007). In addition to agmatine, the catabolic reaction of arginine by ADC also produces CO_2, hence may have milder side effects than those catalyzed by ADI (generates ammonia) and arginase (generates urea). More improtantly, while ADI has little inhibitory effect in ASS-positive cell lines and arginase is thought to have little inhibitory effect in OTC-positive cell lines, ADC, whose catalytic products are not intermediates in the urea cycle, may be advantageous over the other two arginine-depleting enzymes as it may, theoretically, inhibit the growth of cancer cells regardless of their urea cycle enzyme expression profiles.

1.5 Extending the circulating half-lives of drug materials

1.5.1 Pegylation

As introduced in the previous sections, pegylation is the main established method for extending the circulating half-life of anti-cancer enzymes such as aparaginase and rhArg. PEG is a hydrophilic, synthetic polymer, and the process during which one or several PEG molecules are conjugated covalently to the surface of the target material is termed pegylation (Pasut *et al.*, 2008). The size of PEG used in pharmaceutical practice ranges from 400 Da to 50 kDa (Knop *et al.*, 2010). The non-toxic and weakly immunogenic nature of PEG has made it the most widely used type of polymer conjugate for therapeutic proteins (Pasut *et al.*, 2008; Roberts *et al.*, 2002). The effect of pegylation includes the reduction of renal clearance of relatively small molecules through increasing their sizes, the elimination of immunogenicity of heterogeneous proteins through shielding their antigenic epitopes, the prevention of protein degradation by proteolytic enzymes probably through shielding the enzyme-recognition sites on proteins (Roberts *et al.*, 2002), and the improvement of protein solubility due to the hydrophilic property of PEG molecules (Pasut *et al.*, 2008).

The first reported case of pegylation took place in 1977 when PEG was conjugated to bovine serum albumin (BSA) (Abuchowski *et al.*, 1977). Since then, pegylation has been studied as a method for altering the

pharmacological and biological properties of proteins. Pegylated therapies that are currently used in clinical practice include: Adagen (Enzon), the pegylated form of bovine adenosine deiminase (ADA), as an orphan drug for the treatment of ADA deficiency; PEGASYS (Roche), the pegylated interferon α-2a, as a treatment of hepatitis C; and Oncaspar (Enzon), the pegylated L-asparaginase for the treatment of ALL (Knop *et al.*, 2010; Pasut and Veronese, 2009).

In addition to its potential immunogenicity over long-term application, pegylation also has some other defects. The pharmaceutical grade of PEG reagent can be of high price, whereas high PEG-to-drug ratio is often used during pegylation. The standard protocols for the preparation of both PEG-ADI and PEG-rhArg recommend a molar ratio of PEG to enzyme of 40:1 or 50:1 (Cheng *et al.* 2007; Holtsberg *et al.*, 2002; Stone *et al.*, 2012). Therefore, pegylation of drug material may not be a quite cost-effective process. Some downstream procedures, such as the removal of free PEG molecules from the pegylated enzyme, is also required after the process of pegylation.

Another main defect of pegylation for the modification of protein drugs lies in the fact that it may easily affect the protein binding or catalytic activity (Bailon *et al.*, 2001; Kubetzko *et al.*, 2005). It has been reported that PEG-ADI retains only half of the specific activity of native ADI (Ni *et al.*, 2008). Although careful design of the conjugation site may help to minimize the loss of enzyme activity, changes are unavoidable in most cases. In fact, it has been reported by our group members that the activity of ADC has

greatly decreased after pegylation (Section 6.4.1). Therefore, alternative methods should be explored.

1.5.2 Fusion proteins

1.5.2.1 Human serum albumin (HSA) fusion proteins

Apart from serving as potential anti-cancer drug materials, proteins can also play the role of macromolecular conjugates for the modification of anti-cancer chemotherapeutic drugs. Plasma proteins, especially serum albumin, are preferably picked up and accumulate in tumor cells due to the impaired lymphatic drainage of these cells (Brown and Giaccia, 1998; Wunder *et al.*, 1997). After entering tumor cells, plasma proteins are broken down by lysosomal enzymes to provide amino acids for the *de novo* synthesis of tumor proteins (Stehle *et al.*, 1997). Therefore, albumin is a good candidate for tumor targeting agents. For example, doxorubicin carried by the human serum albumin (HSA) nanoparticles has demonstrated effective localization in tumors as well as obvious cytotoxic effect in tumor cells (Bae *et al.*, 2012).

For protein or peptide drugs, genetic fusion is a common method for the generation of HSA-drug conjugates. Serum albumin is abundant in human plasma, with an average concentration of 40 mg/ml (>600 μM) (Sand *et al.*, 2015). As a relatively large monomeric protein of ~67 kDa, HSA may help to prevent its drug conjugates from being excreted through renal filtration by increasing the size of the drug. The long biological half-life of HSA (around 20 days in humans; Peters, 1985) is also a favored property for conjugating materials (Muller *et al.*, 2007). Furthermore, as HSA is of human-origin, it is also believed that through the fusion with HSA, the

immunogenicity of the drug may be alleviated. Albutropin, an HSA-growth hormone fusion protein, has been used for the treatment of growth hormone deficiency (Osborn *et al.*, 2002). Compared to the unmodified growth hormone, the fusion protein has a four-fold longer half-life in rats and a six-fold longer half-life in monkeys (Osborn *et al.*, 2002). Albinterferon α-2b, a fusion of interferon α-2b with HSA, is reported to have an extended circulating half-life of 6-7 days, and has entered phase III trials for the treatment of chronic hepatitis C (Balan, 2006; Subramanian *et al.*, 2007).

HSA-fusion is a key breakthrough for improving the pharmacokinetic properties of drugs. It accomplishes the modification once and for all on a genetic basis, and is a much more economical alternative to chemical methods such as pegylation.

1.5.2.2 The application of albumin binding domain (ABD)

The genetic fusion of a protein to an albumin binding domain (ABD) from streptococcal protein G has been used since the early 1990s (Makrides *et al.*, 1996; Nygren *et al.*, 1991). ABD is a relatively small domain at the N-terminus of streptococcal protein G which has affinity for serum albumin (Akerstrom *et al.*, 1987). *In vivo* studies have shown that the ABD fusion protein is able to bind to serum albumin effectively, and hence stabilizes the protein of interest (Nygren *et al.*, 1991). The circulation half-life of the protein has also been extended (Makrides *et al.*, 1996).

1.6 Objectives of the project

In order to gain a better understanding of ADC, the expression, purification and anti-cancer properties of this enzyme originates from *E. coli* were explored in this project.

The first part of this project mainly consists of the expression and purification of a recombinant *E. coli* biosynthetic ADC tagged with six histidine residues (hereafter referred to as ADC unless specified). Through the determination of the optimal reaction conditions for ADC, an improved method for assaying the specific activity of ADC has also been established.

The project then focuses on the anti-cancer properties of ADC *in vitro*. The effect of ADC on cell viability has been examined in a variety of cell lines of different cancer types. The ability of ADC on the induction of apoptosis, autophagy, and cell cycle arrest was then investigated. In addition, we have tested some combinations of ADC with other anti-cancer small molecules such as doxorubicin and HCQ in cancer cells. Some comparative studies using ADI and BCA has also been conducted.

The project then proceeds to a preliminary *in vivo* study to test the feasibility of ABD fusion for the improvement of circulating half-life of enzyme drugs. Both ADC-ABD and BCA-ABD have been prepared and studied.

By revealing the enzymatic properties, the anti-cancer potential, as well as some defects of ADC, this study may provide more information for the future development of ADC as an anti-cancer drug.

Chapter 2

Materials and methods

2.1 Materials

2.1.1 Protein constructs

2.1.1.1 Protein construct of ADC

The pET expression system was used for the expression of ADC. The gene encoding ADC was slightly modified and inserted into a pET-3a vector (Figure 2.1). Expression of ADC was under the control of a T7 promoter and required the induction of isopropyl β-D-1-thiogalactopyranoside (IPTG). The recombinant vector was then cloned into *E. coli* strain BL21 (DE3). This whole process was done by Ms. Sandra Y. S. Siu who was a former member of our research group.

The ADC used in this project was a slightly modified version based on the native *E. coli* biosynthetic ADC. The modifications of the ADC's DNA sequence are shown in Figure 2.2 and described as follows:

First, the 32 amino acid residues at the N-terminus of native ADC representing the signal peptide sequence had been removed to make ADC remain in the cytoplasm of *E. coli*, which was easier for purification. Because a start codon "ATG" is included in the *NdeI* restriction site

"CATATG" (Figure 2.1), a methionine residue was artificially added to the N terminus of the protein.

Second, a point mutation was made to change the 1299th neucleotide of native ADC from thymine to cytosine. This is a silent mutation therefore has no effect on the amino acid sequence produced. This mutation is necessary to remove the undesired *BamHI* restriction site within the middle of the native ADC DNA sequence, as *BamHI* restriction site is involved in the cloning process of ADC into the pET-3a plasmid.

Finally, a DNA sequence encoding the 6x histidine tag was added to the C-terminus of ADC so that the enzyme can be easily purified by nickel affinity chromatography. According to Ms. Sandra Y. S. Siu, this modification is preferably performed at the C-terminus of ADC, since an N-terminal 6x histidine tag results in much less protein yield and significantly lower enzyme activity (Appendix Figure 1).

An alignment of the protein sequences of native *E. coli* biosynthetic ADC and the ADC used in this project is shown in Figure 2.3.

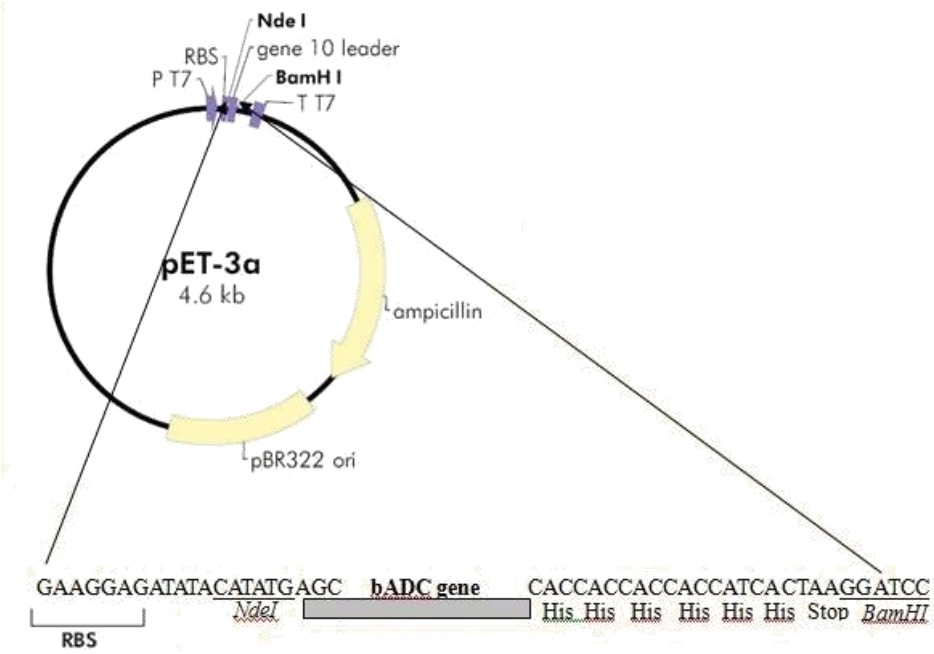

Figure 2.1: Plasmid map of ADC used in this project. This map is provided by Ms. Sandra Y. S. Siu. RBS, ribosome binding site.

Figure 2.2: DNA sequence of ADC used in this project showing the modifications made. Information was provided by Ms. Sandra Y. S. Siu.

Figure 2.3: Alignment of the protein sequences of native *E. coli* biosynthetic ADC (accession number: P21170) and modified recombinant ADC used in this project. Multiple sequence alignment was performed by CLUSTALW. Score of alignment: 98.8942.

2.1.1.2 Protein construct of ADC-ABD

The construct of ADC-ABD was designed by Dr. H. K. Yap in our research group, who also kindly provided *E. coli* cells that expressed ADC-ABD produced from fed-batch fermentation for this project. pRSET expression system was used for the production of ADC-ABD (Figure 2.4). This expression system does not require lactose or IPTG induction, and hence the cell culturing process is easier than that of ADC.

A high affinity version of ABD designed by Jonsson *et al.* (2008) was used in this project. This fragment contains a linker sequence (AVDANS) as well as ABD, and was fused directly to the C-terminus of ADC. When the protein is expressed, a 6x histidine tag provided by the pRSET plasmid is added to the C-terminus of the fusion protein. The alignment of the protein sequences of ADC and ADC-ABD used in this project is shown in Figure 2.5.

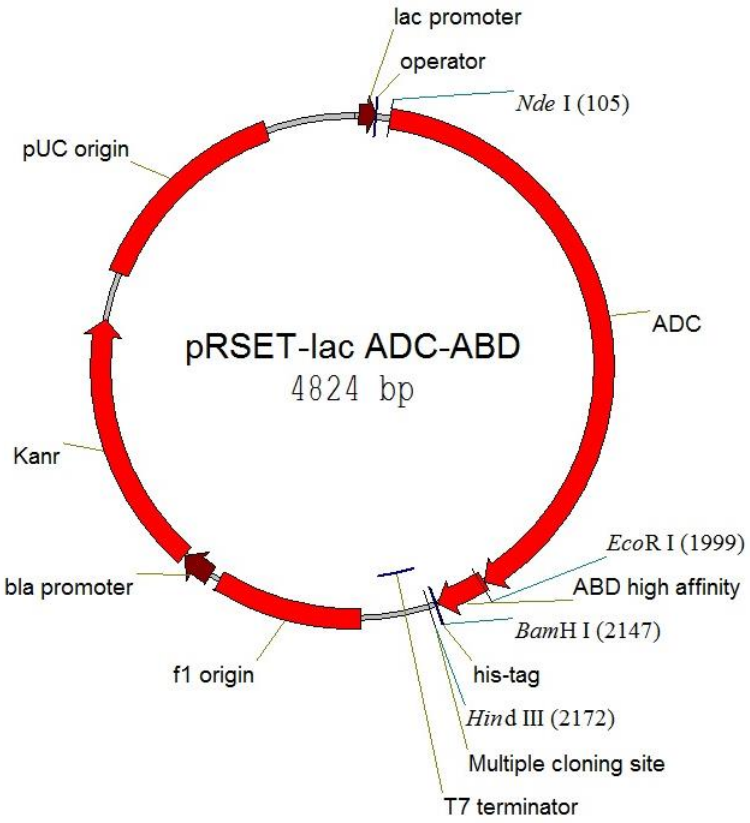

Figure 2.4: Plasmid map of ADC-ABD. This map is provided by Dr. H. K. Yap.

Figure 2.5: Protein sequence alignment of ADC and ADC-ABD used in this project by CLUSTALW. Score of alignment: 99.5261.

2.1.1.3 Protein constructs of BHA and BAH

The protein sequence of BCA used in this project is the same as that used by Bewley *et al.* (1999) (PDB ID: 2CEV) except that it contains a 6x histidine tag at the C terminus.

The constructs of both BCA-6xHis-ABD (BHA) and BCA-ABD-6xHis (BAH) were designed by Mr. Steve H. C. Chong in our research group, who also kindly provided *E. coli* cell stocks that expressed BHA and BAH.

In both BHA and BAH, the BCA portion is a mutated version of BCA with its valine residue at position 20 mutated to proline (V20P), while the ABD portion is the wild-type version of ABD with a linker sequence (AQHDEAVDANS) (Jonsson *et al.*, 2008). The ABD portion is either located at the very C terminus of the fusion protein (in the case of BHA) or fused in between BCA and 6x histidine tag (in the case of BAH). The alignment of the protein sequences of BCA, BHA, and BAH used in this project is shown in Figure 2.6.

```
BCA             MKPISIIGVPMDLGQTRRGVDMGPSAMRYAGVIERLERLHYDIEDLGDIPIGKAERLHEQ
BHA             MKPISIIGVPMDLGQTRRGPDMGPSAMRYAGVIERLERLHYDIEDLGDIPIGKAERLHEQ
BAH             MKPISIIGVPMDLGQTRRGPDMGPSAMRYAGVIERLERLHYDIEDLGDIPIGKAERLHEQ
                ******************** ****************************************

BCA             GDSRLRNLKAVAEANEKLAAAVDQVVQRGRFPLVLGGDHSIAIGTLAGVAKHYERLGVIW
BHA             GDSRLRNLKAVAEANEKLAAAVDQVVQRGRFPLVLGGDHSIAIGTLAGVAKHYERLGVIW
BAH             GDSRLRNLKAVAEANEKLAAAVDQVVQRGRFPLVLGGDHSIAIGTLAGVAKHYERLGVIW
                ************************************************************

BCA             YDAHGDVNTAETSPSGNIHGMPLAASLGFGHPALTQIGGYCPKIKPEHVVLIGVRSLDEG
BHA             YDAHGDVNTAETSPSGNIHGMPLAASLGFGHPALTQIGGYCPKIKPEHVVLIGVRSLDEG
BAH             YDAHGDVNTAETSPSGNIHGMPLAASLGFGHPALTQIGGYCPKIKPEHVVLIGVRSLDEG
                ************************************************************

BCA             EKKFIREKGIKIYTMHEVDRLGMTRVMEETIAYLKERTDGVHLSLDLDGLDPSDAPGVGT
BHA             EKKFIREKGIKIYTMHEVDRLGMTRVMEETIAYLKERTDGVHLSLDLDGLDPSDAPGVGT
BAH             EKKFIREKGIKIYTMHEVDRLGMTRVMEETIAYLKERTDGVHLSLDLDGLDPSDAPGVGT
                ************************************************************

BCA             PVIGGLTYRESHLAMEMLAEAQIITSAEFVEVNPILDERNKTASVAVALMGSLFGEKLMH
BHA             PVIGGLTYRESHLAMEMLAEAQIITSAEFVEVNPILDERNKTASVAVALMGSLFGEKLMH
BAH             PVIGGLTYRESHLAMEMLAEAQIITSAEFVEVNPILDERNKTASVAVALMGSLFGEKLMA
                ************************************************************

BCA             HHHHH-------------------------------------------------------
BHA             HHHHHAQHDEAVDANSLAEAKVLANRELDKYGVSDYYKNLINNAKTVEGVKALIDEILAA
BAH             QHDEAVDAN------SLAEAKVLANRELDKYGVSDYYKNLINNAKTVEGVKALIDEILAA
                :*..

BCA             --------
BHA             LP------
BAH             LPHHHHHH
```

Figure 2.6: Protein sequence alignment of BCA, BHA and BAH used in this project by CLUSTALW. Scores of alignment: BCA versus BHA: 99.6721; BCA versus BAH: 98.0328; BHA versus BAH: 97.5138.

2.1.2 Chemicals and reagents

Nickel (II) sulfate hexahydrate, magnesium chloride anhydrous, agmatine sulfate, L-arginine, L-citrulline, L-ornithine, urea, urease, thiosemicarbazide, sodium hydroxide, HEPES, trichloroacetic acid (TCA), hydrochloric acid, sulfuric acid, phosphoric acid, isopropanol, 2-mercaptoethanol, Triton X-114, amino acid standards, human serum albumin (HSA), dimethyl sulfoxide (DMSO), doxorubicin hydrochloride, verapamil hydrochloride, rapamycin, and hydroxychloroquine (HCQ) sulfate were purchased from Sigma-Aldrich.

LB broth, yeast extract powder, ampicillin, kanamycin, IPTG, imidazole, sodium phosphate (monobasic), sodium phosphate (dibasic), sodium chloride, sodium dodecyl sulfate (SDS), and Tween 20 were purchased from Affymetrix.

Manganese (II) chloride tetrahydrate, iron (III) chloride hexahydrate, bromophenol blue, diacetyl monoxime, and acetic acid were purchased from BDH (VWR).

Ammonium persulfate (APS), 30% acrylamide/bis-acrylamide solution, and TEMED were purchased from Bio-Rad.

Glycerol, glycine, and Tris base were purchased from Amresco.

Methanol and ethanol were purchased from DUKSAN.

Coomassie Brilliant Blue R-250 was purchased from Unichem.

Glutamate dehydrogenase, α-ketoglutaric acid, and NADPH were purchased from Roche.

LY294002 was purchased from Calbiochem.

Arginine-free medium (AFM) was purchased from United States Biological.

Antibodies to GAPDH, LC3, PARP, phospho-Akt, Akt, phospho-ERK1/2, ERK1/2, phospho-mTOR, mTOR, phosphor-p70S6K, p70S6K, and rabbit IgG (HRP-linked) were purchased from Cell Signaling Technology.

Ultra Ninhydrin Reagent Kit, Lithium loading buffer, Lithium buffer 1-5, and Lithium regeneration buffer for amino acid analysis were purchased from Biochrom.

ADI used in this project was kindly provided by Mr. Godfrey Y. M. Lam in our group. BCA used in this project was kindly prepared by Ms. Shirley S. L. Chu in Dr. Thomas W. H. Lo's research group.

2.1.3 Cell lines

Human colorectal carcinoma cell lines HCT116 and LoVo, human colorectal adenocarcinoma cell lines COLO205 were obtained from the U.S. National Cancer Institute (NCI).

Human pancreatic adenocarcinoma cell line BxPC-3 (ATCC number: CRL-1687), human pancreatic carcinoma cell line PANC-1 (ATCC number: CRL-1469), and human foreskin fibroblast cell line HFF-1 (ATCC number: SCRC-1041) were obtained from the American Type Culture Collection (ATCC).

Human colorectal adenocarcinoma cell line SW1116, human cervix adenocarcinoma cell line HeLa, human malignant melanoma cell line A375, human hepatocellular carcinoma cell line HepG2, and human lung carcinoma cell line A549 were provided by Bio-Cancer Treatment International Limited.

Tumor cells were maintained in complete medium unless specified. The complete medium was either DMEM (for A375, A549, HeLa, HepG2, and PANC-1; Life Technologies) or RPMI 1640 (for BxPC-3, COLO 205, HCT116, LoVo, and SW1116; Life Technologies) supplemented with 10% (v/v) fetal bovine serum (FBS; Hyclone) and 100 units/ml penicillin/streptomycin (Life Technologies).

2.2 Protein expression

E. coli cell stocks that expressed ADC, BHA and BAH were provided by Mr. Steve H. C. Chong. To prepare the seed culture, a small amount of *E. coli* BL21 (DE3) glycerol stock was inoculated into 10 ml LB medium supplemented with 100 μg/ml ampicillin in a universal bottle. The seed culture was grown at 37 ℃ with shaking at 700 rpm for overnight (~16 h). 2.5 ml overnight seed culture was then used to inoculate 250 ml of LB medium with 100 μg/ml ampicillin in every 2 L flask. Inoculated cells were grown at 37 ℃ with shaking at 280 rpm for 2-4 h to an OD_{600} of 0.6-0.8. 0.2 mM IPTG was then added to the culture medium to induce the overexpression of target protein. Cells were grown for a further 4 h and harvested at 4500 rpm. Cell pellets were used immediately or stored at -20 ℃.

E. coli cell stock that expressed agmatinase were provided by Dr. H. K. Yap. The expression of agmatinse started with the inoculation of a small amount of *E. coli* glycerol stock into 250 ml 2x TY medium supplemented with 50 μg/ml kanamycin, 50 μM $MnCl_2$ and 0.06% lactose (a sterile solution of 20% (w/v) lactose monohydrate was prepared beforehand) in every 2 L flask. The culture was grown at 28 ℃ with shaking at 280 rpm for ~21-24 h and was harvested at 4500 rpm. Cell pellets were used immediately or stored at -20 ℃.

E. coli cells that expressed ADC-ABD were produced from 500 ml fermentation culture and were provided in the form of a cell pellet by Dr. H. K. Yap.

2.3 Protein purification by nickel affinity chromatography

E. coli cell pellets were resuspended in buffer containing 50 mM Tris-HCl, 100 mM NaCl (pH 7.4; for the purification of ADC and ADC-ABD, 5 μM $MgCl_2$ was supplemented in buffer; for the purification of agmatinase, 5 μM $MnCl_2$ was supplemented in buffer) and were broken by sonication. Cell debris was then removed by centrifuging at 10,000 rpm for 40 min. Supernatant was applied to a 5 ml HiTrap™ chelating column (GE Healthcare) that had been charged with Ni^{2+} and equilibrated with buffer A (20 mM sodium phosphate, 0.5 M NaCl, pH 7.4) using an ÄKTA purifier. Proteins were eluted using a gradient of 0-0.5 M imidazole which was achieved by the combination of buffer A with buffer B (0.5 M imidazole in buffer A) at various ratios. Fractions were analyzed by sodium dodecyl sulfate polyacrylamide gel electrophoresis (SDS-PAGE) using 12% polyacrylamide gels, and those containing the target protein were pooled. Pooled fractions were concentrated and the buffer of the concentrated pooled fractions was exchanged with 20 mM sodium phosphate (pH 7.4) using centrifugal filter device (Amicon) or tangential flow filtration device (Millipore). The membrane cut-off was 50,000 MW for ADC and ADC-ABD and 30,000 MW for BHA, BAH and agmatinase. The retentate was then diluted to a desired concentration and underwent sterile filtration through a 0.2 μm syringe filter and stored at 4 ℃. Cofactors (5 mM $MgCl_2$, 0.1 mM PLP) were supplemented in ADC and ADC-ABD products, and light should be prevented for the storage of these products.

2.4 Protein gel electrophoresis

Protein samples were analyzed by gel electrophoresis to examine their molecular weight and purity or as a step prior to the immunoblot assay.

Samples were mixed with the same amount of 2x loading buffer (20 mM Tris, 100 mM 2-mercaptoethanol, 2% SDS, 20% glycerol and 0.016% bromophenol blue for SDS-PAGE; same ingredients but without 2-mercaptoethanol for native-PAGE). SDS-PAGE samples were then boiled in water for 5 min before being loaded onto the gel. The gel was a composition of 4% stacking gel layered on top of 8-12% separating gel. For SDS-PAGE, molecular weight standards (low range) or Precision Plus Protein Dual Color Standards (Bio-Rad) were used as markers to determine the MW of proteins. Electrophoresis was carried out in a Mini-PROTEAN III dual slab cell (Bio-Rad) filled with 1x running buffer (25 mM Tris, 192 mM glycine and 1% SDS for SDS-PAGE; same ingredients but without SDS for native-PAGE) at 80 V for ~20 min then at 130-180 V for ~50 min-1 h. After electrophoresis, the gel was stained with staining solution (25% methanol, 10% acetic acid, 0.06% Coomassie Brilliant Blue R-250) for ~5 min with agitation. The gel was then destained with destaining solution (10% acetic acid and 10% methanol) with agitation until the background became clear. For storage purpose, the gel was then washed with deionized water (DI water) and air-dried with gel drying films (Promega).

2.5 Determination of protein concentration

In general, protein concentrations were determined by the Bradford's method. Samples were diluted to the desirable concentrations, topped up to 800 µl with MilliQ water, mixed with 200 µl Protein Assay Dye Reagent Concentrate (Bio-Rad), incubated in dark for 10 min, and measured the absorbance at 595 nm. Bovine serum albumin (BSA; Sigma) was used to construct a standard curve for the calculation of protein concentration.

Protein concentration of tumor cell lysates was determined by the Pierce BCA Protein Assay Kit (Thermo Scientific) according to the producer's instruction. BSA was used for the construction of a standard curve.

2.6 Determination of enzyme activity

2.6.1 Diacetyl monoxime (DAMO) method

Enzyme activity was measured by the diacetyl monoxime (DAMO) method which quantifies the produced urea in the reaction mixture (Kanagasabapathy and Kumari, 2000).

Specific activity of ADC and ADC-ABD was determined by coupling the reaction catalyzed by ADC or ADC-ABD to that by agmatinase so that the formation of agmatine could be monitored by the amount of urea, and hence could be tested by the DAMO method. The following standard assay conditions were used unless specified: first, 7.5-30 μl ADC or ADC-ABD sample was diluted to 350 μl with 100 mM HEPES buffer (pH 8.0) containing 50 mM $MgCl_2$ and 0.5 mM PLP, the diluted enzyme was mixed with 150 μl 700 mM L-arginine (pH 8.0) and incubated at 37 ℃ for 5 min, the reaction was stopped by boiling for 10 min; then 50 μl supernatant of the first-step reaction mixture was added to a 350 μl mixture of 0.03 mg *E. coli* agmatinase and 100 mM Glycine-NaOH (pH 9.0), allowed to react for 15 min and stopped by 100 μl 500g/L TCA; the reaction mixture was 2-fold diluted prior to the DAMO assay. One unit of enzyme activity is defined as the amount of ADC/ADC-ABD that catalyzes the production of 1 μmol urea per min under standard assay conditions. Specific activity of the enzyme is expressed as activity units (U) per mg of protein.

For the activity assay of agmatinase, the following standard conditions were used unless specified: first, a 350 μl mixture of 2.5-20 μl agmatinase sample and 100 mM Glycine-NaOH buffer (pH 9.0) was reacted with 50 μl 2 M agmatine sulfate at 45 ℃ for 5 min, the reaction was stopped by 100 μl 500g/L TCA; the reaction mixture was then 10-fold diluted prior to the DAMO assay. One unit of enzyme activity is defined as the amount of agmatinase that catalyzes the production of 1 μmol urea per min under standard assay conditions. Specific activity of the enzyme is expressed as U per mg of protein.

For the activity assay of BHA and BAH, the following standard conditions were used unless specified: first, a 450 μl mixture of 300 μl diluted protein sample (dilution fold: 100, 200, 400 and 800) and 20 mM sodium phosphate buffer (pH 7.4) was reacted with 150 μl 700 mM L-arginine (pH 7.4) at 37 ℃ for 5 min, the reaction was stopped by 250 μl 500g/L TCA; the reaction mixture was then 20-fold diluted prior to the DAMO assay. One unit of enzyme activity is defined as the amount of BCA/BHA/BAH that catalyzes the production of 1 μmol urea per min under standard assay conditions. Specific activity of the enzyme is expressed as U per mg of protein.

2.6.2 Ikemoto method

Two methods were used for determining the activity of BCA and its derivatives in this project: for *in vitro* experiments, activities of the enzymes were determined by the DAMO method as introduced in Section 2.6.1; for *in vivo* experiments, activities of the enzymes were determined by a spectrophotometric method as described by Ikemoto *et al.* (1989) with slight modifications. Basically, 1 μl enzyme sample was added to 500 μl mixture (pH 8.3) of 0.1 M Tris, 50 mM L-arginine, 10 mM α-ketoglutaric acid, 35 U/ml urease, 1 U/ml glutamate dehydrogenase, and 0.3 mM NADPH. The reaction mixture was well mixed by vortex and incubated at 30 ℃ in a spectrophotometer. Absorbance at 340 nm was read, and the reaction kinetics was analyzed by Swift II (GE Healthcare). One unit of enzyme activity is defined as the amount of BCA/BHA/BAH that catalyzes the production of 1 μmol urea per min under standard assay conditions. Specific activity of the enzyme is expressed as U per mg of protein.

2.7 Removal of endotoxin in proteins

The endotoxin content of the proteins was removed by phase separation with Triton X-114 as described by Aida and Pabst (1990). Triton X-114 was added to the protein solution (v/v = 1:100). The solution was mixed by vortex for 1 min at room temperature, then placed on ice for 5 min. After a brief vortex, the solution was incubated in a 37 ℃ water bath for 5 min, and centrifuged at 16,200 rcf for 7 s or longer at room temperature. The upper layer was collected. For each protein sample, these phase extraction processes were repeated for three times to minimize the endotoxin content.

The endotoxin content in protein samples was determined by limulus amebocyte lysate (LAL) test. 100 μl pyrogen-free water was added to a Pyrotell gel-clot formulation vial (containing 0.25 EU/ml endotoxin; Associates of Cape Cod, Inc.) to dissolve the contents in the vial. 100 μl sample was then added to the vial, and the contents in the vial were mixed by vortex. After mixing, the vial was incubated at 37 ℃ for exactly 60 min. Endotoxin level would be lower than the kit sensitivity if the contents remain in solution form, or higher than the kit sensitivity if the contents clot. Control standard endotoxin (Associates of Cape Cod, Inc.) was used as a positive control. A sample with endotoxin content no greater than 200 EU/ml is considered proper for the administration in animals.

2.8 Cell culture

All tumor cell lines were cultured in 25 cm^2 or 75 cm^2 tissue culture flask (TPP) at 37 ℃ in an incubator containing a humidified atmosphere of 95% air and 5% CO_2. When reaching around 90% confluence, cells were diluted and passed to a new tissue culture flask to maintain the cell growth. To pass the cells, medium in the tissue culture flask was first removed. Cells remained adherent in the culture flask were then washed once with sterilized 1x phosphate buffered saline (PBS; pH 7.4), and treated with 1 ml (for cells in 25 cm^2 tissue culture flask) or 3 ml (for cells in 75 cm^2 tissue culture flask) of Trypsin-EDTA liquid (0.25% trypsin, 1 mM EDTA 4Na; Invitrogen) at 37 ℃ to allow for the detachment of cells from the culture flask. After 2-5 min of trypsin treatment, the same volume of medium was added to the tissue culture flask to inactivate trypsin. The mixture was then centrifuged at 1,200 rpm for 3 min at room temperature. After removing the supernatant, 1 ml complete medium was used to resuspend the cell pellet. Depending on the growth rate of each specific cell line, 50 μl to 250 μl of mixture was transferred to a new culture flask supplemented with fresh complete medium.

Cells number was counted through trypan blue staining. 10 μl of cell resuspension which had been diluted to a suitable concentration was mixed with 10 μl of Trypan Blue Solution (0.4%; Life Technologies). 10 μl of the stained mixture was then used to fill a hemocytometer for cell counting

under a microscope. Nonviable cells were stained and viable ones excluded the stain.

To prepare a cell stock, 2-5 x 10^6 cells were suspended in 1 ml mixture of 45% complete medium, 50% FBS and 5% DMSO within a 2.0 ml cryo tube (TPP), and stored in an isopropanol-bathed bucket at -80 ℃ for 24 h. Then frozen cell stocks were then transferred into a tank containing liquid nitrogen for long-term storage. To thaw cells, a vial of frozen cell stock was taken out of the liquid nitrogen tank and warmed in a 37 ℃ water bath with gentle shaking for less than 2 min. The cryoprotective medium was then removed by centrifugation and the cells were resuspended with pre-warmed complete medium at 37 ℃ for culture. Passages below 30 of each cell line were used in this study.

2.9 Cell viability assay

Cells were seeded in 96-well tissue culture plates at 3-6 x 10^3 cells (for 72 h drug treatment; the number was determined by cell types and growth rates) or 10^4 cells (for 24 h treatment) in a volume of 100 μl of complete medium per well, and incubated overnight to allow for cell adhesion to the plate. On the next day, the culture medium was replaced by either complete medium with varying concentrations of reagents or AFM. The plates were then incubated for an additional 24 or 72 h. Cell viability was analyzed by MTT (3-(4,5-dimethylthiazol-2-yl)-2,5-diphenyltetrazolium bromide) assay. MTT reagent was made by dissolving MTT (Invitrogen) in PBS and the working concentration was 5 μg/ml. 10 μl MTT reagent was added to each well and the culture plates were incubated for another 4 h. 100 μl of 0.01 N HCl in 10% SDS was then added to each well and the plates were cultured overnight. The absorbance of the each well at 570 nm was determined against the background of absorbance at 655 nm measured by a spectrophotometer. In living cells, the yellow-colored MTT can be reduced to purple formazan which dissolves in acidified SDS solution. The change of color indicates the redox potential of cells and can be quantified to reflect the cell viability. Non-linear regression with Prism 5.0 (Graphpad Software) was used to fit a sigmoidal curve, and the amount of a compound needed to achieve 50% inhibition of cell viability is defined as IC_{50}. The results of drug combination studies were analyzed by Calcusyn version 2.0 (Biosoft).

2.10 Apoptosis analysis by flow cytometry

2.10.1 Apoptosis analysis by annexin V binding assay

Evaluation of apoptosis was performed using the annexin V-FITC apoptosis detection kit (BD Pharmingen). 1-2 $\times 10^5$ cells per well were seeded in a 6-well plate, grown overnight, and treated with various concentrations of reagents. After 24, 48 or 72 h of incubation, both suspension and adherent cells were collected by treatment with 0.25% trypsin-EDTA for 2-3 min and centrifugation at 1,200 rpm for 3 min. Cell pellet was washed with 1x PBS (pH 7.4), resuspended in binding buffer containing annexin V-FITC and propidium iodide (PI) at room temperature for 15 min in darkness according to the manufacturer's instruction. Cells were then analyzed in a FACSAria flow cytometer (BD Biosciences) within 1 h after staining. Annexin V detects for the translocation of phosphatidylserine (PS) from the inner to the outer leaflet of the cell membrane which is a sign of early apoptosis. PI, as a membrane impermeable dye, detects for the membrane integrity of cells thus reflects the cell viability. 10,000 cells were acquired from each sample. The subsets of cells undergoing early apoptosis (annexin V-positive, PI-negative) and late apoptosis (annexin V-positive, PI-positive) were determined by FASCAria software (BD Biosciences).

2.10.2 Apoptosis analysis by active caspase-3 assay

Evaluation of apoptosis was also performed using the CaspGLOW fluorescein active caspase-3 staining kit (BioVision) according to the manufacturer's instruction. 1.5 x 10^5 of HCT116 cells per well were seeded in a 60-mm dish, grown overnight, and treated with various concentrations of ADC or BCA. After 72 h of incubation, both suspension and adherent cells were collected by treatment with 0.25% trypsin-EDTA for 2 min and centrifugation at 1,200 rpm for 3 min. Cell pellet was washed with 1x PBS (pH 7.4), resuspended in 300 µl pre-warmed complete medium containing 1 µl FITC-DEVD-FMK and incubated at growth condition for 30 min. After staining, cells were washed twice with wash buffer and analyzed using a FACSAria flow cytometer (BD Biosciences). DEVD-FMK is a cell-permeable caspase inhibitor that can bind irreversibly to active caspase-3 in apoptotic cells. 10,000 cells were acquired from each sample. The subsets of cells containing active caspase-3 were determined by FASCAria software (BD Biosciences).

2.10.3 Apoptosis analysis by mitochondrial outer membrane permeabilization (MOMP) assay using JC-1 dye

Evaluation of apoptosis was also achieved by analyzing the changes in MOMP using the JC-1 (Invitrogen) according to the manufacturer's instruction. 10^5 of HCT116 cells per well were seeded in a 6-well plate, grown overnight, and treated with various concentrations of ADC. After 72 h of incubation, both suspension and adherent cells were collected by treatment with 0.25% trypsin-EDTA for 2 min and centrifugation at 1,200 rpm for 3 min. Cell pellet was washed with 1x PBS (pH 7.4), resuspended in 500 µl pre-warmed complete medium containing 1 µl JC-1 and incubated at growth condition for 10 min. After staining, cells were washed twice with 1x PBS (pH 7.4) and analyzed using a FACSAria flow cytometer (BD Biosciences). JC-1 is a cationic dye which establishes membrane potential-dependent accumulation in mitochondria. It appears in aggregated form (red fluorescence) in mitochondria and as monomer (green fluorescence) in cytosol. A shift in JC-1 fluorescence emission from red to green indicates the increase of MOMP which is a sign for mitochondrial pathway of apoptosis. 10,000 cells were acquired from each sample. The subsets of cells showing green or red fluorescence were determined by FASCAria software (BD Biosciences).

2.11 Cell cycle analysis by flow cytometry

10^5 HCT116 or LoVo cells per well were seeded in a 6-well plate, grown overnight, and treated with various doses of ADC or BCA. After 72 h of incubation, both suspension and adherent cells were collected by treatment with 0.25% trypsin-EDTA for 2-3 min and centrifugation at 1,200 rpm for 3 min. Cell pellet was washed with 1x PBS (pH 7.4) and fixed with 75% ice-cold ethanol for at least 30 min. After removing ethanol, fixed cells were stained with PI/RNase staining buffer (BD Biosciences) at room temperature for 15 min in darkness. Stained cells were analyzed by flow cytometry (FACSAria, BD Biosciences). PI intercalates between the bases of DNA, and hence can be used for the evaluation of DNA content. For each data file, data from 10,000 cells were collected, and the percentages of cells in G_0/G_1, S and G_2/M phases were analyzed with ModFit LT 3.0 (Verity Software House).

2.12 Immunoblot assay

HCT116 cells were planted at 5 x 10^5 per well in a 6-well plate or at 10^6 per 60-mm culture dish, allowed to grow overnight, and treated with various doses of reagents. After a certain period of incubation (2-72 h), both suspension and adherent cells were collected by treatment with 0.25% trypsin-EDTA for 2 min and centrifugation at 1,200 rpm for 3 min. Cell pellet was washed with 1x PBS (pH 7.4) and lysed in RIPA lysis buffer (Millipore) containing both Protease Inhibitor Cocktail Set III (EDTA-free; Merck) and phosphatase Inhibitor Cocktail 3 (DMSO solution; Sigma). The lysate was mixed by vortex for a complete lysis and centrifuged at 13,200 rpm for 10 min at 4 ℃. Supernatant was subjected to SDS-PAGE analysis or stored at -80 ℃ if not used immediately.

After SDS-PAGE analysis, the gel was transferred to Immobilon-PSQ transfer membrane (PVDF, 0.2 μm; Millipore) in a tank filled with ice-cold 1x transfer buffer (25 mM Tris base, 0.2 M glycine, 20% methanol and 0.037% SDS) at 100 V for 90 min (or at 300 mA for 3 h when transferring large proteins such as phosphor-mTOR and mTOR) in a cold room. The transferred membrane was blocked with blocking buffer which was 1x TBST (0.02 M Tris base, 0.15 M NaCl, 0.05% Tween 20) containing 5% (w/v) Blotting Grade Blocker (nonfat dry milk; Bio-Rad). The blocking process lasted for 1 h at room temperature with gentle agitation. Then the membrane was washed for 3 x 5 min with 1x TBST at the same conditions. Blocked membranes were incubated with primary antibodies diluted at

1:1,000-1:5,000 in 1x TBST with 5% BSA (Roche) at 4℃ with agitation overnight. On the next day, membrane was first washed for 4 x 5 min with 1x TBST, then incubated with secondary antibodies diluted at 1:5,000-1:20,000 in blocking buffer for 1 h at room temperature with gentle agitation. After another 4 x 5 min washing with 1x TBST, the membrane was incubated with Immobilon Western Chemiluminescent HRP Substrate (Millipore) for ~3 min at room temperature in darkness. The image was then taken by ChemiDoc imaging system (Bio-Rad) and analyzed by Quantity One (Bio-Rad).

2.13 Animal studies

2.13.1 *In vivo* studies of ADC and ADC-ABD

Seven ICR mice were used for the *in vivo* study of ADC and ADC-ABD. All mice were males. Prior to the injection of protein, blood sample was taken from each mouse and used as control (0 h). 6 mice were treated with different doses (1.25 mg, 2.5 mg or 5 mg per mouse) of ADC or ADC-ABD via i.p. or i.v. injection, and another mouse was i.v. injected with 250 μl of 1x PBS (pH 7.4) as control. Blood samples were taken at 2, 6, 24, 48, and 72 h after injection. The serum of each blood sample was collected by centrifugation at 3,000 rpm for 10 min at room temperature. 20 μl of serum was mixed with 20 ul of 1x PBS. The diluted serum was then mixed with an equal volume (40 μl) of 10% SSA (5'-sulfosalicylic acid; Sigma) solution and was allowed to precipitate at 4 ℃ for 1 h or overnight. After centrifugation at full speed for 10 min at 4 ℃, 70 μl of the supernatant was mixed with an equal volume of lithium citrate loading buffer (Biochrom), filtered through 0.4 μm filter disk, and analyzed by amino acid analyzer (Biochrom) for arginine contents.

2.13.2 *In vivo* study of BHA

Six BALB/c mice of 8 weeks old were used for the *in vivo* study of BHA. 3 mice were males and 3 were females. Prior to the injection of BHA, blood sample was taken from each mouse and used as control (0 h). The mice were randomly divided into two groups for i.p. and i.v. injection, respectively. 250 U of BHA was injected to each mouse, and blood samples were taken at 2, 6, 24, 72, and 120 h after injection. The serum of each blood sample was collected by centrifugation at 3,000 rpm for 10 min at room temperature. 16 μl of serum was mixed with 24 ul of 1x PBS (pH 7.4). The diluted serum was then mixed with an equal volume (40 μl) of 10% SSA solution and was allowed to precipitate at 4 ℃ for 1 h or overnight. After centrifugation at full speed for 10 min at 4 ℃, 70 μl of the supernatant was mixed with an equal volume of lithium citrate loading buffer (Biochrom), filtered through 0.4 μm filter disk, and analyzed by amino acid analyzer (Biochrom) for arginine and ornithine contents.

2.14 Statistical analyses

For all statistical analyses, data were analyzed by either two tailed *t*-test or one-way analysis of variance (ANOVA) with post hoc Dunnett's multiple comparison test with $P < 0.05$ considered as significantly different.

Chapter 3

Results: preparation, expression and purification of ADC

3.1 Expression and purification of ADC

Figure 3.1 shows the chromatogram of ADC purification. Two peaks were observed during the elution process using increasing concentrations of imidazole. The first peak occurred at lower concentrations of imidazole, while the second one occurred when imidazole concentration reached ~0.1 M.

According to the SDS-PAGE analysis of the eluted fractions (Figure 3.2), eluted fractions 5 to 10 mainly contain a protein with a molecular weight between 66.2 and 97.4 kDa which is likely to be the ADC monomer (~71.5 kDa calculated based on the amino acid sequence). This result suggests that ADC has been successfully expressed and purified. The peak corresponding to these fractions is the second peak in the chromatogram, indicating the binding of ADC to the nickel column is tighter than that of the impurities to the column.

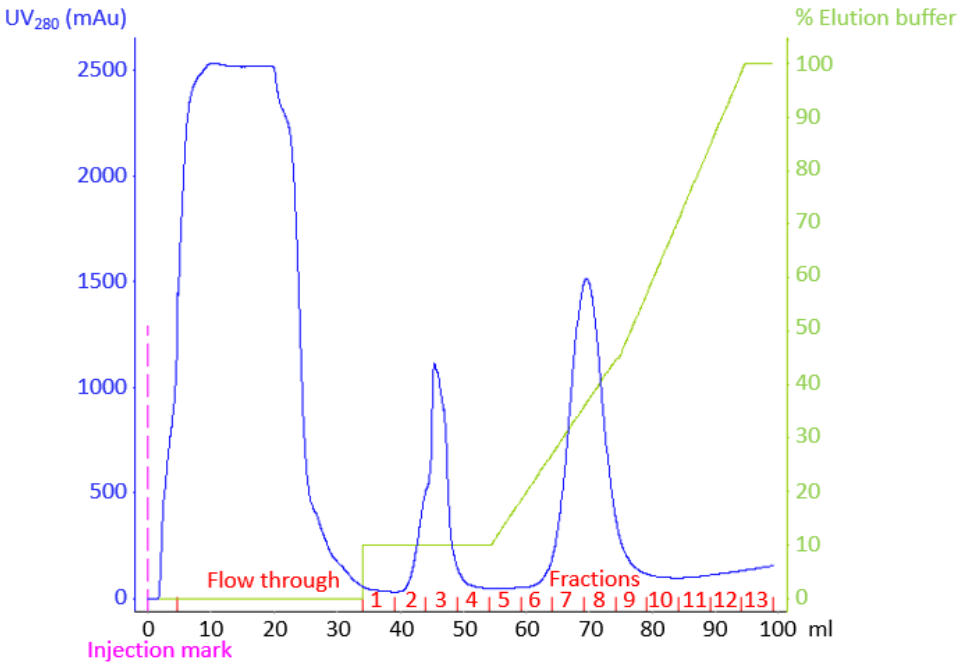

Figure 3.1: Elution profile of the purification of ADC from *E. coli* cells grown in 500 ml shake flask culture by a single step of nickel-charged 5 ml HiTrap™ chelating HP column chromatography. mAU, milli absorption unit; 100% B = 0.5 M imidazole.

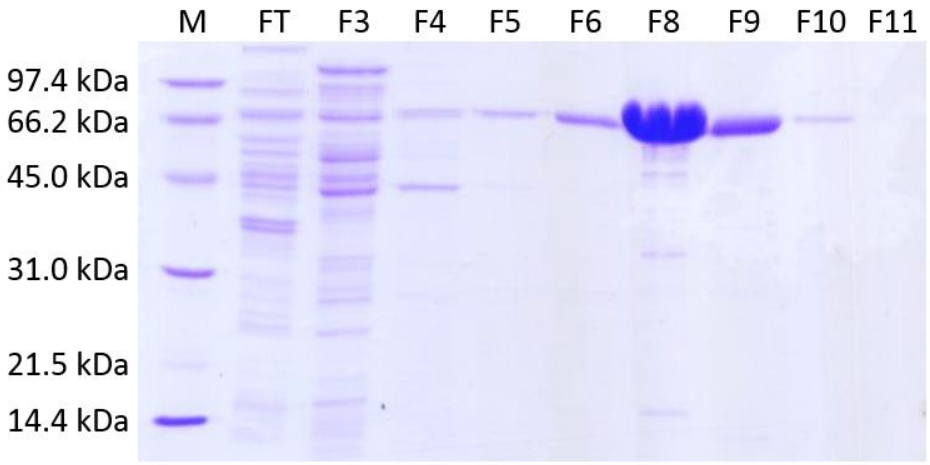

Figure 3.2: SDS-PAGE analysis of the column fractions from nickel affinity chromatography for ADC. M, SDS-PAGE molecular weight standards, low range (Bio-Rad); FT, flow through; F3-F11, eluted fractions from the column.

3.2 Specific activity of ADC

3.2.1 The reactions of ADC and agmatinase should be performed separately to achieve a more accurate measurement of the specific activity of ADC

Previously, researchers in our group measured the activity of ADC in a mixture containing ADC, agmatinase, and the substrate L-arginine. In their assay, arginine was converted to urea under the catalysis of ADC and agmatinase (Figure 3.3), and urea was subsequently quantified by the DAMO assay. The measured specific activity of ADC through this method, however, was very low. Considering ADC and agmatinase may have different optimal pH values, optimal temperatures and kinetics, a reaction condition favored by ADC may not allow the complete conversion of agmatine to putrescine and urea by agmatinase. Therefore in this project, we have proposed an improved method that the reactions of ADC and agmatinase be performed in succession to reflect the real activity of ADC in a more accurate way. The reaction conditions of the assay should also be optimized.

To prove the need for an improved activity assay method, a comparison on the specific activities of ADC between the old method (ADC and agmatinase in the same reaction mixture) and the new method (ADC- and agmatinase-catalyzed reactions were performed in succession while the temperature and pH conditions are same as the old method) was conducted

using four different batches of ADC samples. As the preparation method and storage condition of ADC were not optimized at the time when this experiment was conducted, batch-batch variations of ADC activity were expected. According to the result (Figure 3.4), the new method is more sensitive as it is able to demonstrate the batch-batch variations of ADC activity among the four samples which the old method failed to show. Besides, in all the four ADC samples tested, much higher specific activities are derived when the ADC- and agmatinase-catalyzed reactions are performed separately (Figure 3.4). This proves our hypothesis that in the old method, the assay conditions are not favored by agmatinase, and hence a portion of agmatine produced by ADC-catalyzed reaction is not converted to putrescine and urea. Therefore, it is suggested that the reactions of ADC and agmatinase be performed separately, and the optimal reaction conditions for ADC and agmatinase be determined respectively.

In addition, colorless product was observed when testing the ADC-catalyzed reaction mixture (which contains agmatine but not urea) by DAMO assay, indicating that agmatine is not an interfering molecule.

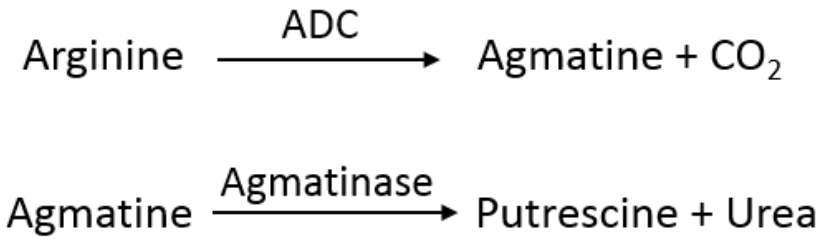

Figure 3.3: The two enzymatic reactions involved in the assay method for ADC activity.

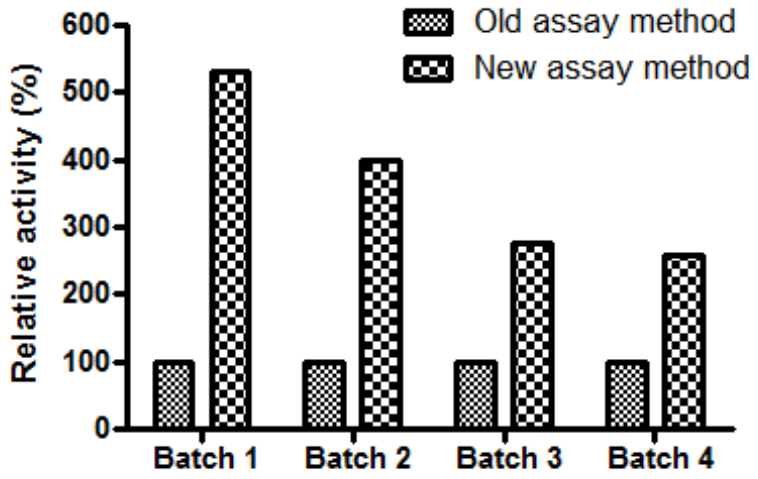

Figure 3.4: Bar chart showing the comparison of the activities of ADC measured by the old method (ADC and agmatinase in a single mixture) and the new method (ADC and agmatinase in subsequent reactions). Data are expressed as percentage of the activity of the corresponding sample measured by the old method. Each bar represents a single measurement. All reactions were performed in 20 mM sodium phosphate buffer at 37 ℃, pH 8.0. Reaction mixtures containing ADC were also supplemented with 1 mM $MgCl_2$ and 0.1 mM PLP. In the new assay method, overnight agmatinase reactions were carried out.

3.2.2 Preparation and characterization of *E. coli* agmatinase

3.2.2.1 Purification of agmatinase by affinity chromatography

Figure 3.5 is the chromatogram showing the purification of 6x histidine-tagged agmatinase from *E. coli* cell lysate. Two peaks were observed during the elution process using increasing concentrations of imidazole. The first peak occurred at lower concentrations of imidazole, while the second one occurred when imidazole concentration reached ~0.3 M.

According to the SDS-PAGE analysis of the eluted fractions (Figure 3.6), fractions 7 to 10 mainly contain a protein with a molecular weight slightly above 31 kDa which is quite close to the calculated molecular weight of agmatinase monomer (~34 kDa). This result indicates that agmatinase has been expressed at a high level and has been successfully purified.

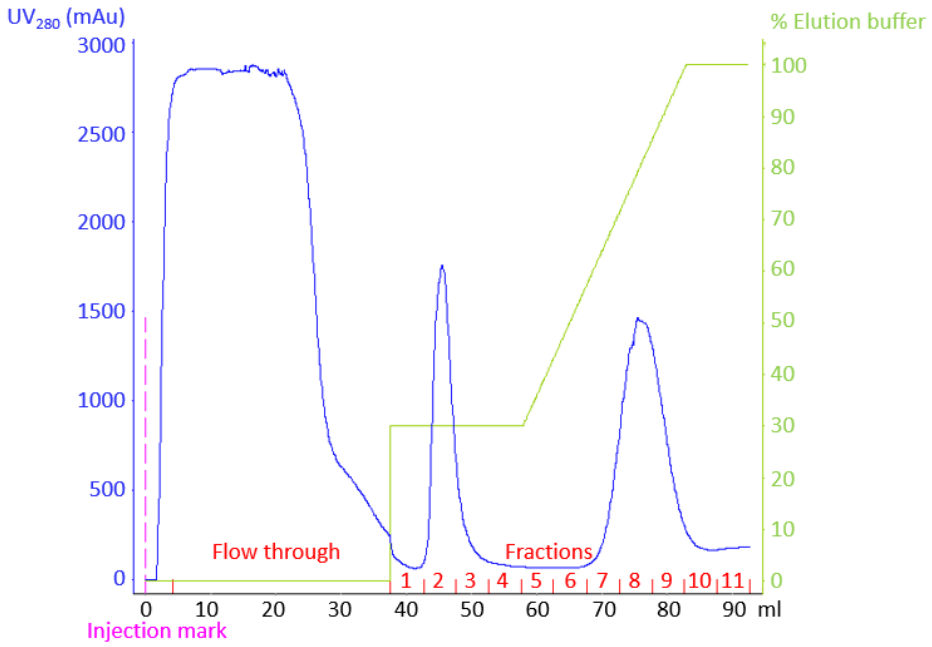

Figure 3.5: Elution profile of the purification of agmatinase from *E. coli* cells grown in 500 ml shake flask culture by a single step of nickel-charged 5 ml HiTrap^{TM} chelating HP column chromatography. mAU, milli absorption unit; 100% B = 0.5 M imidazole.

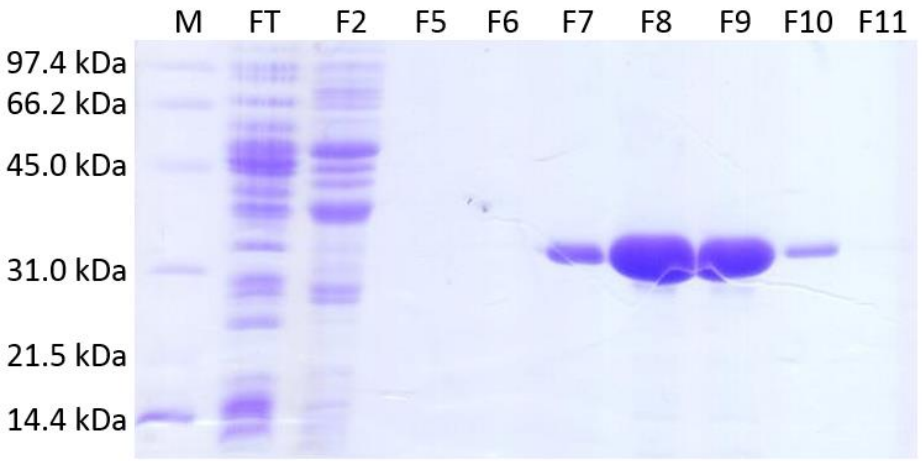

Figure 3.6: SDS-PAGE analysis of the column fractions from nickel affinity chromatography for agmatinase. M, SDS-PAGE molecular weight standards, low range (Bio-Rad); FT, flow through; F2-F11, eluted fractions from the column.

3.2.2.2 The optimal pH for agmatinase

The optimal pH for the purified agmatinase was determined by the DAMO activity assay. The activities of agmatinase in 20 mM sodium phosphate buffer of eight pH values ranging from 6.5 to 10.0 were tested. It is observed from Figure 3.7 that agmatinase favors basic pH, and its activity increases as pH rises, reaching a maximal value at ~pH 10.0 or even higher. Since we prefer a relatively mild reaction condition, pH 9.0 was therefore selected as the pH for agmatinase-catalyzed reaction of the activity assay for ADC. 100 mM glycine-NAOH buffer at pH 9.0 was used for all subsequent reactions of agmatinase unless specified, as it provides better buffering capacity than sodium phosphate buffer at a basic pH.

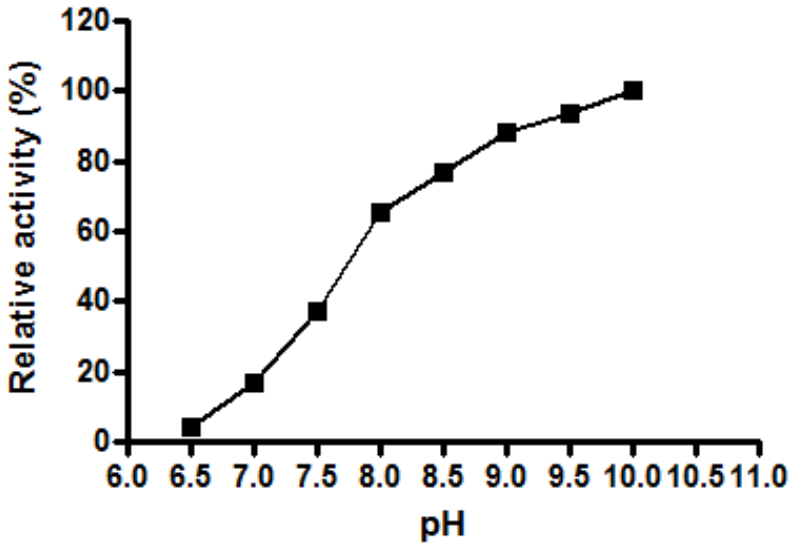

Figure 3.7: Effect of pH on the activity of agmatinase. Data are expressed as percentage of enzyme activity at pH 10.0. Each point represents the mean of a single experiment performed in duplicate. All reactions were performed in 20 mM sodium phosphate buffer at 37 ℃.

3.2.2.3 The optimal temperature for agmatinase

According to some literatures, assays for the activity of agmatinase are conducted at 37 ℃ (Hyung *et al.*, 2004; Salas *et al.*, 2004; Satishchandran and Boyle, 1986). It is, however, also notable that one study pointed out the activity of agmatinase retained after being incubated at 60 ℃ for 20 min (Carvajal *et al.*, 2004). To examine whether the activity of *E. coli* agmatinase is affected by temperature, temperatures ranging from 20 to 50 ℃ were tested in this project. The results show that agmatinase prefers reaction temperatures higher than 37 ℃ and its activity is maximal at ~45 ℃ (Figure 3.8). Therefore 45 ℃ was selected as the temperature for all subsequent reactions of agmatinase.

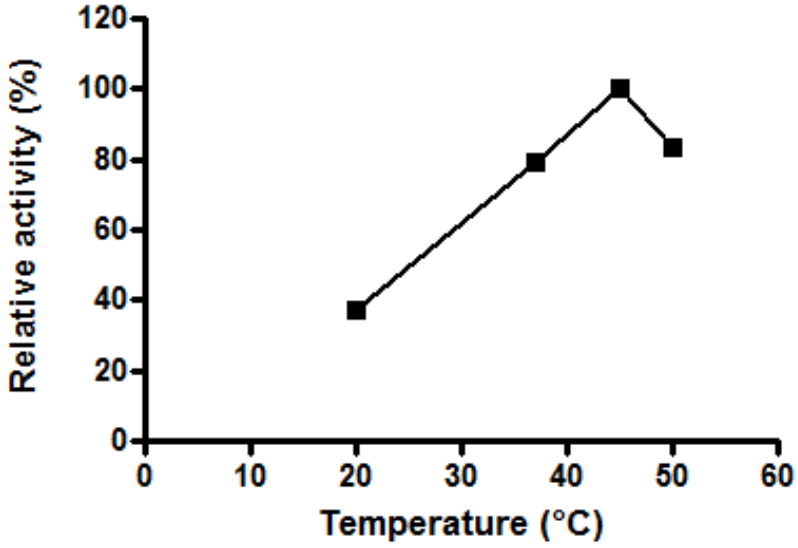

Figure 3.8: Effect of temperature on the activity of agmatinase. Data are expressed as percentage of enzyme activity at 45 ℃. Each point represents the mean of a single experiment performed in duplicate. All reactions were performed in 20 mM sodium phosphate buffer at pH 9.0.

3.2.2.4 Specific activity of agmatinase

To gain a better understanding of the enzymatic properties of agmatinase, specific activity of this enzyme was also examined. 100 μmol agmatine sulphate was used for each reaction to ensure there would be excess amount of substrate.

As measured in our study, specific activity of freshly prepared agmatinase is 101.17 ± 6.31 U/mg (at 45 ℃, pH 9.0). One unit of enzyme activity is defined as that amount of agmatinase that catalyzes the production of 1 μmol urea per min under standard assay conditions. This result is much higher than the value of 62 U/mg obtained by Salas *et al.* (2004) at pH 9.0 (temperature not specified). Such a difference may due to the differences in reaction temperature, substrate amount, reaction time, type of buffer, and enzyme quality between these two studies.

The measured specific activity of agmatinase provides important information to help us design a reaction that may ensure the maximal conversion of agmatine produced by ADC-catalyzed reaction to putrescine and urea.

3.2.3 Optimal pH for ADC

The activities of ADC in 20 mM sodium phosphate buffer of nine pH values ranging from 6.0 to 8.6 were tested. It is observed from Figure 3.9 that ADC shows maximum activity at pH 8.0, and its activity is almost fully retained when pH rises to 8.2. However, ADC only retains around half of its full activity at a physiological pH (Figure 3.8). Our measured optimal pH for ADC is quite close to the result of pH 8.4 derived by Wu and Morris (1973a) using 100 mM HEPES. Although another research group has reported that the same type of ADC functions optimally at pH 7.2-7.4 (buffer not specified, may be 100 mM HEPES or Tris-HCl) (Song *et al.*, 2010), their data variations seem to be too great to draw any persuasive conclusion.

Therefore, pH 8.0 was selected as the optimal pH for ADC-catalyzed reaction of the activity assay. This project then followed the suggestion by Wu and Morris (1973a) to use 100 mM HEPES buffer in all subsequent activity assays for ADC. Phosphate buffer is reported to exert an inhibitory effect on the activity of ADC (Wu and Morris, 1973a). However, we obtained similar specific activity values from sodium phosphate buffer, Tris-HCl buffer and HEPES buffer at 37 ℃ and pH 8.0 for ADC-ABD (Appendix Figure 2). Tris-HCl buffer is not favored for the activity test of ADC because its pH at storage condition (4 ℃ or 25 ℃) is much higher than that at activity assay condition (37 ℃).

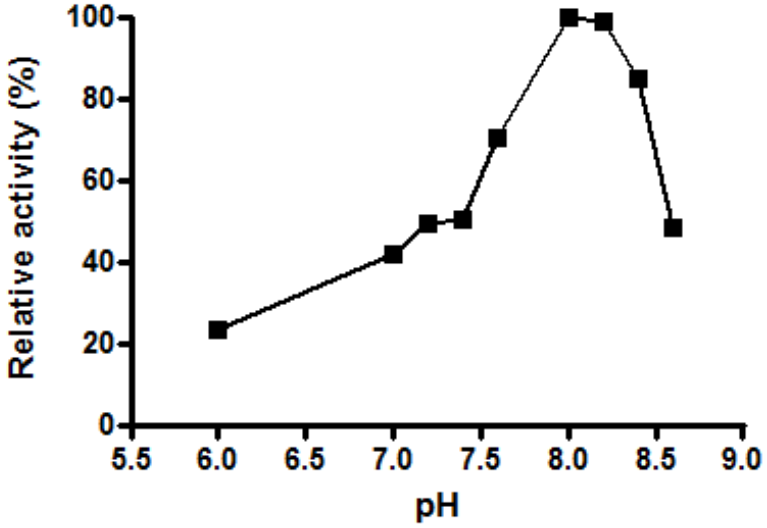

Figure 3.9: Effect of pH on the activity of ADC. Data are expressed as percentage of enzyme activity at pH 8.0. Each point represents a single measurement. All ADC-catalyzed reactions were performed in 20 mM sodium phosphate buffer (supplemented with 1 mM $MgCl_2$ and 0.1 mM PLP) at 37 ℃.

3.2.4 Optimization of the cofactor concentrations for the activity assay of ADC

The effect of cofactors on the activity of ADC was investigated by fixing the concentration of one cofactor in the reaction mixture while testing the effect of another at a time. The rate of arginine decarboxylation catalyzed by ADC shows hyperbolic dependence on both Mg^{2+} and PLP concentrations (Figure 3.10). The activity of ADC reaches its maximum value when the reaction mixture contains 14 mM $MgCl_2$ (Figure 3.10 A) and 0.14 mM PLP (Figure 3.10 B). Surprisingly, excessive amount of both cofactors exert inhibitory effects on the activity of ADC instead of maintaining ADC activity at the maximal value (Figure 3.10). The possible reason for such a phenomenon is that too much cofactors may result in non-specific binding to ADC and hence interfere with the ADC activity. Therefore, 10.5-35 mM $MgCl_2$ and 0.07-0.35 mM PLP should be used to achieve maximal activity of ADC. We suggest a reaction mixture containing 35 mM $MgCl_2$ and 0.35 mM PLP for the standard activity assay for ADC, as this combination of cofactor concentrations results in high ADC activity not only in purified ADC samples but also in *E. coli* cell lysates (Appendix Figure 3).

A

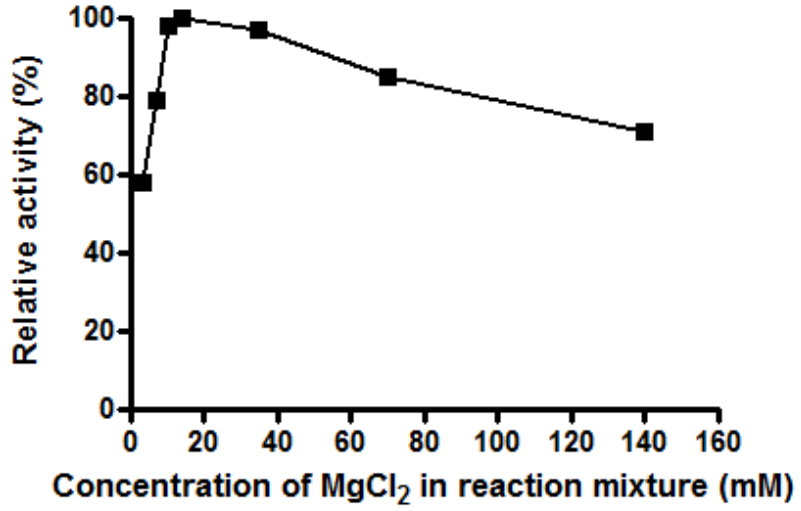

B

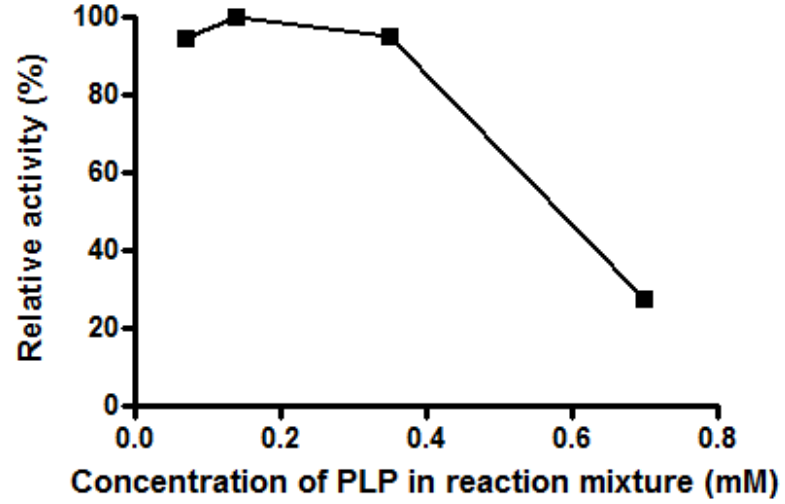

Figure 3.10: Effect of cofactors on the activity of ADC. Each point represents a single measurement. (A) Effect of $MgCl_2$ on the activity of ADC. Data are expressed as percentage of enzyme activity at 14 mM $MgCl_2$. All ADC-catalyzed reactions were performed in 100 mM HEPES buffer (supplemented with 0.07 mM PLP) at 37 ℃. (B) Effect of PLP on the activity of ADC. Data are expressed as percentage of enzyme activity at 0.14 mM PLP. All ADC-catalyzed reactions were performed in 100 mM HEPES buffer (supplemented with 35 mM $MgCl_2$) at 37 ℃.

3.2.5 Specific activity of ADC measured by the improved assay method

Based on our assay method, specific activity of freshly prepared ADC is 28.88 ± 2.68 U/mg (at 37 ℃, pH 8.0). One unit of enzyme activity is defined as the amount of ADC that catalyzes the production of 1 μmol urea per min under standard assay conditions. This result is higher than the previously reported value of 16.4 U/mg at 37 ℃ pH 8.4 (Wu and Morris, 1973a). Despite that Wu and Morris (1973a) used a direct method by measuring the CO_2 produced by ADC-catalyzed reaction while our method is an indirect measurement, it is suggested the differences in buffer pH and the concentration of magnesium ions used in the assays are the main reasons for the differences between our measured specific activities of ADC. The assay by Wu and Morris (1973a) was conducted at pH 8.4 with 4 mM Mg^{2+}, while the assay in this project was excecuted at pH 8.0 with a reaction mixture containing ~35 mM Mg^{2+}.

3.3 Overview of ADC purification from shake flask culture

The preparation of ADC from *E. coli* cells can be summarized into four main stages: first, *E. coli* cell pellet was resuspended in buffer and lysed by sonication; the cell debris was then removed by centrifugation; supernatant containing soluble proteins was applied to the nickel affinity column; finally, eluted fractions containing relatively pure ADC were pooled together, concentrated and exchanged to the buffer for storage, supplemented with cofactors, underwent sterile filtration to become the final product. Samples drawn from these four stages were analyzed by SDS-PAGE and the results are shown in Figure 3.11.

The strong T7 promoter of the expression system used has resulted in high level of ADC expression. According to the analysis by Quantity One (Bio-Rad), ADC comprises ~43% of the cells total soluble protein (Figure 3.11, lane S). Protein purification by nickel affinity column chromatography has removed most contaminates and the purity of ADC is ~92% (Figure 3.11, lane P). As the final product is more concentrated, some impurities are more obviously observed on the gel. However, considering the proportion of these impurities is quite small, the purification result is still acceptable.

Table 3.1 lists the details of a typical purification process. 110 mg of ADC protein has been purified from 1 L bacterial culture grown in shake flask.

A notable observation is that comparing the final ADC product to the whole *E. coli* lysate, the fold of purification is only 2.49 according to the analysis of SDS-PAGE band intensity by Quantity One (Bio-Rad) (Figure 3.11), and 2.02 according to the calculated enzyme activity (Table 3.1). Such low values of purification fold are atypical yet reasonable. As ADC comprises almost half of the total proteins in *E. coli* cells due to the strong protein expression system used in this project, the improvement that can be achieved on fold of purification is quite limited.

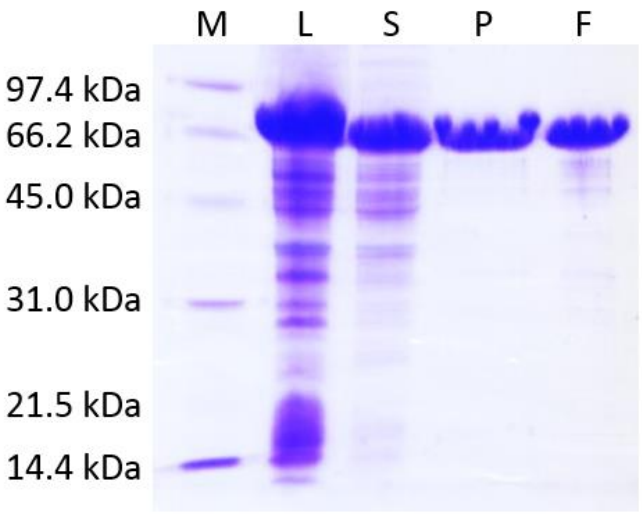

Figure 3.11: Representative image showing the SDS-PAGE analysis of a typical purification process for ADC from *E. coli* cell lysate obtained from 500 ml shake flask culture. M, SDS-PAGE molecular weight standards, low range (Bio-Rad); L, induced whole-bacterial lysate; S, the sonicated supernatant containing all soluble proteins which was to be loaded onto a nickel affinity column; P, pooled eluted fractions from the nickel affinity column containing relatively pure ADC; F, ADC final product after buffer exchange and supplementation of cofactors.

Table 3.1: Purification of recombinant *E. coli* biosynthetic ADC from 1 L shake flask culture.

Purification step	Total enzyme activity (U)	Total protein (mg)	Specific enzyme activity (U/mg)	Fold purification	% Recovery
Whole cell lysate	4113.5	304.7	13.5	1.00	100.00%
Soluble proteins	3757.0	221.0	17.0	1.26	91.33%
Affinity column pooled fractions	3144.1	111.1	28.3	2.10	76.43%
Final Product	3005.7	110.1	27.3	2.02	73.07%

3.4 Long-term storage of ADC

The final product of ADC contained ~3-4 mg/ml protein in 20 mM sodium phosphate buffer supplemented with 5 mM $MgCl_2$ and 0.1 mM PLP, and was stored at 4 ℃ in darkness. Surprisingly, the optimal pH for ADC activity does not fit for the storage of ADC. When stored at pH 8.0, ADC activity fell to around one-fourth of its original value after 4 months of storage. Therefore pH 7.4 was used as the pH for the storage of ADC.

Three batches of ADC were tested for their specific activity when freshly prepared, as well as at several months after their preparation. The protein concentrations and specific activities of these three batches of ADC all remained quite stable during the whole storage period (Figure 3.12), although the specific activity of ADC experienced a slight decrease over time. The fluctuation of results may due to the variation among different batches of reagents for the activity test. Some reagents, such as those for DAMO assay, are shared within the research group. As these shared reagents are prepared by different group members from time to time, their performance may vary slightly.

When observed with naked eyes, it has been found that the color of ADC solution changes from yellow to light yellow, or even transparent, during longer storage period (for example, 24 months). This observation indicates that the decrease of specific activity of ADC may due to the degradation of PLP.

Based on our data, we suggest ADC can remain relatively stable for 6-12 months when stored at 4 ℃ in darkness in the suggested formulation. Therefore in this project, only those batches of ADC that had been stored for less than 6 months were used for tissue culture and animal experiments.

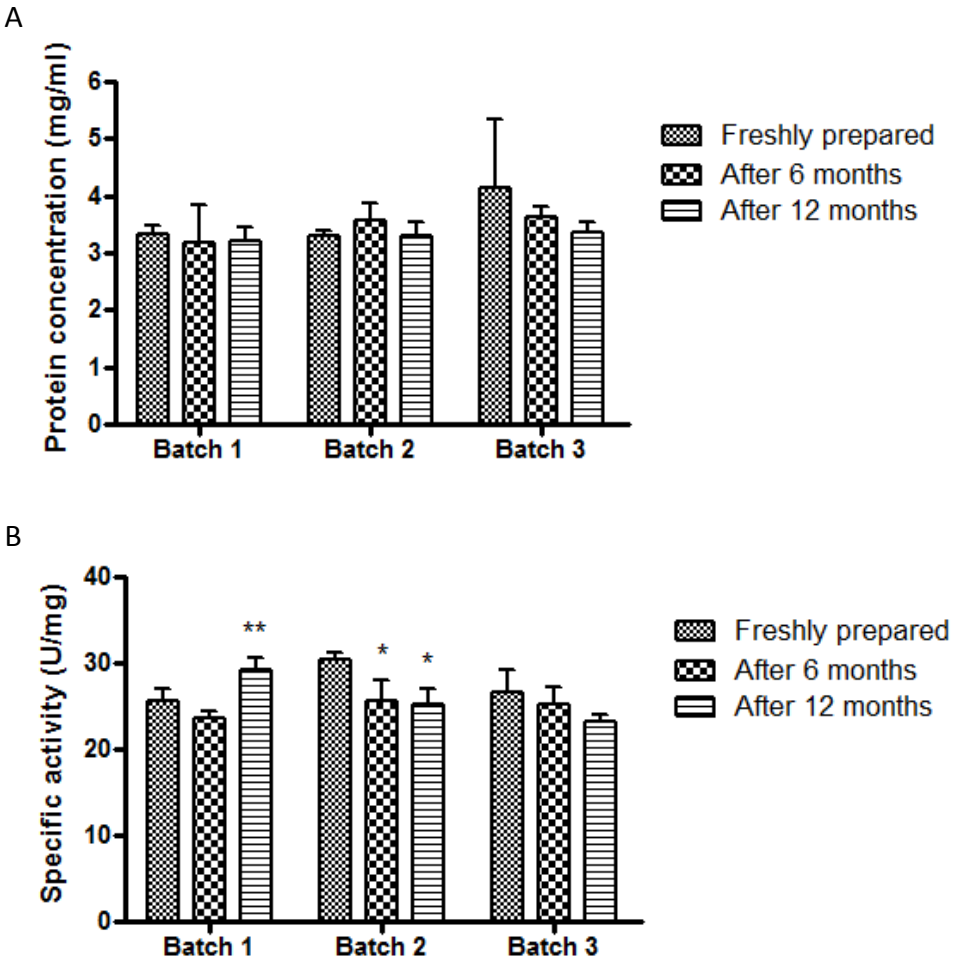

Figure 3.12: Effect of long-term storage on protein concentration and specific activity of ADC. All batches of ADC were formulated at ~3-4 mg/ml in 20 mM sodium phosphate buffer supplemented with 5 mM $MgCl_2$ and 0.1 mM PLP, and were stored at 4 ℃ in darkness. (A) Changes of protein concentration of ADC upon storage. Data are expressed as mean ± SD of a single experiment performed in duplicate; (B) Changes of specific activity of ADC upon storage. Data are expressed as mean ± SD of a single experiment performed in triplicate. All ADC-catalyzed reactions were performed under standard assay conditions (37 ℃, pH 8.0). *, $P < 0.05$; **, $P < 0.01$ (versus corresponding freshly prepared ADC).

Chapter 4

Results: anti-cancer properties of ADC *in vitro*

4.1 ADC reduces cell viability in ten human cancer cell lines

4.1.1 ADC inhibits the proliferation of ten human cancer cell lines in a dose-dependent manner

Ten cell lines of different cancer types, including liver cancer (HepG2), lung cancer (A549), cervical cancer (HeLa), melanoma (A375), pancreatic cancer (BxPC-3, PANC-1), and colorectal cancer (HCT116, LoVo, COLO 205, SW1116), as well as a non-tumorous cell line, human foreskin fibroblast HFF-1, were tested for their sensitivities to ADC. After 72 h of treatment with ADC at a series of concentrations, cell viability was tested by the MTT assay.

As summarized in Table 4.1, the treatments of ADC in ten cell lines of different cancer types all result in notable inhibition of cell growth, with IC_{50} values of ADC ranging from 3.8 to 46.5 μg/ml, indicating that ADC has a broad anti-cancer spectrum. Cell sensitivity to ADC appears to be dose-dependent. For each cell line, the cytotoxicity of ADC increases as the dose of ADC increases, and finally reaches a plateau which is regarded as the maximum cytotoxicity (Figure 4.1). In this project, maximum cytotoxicity is expressed as the percentage of nonviable cells achieved by

the maximum concentration of ADC tested (50 μg/ml for HeLa; 100 μg/ml for the rest of cell lines) relative to control (0 μg/ml ADC). At the highest tested concentration of ADC, ~ 62% - 93% of tumor cells are growth-inhibited (Table 4.1). Figure 4.2 shows micrographs of HCT116 cell growth and proliferation upon ADC treatment.

In contrast, around 70% of the non-tumorous HFF-1 cells remain viable even when the maximum dose (100 μg/ml) of ADC is used (Figure 4.1). The relative resistance of HFF-1 to ADC treatment provides some evidence that ADC may be a potential selective therapeutic agent for cancer.

Table 4.1: IC_{50} and maximum cytotoxicity of ADC in ten cancer cell lines. IC_{50} value is defined as the amount of ADC needed to achieve 50% inhibition of cell viability. Maximum cytotoxicity is expressed as the percentage of nonviable cells achieved by the maximum concentration of ADC tested (50 μg/ml for HeLa; 100 μg/ml for the rest of cell lines) relative to control (0 μg/ml ADC). Data are expressed at the mean of three experiments performed in triplicate. ADC treatment period: 72 h.

Cancer Type	Cell Line	IC_{50} (μg/ml)	Maximum cytotoxicity (%)
Melanoma	A375	5.61	84.76
Pancreatic	PANC-1	4.65	82.98
	BxPC-3	16.85	93.16
Colorectal	HCT116	12.23	84.35
	COLO 205	19.40	81.62
	LoVo	38.09	66.17
	SW1116	21.30	73.69
Lung	A549	12.29	69.13
Liver	HepG2	30.75	61.87
Cervical	HeLa	3.82	86.49
Non-tumorous	HFF-1	> 100	< 50

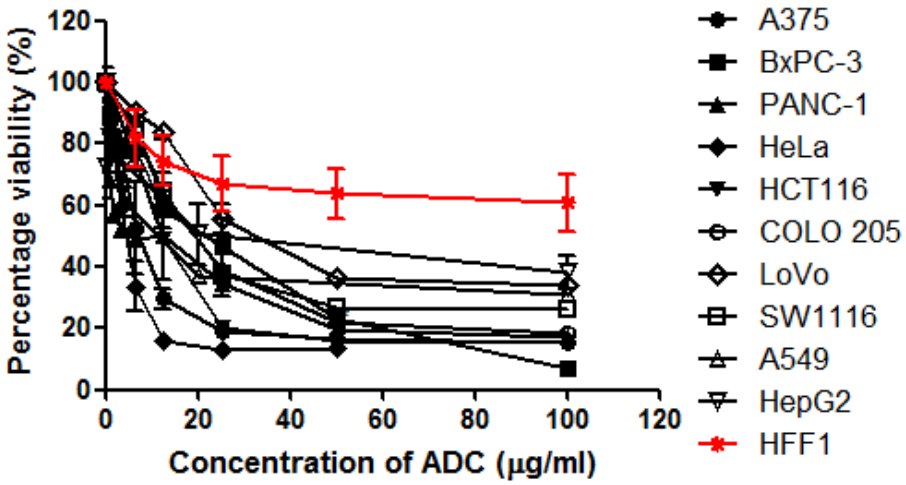

Figure 4.1: Dose-response curves showing the effect of ADC in ten cancer cell lines (black) and one non-tumorous cell line (red). Cells were incubated with different concentrations of ADC for 72 h prior to MTT assay. Data are expressed as percentage of control treatment (0 µg/ml ADC) and are the mean ± SEM of three experiments each performed in triplicate.

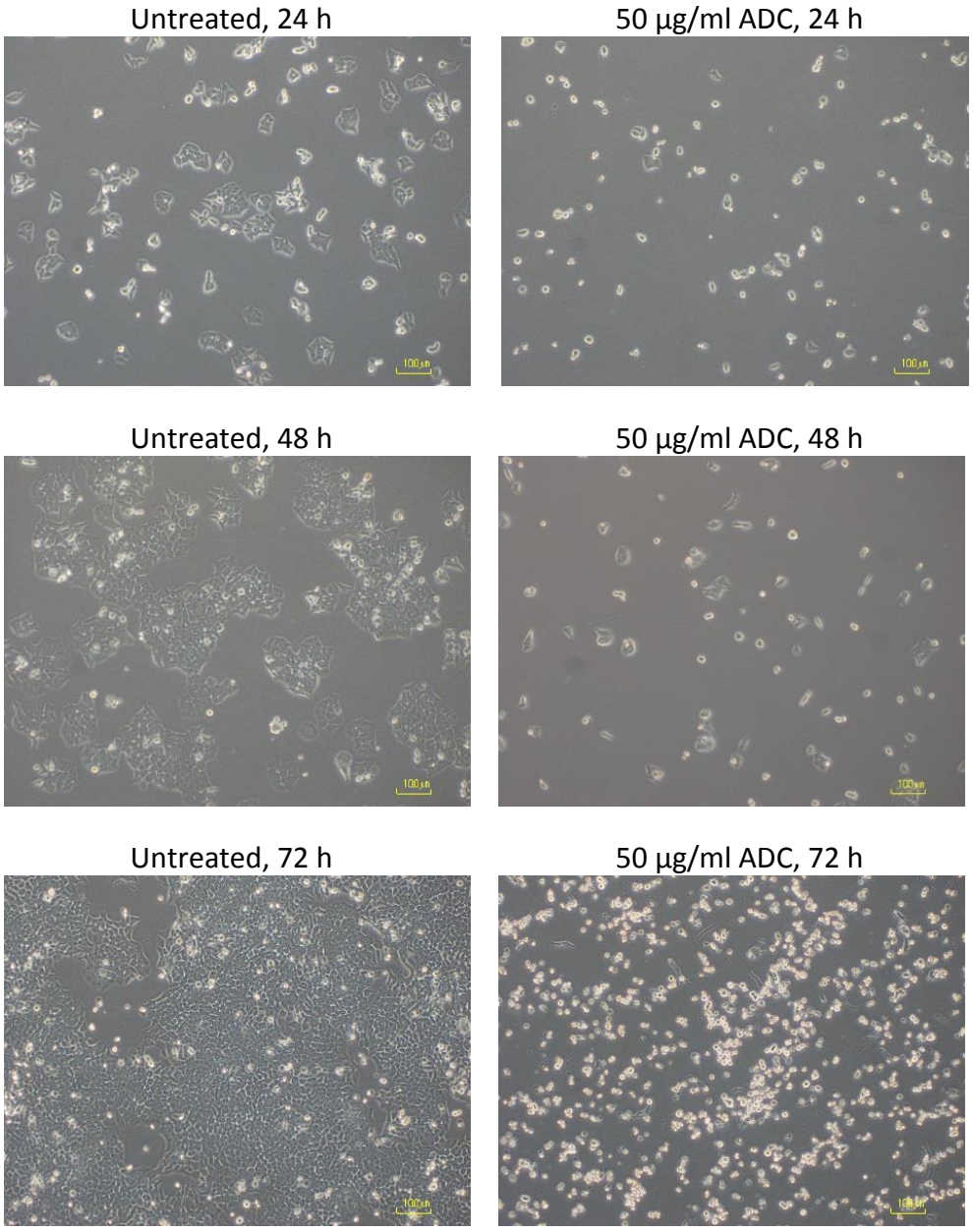

Figure 4.2: Micrographs of HCT116 cells upon ADC treatment. Left column (untreated): HCT116 cells were grown in complete medium with cofactors (1 mM $MgCl_2$, 0.1 mM PLP) for 24, 48, and 72 h; right column (50 µg/ml ADC): HCT116 cells were grown in complete medium with cofactors and 50 µg/ml ADC for the same periods. Scale bar, 100 µm.

4.1.2 ADC inhibits the proliferation of five human cancer cell lines in an ASS-independent manner compared to ADI and BCA

The cytotoxicities of ADI, BCA and ADC were determined in a comparative study in five tumor cell lines: A375, HeLa, BxPC-3, PANC-1, and HCT116. A375 is a typical melanoma cell line which has been frequently used in studies on ADI, and has been reported to be ASS-negative as well as ADI-sensitive in all the studies (Manca *et al.*, 2011; Sugimura *et al.*, 1992; Tsai *et al.*, 2009, Tsai *et al.*, 2012; Wu *et al.*, 2011). The cervical cancer cell line HeLa, in contrast, is ASS-positive with high ASS activity (Cheng *et al.*, 2007; Shen *et al.*, 2003) and has been found to be ADI-resistant (Shen *et al.*, 2003; Sugimura *et al.*, 1992; Wu *et al.*, 2011). It has also been reported that HeLa cells express an increased amount of ASS in response to ADI treatment which further accounts for their drug resistance (Wu *et al.*, 2011). HCT116, unlike the other colorectal cancer cell line counterparts which are highly ASS-positive, expresses only a low level of ASS (Appendix Figure 4). PANC-1 and BxPC-3 are both pancreatic cancer cell lines with low or medium levels of ASS (Bowles *et al.*, 2008; Appendix Figure 4).

As both ADI- and BCA-catalyzed reactions are parts of the urea cycle, it is hypothesized that the anti-tumor effects of ADI and BCA are both related to cellular ASS level. In contrast, the anti-tumor effect of ADC may be relatively less affected by the presence of ASS, as neither catalytic products of ADC are intermediates of the urea cycle.

Our results have demonstrated that ADI, BCA and ADC all exert some inhibitory effects in the cell lines studied. ADI is effective against A375, HCT116, BxPC-3, PANC-1 but not HeLa cells, while both BCA and ADC are effective against all these five cancer cell lines tested (Table 4.2). Generally, ADC is the least potent arginine-depleting enzyme, yet it is still advantageous over ADI and BCA in terms of efficacy, especially in ASS-positive cancer cells (Table 4.2).

As expected, sensitivity of tumor cells to ADI displays a clear relationship to the cellular ASS level (Table 4.2). ADI treatment is most effective against ASS-negative A375 cells, as more than 90% of the cells become nonviable upon the treatment of the maximum dose of ADI; BxPC-3 and PANC-1 cells are defined as "partially ADI-sensitive" since only less than 60% of these cells are inhibited when the maximum dose of ADI is applied; HeLa cells are found to be ADI-resistant (Table 4.2) which agrees with the findings reported in previous literatures (Shen *et al.*, 2003; Sugimura *et al.*, 1992; Wu *et al.*, 2011).

For BCA, there also seems to be a trend that the IC_{50} value increases while the maximum cytotoxicity decreases along with an increase in cellular ASS level yet more cell lines should be studied before drawing a solid conclusion (Table 4.2). It is notable that PANC-1 is relatively more resistant to BCA than BxPC-3 despite its original ASS level is lower (Appendix Figure 4). This observation can be explained by a previous finding that the treatment of arginase has induced the ASS level in PANC-1 cells (Glazer *et*

al., 2010). Therefore, the ASS level in PANC-1 cells is defined as "low/medium, and inducible" in this project (Table 4.2).

In the case of ADC, however, no clear relationships between cellular ASS level and cell sensitivity to ADC has been observed (Table 4.2). This result meets our expectation that ADC may inhibit tumor cell growth in a more ASS-independent manner compared to ADI and BCA. A systematic study on the induction of ASS protein expression by the three arginine-depleting enzymes in different cancer cell lines should be conducted in the future go generate a more solid conclusion.

Table 4.2: IC_{50} and maximum cytotoxicity of ADI, BCA and ADC in five cancer cell lines. Cells were treated for 72 h before MTT analysis. Data are the mean of three experiments performed in triplicate. IC_{50} value is defined as the amount of enzyme needed to achieve 50% inhibition of cell viability. Maximum cytotoxicity is expressed as the maximum percentage of nonviable cells achieved by each enzyme. ADI-resistant cells are defined as cells of which more than 50% survive under the maximum dose of ADI tested.

Cancer Type	Cell Line	ASS protein level	IC_{50} (μg/ml)			Maximum cytotoxicity (%)		
			ADI	BCA	ADC	ADI	BCA	ADC
Melanoma	A375	Undetectable, uninducible	0.03	0.12	5.61	93.92	86.92	84.76
Colorectal	HCT116	Low	0.10	0.22	12.23	72.18	81.05	84.35
Pancreatic	BxPC-3	Medium	0.09	0.44	16.85	57.53	84.82	93.16
	PANC-1	Low/medium, inducible	0.04	1.81	4.65	55.68	63.01	82.98
Cervical	HeLa	Low/high, inducible	Resistant	1.25	3.82	< 50	61.14	86.49

4.1.3 The anti-proliferation effect of ADC is less vulnerable to extracellular citrulline compared to BCA

Apart from ASS, OTC is another key enzyme in the urea cycle. Since all the cell lines studied in this project are found to be OTC-negative (Appendix Figure 4), a cell line that expresses high level of OTC protein should be artificially constructed to examine whether cellular OTC expression can affect the cytotoxicity of arginine-depleting enzymes.

OTC-positive cell line construction using adenoviruses carrying gene encoding OTC to infect the tumor cells has been carried out in HeLa cells in this project. HeLa was chosen because this cell line is easy to infect. As a control, adenovirus carrying gene encoding green fluorescent protein (GFP) is used to infect HeLa cells so that the efficiency of infection can be evaluated under a fluorescent microscope. The infection efficiency, however, was far from satisfactory (Appendix Figure 5). Therefore we switched to another strategy by adding excessive citrulline (1.15 mM) to the culture medium to mimic an environment in which OTC-positive cells grow. The effect of excessive citrulline on the ADC- and BCA-induced cell death was then tested.

The results show that excessive extracellular citrulline has little impact on the anti-tumor effects of both ADC and BCA in ASS-negative A375 cells, as the dose-response curves of citrulline-treated group and control group almost fully overlap (Figure 4.3). In ASS-positive tumor cells, the

supplementation of excessive citrulline has demonstrated rescuing effect of cells from both ADC and BCA treatments, although the effect of ADC seems to be less affected than that of BCA (Figure 4.3). In HCT116 cells which expresses low level of ASS, the supplementation of citrulline has little impact on the cells treated with ADC but rescues a small number of cells treated with BCA (Figure 4.3). In COLO 205 cells which expresses medium level of ASS, excessive extracellular citrulline recovers ~70% of cells from ADC treatment, whilst making the cells almost totally survived from BCA treatment (Figure 4.3).

Our results have demonstrated that ASS is the rate-limiting enzyme for cell growth under citrulline-rich and arginine-poor conditions. These results also indicate that ADC may be more effective than BCA in tumor cells with high levels of both ASS and OTC.

A375:

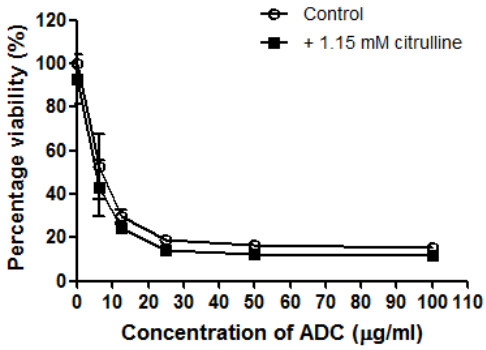

A375:

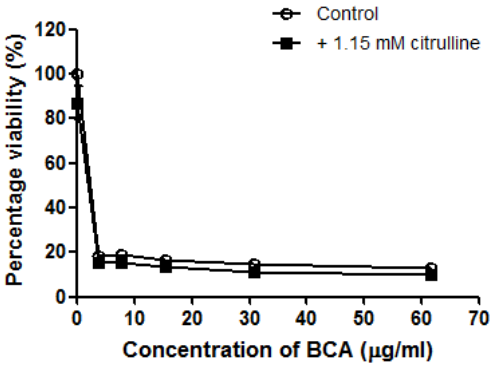

HCT116:

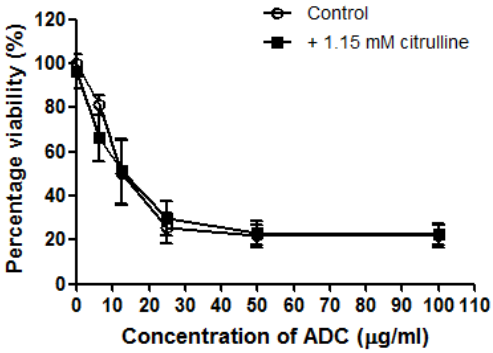

HCT116:

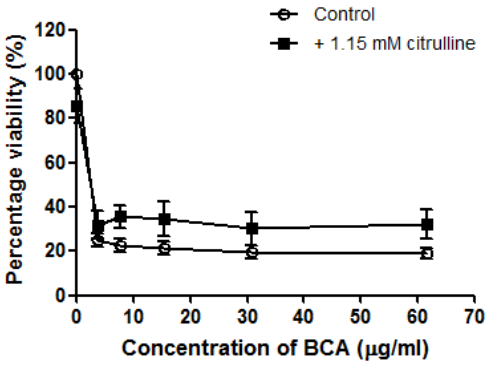

COLO 205:

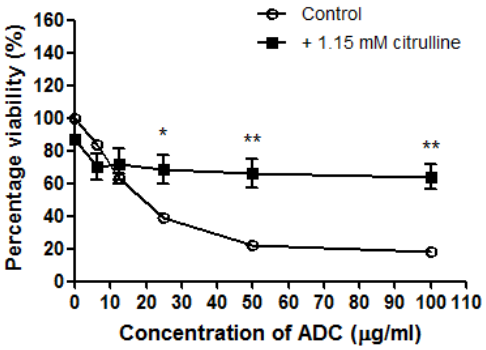

COLO 205:

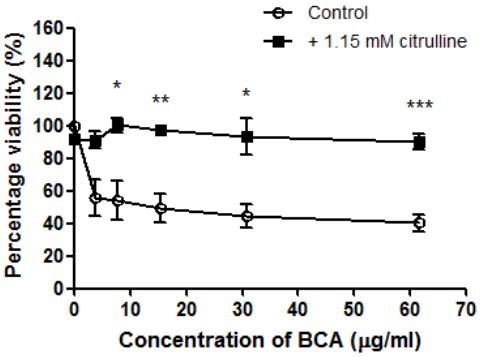

Figure 4.3: *In vitro* growth inhibition curves of ADC and BCA in A375, HCT116, and COLO 205 cells. Cells were treated with ADC or BCA for 72 h in complete medium (control) or complete medium supplemented with 1.15 mM citrulline. Data are expressed as percentage of the cell population at 0 μg/ml enzyme in control group and are the mean ± SEM of three experiments each performed in triplicate. *, $P < 0.05$; **, $P < 0.01$; ***, $P < 0.001$ (versus corresponding enzyme concentration in control group).

4.1.4 The anti-proliferation effect of ADC is dependent on the concentrations of its cofactors in the cell culture environment

Although the formulation of ADC already contains both $MgCl_2$ and PLP, supplementation of additional cofactors in the culture medium is still suggested based on the experience from DAMO enzyme activity assay. Here we tested the importance of cofactors for the cytotoxicity of ADC by comparing the IC_{50} values of ADC in culture medium with and without $MgCl_2$ (1 mM) and/or PLP (0.1 mM), using HCT116 and SW1116 cell lines.

According to the results, the potency of ADC in cancer cells is affected by the amount of cofactors present in the culture medium. It is found that the addition of either $MgCl_2$ or PLP, or both, decrease the IC_{50} values of ADC in both HCT116 and SW1116 cells (Table 4.3). Compared to $MgCl_2$, PLP seems to play a more important role in boosting the anti-cancer potency of ADC (Table 4.3). When both cofactors are added to the medium, the lowest IC_{50} value among all treatment groups is achieved (Table 4.3). Therefore it is recommended that both $MgCl_2$ and PLP be supplemented in the culture medium for *in vitro* studies of ADC to achieve better cytotoxic effects.

Table 4.3: Supplementation of cofactors in the culture medium affects the IC_{50} values of ADC in HCT116 and SW1116 cells. Cells were treated for 72 h before MTT analysis. IC_{50} values are calculated based on the results of three experiments performed in triplicate.

Tumor cell line	IC_{50} of ADC (μg/ml)			
	No cofactors	1 mM $MgCl_2$	0.1 mM PLP	1 mM $MgCl_2$ + 0.1 mM PLP
HCT116	53.17	36.82	18.90	12.23
SW1116	76.63	47.90	37.70	21.30

4.1.5 The role of agmatine in the anti-proliferation effect of ADC

It has been reported that agmatine, the product of ADC-catalyzed reaction, has anti-cancer effect (Isome *et al.*, 2007; Molderings *et al.*, 2004; Wang *et al.*, 2005; Wolf *et al.*, 2007). Therefore we would like to study whether the cytotoxicity of ADC is due to arginine depletion or agmatine production or both.

The effects of agmatine in three colorectal cancer cell lines, HCT116, LoVo, and COLO 205, as well as in one pancreatic cancer cell line, BxPC-3, were first examined. Agmatine sulphate was used. It has been found that the IC_{50} values of agmatine in the three colorectal cancer cell lines tested are all ~2 mM (Table 4.4). This result is consistent with the previously reported data (Mayeur *et al.* 2005, Wolf *et al.*, 2007). The pancreatic cancer cell line, BxPc-3, is more sensitive to agmatine treatment with an IC_{50} value of ~1 mM (Table 4.4). Consequently, it is suggested that agmatine itself has some anti-proliferation effect in these four cancer cell lines tested, and the cell sensitivity to agmatine may be cancer type-dependent.

A following experiment then examined the effect of arginine-depletion in five cancer cell lines using arginine-free medium (AFM), and compared that with the inhibitory effect of the maximum ADC concentration (100 μg/ml). According to Figure 4.3, the maximum dose of ADC (100 μg/ml) achieves similar anti-proliferation effect to that of AFM in A375, HCT116, COLO 205 and SW1116 cells. This may indicate that the production of

agmatine through ADC-catalyzed reaction has little impact on the growth of these cells when high doses of ADC are used.

Interestingly, BxPC-3 cells respond to AFM and ADC in a distinct way. It is found that AFM has much lower efficacy than ADC in BxPC-3 cells (Figure 4.4). This can be explained by the fact that BxPC-3 is more sensitive to agmatine than the other cell lines tested. Besides, the growth rate of BxPC-3 is much slower than the other four cell lines tested, and hence BxPC-3 cells may be less vulnerable to nutrient-depletion.

To further examine the role of agmatine in the anti-tumor effect of ADC in BxPC-3 cells, the cells were subjected to the treatment of ADC combined with agmatinase. A rescuing effect of agmatinase was expected in BxPC-3 cells, since the harmful agmatine would be removed and the pro-proliferative putrescine would be generated. Excessive agmatinase (~99 μg/ml), when administered alone, has no significant impact on the viability of BxPC-3 cells (Figure 4.5). When combined with ADC, it has been observed that agmatinase rescues a small portion of BxPC-3 cells from 100 μg/ml ADC (Figure 4.5) which fits our hypothesis. Thus, ADC may inhibit the growth of BxPC-3 cells through both arginine-depletion and agmatine production, and arginine depletion seems to be the main reason for BxPC-3 cell death.

Table 4.4: IC_{50} of agmatine in four cancer cell lines. Cells were treated with agmatine sulphate for 72 h before MTT analysis. IC_{50} values are calculated based on the results of three experiments performed in triplicate.

Cancer type	Cell line	IC_{50} of agmatine (mM)
Pancreatic	BxPC-3	1.09
Colorectal	HCT116	1.79
	LoVo	2.24
	COLO 205	1.85

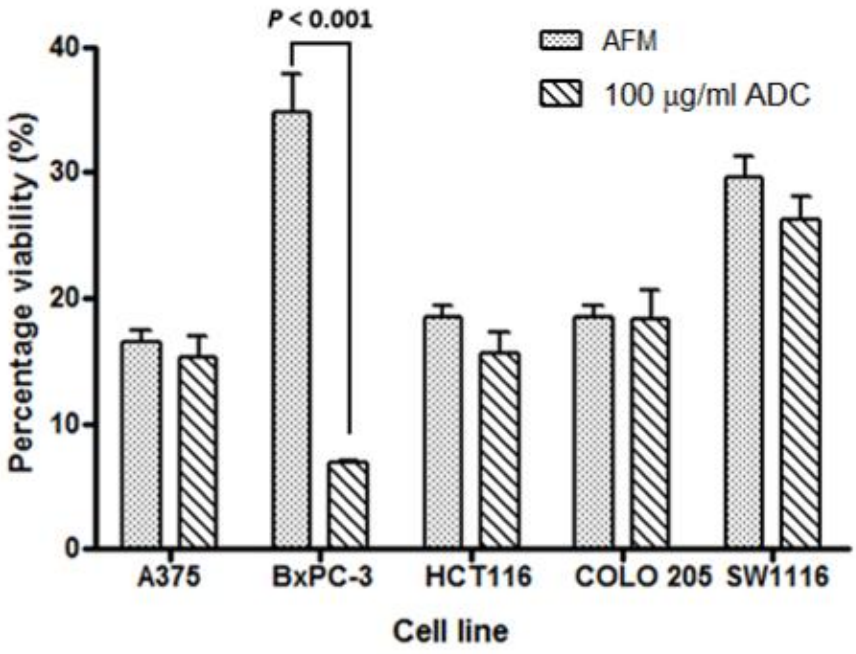

Figure 4.4: Bar chart comparing the effects of AFM and the maximum dose of ADC (100 µg/ml) on cell viability. Cells were treated for 72 h before MTT analysis. Data are expressed as the percentage of viable cells compared to control (complete medium) in the form of mean ± SEM of three experiments performed in triplicate.

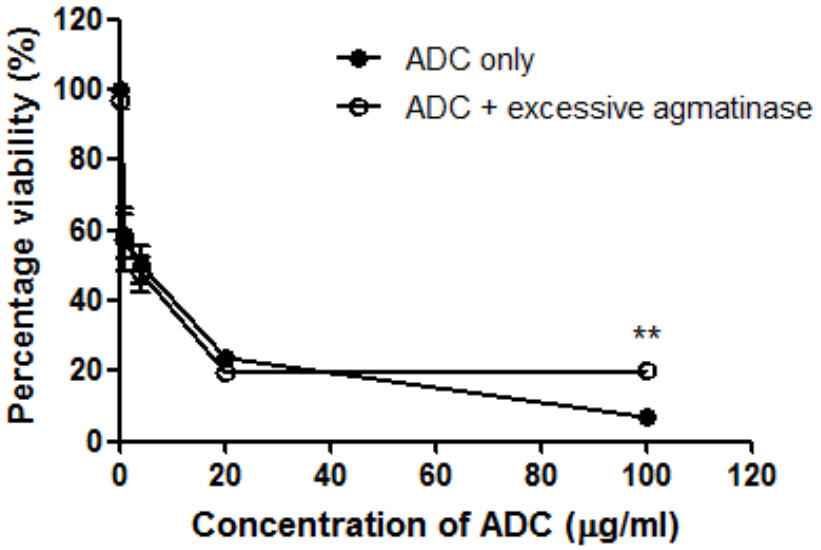

Figure 4.5: *In vitro* growth inhibition curves of ADC with and without excessive agmatinase in BxPC-3 cells. Cells were cultured in complete medium with or without ~99 µg/ml agmatinase for 72 h prior to MTT assay. Data are expressed as percentage of control (0 µg/ml ADC, 0 µg/ml agmatinase) and are the mean ± SEM of three experiments each performed in triplicate. **, $P < 0.01$ (ADC + excessive agmatinase versus ADC only).

4.2 ADC induces apoptosis in HCT116 cells

4.2.1 ADC induces apoptosis in a time-dependent manner in HCT116 cells and is a stronger apoptosis inducer than BCA

To study whether the reduced cell viability upon ADC treatment is due to apoptosis, HCT116 cells were grown in the absence or presence of 50 μg/ml ADC for 24, 48, and 72 h and were subjected to annexin V-FITC staining and flow cytometry analysis. Annexin V is a recombinant protein that has a strong, specific interaction with PS, and is therefore used for the detection of apoptosis (Elmore, 2007).

Prior to cell harvest, an observation under the light microscope has shown that decreased cell population as well as numbers of small, round, detached vesicles are found in all ADC-treated groups (Figure 4.2). According to the images taken by time-lapse microscopy, these vesicles are likely to be apoptotic bodies as they are blebbings emerged from the cells and their number increases with time upon ADC treatment (Figure 4.6). When stained with annexin V-FITC and observed under a fluorescent microscope, more green cells are found in the ADC-treated group, indicating the externalization of PS – a sign for early apoptosis (Appendix Figure 6).

According to the flow cytometry results, apoptosis is induced in HCT116 cells in a time-dependent manner upon ADC treatment. At 24, 48, and 72 h post-ADC-treatment, ~35%, 52%, and 57% of HCT116 cells

undergo apoptosis, respectively (Figure 4.7). BCA also induces apoptosis in HCT116 cells in a similar way (Figure 4.7). However, ADC seems to be a much stronger apoptosis inducer than BCA in HCT116 cells, as only ~16%, 21%, and 25% of cells undergo apoptosis at 24, 48, and 72 h when 50 μg/ml of BCA is used (Figure 4.7).

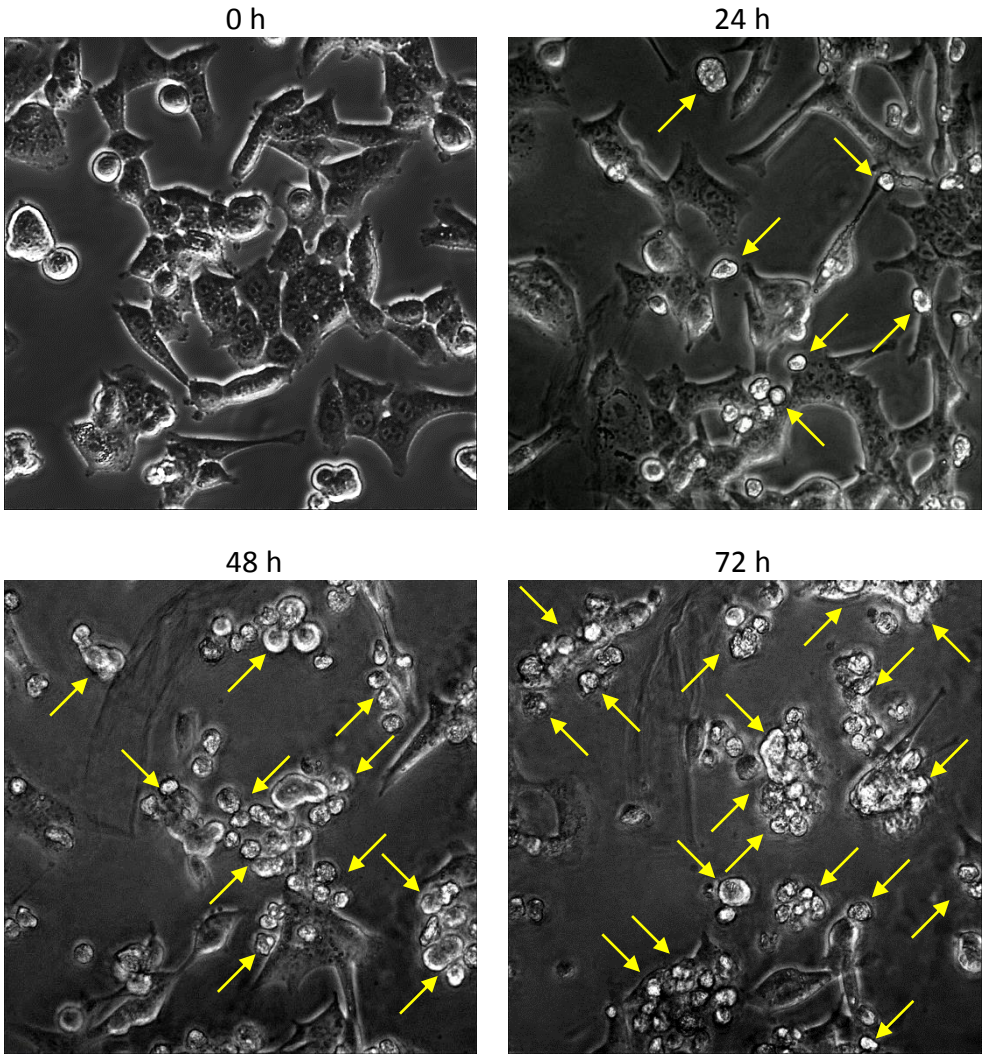

Figure 4.6: Micrographs of HCT116 cells incubated in medium with 50 µg/ml ADC at 0, 24, 48, and 72 h. Images were taken by the time-lapse microscopy. Arrowheads indicate apoptotic bodies. Magnification = 400x.

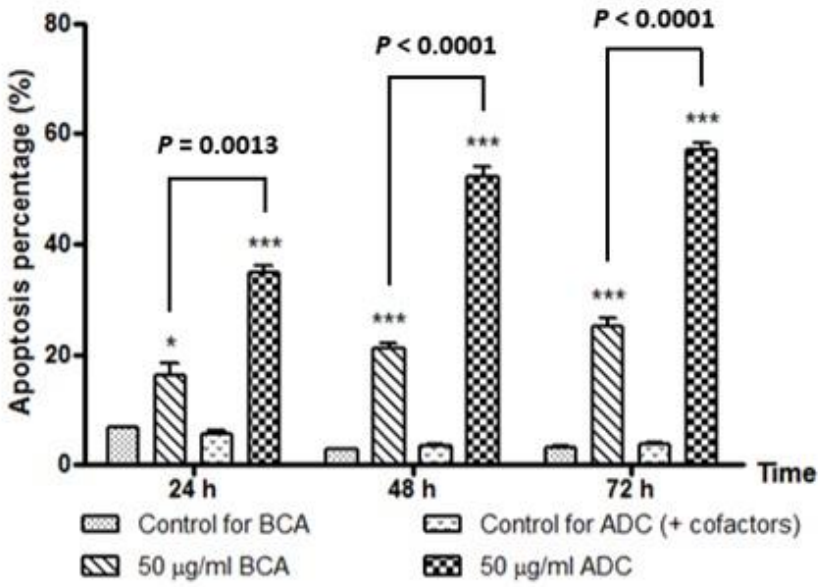

Figure 4.7: Bar graph showing mean ± SEM of the apoptosis percentage in HCT116 cells after 24, 48, or 72 h of treatment with ADC or BCA. *, $P < 0.05$; ***, $P < 0.001$ (versus corresponding control). n = 3.

4.2.2 ADC induces apoptosis in HCT116 and LoVo cells in a dose-dependent manner

To investigate ADC-induced apoptosis in more details, HCT116 cells were grown in the presence of different concentrations of ADC for 72 h and then harvested for the examination of apoptosis. Comparing to the control group (0 μg/ml ADC, 2.93% cells undergo apoptosis), the apoptotic cell population remains relatively unchanged at 6.25 μg/ml ADC (4% cells undergo apoptosis), but increases by 4.9-, 18.1-, 21.2-, and 21.8-fold at 12.5, 25, 50, and 100 μg/ml ADC, respectively (Figure 4.8 A, C). The dose-dependent apoptosis-inducing effect of ADC is also observed in LoVo cells (Figure 4.8 B). Similarly, BCA triggers apoptosis in HCT116 and LoVo cells in a dose-dependent manner (Appendix Figure 7). It is also observed that compared to HCT116 cells, LoVo cells show a higher basal level of apoptosis both in complete medium (~16%, Appendix Figure 7 B) and in complete medium supplemented with cofactors (~23%, Figure 4.8 B) which deserves further examination. No necrotic cell population has been detected in ADC- or BCA-treated HCT116 and LoVo cells.

A

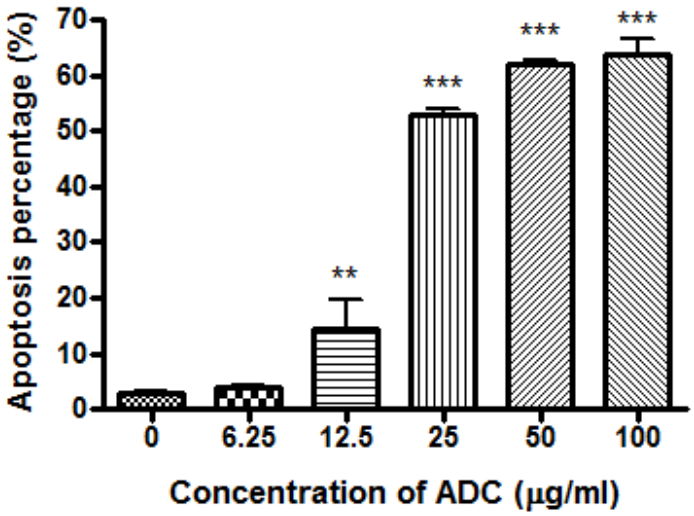
Apoptosis percentage (%)
70
60
50
40
30
20
10
0
**
***
***
***
0
6.25
12.5
25
50
100
Concentration of ADC (μg/ml)

B

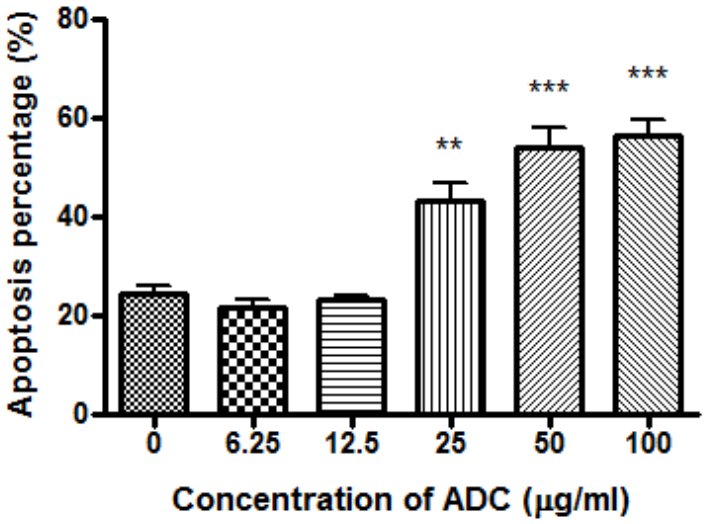
Apoptosis percentage (%)
80
60
40
20
0
**
***
***
0
6.25
12.5
25
50
100
Concentration of ADC (μg/ml)

C

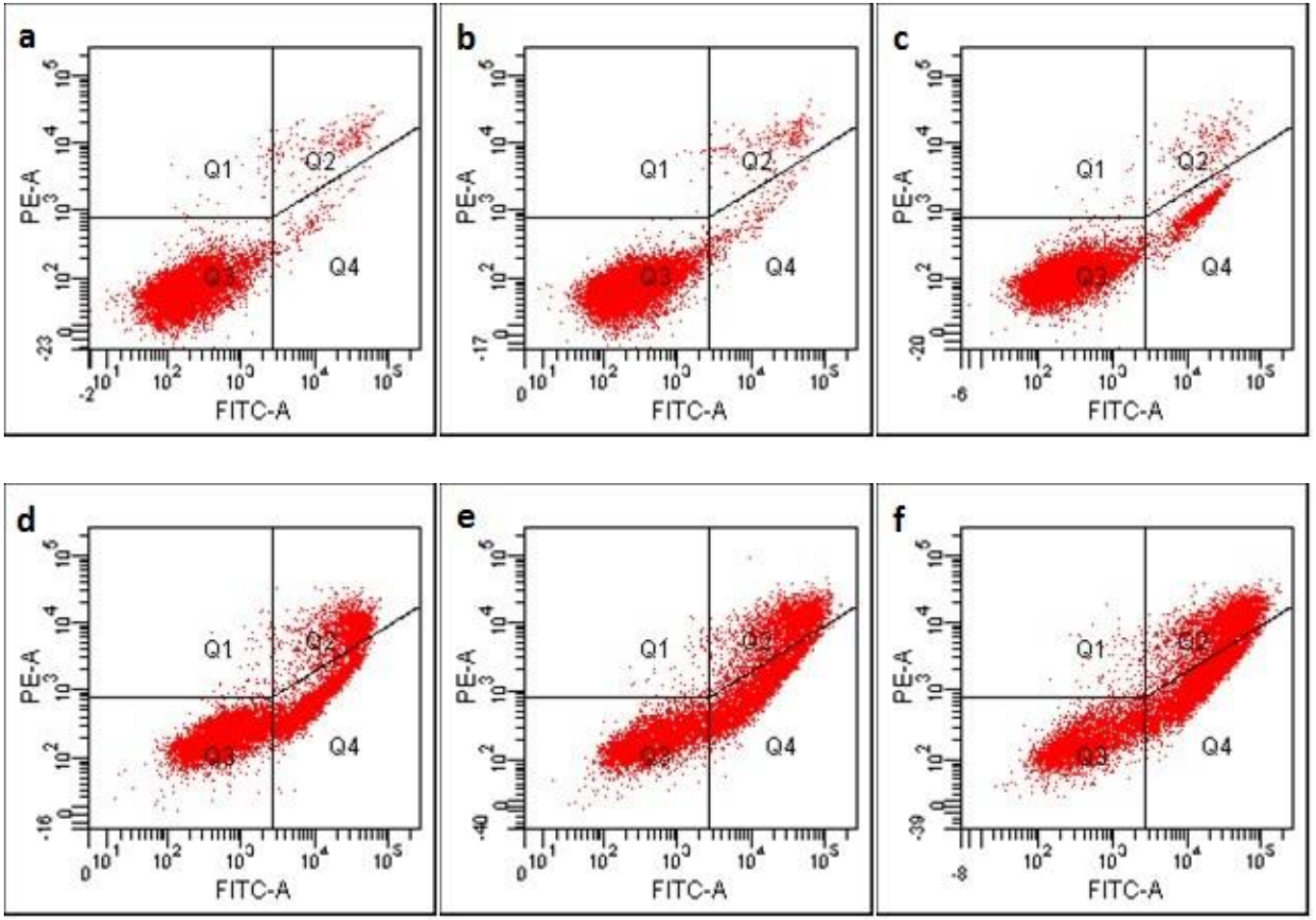

Figure 4.8: ADC induces apoptosis in HCT116 and LoVo cells in a dose-dependent manner. (A) Bar graph showing mean ± SEM of the apoptosis percentage in HCT116 cells after 72 h of treatment with different concentrations of ADC (n = 3); (B) Bar graph showing mean ± SEM of the apoptosis percentage in LoVo cells after 72 h of treatment with different concentrations of ADC (n = 3).**, $P < 0.01$; ***, $P < 0.001$ (versus 0 μg/ml control); (C) Representative data from triplicated experiments showing the pro-apoptotic effect of ADC in HCT116 cells. Q1: necrotic cells; Q2: late apoptotic cells; Q3: living cells; and Q4: early apoptotic cells. (a) 0 μg/ml ADC (control); (b) 6.25 μg/ml ADC; (c) 12.5 μg/ml ADC; (d) 25 μg/ml ADC; (e) 50 μg/ml ADC; (f) 100 μg/ml ADC.

4.2.3 ADC-induced apoptosis in HCT116 cells follows the mitochondrial pathway

The mechanism of ADC-induced apoptosis in HCT116 cells was then studied. Based on the findings by Sheen *et al.* (2011) that leucine deprivation causes cell death through the mitochondrial apoptotic pathway, it is hypothesized that the lack of arginine may also act as a negative stimulus of apoptosis by increasing the permeability of mitochondria, and may hence cause the release of pro-apoptotic proteins into the cytosol.

HCT116 cells were treated with 50 μg/ml ADC for 72 h, stained with JC-1, and analyzed by flow cytometry. As a cationic dye, JC-1 accumulates potential-dependently in the form of red fluorescent aggregates in mitochondria, and it dissociates into green fluorescent monomers when diffused into cytosol due to the change of electrochemical gradient of mitochondrial outer membrane (MOM). As shown in Figure 4.9, the decrease of red/green fluorescence intensity ratio in ADC-treated HCT116 cells indicates the depolarization of mitochondria and increase of mitochondrial outer membrane permeabilization (MOMP). The percentage of ADC-treated HCT116 cells with increased MOMP is ~50% which is quite comparable to the apoptotic population (~57%, Section 4.2.1). This result suggests that a major portion of HCT116 cell population dies through the mitochondrial apoptotic pathway upon ADC treatment which is reasonable, as ADI has also been reported to reduce the mitochondrial

membrane potential in the ASS-deficient breast cancer cell line MDA-MB-231 (Qiu *et al.*, 2014).

In contrast, a preliminary experiment on LoVo cells shows that the effect of ADC on MOMP is less obvious in this cell line (Appendix Figure 8). Even in untreated LoVo cells, a high basal level of increased MOMP has been detected (Appendix Figure 8) which is consistent with the high basal level of apoptosis observed in this cell line (Section 4.2.2).

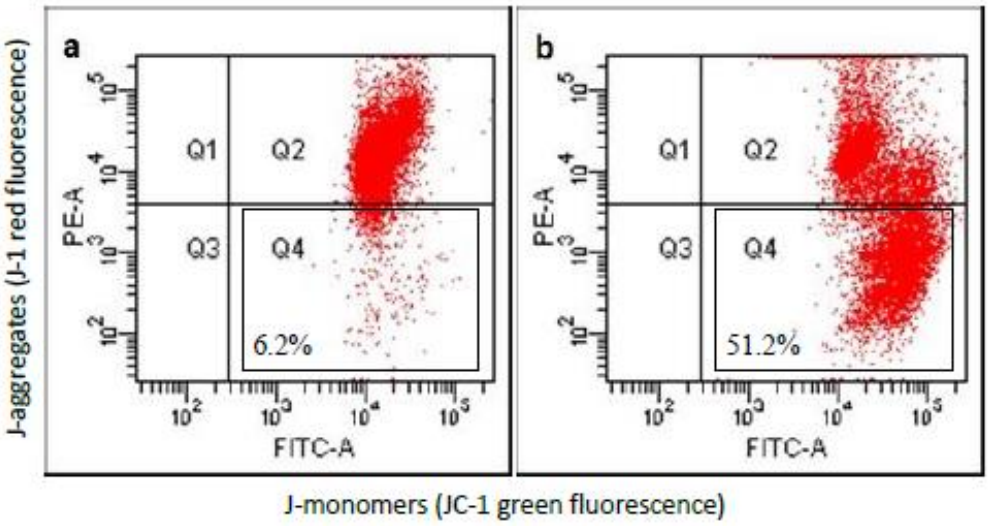

Figure 4.9: Representative data from triplicated experiments showing changes in MOMP in ADC-treated HCT116 cells using JC-1 dye and flow cytometry. Cells were grown for 72 h prior to analysis. a, control (0 μg/ml ADC); b, 50 μg/ml ADC.

4.2.4 ADC-induced apoptosis is caspase-3-dependent in HCT116 cells and caspase-3-independent in LoVo cells

As the release of mitochondrial contents can activate caspases to execute apoptosis, we then detected whether caspases had truly been activated by focusing on caspase-3, a typical caspase in apoptotic study.

When treated with 50 μg/ml of ADC for 72 h, ~51% of ADC-treated HCT116 cells become caspase-3-activated (Figure 4.10 A), which is quite consistent with the apoptotic population (~57%, Section 4.2.1). This result suggests that apoptosis induced by ADC in HCT116 cells is caspase-3-dependent. Similarly, the majority of apoptotic HCT116 cells in the BCA treatment group may follow the caspase-3-dependent pathway (Appendix Figure 7 A, Appendix Figure 9 A)

Further examination on the cleavage of poly (ADP-ribose) polymerase (PARP), a known substrate of caspase-3, shows that cleavage of PARP in HCT116 cells is invisible until after 12 h of ADC treatment (Figure 4.11). This finding is consistent with the flow cytometry results and also provides some clues on the timing of ADC-induced apoptosis in HCT116 cells.

Compared to HCT116, the case of LoVo cells is more complicated. Consistent with the relatively high basal level of apoptosis, high basal level of active caspase-3 (Figure 4.10, Appendix Figure 9 B) and cleaved PARP (Figure 4.11 B) are observed in LoVo cells. Compared to cells grown in complete medium (12% cells with active caspase-3), the treatment of either

21 or 42 μg/ml of BCA further increases the percentage of LoVo cells with activate caspase-3 to ~25% (Appendix Figure 9 B) yet such a proportion is only around half of the apoptotic population (52%, Appendix Figure 7 B). The addition of ADC, nevertheless, does not induce further activation of caspase-3 and cleavage of PARP in LoVo cells (Figure 4.10 B, Figure 4.11 B). Therefore, in LoVo cells, the apoptosis-inducing effect triggered by ADC may be caspase-3-independent, while the effect triggered by BCA may be a combination of caspase-3-dependent and caspase-3-independent events. These distinct responses of HCT116 and LoVo cells towards ADC and BCA suggest that the detailed apoptotic pathway induced by enzymatic arginine deprivation is not only cell line-dependent but also enzyme-dependent.

A

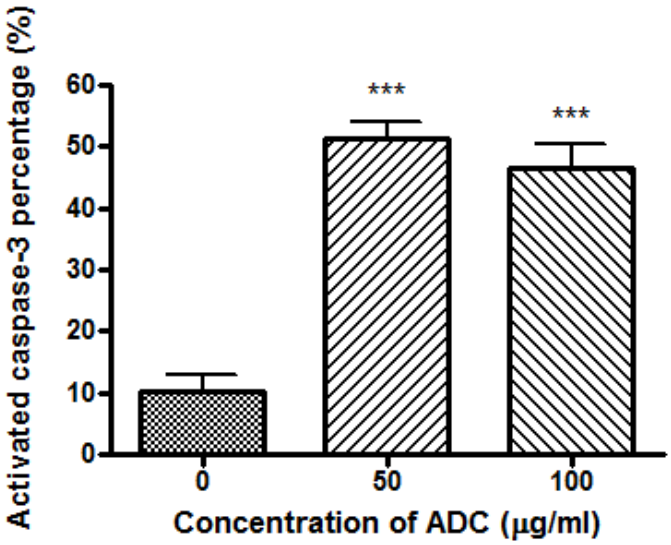

B

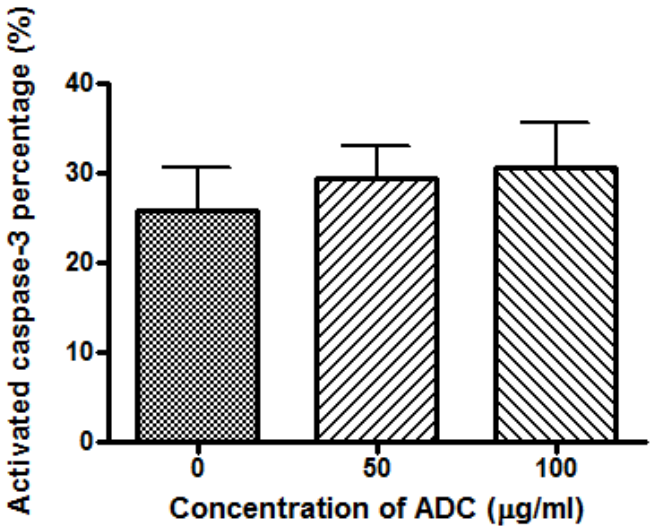

Figure 4.10: FITC-DEVD-FMK staining and flow cytometry results showing the percentage of (A) HCT116 and (B) LoVo cell population with active caspase-3 upon ADC treatment. Data are expressed as mean ± SEM of three individual experiments. ***, $P < 0.001$ (versus 0 µg/ml control).

A

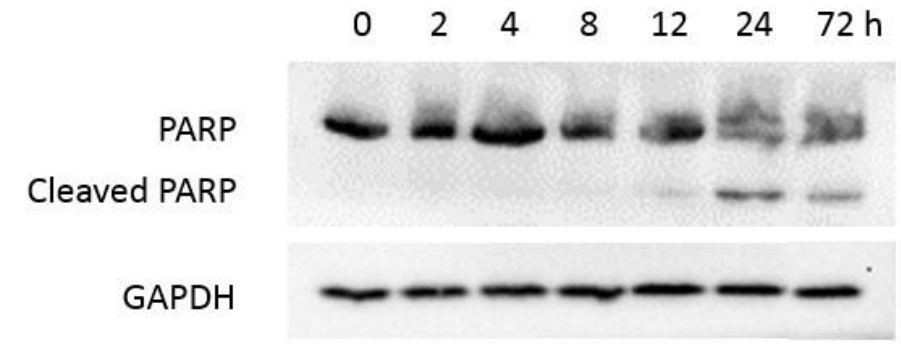

B

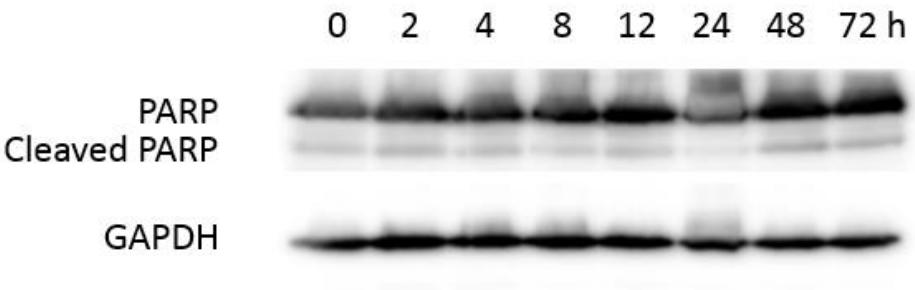

Figure 4.11: Immunoblot analysis showing the time-dependent effect of 50 μg/ml ADC on the cleavage of PARP in (A) HCT116 cells and (B) LoVo cells.

4.2.5 ADC inhibits the ERK signaling pathway in HCT116 cells

Extracellular signal-regulated kinase (ERK; ERK1 and ERK2) is a key regulator for cell growth and proliferation and has been identified as a pro-survival factor with anti-apoptotic effect in most cases (Lu and Xu, 2006). The effect of ADC on ERK1/2 was therefore examined in this project. According to the immunoblot result shown in Figure 4.12, phosphorylated ERK1/2 is detected in untreated HCT116 cells, indicating the activation of ERK pathway under normal growth conditions. Both rapamycin (an mTOR inhibitor) and LY294002 (a PI3K inhibitor) do not alter the phosphorylation of ERK1/2 (Figure 4.12). In contrast, treatments with ADC and BCA both decrease the level of p-ERK1/2 which may provide a mechanistic explanation for their induction of apoptosis in HCT116 cells (Figure 4.12). In stark contrast to the downregulation of ERK activity by BCA and ADC in HCT116 cells observed in this study, it has been reported that ERK is activated upon ADI-PEG20 treatment in several melanoma cell lines (Tsai *et al.*, 2012). The activation of ERK signaling pathway by ADI-PEG20 is believed to be related to the upregulation of cellular ASS and the cell resistance to ADI (Tsai *et al.*, 2012).

Interestingly, treatment with AFM only slightly decreases the level of phosphorylated ERK1/2 (Figure 4.12), suggesting that arginine-depletion is not the main reason for the inhibitory effect on ERK1/2 by ADC and BCA. Therefore, both ADC and BCA may act on the ERK pathway through mechanisms other than arginine-depletion. Experiments testing whether the

catalytic products of ADC and BCA (agmatine and ornithine, respectively) can affect the ERK signaling should be conducted in the future. Alternate time points should also be studied.

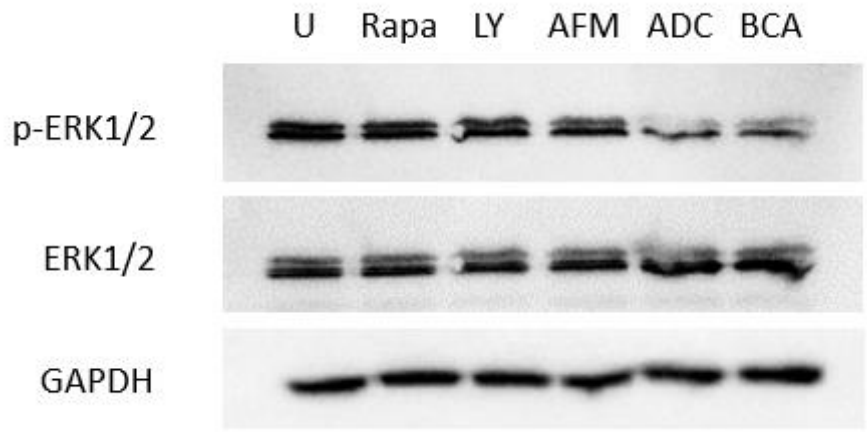

Figure 4.12: Immunoblot analysis showing the effects of different treatments on the ERK1/2 activity in HCT116 cells. Cells were grown in complete medium with the specified reagents for 24 h before analysis. U, untreated cells grown in complete medium; Rapa, 10 nM rapamycin; LY, 25 μM LY294002; AFM, arginine-free medium; ADC, 50 μg/ml ADC; BCA, 50 μg/ml BCA.

4.3 ADC may not induce autophagy in HCT116 and LoVo cells

Apart from apoptosis, autophagy is another possible pathway triggered by arginine-depletion. Previous research has found that ADI triggers autophagy in prostate cancer and melanoma cells (Kim, Bold *et al.*, 2009; Kim, Coates *et al.*, 2009; Savaraj *et al.*, 2010). In this project, the autophagy-inducing effect of ADC was explored.

HCT116 and LoVo cells were treated with 50 μg/ml ADC for different periods and were analyzed by immunoblot assay. As shown in Figure 4.13, LC3-II in both cell lines is detectable at all the time points studied, indicating the ongoing of autophagy which involves the conversion of LC3-I to LC3-II. At time zero, autophagy occurs at a basal level. At 12 and 24 h of ADC treatment, the increased intensity of not only LC3-II but also LC3-I in HCT116 cells indicates that the degradation of these molecules may have been temporarily inhibited (Figure 4.13 A). In LoVo cells, on the other hand, the levels of both LC3 molecules remain relatively constant throughout the 72 h of ADC treatment period, suggesting that LoVo cells may have a higher basal level of autophagy, and the autophagy process is not likely to be intensified by the treatment of ADC (Figure 4.13 B).

We then examined the effect of HCQ, an autophagy inhibitor, in HCT116 cells. The IC_{50} value of HCQ in HCT116 cell line is around 50 μM (Table 4.5). We then tested whether the supplementation of HCQ, at a relative less toxic dose, would have an impact on the anti-cancer effect of

ADC. The preliminary MTT assay result shows that the addition of 25 μM HCQ generally has no impact on HCT116 cells treated with various concentrations of ADC (Figure 4.14). This result, together with the previous one on the levels of LC3 molecules, suggest that ADC may not induce autophagy in HCT116 cells.

To further confirm our hypothesis, the combination effect of ADC and HCQ was studied. It is found that ADC has an antagonistic effect with HCQ at both 24 h and 72 h of treatment periods (Table 4.6, Table 4.7, and Figure 4.15), indicating that these two reagents may induce cell death through distinct pathways.

A

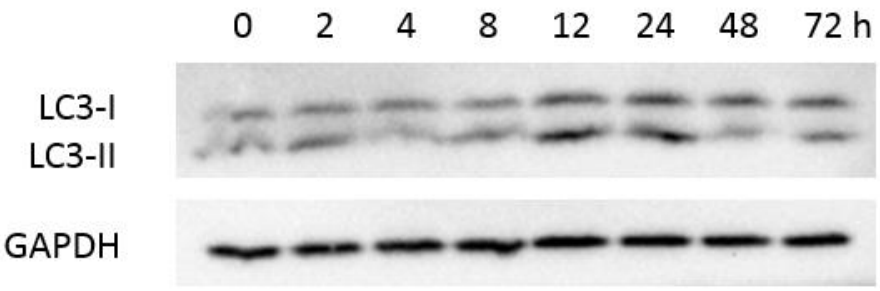

B

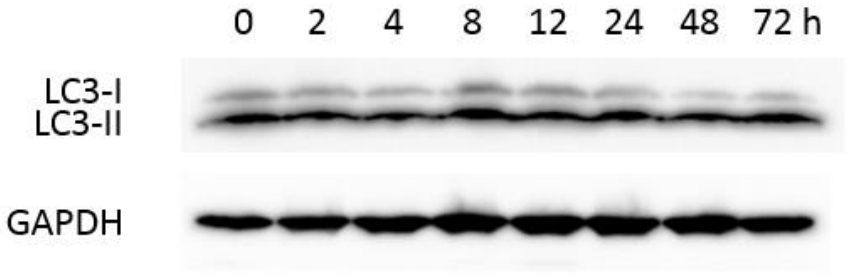

Figure 4.13: Immunoblot analysis showing the effect of 50 μg/ml ADC on LC3 in (A) HCT116 and (B) LoVo cells.

Table 4.5: IC_{50} of HCQ in HCT116 cells. Cells were treated with HCQ for 24 and 72 h prior to MTT assay. IC_{50} values are calculated based on the results of three experiments performed in triplicate.

Tumor cell line	IC_{50} of HCQ (μM)	
	24 h	72 h
HCT116	56.85	47.53

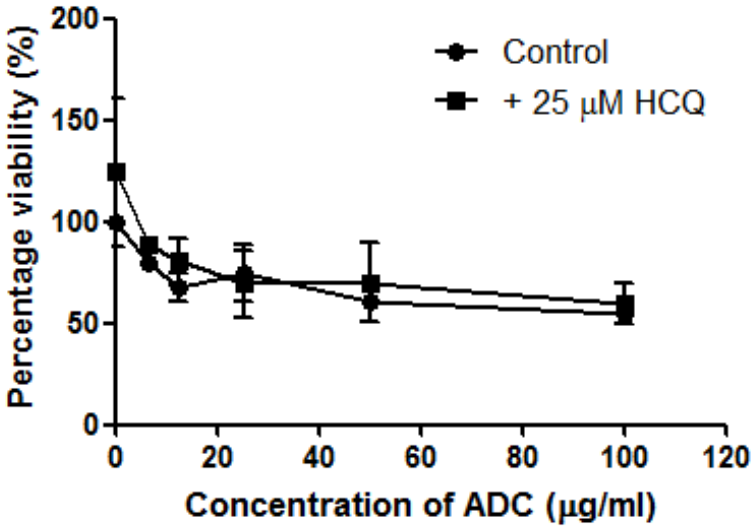

Figure 4.14: *In vitro* growth inhibition curves showing the effect of HCQ in ADC-treated HCT116 cells (preliminary). Cells were incubated with different concentrations of ADC for 24 h in complete medium (control) or medium supplemented with 25 μM HCQ. Data are expressed as percentage of the cell population at 0 μg/ml ADC in control group and are the mean ± SEM of two experiments performed in triplicate.

Table 4.6: Combination index (CI) values of the combination therapy of ADC and HCQ at the ratio of 1:2 in HCT116 cells. Cells were treated for 24 h prior to MTT assay. The data are calculated by Calcusyn based on the results of three experiments performed in triplicate. A combination is defined as synergistic when CI value is less than 1, additive when CI equals to 1, and antagonistic when CI is greater than 1 (Chou and Talalay, 1984).

Arginine-depleting enzyme	CI at IC_{50}	CI at IC_{75}	CI at IC_{90}
ADC	2.11	1.73	1.77

r = 0.98

Table 4.7: CI values of the combination therapy of arginine-depleting enzymes and HCQ at the ratio of 1:1 (ADC: HCQ) and 1:0.616 (BCA: HCQ) in HCT116 cells. Cells were treated for 72 h prior to MTT assay. The data are calculated by Calcusyn based on the results of three experiments performed in triplicate.

Arginine-depleting enzyme	CI at IC_{50}	CI at IC_{75}	CI at IC_{90}
ADC	3.97	2.24	1.48
BCA	828.47	3.86	2.38

r = 0.80 for ADC + HCQ; r = 0.97 for BCA + HCQ

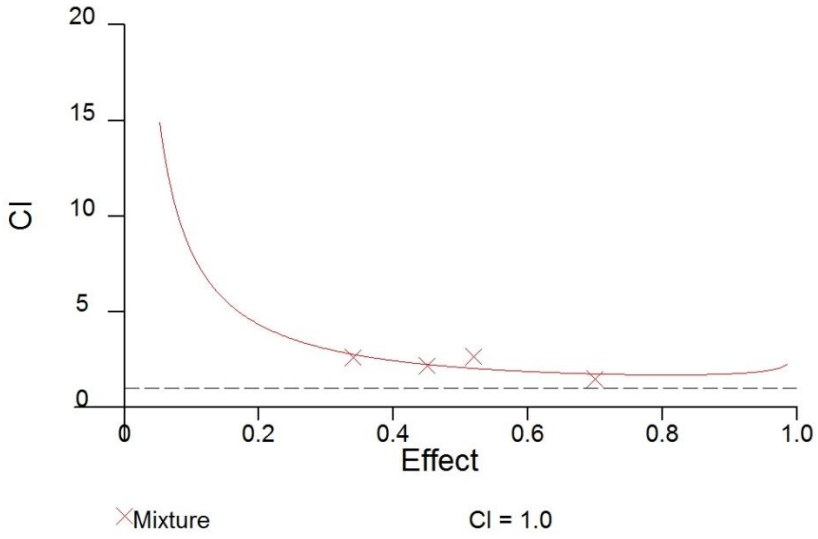

Figure 4.15: Illustrative Fa-CI plot for the combination effect of ADC and HCQ at a 1:2 fixed drug ratio in HCT116 cells. Cells were treated for 24 h prior to MTT assay. The graph is generated by Calcusyn based on the results of three experiments performed in triplicate. Fa: fraction of the system affected.

4.4 ADC induces S and/or G_2/M phase cell cycle arrest in HCT116 and LoVo cells

To investigate the effect of ADC on cell cycle progression, HCT116 cells were exposed to different concentrations of ADC for 72 h and analyzed by flow cytometry for their cell cycle profiles. In the absence of ADC, the cell populations at G_0/G_1, S and G_2/M phases are ~69%, 21% and 10%, respectively (Table 4.8). The S phase subpopulation remains steady at low doses of ADC, but rises at 25, 50 and 100 μg/ml ADC in a dose-dependent manner (Table 4.8). The G_2/M phase proportion slightly increases in response to ADC treatment and peaks at 25 μg/ml ADC (Table 4.8). BCA also results in S and G_2/M phase arrest in HCT116 cells (Appendix Table 1).

To explore whether this cell cycle arrest pattern is unique for HCT116 cell line, LoVo cells were used for the same study. Results have shown that LoVo cells arrest at G_2/M phase following the exposure to low doses of ADC and switch to S phase arrest when the doses of ADC become higher (Table 4.9), but only arrest at S phase when treated with BCA (Appendix Table 2).

ADI treated tumor cells often arrest at G_0/G_1 phase (Gong *et al.*, 1999; Gong *et al.*, 2000; Kim, Kim *et al.*, 2009). As the effect of neither ADI nor arginase in colorectal cancer cells has been reported, the previous findings may not provide much reference to this project. However, S and/or G_2/M

phase arrest is not a preserve of ADC- and BCA-treated colorectal tumor cells. While there are reports that ADI induces G_0/G_1 cell cycle arrest in cell lines such as SNU-1 (stomach adenocarcinoma), SH-EP (neuroblastoma), and DU145 (prostate carcinoma) (Kang *et al.*, 2000; Kim, Kim *et al.*, 2009), S phase arrest is observed in some other ADI-treated cell lines including WAC2 (neuroblastoma), SaOS (osteosarcoma), and Jurkat (leukemia) (Gong *et al.*, 1999; Gong *et al.*, 2000). S and G_2/M arrest have also been observed in hepatocellular carcinoma (HCC) cell lines treated with pegylated recombinant human arginase I (rhArg-PEG) (Lam *et al.*, 2009). It is reported that rhArg-PEG results in S phase arrest in HepG2 and PLC/PRF/5 cells while G_2/M arrest in Hep3B cells (Lam *et al.*, 2009).

Table 4.8: Cell cycle distribution of HCT116 after 72 h of treatment with ADC, as measured by PI staining and flow cytometry. Data are shown as mean ± SD (n = 3). One-way ANOVA reveals significant effects of ADC on S and G_2/M phase subpopulations. *Post hoc* Dunnett's test of treatment versus control: **, $P < 0.01$.

ADC (μg/ml)	G_0/G_1 (%)	S (%)	G_2/M (%)
0	68.9 ± 2.78	20.9 ± 1.38	10.2 ± 1.60
6.25	65.3 ± 6.55	19.1 ± 5.51	15.4 ± 1.06
12.5	64.9 ± 0.69	19.7 ± 0.61	15.4 ± 0.15
25	54.0 ± 3.24	29.0 ± 3.11	17.0 ± 2.74**
50	48.0 ± 4.11	37.0 ± 4.37**	15.0 ± 0.54
100	48.5 ± 4.29	35.8 ± 2.23**	15.7 ± 3.88

Table 4.9: Cell cycle redistribution of LoVo cells after 72 h of treatment with ADC, as measured by PI staining and flow cytometry. Data are shown as mean ± SD (n = 3). One-way ANOVA reveals significant effects of ADC on S and G_2/M phase subpopulations. *Post hoc* Dunnett's test of treatment versus control: **, $P < 0.01$.

ADC (μg/ml)	G_0/G_1 (%)	S (%)	G_2/M (%)
0	44.1 ± 2.45	43.5 ± 3.52	12.4 ± 2.18
6.25	37.4 ± 2.67	45.7 ± 3.21	16.9 ± 0.55**
12.5	39.7 ± 4.67	42.4 ± 3.23	17.9 ± 1.77**
25	32.8 ± 4.76	53.0 ± 4.83	14.2 ± 1.40
50	34.0 ± 3.61	58.9 ± 3.43**	7.2 ± 0.20**
100	26.2 ± 1.42	72.6 ± 0.46**	1.2 ± 1.03**

4.5 Drug combination studies

4.5.1 ADC shows concentration-dependent interaction with doxorubicin in HCT116 cells

Doxorubicin, an anthracycline antibiotic agent, is regarded as one of the most potent chemotherapeutic drugs approved by FDA (Carvalho *et al.*, 2009). For decades, doxorubicin has been acknowledged for its effect against rapid dividing cells due to its ability of causing DNA damages as well as producing free radicals. However, doxorubicin exhibits severe side effects as it is also toxic to non-cancerous cells (Tacar *et al.*, 2013).

An *in vivo* study has demonstrated that doxorubicin has little effect when used alone in colorectal tumor cells but shows moderate effect when used together with other chemotherapeutic agents including 5-FU and cyclophosphamide (Corbett *et al.*, 1977). Therefore, we would like to study whether the combination of ADC can make doxorubicin a more potent drug in colorectal tumor cells.

Combinations of doxorubicin with arginine-depleting enzymes were analyzed in HCT116 cells with ratios of 40:1 (doxorubicin: ADC) and 6:1 (doxorubicin: BCA) by MTT assay. As illustrated by Table 4.10 and Figure 4.16, ADC and doxorubicin are antagonistic at IC_{50}, but exhibit synergy at IC_{75} and IC_{90}. Similarly, BCA and doxorubicin are antagonistic at low and intermediate concentrations, but are synergistic at IC_{90} (Table 4.10).

As suboptimal drug dosages may increase the likelihood of drug-resistance (Bulgheroni *et al.*, 2004), synergy at higher concentrations of anti-cancer agents is therefore more relevant for therapy (Chou, 2010). However, *in vitro* studies are not enough to demonstrate the potential of ADC as an anti-cancer drug in combination with doxorubicin, as pharmacokinetic factors should also be taken into consideration in *in vivo* and clinical studies. Besides, the toxicity of combined drugs for the patients is an important issue. Hence the combination of ADC and BCA with doxorubicin on the treatment of colorectal cancer is promising yet challenging at this moment.

Table 4.10: CI values of the combination therapy of arginine-depleting enzymes and doxorubicin at the ratio of 1:40 (ADC: doxorubicin) and 1:6 (BCA: doxorubicin) in HCT116 cells. Cells were treated for 72 h prior to MTT assay. Data are calculated by Calcusyn based on the results of three experiments performed in triplicate.

Arginine-depleting enzyme	CI at IC_{50}	CI at IC_{75}	CI at IC_{90}
ADC	1.24	0.98	0.85
BCA	2904.76	3.24	0.23

r = 0.96 for both ADC and BCA combinations with doxorubixin

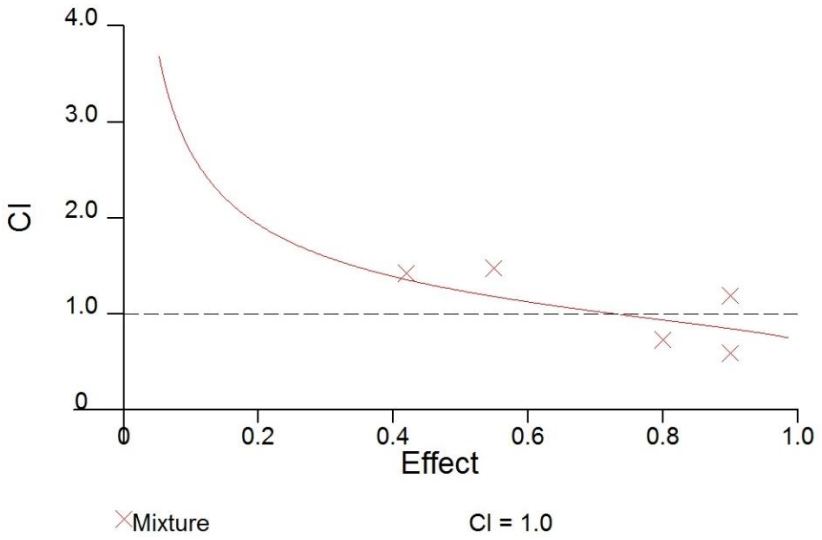

Figure 4.16: Illustrative Fa-CI plot for the combination effect of ADC and doxorubicin at a 1:40 fixed drug ratio in HCT116 cells. Cells were treated for 72 h prior to MTT assay. The graph is generated by Calcusyn based on the results of three experiments performed in triplicate.

4.5.2 ADC shows antagonism with verapamil in HCT116 cells

Verapamil is a drug for the treatment of various diseases including cardiac arrhythmias and hypertension (Meister *et al.*, 2010). Its phenylalkylamine derivative inhibits the calcium flux into the cells (McTavish and Sorkin, 1989). It has also shown some effects against cancer cells, usually used as a combination drug. Muller *et al.* (1994) shows that verapamil can reduce drug resistance in leukemia cells. *In vitro* experiments have found that verapamil is able to enhance the effect of the drug bortezomib in myeloma (Meister *et al.*, 2010) and mantle cell lymphoma cells (Chen *et al.*, 2012). Another group of researchers have also pointed out that verapamil has synergistic effect with gambogic acid in HepG2 (human hepatocellular carcinoma) and K-562 (human chronic myelogenous leukemia) cells through the inhibition of proteasome as well as the production of reactive oxygen species (ROS) (Liu *et al.*, 2014).

To investigate whether the addition of verapamil could enhance the cytotoxic effect of arginine-depleting enzymes, combinations of verapamil with arginine-depleting enzymes were analyzed in HCT116 cells with ratios of 1:1 (verapamil: ADC) and ~0.62:1 (verapamil: BCA) by MTT assay. As shown in Table 4.11 and Figure 4.17, combinations using ADC and verapamil are antagonistic at all concentrations tested. Similar results are observed in BCA and verapamil combinations, with the exception of IC_{90} where the effect is synergistic (Table 4.11). In general, verapamil is not considered as a suitable combination drug for ADC and BCA.

Table 4.11: CI values of the combination therapy of arginine-depleting enzymes and verapamil at the ratio of 1:1 (ADC: verapamil) and 1:0.616 (BCA: verapamil) in HCT116 cells. Cells were treated for 72 h prior to MTT assay. Data are calculated by Calcusyn based on the results of three experiments performed in triplicate.

Arginine-depleting enzyme	CI at IC_{50}	CI at IC_{75}	CI at IC_{90}
ADC	1.12	1.29	1.50
BCA	1594.21	13.55	0.47

r = 0.95 for ADC + verapamil; r = 0.99 for BCA + verapamil

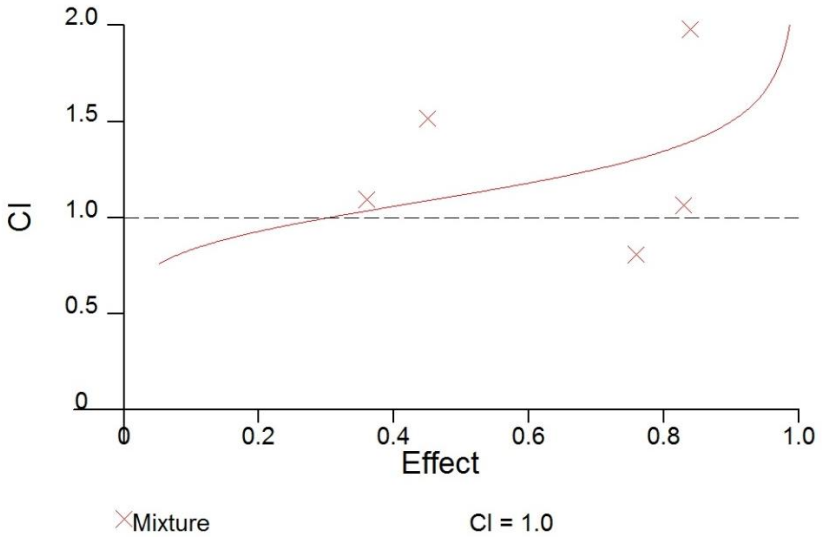

Figure 4.17: Illustrative Fa-CI plot for the combination effect of ADC and verapamil at a 1:1 fixed drug ratio in HCT116 cells. Cells were treated for 72 h prior to MTT assay. The graph is generated by Calcusyn based on the results of three experiments performed in triplicate.

4.5.3 ADC shows concentration-dependent interaction with LY204002 in HCT116 cells

PI3K/Akt is an important signaling pathway for cell growth and proliferation. Therefore the effect of ADC on this pathway was examined.

According to the immunoblot result in Figure 4.18 A, treatments of AFM, BCA and ADC all lead to increased phosphorylated Akt, indicating the possible activation of PI3K/Akt pathway in HCT116 cells upon arginine starvation. Treatment with AFM only slightly increases the level of phosphorylated Akt, suggesting that arginine-depletion is not the only reason for the activation of Akt by ADC and BCA in HCT116 cells (Figure 4.18 A). Therefore, both ADC and BCA may act on the Akt pathway through other mechanisms besides arginine-depletion, such as their production of agmatine and ornithine, respectively. In this experiment, phosphorylated Akt is not detected in untreated HCT116 cells (Figure 4.18 A), yet another experiment with higher amount of proteins reveals that untreated HCT116 possesses low level of phosphorylated Akt (Figure 4.18 B). This second experiment also confirms that ADC can activate Akt in HCT116 cells (Figure 4.18 B). When examining the downstream molecules such as mTOR and p70S6K, however, the effect of ADC is less obvious (Figure 4.18 B), which is probably because mTOR and p70S6K are also regulated by other upstream signaling molecules.

As ADC has been found to inhibit the ERK1/2 activity (Section 4.2.5), we would like to examine if the dual inhibition of ERK and PI3K/Akt pathways through a combination of ADC and a PI3K inhibitor can result in further cell death. Therefore, HCT116 cells were grown in combinations of LY294001 with ADC at a constant ratio of 1:1.25 (LY294002: ADC) for 72 h and analyzed by MTT assay. The IC_{50} value of LY294002 alone in HCT116 cells is 22.36 mM. According to the results in Table 4.12 and Figure 4.19, ADC and LY294002 are antagonistic at lower concentrations but tend to be synergistic at IC_{90}.

Interestingly, according to the immunoblot result, LY294002 at a concentration close to its IC_{50} value in HCT116 cells does not act as a PI3K inhibitor but instead increases the proportion of phosphorylated Akt (Figure 4.18 A). While this finding may explain the antagonistic interaction between ADC and LY294002 at low concentrations, there may be a need to examine the quality of LY294002 used in this project. Further studies with different doses of LY294002 on cellular Akt activity at multiple time intervals should be examined to generate a full picture of this issue.

A

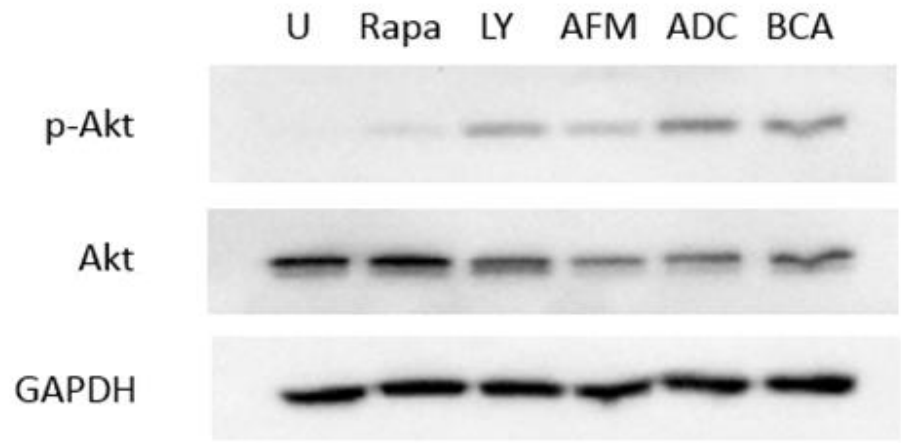

B

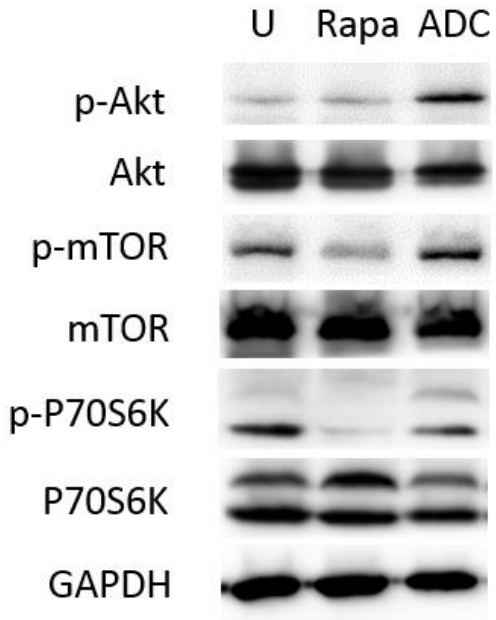

Figure 4.18: Immunoblot analysis showing the effects of different treatments on the Akt activity in HCT116 cells. Cells were grown in complete medium with different reagents for 24 h before analysis. U, untreated cells grown in complete medium; Rapa, 10 nM rapamycin; LY, 25 μM LY294002; AFM, arginine-free medium; ADC, 50 μg/ml ADC; BCA, 50 μg/ml BCA.

Table 4.12: CI values of the combination therapy of ADC and LY294002 at the ratio of 1:0.8 (ADC: LY294002) in HCT116 cells. Cells were treated for 72 h prior to MTT assay. Data are calculated by Calcusyn based on the results of three experiments performed in triplicate.

Arginine-depleting enzyme	CI at IC_{50}	CI at IC_{75}	CI at IC_{90}
ADC	1.88	1.18	0.81

r =0.98986

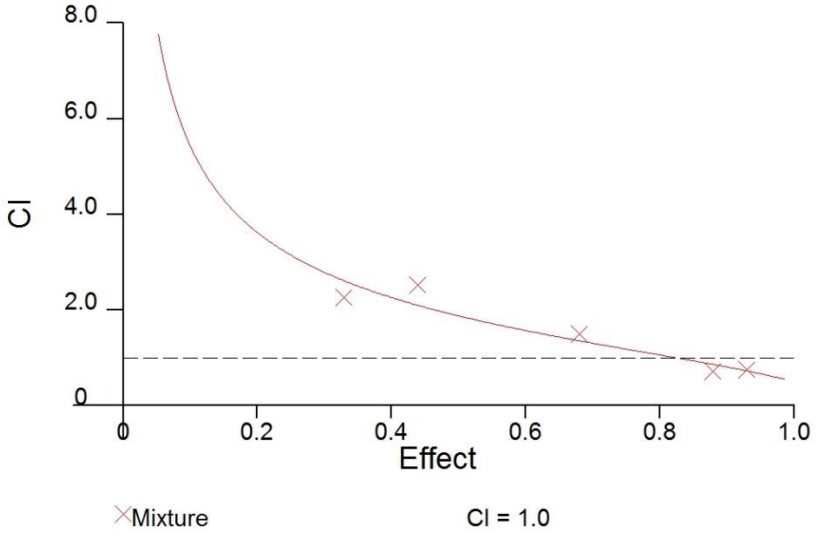

Figure 4.19: Illustrative Fa-CI plot for the combination effect of ADC and LY294002 at a 1:0.8 fixed drug ratio in HCT116 cells. Cells were treated for 72 h prior to MTT assay. The graph is generated by Calcusyn based on the results of three experiments performed in triplicate.

Chapter 5

Results: ADC-ABD and a preview of its usage in *in vivo* studies

5.1 Expression and purification of ADC-ABD

Figure 5.1 shows the chromatogram of ADC-ABD purification. During elution, the first peak which was considered to contain non-specific proteins occurred when the column is washed with 0.06 M imidazole (Figure 5.1). When the concentration of imidazole was raised to 0.15 M, the second peak occurred and reached its summit at around 0.3 M imidazole (Figure 5.1). Compared to ADC which starts to be eluted at ~0.1 M imidazole (Figure 3.1), the elution time for ADC-ABD requires higher imidazole concentration, indicating that ADC-ABD binds to the nickel affinity column more tightly than ADC.

According to the SDS-PAGE gel image, the second peak mainly consists of a target protein of around 76 kDa (Figure 5.2, lanes F6-F14). This target protein is likely to be ADC-ABD since the calculated molecular weight of ADC-ABD monomer based on its amino acid sequence is 77.38 kDa. Therefore, ADC-ABD has been successfully expressed and purified. Fractions containing relatively pure ADC were pooled together and exchanged buffer using centrifugal filter device (Amicon). The 50,000 MW

cut-off of the membrane helps to further remove some of the unwanted small proteins in the sample.

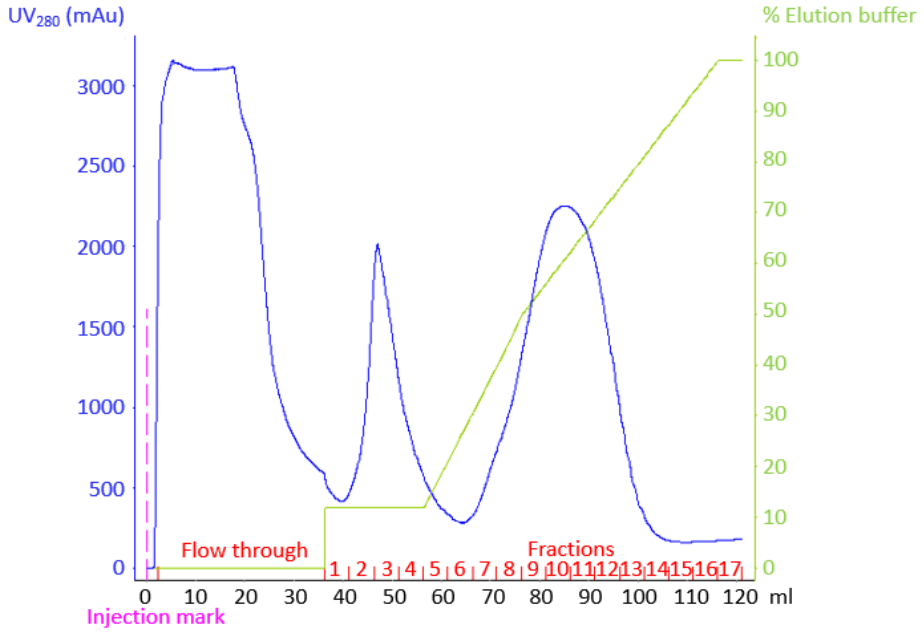

Figure 5.1: Elution profile of the purification of ADC-ABD from 5 g *E. coli* wet cell pellet (produced by fed-batch fermentation) by a single step of nickel-charged 5 ml HiTrap^{TM} chelating HP column chromatography. mAU, milli absorption unit; 100% B = 0.5 M imidazole.

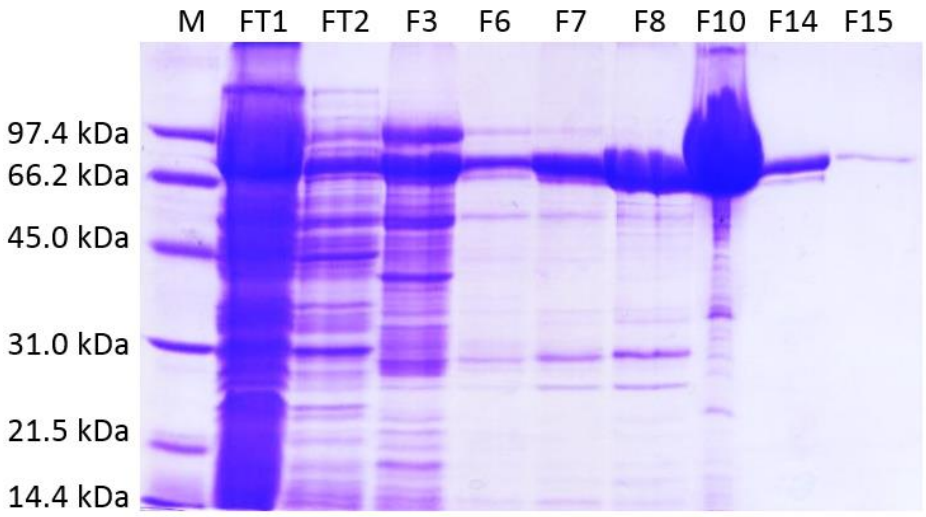

Figure 5.2: SDS-PAGE analysis of the column fractions from nickel affinity chromatography for ADC-ABD. M, SDS-PAGE molecular weight standards, low range (Bio-Rad); FT1, flow through at an earlier stage; FT2, flow through at a later stage; F3-F15, eluted fractions from the column.

5.2 Overview of shake flask expression and purification of ADC-ABD

Since an alternate expression system was used, the expression of ADC-ABD by shake flask culture is ~50 mg/L *E. coli* culture and is only half of the value of ADC. However, much higher expression level of ADC-ABD can be achieved when using *E. coli* cells cultured by fed-batch fermentation. According to Dr. H. K. Yap, when using large-scale fermentation method, the yield of ADC-ABD is estimated to be ~1.2 g/L *E. coli* culture.

Our method results in ~3 fold of purification of ADC-ABD, and the yield of ADC-ABD is around 76%. The purity of the ADC-ABD final product is satisfactory as shown in Figure 5.3.

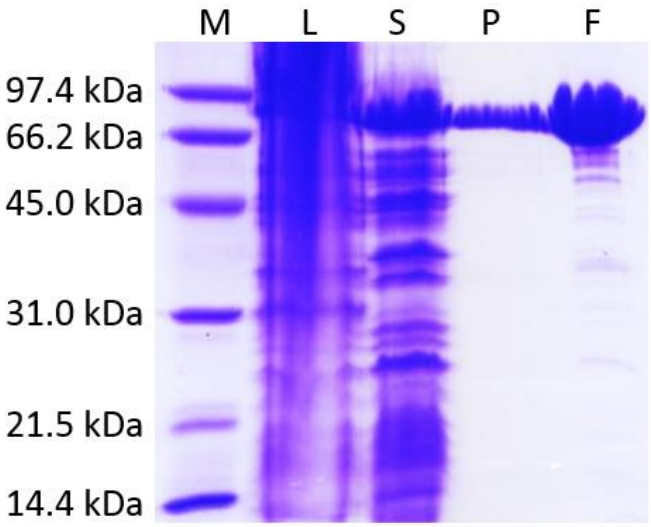

Figure 5.3: Representative image showing the SDS-PAGE analysis of a typical purification process for ADC-ABD from 9.4 g *E. coli* wet cell pellet (produced by fed-batch fermentation). M, SDS-PAGE molecular weight standards, low range (Bio-Rad); L, induced whole-bacterial lysate; S, the sonicated supernatant containing all soluble proteins which was to be loaded onto a nickel affinity column; P, pooled eluted fractions from the nickel affinity column containing relatively pure ADC-ABD; F, ADC-ABD final product after buffer exchange and supplementation of cofactors.

5.3 Specific activity and stability of ADC-ABD

The specific activity of ADC-ABD was measured by the same method as that for ADC. One unit of enzyme activity is defined as the amount of enzyme that catalyzes the production of 1 μmol urea per min under standard assay conditions. Based on our assay method, specific activity of freshly prepared ADC-ABD is 25.02 ± 1.17 U/mg (at 37 ℃, pH 8.0). This value, although slightly lower than that of ADC (28.88 ± 2.68 U/mg), indicates that the fusion of ABD has not altered much of the ADC activity.

Same as ADC, the final product of ADC-ABD contains ~4 mg/ml protein in 20 mM sodium phosphate buffer at pH 7.4 supplemented with 5 mM $MgCl_2$ and 0.1 mM PLP, and is stored at 4 ℃ in darkness. The protein concentration and specific activity of ADC-ABD seem to be relatively stable for at least 6 months as well (Figure 5.4). Yet more batches of proteins should be studied before drawing a solid conclusion.

A

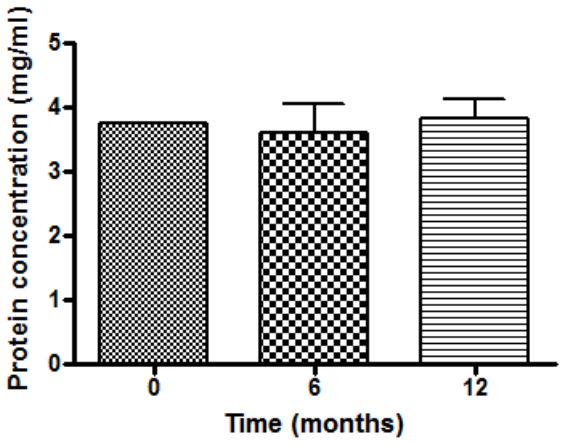

B

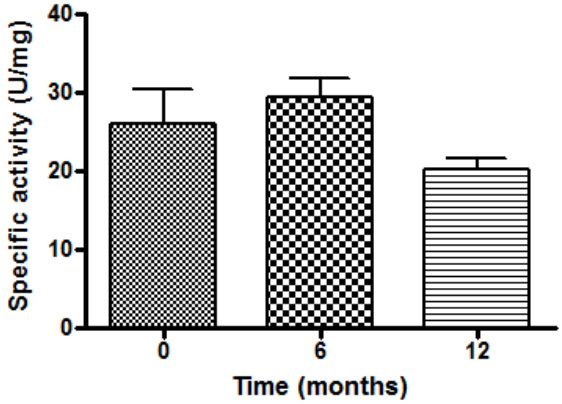

Figure 5.4: Effect of long-term storage on protein concentration and specific activity of ADC-ABD. ADC-ABD was formulated at ~4 mg/ml protein in 20 mM sodium phosphate buffer supplemented with 5 mM $MgCl_2$ and 0.1 mM PLP, and was stored at 4 ℃ in darkness. Data are expressed as mean ± SD of a single experiment performed in triplicate. All ADC-ABD-catalyzed reactions were performed under standard assay conditions (37 ℃, pH 8.0).

5.4 Removal of endotoxin from ADC and ADC-ABD

Protein concentrations and enzymatic activities before and after endotoxin removal were tested. For both ADC and ADC-ABD, ~90% proteins are recovered after endotoxin removal process, and the enzyme activities are not much affected (Figure 5.5). Therefore, phase separation by Triton X-114 is proved to be a proper method to remove endotoxin from ADC and ADC-ABD.

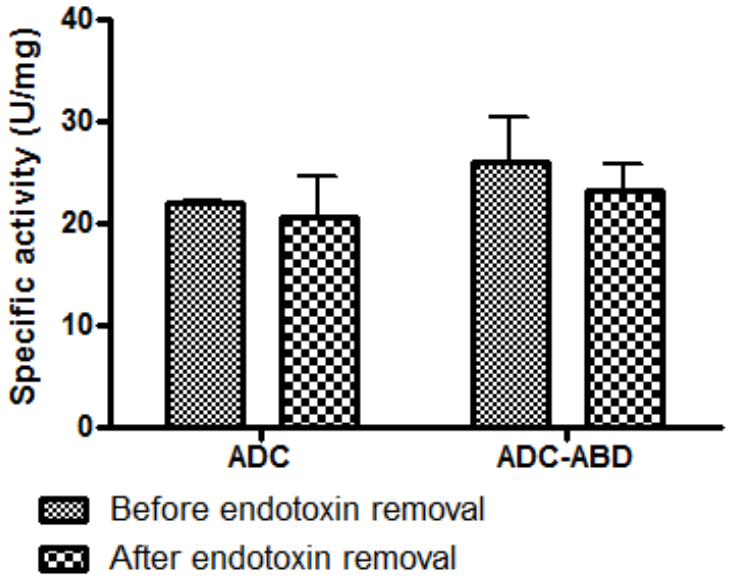

Figure 5.5: Effect of endotoxin removal by Triton X-114 on the activities of ADC and ADC-ABD. Data are expressed as mean ± SD of a single experiment performed in triplicate. All ADC- and ADC-ABD-catalyzed reactions were performed under standard assay conditions (37 ℃, pH 8.0).

5.5 *In vitro* anti-cancer properties of ADC-ABD

After 72 h of treatment with increasing concentrations of ADC-ABD, the viability of three colorectal cancer cell lines was tested by MTT assay and the results were compared with those of ADC.

As summarized in Table 5.1, ADC-ABD inhibits the growth of all the three colorectal cancer cell lines tested. Surprisingly, ADC-ABD is much more potent in all these three cell lines than ADC. It has also been observed that ADC-ABD is less effective than ADC in HCT116 cells yet exhibits similar maximum cytotoxicity as ADC in COLO 205 and LoVo cells.

Table 5.1: A comparison of the effects of ADC and ADC-ABD in three colorectal cancer cell lines. Cells were incubated in medium with one of the arginine-depleting enzymes for 72 h before MTT analysis. The IC_{50} value is calculated based on the results of three experiments performed in triplicate and is defined as the amount of an enzyme needed to achieve 50% inhibition of cell viability. Maximum cytotoxicity is expressed as the maximum percentage of nonviable cells achieved by 100 μg/ml of each enzyme which is the mean of three experiments performed in triplicate.

Cell Line	IC_{50} (μg/ml)		Maximum cytotoxicity (%)	
	ADC	ADC-ABD	ADC	ADC-ABD
HCT116	12.23	2.46	84.35	71.44
COLO 205	19.40	2.66	81.62	79.90
LoVo	38.09	17.81	66.17	62.06

5.6 *In vitro* binding to albumin of ADC-ABD

To investigate whether ADC-ABD could bind to serum albumin as expected, ADC-ABD was mixed with HSA at different ratios and analyzed on 10% native-PAGE gel. When the two proteins are mixed together, a new band which probably resembles the HSA-ADC-ABD complex is observed (Figure 5.6). According to native-PAGE analysis, the interaction between HSA and ADC-ABD is quite weak, as free HSA and ADC-ABD molecules are observed at almost every HSA-to-ADC-ABD ratio tested (Figure 5.6). It should be noticed that native-PAGE provides only a rough detection for the interaction between ABD fusion protein and albumin. Standard assay methods such as surface plasmon resonance should be tried in the future studies to examine the interaction between HSA and ADC-ABD in a more accurate way.

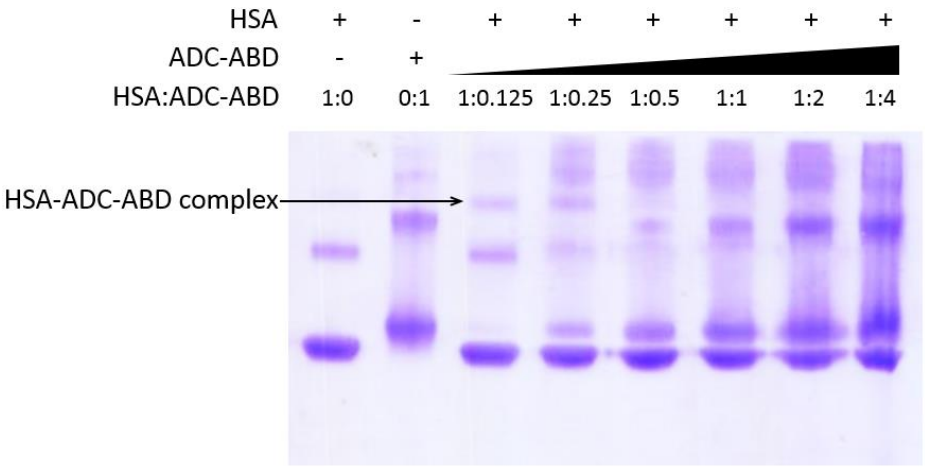

Figure 5.6: Native-PAGE analysis of the interaction between HSA and ADC-ABD. 4 μg of HSA was constantly loaded to each HSA-positive lane, Different amounts of ADC-ABD were used as indicated by the HSA: ADC-ABD ratio.

5.7 *In vivo* performance of ADC-ABD

In this preliminary study, ADC and ADC-ABD were administered to mice, and their arginine-depleting effects were investigated. As these two enzymes have not been studied *in vivo* so far, their proper dosages in mice are also aimed to be determined. ICR mice were chosen over BALB/c mice in this study as they are of bigger size, and hence are easier to handle and are able to tolerate higher doses of drugs. Various concentrations of ADC and ADC-ABD were injected to ICR mice. Lower dose of enzyme (1.25 mg) was administered intravenously, and higher doses (2.5 and 5 mg) were administered intraperitoneally since their volumes were too large for i.v. injection.

As shown in Figure 5.7, ADC depletes the plasma arginine in mice in a dose-dependent manner. The plasma arginine is around 50 μM at 2 h after injection of 1.25 mg ADC (Figure 5.7 A), but remains at an undetectable level at the same time point after injections of 2.5 and 5 mg ADC (Figure 5.7 B, C). In contrast, all doses of ADC-ABD tested are able to maintain plasma arginine at an undetectable level within 2 h after injection (Figure 5.7). We have also observed that when 2.5 mg enzyme is administered, the plasma arginine returns to normal level more slowly in the mouse treated with ADC-ABD than in the one treated with ADC (Figure 5.7 B). However, the same observation is not found in mice treated with 5 mg enzymes (Figure 5.7 C). Considering that for all concentrations of ADC-ABD tested, the

plasma arginine returns to a normal level at 48 h after injection and remains stable thereafter (Figure 5.9), it seems that ADC-ABD fails to prolong the circulating half-life of ADC in a significant manner according to our study.

A possible reason for such a result may be the weak interaction between ADC-ABD and mice serum albumin. The linker between the ADC and ABD (amino acid sequence: AVDANS) may be too short to make the ABD region protruded enough to the environment to interact effectively with albumin. Therefore, it is suggested that the construct of ADC-ABD be redesigned in the future.

Another possible reason is that the concentrations of surrounding cofactors are much diluted when ADC-ABD is administered to mice. The lack of sufficient cofactors may also be responsible for the short circulating half-life of ADC-ABD *in vivo*, as cofactors are found to play important roles in the activity of ADC (Sections 3.2.4 and 4.1.4). Therefore, continuous supplementation of cofactors is suggested in the future experiments on ADC and ADC-ABD.

Some other valuable experiences are also gained from this preliminary study. All mice showed good tolerance with the enzymes administered, as no obvious side effects were observed during the whole study period. The proper doses of ADC and ADC-ABD are recommended to be 2.5 to 5 mg (or more) per ICR mouse. Moreover, the method of administration seems to have no influence on the *in vivo* arginine-depletion ability when enough enzyme is used (Figure 5.7 B, C).

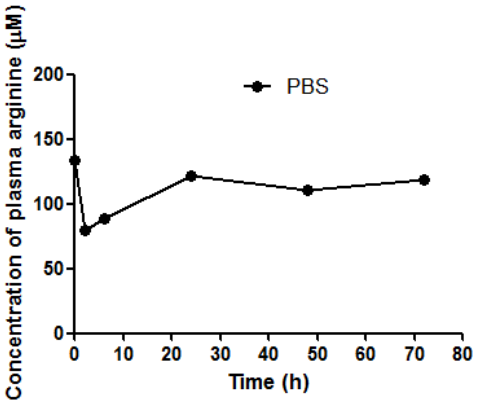
Concentration of plasma arginine (μM)
PBS
Time (h)

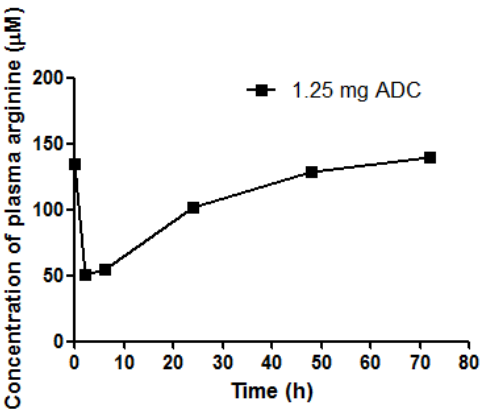
Concentration of plasma arginine (μM)
1.25 mg ADC
Time (h)

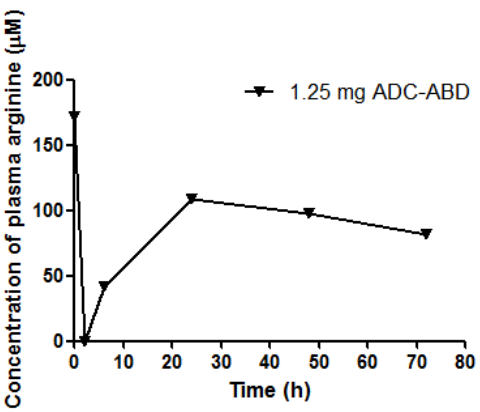
Concentration of plasma arginine (μM)
1.25 mg ADC-ABD
Time (h)

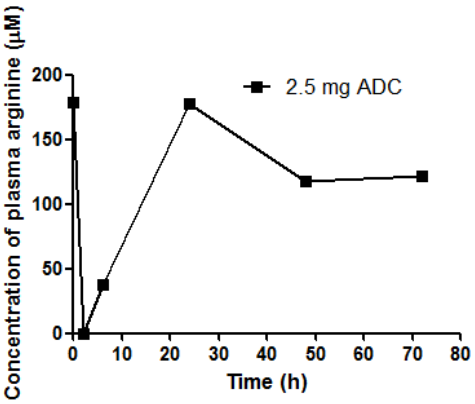
Concentration of plasma arginine (μM)
2.5 mg ADC
Time (h)

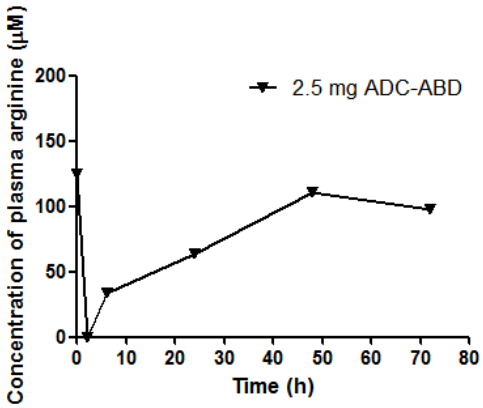
Concentration of plasma arginine (μM)
2.5 mg ADC-ABD
Time (h)

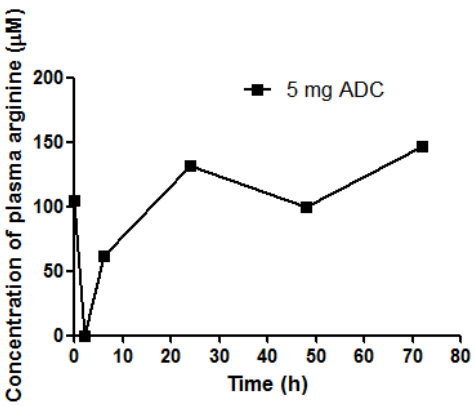
Concentration of plasma arginine (μM)
5 mg ADC
Time (h)

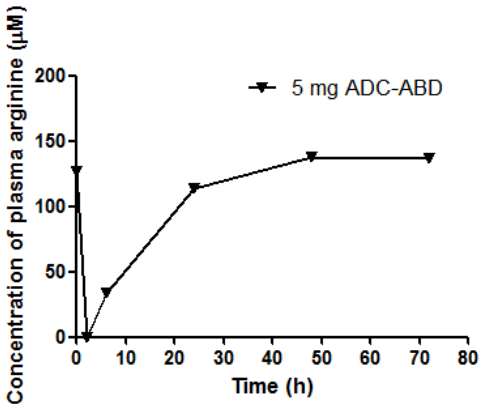
Concentration of plasma arginine (μM)
5 mg ADC-ABD
Time (h)

Figure 5.7: The pharmacodynamics of ADC and ADC-ABD on plasma arginine in mice. ICR mice were each injected with 1.25 mg (i.v.), 2.5 mg (i.p.), or 5 mg (i.p.) ADC or ADC-ABD. Plasma was collected at 2, 6, 24, 28, and 72 h after injection. Time 0 refers to the serum sample collected prior to the injection. The amount of arginine in each sample is determined by amino acid analysis. Arginine concentrations below the detection level are regarded as 0 μM in these plots. Each point represents a single mice plasma sample.

5.8 Further investigations into the ABD fusion strategy using BCA

5.8.1 Expression and purification of BHA

According to the chromatogram of BHA purification, three peaks were observed during the elution process using increasing concentrations of imidazole (Figure 5.8). The first two peaks were merged together, succeeded by the third peak that occurred when imidazole concentration reached ~0.13 M (Figure 5.8). When analyzed by SDS-PAGE, it has been found that the third peak mainly consists of a target protein of around 40 kDa (Figure 5.9, lanes F4-F8). This target protein is likely to be BHA since the calculated molecular weight of BHA monomer based on its amino acid sequence is 39.44 kDa. Therefore, it is suggested that BHA has been successfully expressed and purified. Fractions containing relatively pure BHA were pooled together for further processes.

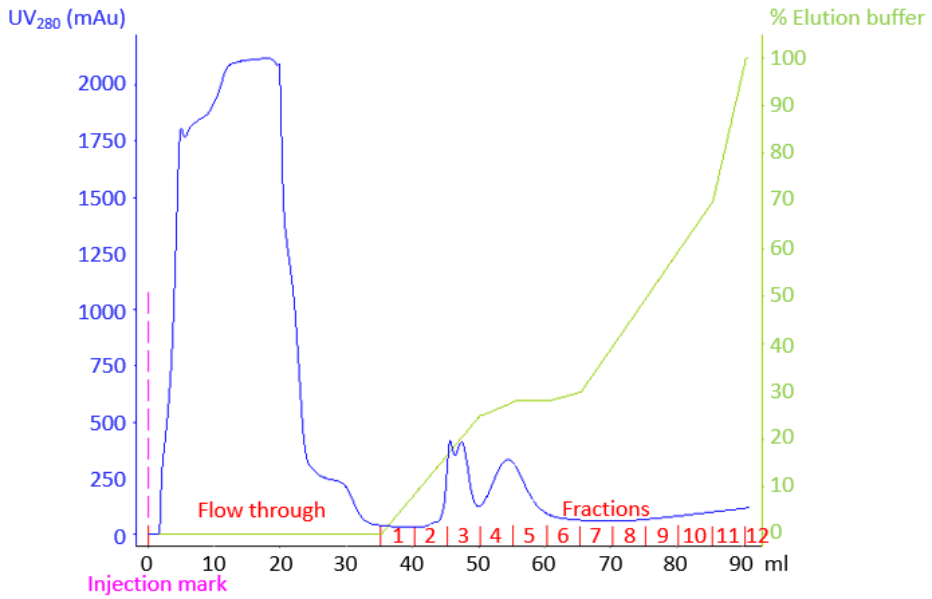

Figure 5.8: Elution profile of the purification of BHA from *E. coli* cells grown in 500 ml shake flask culture by a single step of nickel-charged 5 ml HiTrap^{TM} chelating HP column chromatography. mAU, milli absorption unit; 100% B = 0.5 M imidazole.

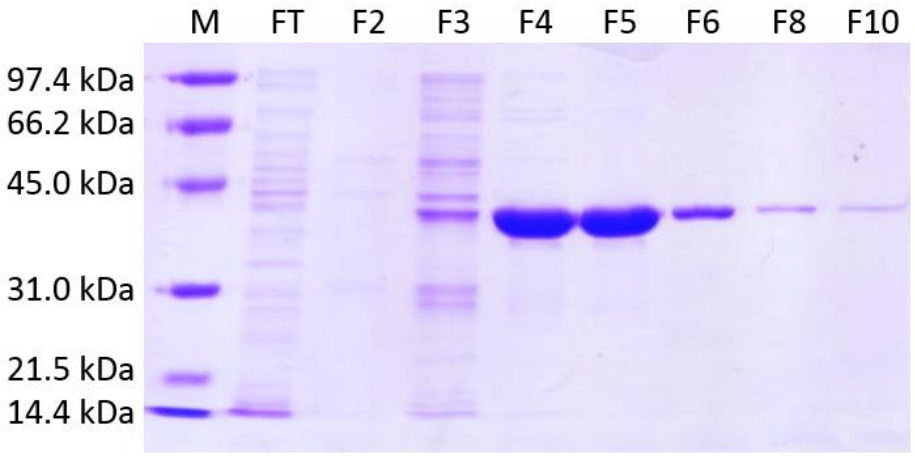

Figure 5.9: SDS-PAGE analysis of the column fractions from nickel affinity chromatography for BHA. M, SDS-PAGE molecular weight standards, low range (Bio-Rad); FT, flow through; F2-F10, eluted fractions from the column.

5.8.2 Expression and purification of BAH

According to the chromatogram of BAH purification, three peaks were observed during the elution process using increasing concentrations of imidazole (Figure 5.10). The second and third peaks were merged together and occurred when imidazole concentration reached ~0.18 M (Figure 5.10). When analyzed by SDS-PAGE, it has been found that this merged peak mainly consists of a target protein of around 40 kDa (Figure 5.11, lanes F6-F14) which is likely to be BAH. Compared to BHA which is eluted at ~0.13 M imidazole, BAH seems to bind more tightly to the nickel affinity column. This is probably because the ABD domain, when inserted between BCA and the 6x histidine tag, helps to make the 6x histidine tag more exposed, and hence the BAH can interact with the nickel ions in the column more effectively than BHA.

Fractions containing relatively pure BAH were pooled together and exchanged buffer using tangential flow filtration device (Millipore) instead of a centrifugal filter device, as this protein is prone to precipitate at high concentration. However, the protein was still severely precipitated during the buffer exchange process, leading to a great loss of protein. It is proposed that BAH is only soluble at a high salt concentration, probably due to its structure. When buffer is exchanged to 20 mM sodium phosphate, the protein may become unstable.

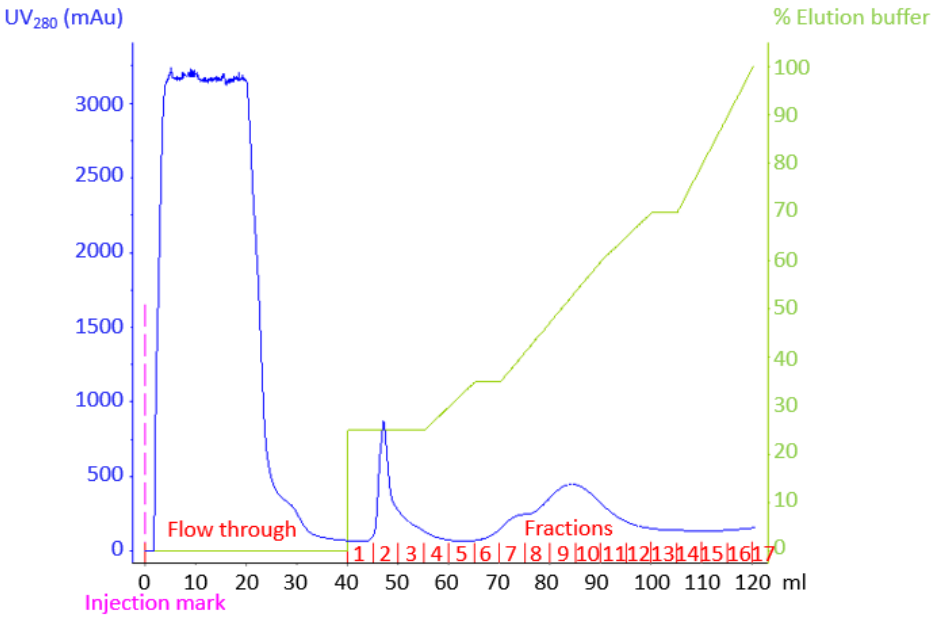

Figure 5.10: Elution profile of the purification of BAH from *E. coli* cells grown in 500 ml shake flask culture by a single step of nickel-charged 5 ml HiTrap^{TM} chelating HP column chromatography. mAU, milli absorption unit; 100% B = 0.5 M imidazole.

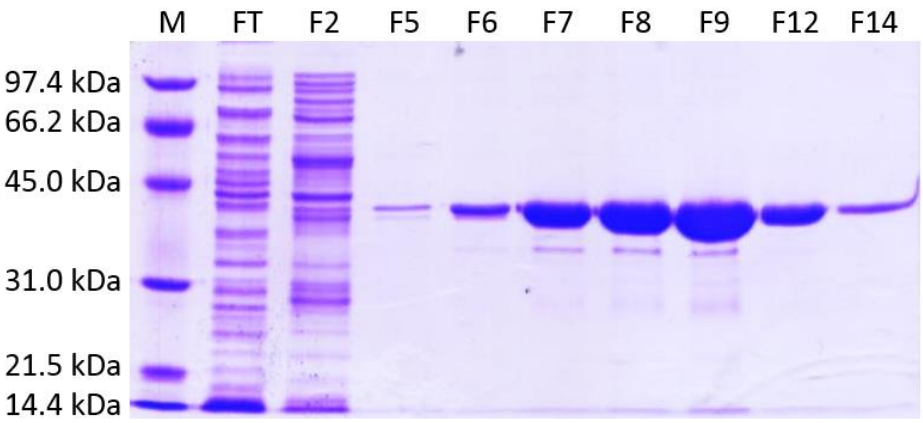

Figure 5.11: SDS-PAGE analysis of the column fractions from nickel affinity chromatography for BAH. M, SDS-PAGE molecular weight standards, low range (Bio-Rad); FT, flow through; F2-F14, eluted fractions from the column.

5.8.3 Specific activities of BHA and BAH

Two methods are used for determining the activities of BCA and its derivatives in our research group. For *in vitro* experiments, activities of the enzymes are determined by the DAMO method at 37 ℃, pH 7.4. For *in vivo* experiments, activities of the enzymes are determined by a spectrophotometric method as described by Ikemoto *et al.* (1989). One unit of enzyme activity is defined as the amount of BCA/BHA/BAH that catalyzes the production of 1 μmol urea per min under standard assay conditions. Specific activity of the enzyme is expressed as activity units per mg of protein.

Under standard DAMO assay conditions (37 ℃, pH 7.4), freshly purified BHA has a specific activity value of 220.6 ± 15.8 U/mg, which is close to the value of BCA (around 243.30 U/mg according to Ms. Shirley S. L. Chu). After one month of storage at 4 ℃, pH 7.4, the specific activity of the same BHA sample decreased to 164.5 ± 10.9 U/mg, indicating that BHA is not very stable under the storage conditions used.

When analyzed by Ikemoto assays under standard conditions (37 ℃, pH 8.3), the measured specific activity value of BHA is smaller, probably because the pH used in this method is suboptimal for BHA. Similar to ADC and ADC-ABD, endotoxin removal process by Triton X-114 phase separation does not affect the specific activities of BHA and BAH (Table 5.2). When measured by the Ikemoto methods, freshly purified BHA is of

142.23 ± 6.75 U/mg before endotoxin removal, and 144.78 ± 14.39 U/mg after endotoxin removal. The specific activities of both BHA and BAH seem to have slightly increased after endotoxin removal (Table 5.2), probably because some lipophilic impurities have been removed during this process. However, the specific activity and the protein amount of BAH are so low (Table 5.2) that this enzyme cannot be used in animal experiments.

Table 5.2: A comparison of the enzymatic activities before and after endotoxin removal, assayed by Ikemoto method. One unit of enzyme activity is defined as the amount of enzyme that catalyzes the production of 1 μmol urea per min under standard assay conditions (37 ℃, pH 8.3).

Protein	Specific activity (U/mg)	
	Before endotoxin removal	After endotoxin removal
BHA	142.23 ± 6.75	144.78 ± 14.39
BAH	8.15 ± 0.42	11.07 ± 1.76

5.8.4 *In vivo* performance of BHA

The *in vivo* arginine-depleting effect of BHA was studied in BALB/c mice and is compared with that of BCA, as shown in Figure 5.12 and 5.13. According to the results provided by Dr. Stephen C. F. Kim, plasma arginine level quickly returns to normal within 24 h after the injection of BCA (Figure 5.12). In contrast, an undetectable level of serum arginine has been remained for at least 24 h after injection of BHA (Figure 5.12). This result indicates the fusion of ABD has prolonged the circulating half-life of BCA *in vivo*. Although further modifications of the fusion protein construct should be made, our results at this moment have already proved that ABD fusion is a feasible and promising strategy for improving the pharmacodynamic properties of arginine-depleting enzymes.

As the product of BCA-catalyzed reaction, ornithine was also examined in our study. The level of plasma ornithine slightly decreases after the injection of BHA, and remains slightly below the original level even at 120 h after injection (Figure 5.13). This may due to the reconversion of ornithine to arginine by the liver in order to synthesize enough arginine to meet the metabolic needs under the stress of arginine-depletion.

The route of administration seems to have no influence on the arginine-depleting effect of BHA *in vivo* (Figure 5.12 and Figure 5.13). Besides, all mice have shown good tolerance with the administration of BHA as no obvious side effects have been observed.

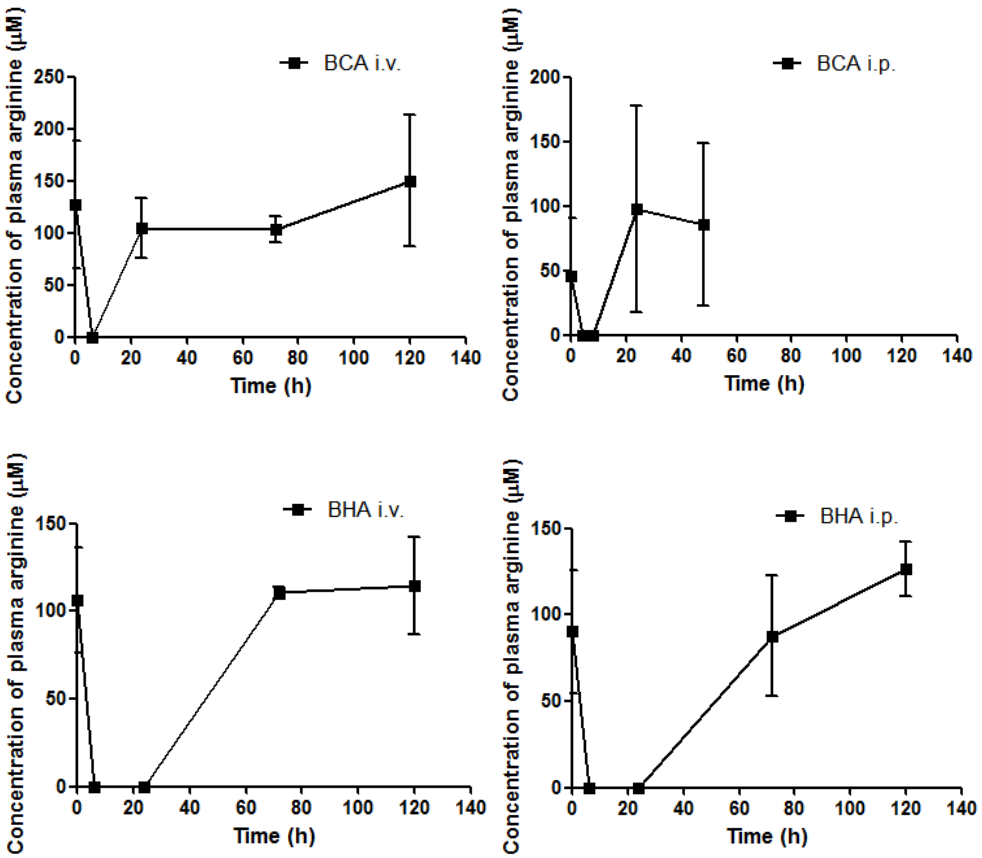

Figure 5.12: The pharmacodynamics of BCA and BHA on plasma arginine in mice. Each BALB/c mice was injected i.v. or i.p. with 250 U BCA or BHA. Plasma was collected at the indicated time points after injection. Time 0 refers to the serum sample collected prior to the injection. The amount of arginine in each sample is determined by amino acid analysis. Arginine concentrations below the detection level are regarded as 0 μM in these plots. Each point represents mean ± SD of three mice. Data on BCA are provided by Dr. Stephen C. F. Kim.

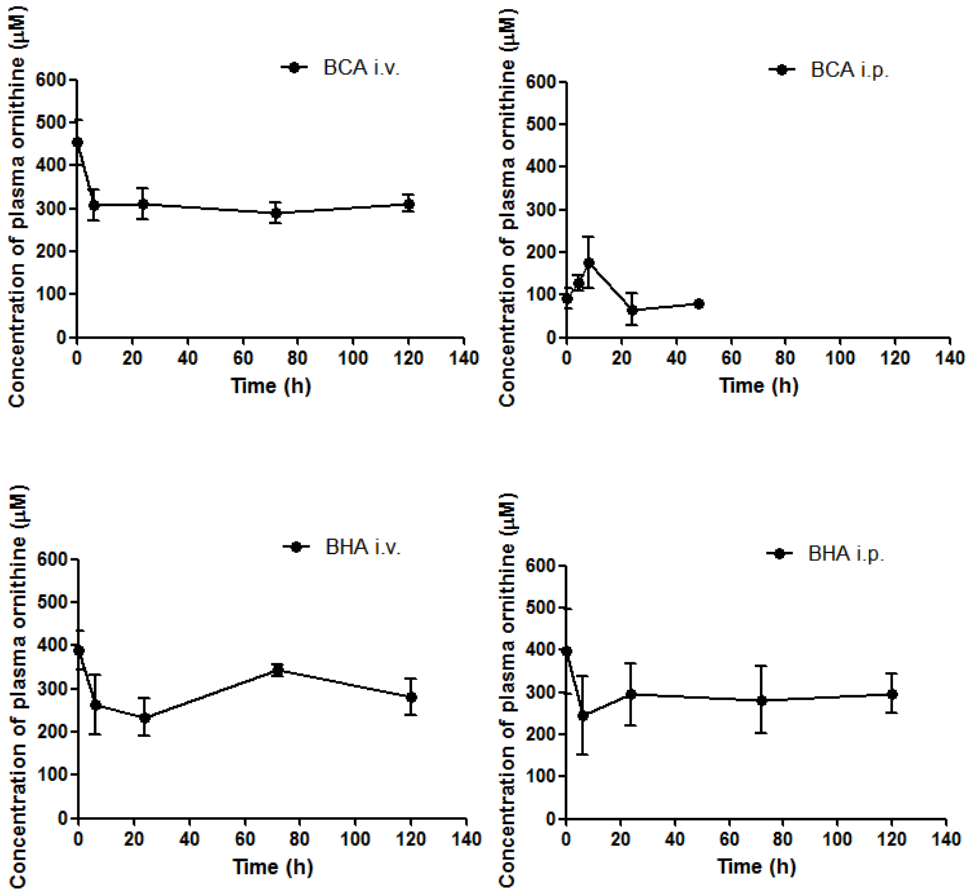

Figure 5.13: The pharmacodynamics of BCA and BHA on plasma ornithine in mice. Each BALB/c mice was injected i.v. or i.p. with 250 U BCA or BHA. Plasma was collected at the indicated time points after injection. The amount of ornithine in each sample is determined by amino acid analysis. Time 0 refers to the serum sample collected prior to the injection. Each point represents mean ± SD of three mice. Data on BCA are provided by Dr. Stephen C. F. Kim.

Chapter 6

Discussions

6.1 Preparation of ADC

6.1.1 The reason for choosing *E. coli* biosynthetic ADC in this study

ADC has been found in various types of organisms, including bacteria, fungi, parasites, plants, marine animals, and mammals. As a potential drug material, ADC of human origins is the first to consider since it may cause less immunological response in patients. However, ADCs originate from human and other mammals are membrane-associated (Zhu *et al.*, 2004), and thus are difficult to produce in large quantities.

In plants such as rice and Arabidopsis, heat stress induces elevated putrescine level which acts as a protective mechanism for plants, and this response is related with the induction of ADC activity (Roy and Ghosh, 1996; Sagor *et al.*, 2013). Plant ADCs are generally of low catalytic activities. ADCs in oat and barley are reported to have activities of around 6000-8000 nmol CO_2 per h per g of fresh leaf extract which are much higher than those of many other plant species (Birecka *et al.*, 1985). The activity of oat ADC, when expressed in transgenic tobacco, is around 100 nmol CO_2 per h per mg protein at most (Masgrau *et al.*, 1997). In contrast, the unit of bacterial ADC specific activity is usually μmol CO_2 per min per mg protein

(Blethen *et al.*, 1968; Graham *et al.*, 2002; Wu and Morris, 1973a). Regardless of the differences in analytical methods among research groups, a conclusion that plant ADCs are of much lower catalytic activities than their bacteria and mammalian counterparts can still be safely drawn.

The establishment of multiple ways to reduce the immunogenicity of heterogenous proteins, such as pegylation and nanoparticle drug delivery system, has expanded our therapeutic choices. As a result, bacterial enzymes have become useful materials in cancer therapy. Asparaginase from *E. coli* and *E. chrysanthemi* has already been used in clinical practice for the treatment of ALL (Pasut *et al.*, 2008). ADI from Mycoplasma species has also resulted in exciting response rate in patients with HCC and melanoma (Ascierto *et al.*, 2005; Izzo *et al.*, 2004). Therefore, ADC originates from bacterial species such as *E. coli* became a focus of our study.

In *E. coli*, two isoforms of ADC have been detected. Biodegradative ADC is only activated in an acidic environment and loses most of its activity at physiological pH (Blethen *et al.*, 1968), thus making it unfavorable as an anti-cancer agent. In contrast, Wu and Morris (1973a) reported that the optimal pH of biosynthetic ADC is much closer to physiological pH. Their conclusion has also been proven by this project. Another bacterial ADC which originates from *Bacillus subtilis* has previously been studied in gastric cancer MKN-45 cells by our group members. It has been found that *B. subtilis* ADC is less potent than *E. coli* biosynthetic ADC. As a result, *E. coli* biosynthetic ADC was chosen in this project.

6.1.2 Expression, purification, endotoxin removal, and long-term storage of ADC

Despite some protein loss during the affinity chromatography, a considerable final yield of ADC was still obtained in this project. In a typical experiment, around 110 mg ADC is purified from *E. coli* grown in 1 L culture medium. When scaled up from shake flask culture to fermentation, the yield of ADC is even much more delightful. According to Dr. H. K. Yap in our group, the yield of ADC from fermentation is 2.0-2.5 g/L of *E. coli* cell culture.

As ADC used in this project is bacteria-originated, an important consideration is to find a proper method for removing endotoxins in the final protein product. The theoretical pI is 5.03 for ADC and 5.12 for ADC-ABD (calculated by Compute pI/Mw; ExPASy). Since endotoxin also has an acidic pI value of around 2 (Shi *et al.*, 2001), it is difficult to be separated from either ADC or ADC-ABD by any ion exchange. Phase separation by the nonionic detergent Triton X-114 thus appears to be a better choice in this situation. Triton X-114 is homogeneous at low temperatures but partitions into an aqueous phase and a detergent phase at temperatures above its cloud point (23 ℃) (Bordier, 1981). In this way, hydrophilic and hydrophobic proteins in a solution containing Triton X-114 can be separated. The results on ADC, ADC-ABD, BHA, and BAH have all shown that phase separation by Triton X-114 can reduce the endotoxin contents in proteins to a satisfactory level and has little impact on protein amount as

well as enzyme activity. Therefore, Triton X-114 phase separation is recommended as a simple yet effective and universal method for endotoxin removal.

There is, however, still potential for improvement on our present purification methods. Some impurities, although of tiny amount, are still detected in the final product of ADC, making ADC difficult to meet the diagnostic and therapeutic requirements at this moment. To improve, some refinery purification processes, such as ion exchange or hydroxyapatite chromatography, should be recruited in addition to affinity chromatography in the future.

To sum up, ADC is of high yield and good purity by simple and cost-effective preparation procedures. Its bacterial stock is of high stability for more than three years at -80 ℃ while its protein stock is stable for at least six months at 4 ℃ in solution form. Generally speaking, ADC is a promising druggable material on the aspect of production.

6.1.3 The improved activity assay method and the specific activity of ADC

The most widely used method for the determination of ADC specific activity is probably the one through the detection of $^{14}CO_2$ produced from (1-^{14}C)-arginine (Burrell *et al.*, 2010; Morrissey *et al.*, 1995; Regunathan and Reis, 2000; Wu and Morris, 1973a; Zhu *et al.*, 2004). This method, however, is infeasible in this project as it requires specific equipment and reagents.

Some other methods for measuring the activity of ADC have also been reported. Goldschmidt and Lockhart (1971a, 1971b) have introduced a simple method which involves the extraction of agmatine with n-butanol and the subsequent detection of extracted agmatine by formulated diacetyl agents. The extraction process, although is necessary to avoid the formulation of diacetyl agents from reacting with arginine in solution (Goldschmidt and Lockhart, 1971b), may be hard to ensure the accuracy of a quantitative analysis.

Our thought then turned towards the detection of urea generated from arginine through a combination of ADC- and agmatinase-catalyzed reactions, since our lab has already been using an established DAMO method for detecting the urea produced by arginase-catalyzed deprivation of arginine. Under strong acidic conditions, urea reacts with DAMO to yield colored product whose intensity can be measured at 540 nm

(Kanagasabapathy and Kumari, 2000). The previously established activity method for ADC in our research group, as described in Section 3.2.1, allows ADC and agmatinase to react in the same mixture, and results in an extremely low ADC activity of around 1 μmol urea per min per mg protein at 37 ℃ and pH 8.0. Such a result is inconsistent with the findings that ADC can effectively inhibit the growth of tumor cells. Therefore, it was speculated that ADC and agmatinase might have distinct optimal reaction conditions, and their reactions must be conducted separately. We first incubated the reaction products of ADC with agmatinase overnight to make sure the incubation time was long enough to allow as much agmatine be converted to putrescine and urea as possible, and then compared the result to that derived by the old assay method. Through this preliminary trial we have proved our speculation that the activity of ADC has been underestimated previously, and a more accurate assay method is needed to be designed.

The improved activity assay method established in this project is regarded as a reliable one as it is repeatable in different trials and provides reasonable results regarding the data of Wu and Morris (1973a) as a reference. It is also proven to be a simple method that can be easily mastered by researchers without any previous experience on protein activity assay. Unlike the detection of $^{14}CO_2$, this assay method requires less equipment and is more cost-effective. Compared to the previous method in our group which requires as much as 1.1 mg purified ADC per test, this improved method also enhances the experimental throughput as only 0.02-0.15 mg ADC is required for each test. The mere limitation of this improved

method is that it may be difficult to determine the K_m and k_{cat} of ADC, as it consists of two enzymatic reactions which need to be performed in sequence.

Through the modification of the activity assay method, we have also gained much knowledge on the enzymatic properties of *E. coli* agmatinase, including its optimal reaction temperature and pH. *E. coli* agmatinase is also an enzyme with easy and cost-effective preparation processes. As agmatinase is able to hydrolyze agmatine, it was used together with ADC for some anti-cancer mechanism studies in this project, and will continue to be a useful research tool in the future.

6.1.4 The effect of cofactors on the structure, specific activity, and anti-cancer properties of ADC

Biosynthetic ADC is a unique enzyme as it requires two cofactors: magnesium ions and PLP. At pH 8, magnesium ions are essential for the dimer and tetramer formation of ADC, and they also coordinate the binding between ADC and PLP (Wu and Morris, 1973b). PLP accounts for the catalytic activity of ADC as Wu and Morris (1973b) have pointed out that there is a Schiff base formed between PLP and a lysine residue of ADC which is a part of the typical PLP-decarboxylation mechanism according to O'Leary (1992). Therefore, both cofactors are crucial for the catalytic activity of ADC, and PLP seems to be of higher importance than magnesium ions which has been proven by this project (Section 4.1.4).

According to the structural study of Forouhar *et al.* (2010), PLP binds to ADC through a covalent bond as well as some non-covalent forces including hydrogen bonds as well as π-stacking interaction. We hypothesize that the requirement of additional PLP supplementation to ensure the optimal activity of ADC may due to the degradation of ADC-bound PLP. Prior to this project, similar conclusions that the supplementation of additional cofactors is necessary for the enzymatic activity have been drawn by researchers studying other PLP-dependent enzymes such as methioninase. For example, Sun *et al.* (2003) have supplemented additional PLP in buffer for the activity assay and storage of methioninase. Even for *in vivo* studies of methioninase, a supplementary of PLP provided by osmotic

mini-pumps implanted in mice can help to maintain low plasma methionine level for a longer period (Sun *et al.*, 2003).

6.2 Anti-cancer properties of ADC

6.2.1 Colorectal cancer as a focus of this project

Globally, colorectal cancer has become the third most frequently diagnosed cancer type in males and the second in females (Jemal *et al.*, 2011). The incidence of colorectal cancer is higher in economically developed regions such as Australia, New Zealand, Europe, and North America while is much lower in Africa and South-Central Asia (Jemal *et al.*, 2011). Although not being the top priority for prevention and therapy, colorectal cancer is still one of the major cancers in mainland China. The incidence of colorectal cancer ranked the fifth in both Chinese males (7.7%) and females (8.0%) in 2008 (Wang *et al.*, 2012). The mortality of colorectal cancer increases with age (Zheng *et al.*, 2012), and has been slowly yet steadily increasing during the past thirty years, ranking the fifth in both urban (9.78/100,000) and rural mainland China (5.96/100,000) in 2004-2005 (Zhao *et al.*, 2010). Compared to mainland China, Hong Kong is facing a more severe problem of colorectal cancer. The incidence of colorectal cancer in Hong Kong has more than doubled over the past decade (Yau, 2013). While lung cancer has long been occupying the top spot in terms of incidence in Hong Kong (Yau, 2013), in 2011, it was beaten into the second place by colorectal cancer (Hong Kong Cancer Registry, Hospital Authority, 2013). According to the Hong Kong Cancer Registry, Hospital Authority (2013), there were 4,450 new cases of colorectal cancer and 3,789 reported deaths from colorectal cancer in 2011.

Apart from factors such as inflammatory bowel disease, colorectal polyp and adenoma, as well as family history of colorectal cancer, it is commonly agreed that many life habits that have emerged in recent decades, including the consumption of red and processed meat, low intake of dietary fiber, and lack of physical activities, all contribute to the pathogenesis of colorectal cancer (Zheng *et al.*, 2012). Screening tests such as sigmoid-oscopy are able to detect colorectal cancer at an earlier stage, and hence can greatly reduce the death rate (DeSantis *et al.*, 2014; Jemal *et al.*, 2011; Zheng *et al.*, 2012). These screening tests, however, have not yet been popularized in less-developed countries (Jemal *et al.*, 2011). Even in well-developed countries such as the United States, in early 2014, only 59% of the population above age 50 received colorectal cancer screening as recommended (DeSantis *et al.*, 2014).

Surgery is the most common treatment of early-stage (stage I and II) colorectal cancer, while chemotherapy is often the main treatment for advanced colorectal cancers (DeSantis *et al.*, 2014). Several combinations of conventional chemotherapies, such as FOLFOX (oxaliplatin plus 5-FU and leucovorin), FOLFIRI (irinotecan plus 5-FU and leucovorin), and XELOX (or CAPOX; oxaliplatin plus capecitabine) are recommended as the first- and second-line treatments of patients with metastatic colorectal cancer (Cassidy *et al.*, 2011; Goldberg *et al.*, 2004; Tournigand *et al.*, 2004). Side effects of these treatments include nausea, vomiting, diarrhea, neutropenia, febrile neutropenia, paresthesia, and dehydration (Goldberg *et*

al., 2004). Powerful therapeutic methods with milder side effects are still under exploration.

Human colorectal cancer cell lines are reported to have similar gene mutation profiles as primary colorectal tumors, and are considered as proper models for drug development against colorectal cancer (Mouradov *et al.*, 2014). Colorectal cancers are generally of high ASS levels (Delage *et al.*, 2010), and thus have been a restricted area for the studies of ADI so far. Contrarily, we have made a preliminary yet successful step in this area by demonstrating the effectiveness of ADC in four colorectal cancer cell lines with different levels of ASS protein expression. Such findings have revealed a main potential advantage of ADC over ADI. In addition, ADC may be a promising agent against colorectal cancer in particular, as its anti-proliferative catalytic product agmatine has been reported to accumulate in several human colon carcinoma cells via specific agmatine transporters (Heinen *et al.*, 2003; Mayeur *et al.*, 2005; Molderings *et al.*, 2003).

Apart from colorectal cancer, ADC also exerts inhibitory effect on cell lines of other cancer types. For example, we have demonstrated that ADC has inhibitory effect on the cervical cancer cell line HeLa which is ADI-resistant. We have also found that ADC is very effective against pancreatic cancer cell lines BxPC-3 and PANC-1. Therefore, we believe that ADC may also have a promising future in the treatment of other cancer types.

6.2.2 Reliability of MTT assay in reflecting the cell viability

MTT assay is a colorimetric method for measuring the mitochondrial activity of cells, and is one of the most commonly used methods for the detection of cell viability or cytotoxicity. In living and metabolically active cells, succinate dehydrogenase in mitochondria cleaves the tetrazolium ring of MTT, and hence converts the water soluble MTT to an insoluble purple formazan compound (Fotakis and Timbrell, 2006). MTT provides a rapid and precise quantitative measurement of the number and activity of living cells (Mosmann, 1983).

The lactate dehydrogenase (LDH) assay which measures the leakage of LDH from damaged cells into culture medium, is another commonly used method for the determination of cell growth and viability. Compared to the LDH assay, MTT assay is a more sensitive method to detect early cytotoxic events (Fotakis and Timbrell, 2006), and is more reliable on the determination of cytotoxicity that only affects intracellular events (Weyermann *et al.*, 2005). It has been reported that certain renal carcinoma cell lines treated with ADI show similar amount of LDH release as control (Yoon *et al.*, 2007). Although such result is meaningful as it suggests the ongoing of cell cycle arrest upon ADI treatment (Yoon *et al.*, 2007), it also indicates that the LDH assay is not a suitable method for the quantification of cytotoxicity of arginine-depleting enzymes.

MTT assay also has certain advantages over the other methods on the

evaluation of cell viability. Compared to the neutral red assay in which the neutral red accumulates in the lysosomes of living cells, MTT assay is thought to be much more sensitive in certain cases (Weyermann *et al.*, 2005). Trypan blue exclusion assay may not be suitable for samples with low viability, and is also problematic for measuring the proportion of viable cells after ADC treatment as most dead cells have undergone apoptosis to form apoptotic bodies which make it difficult to determine the actual cell numbers. In contrast, the quick, cheap, easy and relatively reliable properties of MTT all make it a preferred method for the determination of cytotoxicity in this project.

However, MTT may sometimes overestimate the cell viability if an experiment involves inhibitors of the mitochondrial enzymes. A group of researchers have found that the IC_{50} value of epigallocatechin gallate (EGCG) determined by MTT assay is higher than those determined by other methods because EGCG promotes mitochondrial functions (Wang *et al.*, 2010). On the other hand, MTT may underestimate the number of viable cells, as some cells may be living with low metabolic activities. MTT assay is also not recommended for determining the cytotoxicity of reagents that can generate superoxide, as superoxide can reduce MTT to formazan products (Wang *et al.*, 2011). Therefore, our results were further validated by a series of flow cytometry experiments that can directly quantify cell apoptosis and cell cycle arrest.

It is observed in this project that none of the anti-cancer reagents used can achieve 100% cytotoxicity. The maximum cytotoxicity of ADI is ~94%

in A375 cells, and the maximum cytotoxicity of ADC is ~93% in BxPC-3 cells. Even chemotherapeutic drugs such as doxorubicin and verapamil cannot kill 100% of cancer cells based on our MTT results. As we always make sure that the highest dose and the second highest dose of a certain agent achieve similar cytotoxic effects, we are quite confident that the maximum cytotoxicities measured in this project are close to the actual values. Therefore, it is possible that MTT assay may have overestimated the cell viability in this project, or that some resistant cells, probably cancer stem cells, may have survived from drug treatments. As multiple agents with various anti-cancer mechanisms are involved in this project, we also suggest the cell viability be measured with some other methods such as LDH assay and alamar blue assay along with MTT assay in the future to provide more information on cell viability.

6.2.3 Comparisons of ADI, BCA and ADC on their anti-cancer properties

In this project, the anti-cancer effect of three different arginine-depleting enzymes with distinct catabolic pathways of arginine, namely ADI, BCA and ADC, were studied. Their enzymatic reactions as well as their relationships with the urea cycle are depicted in Figure 6.1. Among these three enzymes, ADI is the best-studied arginine-depleting enzyme at the moment, as it has already completed phase I and II trials on patients with HCC and melanoma (Ascierto *et al.*, 2005; Izzo *et al.*, 2004), and is undergoing more clinical trials, including a phase III clinical trial on patients with advanced HCC (Polaris Group, 2011a), phase II trials on patients with leukemia and lymphoma (Polaris Group, 2013b, 2013c), and a few phase I studies in which ADI is used as part of a combination therapy (Polaris Group, 2011b, 2013a, 2014). BCA, although without much published information, shares the same mechanism with the better-studied hArg, and is therefore believed to be a powerful anti-cancer enzyme. In contrast, ADC has long been kept away from the spotlight, despite that an early study by Philip *et al.* (2003) has shown the inhibitory effect of ADC in HeLa and L1210 cells.

Since ADC and its catalytic products are not involved in the urea cycle (Figure 6.1), it is hypothesized that the anti-cancer effect of ADC is less affected by the urea cycle enzyme expression profile of tumor cells. In this project, we tested the effect of ADC in ten tumor cell lines of different

cancer types, and have demonstrated that ADC is effective against all these cell lines regardless of their ASS levels.

We have, in particular, compared the effect of ADI, BCA, and ADC in five cancer cell lines with different ASS levels. It is now widely agreed that cellular ASS, either constitutive or inducible, helps to convert citrulline to arginine and hence results in the resistance of tumor cells to ADI treatment (Delage *et al.*, 2010; Savaraj *et al.*, 2010; Shen *et al.*, 2003). Our experimental results fit this hypothesis as we have observed a trend that the efficacy of ADI decreases as cellular level of ASS increases (Table 4.2). It should be noticed that ASS is the rate-limiting enzyme in the urea cycle (Haines *et al.*, 2011), and low cellular level of ASS may not be sufficient to maintain cell growth through the *de novo* synthesis of arginine from citrulline (Shen *et al.*, 2003). Consequently, we have observed that cells with lower levels of ASS protein, such as BxPC-3, PANC-1 and HCT116, are all sensitive to ADI treatment. We have also demonstrated that HeLa cells which is reported to be highly ASS-positive upon ADI treatment (Cheng *et al.*, 2007; Shen *et al.*, 2003; Wu *et al.*, 2011), have more than 50% of the cell population survived from the maximum dose of ADI (Table 4.2). This finding is similar to those reported by previous publications (Shen *et al.*, 2003; Sugimura *et al.*, 1992; Wu *et al.*, 2011). In addition, we have, as expected, shown that HeLa cells are sensitive to BCA and ADC treatment, especially the latter (Table 4.2). Some other ADC-sensitive cell lines, such as LoVo, COLO 205, and SW1116, all have high ASS protein levels (Appendix Figure 4) and are likely to be ADI-resistant as well. Future

experiments should be focused on these cell lines to verify the potential advantage of ADC over ADI in the treatment of ASS-positive cancers.

A series of experiments were then conducted to compare the anti-cancer effects of BCA and ADC in ASS-positive cancer cells. As BCA and ADC catalyze the catabolism of arginine to different products, it is hypothesized that tumors with both ASS and OTC expressed will be resistant to BCA but not ADC. We failed to testify this hypothesis in this project, as it was difficult to find a natural tumor cell line that would express both ASS and OTC, and it was also challenging to construct such a cell line. The fact that few tumors express OTC may indicate the broad anti-cancer spectrum of both BCA and ADC. Yet related explorations will continuously be made in the future.

Instead of working on an ASS and OTC double positive cancer cell line, we have tried to mimic a situation of cells expressing excessive amount of OTC by a citrulline supplementation experiment (Section 4.1.3). We have found that in ASS-positive tumor cells, the supplementation of excessive citrulline exerts rescuing effect on cells from both ADC and BCA treatments, and the extent of rescue increases as cellular ASS level increases. Such finding agrees with that of Agrawal *et al.* (2012). We have also demonstrated that ASS-positive tumor cells under citrulline-rich conditions are more vulnerable to ADC than BCA, and we suspect such vulnerability may due to the production of anti-proliferative agmatine by ADC-catalyzed decarboxylation of arginine. As citrulline added in this experiment (1.15 mM) is in excessive amount while the concentration of

citrulline in human plasma is only around 40 μM (Crenn *et al.*, 2000), there may be no need to worry that the human plasma citrulline will affect the anti-cancer activity of ADC. Nevertheless, our results do indicate the theoretical possibility of the existence of an ADC-resistant cell line. In order to be ADC-resistant, the cells must express high levels of both ASS and OTC, be insensitive to agmatine, and be supplied with sufficient arginine or any other urea cycle intermediate.

Our citrulline supplementation experiment, although is not able to truly reflect the living conditions of OTC-positive cells, is still a meaningful trial as it indirectly reflects the cellular ASS activity. We therefore recommend that in the future, citrulline supplementation experiments be conducted along with RT-PCR and immunoblot assay, in order to detect cellular ASS at mRNA level, protein level, and enzyme activity level, thus may provide more complete information to predict cell sensitivities to ADI treatment.

The anti-cancer potency and efficacy of ADI, BCA and ADC were also compared in this project. Through the studies in four cancer cell lines with low or medium ASS expression, it is observed that ADI has highest potency in all of these four cell lines, followed by BCA and ADC (Table 4.2). This is likely due to the differences in specific activity and enzyme efficiency among these three arginine-depleting enzymes. According to the previous studies, K_m for L-arginine and specific activity of *Mycoplasma arginini* ADI are 0.2 mM and 50 μmol citrulline per min per mg protein at 37 ℃, pH 6.5 (Takaku *et al.*, 1992), K_m for L-arginine and specific activity of BCA are 3.2 mM and ~170 μmol urea per min per mg protein at 25 ℃, pH 7.4 (Leung

and Lo, 2013), while K_m for L-arginine and specific activity of *E. coli* biosynthetic ADC are 0.03 mM and 16.4 μmol CO_2 per min per mg protein at 37 ℃, pH 8.4 (Wu and Morris, 1973a). As the assay conditions vary and the k_{cat} values of these enzymes are unreported, it is hard to observe a clear relationship between the enzymatic properties and the anti-cancer potency based on our current knowledge. We propose that ADC is less potent probably because it only retains around half of its full activity at physiological pH (Figure 3.8). Yet ADC is still much more potent compared to some other anti-cancer enzymes such as methioninase. It has been reported that the IC_{50} of L-mehioninase from *A. flavipes* is 2.5 U/ml (~162 μg/ml) in HCT116 cells (El-Sayed *et al.*, 2012), while the IC_{50} of ADC is 12.23 μg/ml according to our studies.

On the other hand, we are excited to find that ADC exhibits greater efficacy than ADI and BCA in three of the four cell lines tested, namely, HCT116, BxPC-3 and PANC-1 (Table 4.2). The different performances of ADI, BCA and ADC in cancer cells may due to their distinct catalytic pathways as summarized in Figure 6.1. The main catalytic products of ADI, BCA and ADC are citrulline, ornithine, and agmatine, respectively. Citrulline, as mentioned, can be converted back to arginine in cells with functional ASS. Ornithine itself, although may slightly inhibit tumor growth in some cell lines as observed in a preliminary test in this project (Appendix Figure 10), can be converted to the cytoprotective putrescine by ODC in human body. Besides, it has been reported that ODC is overexpressed in tumors of pancreatic cancer, prostate cancer and breast cancer (Black Jr. and

Chang, 1982; Deng *et al.*, 2008; Mohan *et al.*, 1999; Young *et al.*, 2006). Considering such findings, BCA may be a doubtful choice for the treatment of these cancers as the ornithine produced by BCA reaction can be easily converted to the pro-survival putrescine in this case. Agamatine, the catalytic product of ADC, is an anti-proliferative compound (Isome *et al.*, 2007; Molderings *et al.*, 2004; Wang *et al.*, 2005; Wolf *et al.*, 2007). It is even more exciting to learn that agmatinase, the enzyme that can degrade the anti-survival agmatine to the pro-survival putresciene, is diminished in some tumors such as those of renal cell carcinoma compared to normal human tissues (Dallmann *et al.*, 2004). These previous studies all provide possible explanations for the higher efficacy of ADC over ADI and BCA, and offer a promising prospect that ADC may be specifically against tumor cells rather than normal cells.

Based on our results together with the published findings, we believe that ADC, as an alternative arginine-depleting enzyme, is worthy to be further studied, and a more solid conclusion that ADC is advantageous over the other arginine-depleting enzymes (or even over the other anti-cancer agents) on certain types of cancers is likely be derived in the future.

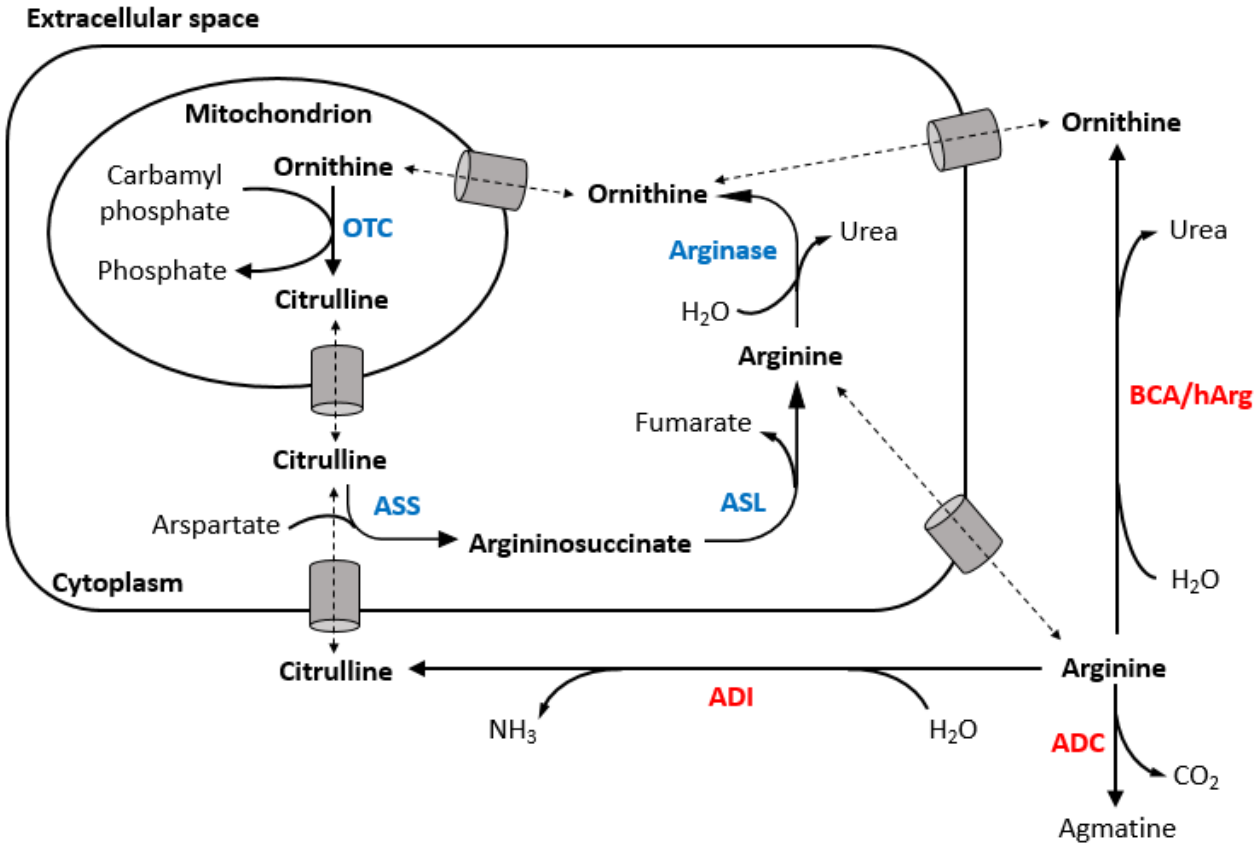

Figure 6.1: Schematic diagram showing the enzymatic reactions of ADI, BCA, hArg, and ADC as well as their relationships with the urea cycle. Enzymes involved in the urea cycle are indicated in blue. The cylinders denote the transporters. The dashed lines indicate the transportation of urea cycle intermediates. This diagram is a modified version of the one proposed by Mian and Lee (2002).

6.2.4 The role of arginine deprivation-induced autophagy on cancer cells

Unlike apoptosis which results in cell death, the role of autophagy in cell fate is much more complicated. Kim, Coates *et al.* (2009) have suggested that autophagy protects prostate cancer cells from ADI-induced cell death, as their study on prostate cancer cell line CWR22Rv1 with 0.1 μg/ml ADI-PEG20 and 25 μM CQ has shown the combination of these two reagents resulted in a significantly elevated apoptosis population after 48 and 72 h of treatment. Similar conclusions have been drawn by other research groups studying the effect of ADI in melanoma and lung cancer cell lines (Kelly *et al.*, 2012; Savaraj *et al.*, 2010). A study on hArg has also pointed out that inhibition of autophagy through the addition of CQ can significantly increase the cytotoxicity of hArg in leukemia cell lines (Tanios *et al.*, 2013). Although autophagy has been widely agreed to play an important role in cell survival mechanism, it is also characterized as type 2 programmed cell death. For example, a more recent study by Qiu *et al.* (2014) has suggested that ADI induces autophagic cell death in breast cancer cells, as they found the addition of 10 μM CQ slightly rescued the cells from ADI-PEG20.

Surprisingly, unlike these previous studies which all suggest that autophagy can be induced by enzymatic degradation of arginine, we failed to detect the ongoing of autophagy in ADC-treated HCT116 and LoVo cells with immunoblot assay for the change of LC3 intensity and drug

combination study of ADC and HCQ. The first possibility may be that ADC fails to deprive arginine in cell culture medium. However, this possibility is ruled out by a preliminary experiment which suggests that arginine level in HCT116 cell culture medium is successfully lowered by ADC and becomes undetectable after 24 h of ADC treatment (Appendix Figure 11). Another possible explanation, supported by the previously published opinion that autophagy is a cellular event prior to apoptosis (Maiuri *et al.*, 2007; Marino *et al.*, 2014), is that ADC-induced autophagy in HCT116 and LoVo cells is too transient to be detected by our experiments (in which 2 h is the earliest time point to study). In this case, the impact of autophagy on cancer cells may be minor. In addition, it is also possible that ADC inhibits intensive autophagy in HCT116 and LoVo cells with unknown mechanisms.

Together with the previous findings, our study may indicate that the ongoing of autophagy and its role in cell fate is enzyme- and cell line-dependent. We also suggest that the details of the relationship between ADC and autophagy in colorectal cancer cells be further examined in the future.

6.3 The possibility of enhancing the anti-cancer effect of ADC through drug combination

In the treatment of dreadful diseases such as cancer and AIDS, drug combination is a well-accepted strategy as it may achieve satisfactory therapeutic effect while reducing the drug doses, side effects, and drug resistance (Chou, 2010). Drug interactions are categorized based on the CI value calculated by the Chou-Talalay method, and are defined as synergism (CI < 1), additive effect (CI = 1), or antagonism (CI > 1) (Chou and Talalay, 1984). The selection of combination agents with potential synergistic effect to the target drug requires a great deal of experience. The developer of the famous Chou-Talalay method even suggests the difficulty of predicting synergism by drug mechanisms in reality (Chou, 2010). As few studies on the anti-cancer properties of ADC have been conducted prior to this project, and it may take a long period to reveal the detailed anti-cancer mechanisms of ADC, we had to rely on some guesswork to select a few agents and test their combination effects with ADC. In this project, four agents with anti-cancer potential, namely HCQ, doxorubicin, verapamil, and LY294002, were tested in combination with ADC in HCT116 cells.

CQ and HCQ are antimalarial drugs with promising anti-cancer effects (Janku *et al.*, 2011; Kimura *et al.*, 2013). After entering the lysosome, CQ and HCQ become protonated and block the acidification of lysosome, thus inhibit autophagy at a late stage (Kimura *et al.*, 2013; Yang *et al.*, 2011). Both CQ and HCQ have been studied in a variety of preclinical and clinical

trials in combination with different chemotherapeutic drugs or small molecule drugs (Amaravadi *et al.*, 2011; Yang *et al.*, 2011). Compared to CQ, HCQ is much safer (Gunja *et al.* 2009; Smith and Klein-Schwartz, 2005), and thus is preferred in this project. Unlike our hypothesis that HCQ may further increase the cytotoxicity of ADC through the blockage of cytoprotective autophagy, our combination studies showed that ADC interacted antagonistically with HCQ in HCT116 at both 24 and 72 h of drug treatment periods (Table 4.6 and Table 4.7). As a result, HCQ is not a suitable combination drug for ADC in such a situation.

We also tested the combination of ADC with doxorubicin, a well-established chemotherapeutic drug that have been used for the treatment of cancer for over 30 years (Tacar *et al.*, 2013). Doxorubicin intercalates into DNA to disrupt DNA replication, and thus leads to apoptosis (Carvalho *et al.*, 2009; Tacar *et al.*, 2013). Although doxorubicin is effective against a wide range of cancers, it is also highly toxic to non-tumorous tissues (Carvalho *et al.*, 2009). The combination study of ADC with doxorubicin in this project aimed at decreasing the dose of doxorubicin while achieving similar anti-cancer effect. Our results have shown that not only ADC but also BCA are synergistic with doxorubicin at high doses (Section 4.5.1), and such combination effects deserve to be further tested *in vivo*. In fact, a phase I clinical trial of ADI-PEG20 plus doxorubicin in patients with HER2-negative metastatic breast cancer is ongoing at present (Polaris Group, 2013a). It is expected the result of this clinical trial, in the future, may give

more hints on the feasibility of the combination of doxorubicin with an arginine-depleting enzyme.

Verapamil has been used as a drug for cardiac diseases, hypertension, as well as cluster headaches (Meister *et al.*, 2010). As a calcium channel blocker, verapamil inhibits the influx of calcium ions into cells (McTavish and Sorkin, 1989). It is believed that verapamil can inhibit the activity of calmodulin through the changing of intracellular calcium environment, and thus prevent chemo-resistant cells from actively removing the chemotherapeutic agents (Simpson, 1985). As a result, verapamil is often studied in combination with small molecule drugs against cancer (Chen *et al.*, 2012; Liu *et al.*, 2014; Meister *et al.*, 2010). As verapamil is not likely to affect the anti-cancer mechanisms of ADC and BCA, the combination studies of verapamil with arginine-depleting enzymes in this project are not expected to yield synergistic results, but instead can be regarded as negative controls. We found that ADC and verapamil were antagonistic in HCT116 cells at all concentrations tested (Section 4.5.2). Similar results were observed in BCA and verapamil combinations, with the exception of IC_{90} at which the effect was synergistic (Table 4.11). We propose that verapamil is not a suitable combination drug for ADC as the result is not promising according to our study.

The last combination agent to study in this project, LY204002, was selected based on our mechanism studies that ADC can inhibit ERK while upregulating Akt in HCT116 cells (Figure 4.12 and Figure 4.18). It has been reported that the dual inhibition of Ras/MEK/ERK and PI3K/Akt/mTOR

pathways may result in greater drug efficacy compared with inhibition of either pathway alone in the treatment of cancer (Renshaw *et al.*, 2013; Saini *et al.*, 2013; Shimizu *et al.*, 2012). LY294002, as a pan-PI3K inhibitor, was expected to demonstrate synergistic effect with ADC in this project. In reality, we found that the interaction between LY294002 and ADC is quite dose-dependent, as these two agents are antagonistic at IC_{50}, antagonistic or nearly additive at IC_{75}, and synergistic at IC_{90} (Table 4.12). In a previous study of ADI in melanoma cell lines, the researchers also reported an upregulation of Akt activity upon ADI-PEG20 treatment, as well as an additive effect on cell growth inhibition when ADI-PEG20 was used together with LY294002 (Tsai *et al.*, 2012). Their studies also showed that LY294002 could enhance the anti-tumor activity of ADI-PEG20 in mice xenografts (Tsai *et al.*, 2012). As both ADI and ADC are arginine-depleting enzymes and may share some similar anti-tumor mechanism, the results of Tsai *et al.* (2012) may indicate a promising future of ADC in combination with PI3K/Akt/mTOR inhibitors in the treatment of cancer.

6.4 ABD fusion strategy

6.4.1 The reason for constructing ADC-ABD

When searching for a strategy to eliminate the immunogenicity of ADC while extending its circulating half-lfe, pegylation was our first consideration since it has been proved to be effective on a variety of enzymes such as apsaraginase, methioninase, ADI, hArg (Pasut *et al.*, 2008), and BCA (Leung and Lo, 2013). Two PEG molecules, methoxy-PEG-maleimide (mPEG-MAL; reacts with cysteine residues), and mPEG-SPA (reacts with lysine residues), were therefore tested by our former group member, Mr. Angus C. L. Chan, prior to this project.

As shown in Figure 2.3, the protein sequence of ADC used in this project contains 8 cysteine and 18 lysine residues. According to the structural study of ADC, the 8th cysteine (cysteine 497) is crucial for the catalytic function of ADC, and is also responsible for the binding of substrate (Forouhar *et al.*, 2010). This conclusion is supported by our observation that mPEG-MAL results in significant activity loss of ADC (Appendix Figure 12 A). The 4th lysine residue (lysine 96) of ADC is also required for a functional ADC, as it locates at the PLP binding site of the enzyme (Forouhar *et al.*, 2010). Probably due to a competition of PLP and mPEG-SPA for this lysine residue, pegylation of mPEG-SPA with ADC holoenzyme retained the activity of ADC (Appendix Figure 12 A) yet results in inefficient pegylation (Appendix Figure 12 B), while pegylation

with ADC apoenzyme improves the pegylation efficiency (Appendix Figure 12 B) but leads to nonfunctional ADC (Appendix Figure 12 C). And hence the concern of pegylation of ADC with mPEG-SPA is to reach a compromise between enzyme activity and pegylation efficiency. Although some other types of PEG molecules can be tested in the future, pegylation is still not favored in this project compared to fusion protein strategies, as it is neither cost-effective nor time-effective, and may result in the formation of anti-PEG antibodies in animals and humans.

Compared to pegylation, the conjugation with HSA is a more recent strategy for the improvement of drug properties. HSA has been conjugated with various chemotherapeutic drugs including methotrexate, doxorubicin, and chlorambucil to prolong their circulating half-lives (Stehle *et al.*, 1997). In addition, a fusion of recombinant bispecific antibody to HSA has increased circulation time of the antibody while still retaining its retargeting effect on T lymphocytes to tumor cells (Muller *et al.*, 2007). The fusion protein of interferon α-2b with HSA (albinterferon) has been found to have extended the half-life of interferon while being efficacious and well tolerated in patients with hepatitis C (Subramanian *et al.*, 2007).

It should be noticed that all these successful examples are the conjugation or fusion of HSA to small molecule drugs. In contrast, ADC is a large protein molecule as it is a homo-tetramer with each monomer of around 71 kDa. While there may be no need to further increase the size of ADC as it is large enough not to be removed by renal clearance, the fusion of a large molecule like HSA (~67 kDa) will take up more space and thus

may hinder the correct structural formation of ADC during protein synthesis. Therefore, the fusion of ADC to the peptide ABD which can bind to HSA is preferred in this project. Successful examples of ABD fusion proteins include the single-chain diabody-ABD fusion which mediates the T cell retargeting to tumor cells (Hopp *et al.*, 2010), and the Affibody $Z_{HER2:342}$-ABD fusion which targets HER2 (Andersen *et al.*, 2011). The effect of ABD fusion may be comparable with that of HSA-fusion, as it has been reported that for a bispecific single-chain diabody, the circulating half-life of its ABD fusion in mice model is similar to that of its HSA-fusion (Stork *et al.*, 2007). Apart from the fusion to small proteins and peptides, ABD can also be fused with large protein molecules. For example, Makrides *et al.* (1996) have demonstrated the binding of ABD fused with human soluble complement receptor type 1 (sCR1) to rat serum albumin and the consequently extended *in vivo* half-life. Their results have provided a practical basis for the application of ABD fusion strategy on the improvement of ADC performance.

6.4.2 Preparation of ADC-ABD and BCA-ABD

The expression system of ADC-ABD is distinct from that of ADC, as these two constructs are designed and prepared by different members in our group. As a result, the yield of ADC-ABD from shake flask culture is 50% less than that of ADC. Similar situation has been reported when the bacterial culturing process is scaled up to fed-batch fermentation according to Dr. H. K. Yap in our group. Nevertheless, 50 mg ADC-ABD per L of shake flask culture and 1.2 g ADC-ABD per L of fed-batch fermentation culture are still satisfactory protein yields. For BCA-ABD fusion proteins, extremely high protein yield of up to 290 mg protein per L of shake flask culture has been obtained in the case of BHA, while little protein has been obtained in the case of BAH due to its instability during purification and formulation processes.

The yields of ABD fusion proteins are highly dependent on the expression systems used. It has been reported that the yield of ABD fused with sCR1 ranges from 0.4 to 1.1 ug per 24 h per ml of Chinese hamster ovary cell culture (Makrides *et al.*, 1996). Around 2-15 mg single-chain diabody-ABD fusion proteins can be obtained from every L of HEK293 cell culture (Hopp *et al.*, 2010; Stork *et al.*, 2007). The yield of ABD-TolA fusion protein expressed in *E. coli* BL21 host is 20 mg/L LB broth medium (Ahmad *et al.*, 2012). In comparison, the yields of both ADC-ABD and BHA are much higher. Our results have demonstrated that the production of both ADC-ABD and BHA are simple and cost-effective. Same as ADC,

these fusion proteins are readily available materials for cancer studies in the future.

6.4.3 The effect of ABD fusion on the properties of ADC and BCA

Although ABD is a small peptide fragment of ~6 kDa, the effect of its fusion on the structure of the target protein cannot be ignored. In this section, we would like to discuss the impact of ABD fusion on ADC and BCA enzyme properties, as well as the function of ABD, on the aspects of protein preparation, enzyme activities, *in vitro* cytotoxicities, and *in vivo* arginine deprivation effects.

Our first observation that ABD fusion may have slightly altered the structure of ADC is derived from the protein purification process, as higher imidazole concentration is required to elute ADC-ABD compared to ADC (Figure 5.1 versus Figure 3.1). We propose that the insertion of ABD in between ADC and the 6x histidine tag has made the 6x histidine tag more exposed to the surrounding environment, and hence has allowed for a tighter binding between the fusion protein and the nickel affinity column. Similar observation has been found in the cases of BCA-ABD fusion proteins, as higher imidazole concentration is required for the elution of BAH compared to BHA (Figure 5.10 versus Figure 5.8). Besides, ABD fusion also results in the precipitation of BAH during the buffer exchange process, as described in Section 5.8.2.

When analyzing the enzyme activity, it is exciting to find that ADC-ABD and BHA both retain the activity of their native counterparts. We also

have observed that the specific activity of ADC-ABD upon long-term storage follows the same decreasing pattern as that of ADC.

Despite the similar catalytic activities between ADC and ADC-ABD, an intriguing result has shown that ADC-ABD, although slightly less effective, is much more potent than ADC in all the three colorectal cancer cell lines tested (Table 5.1). The reason for the boosting effect on the cytotoxicity of ADC by ABD fusion remains a mystery at the moment. We hypothesize that ADC-ABD may be more long-lasting than ADC during cell culture experiments through its interaction with bovine serum albumin in the culture medium. This hypothesis has not been testified by the native-PAGE, as native-PAGE is not sensitive enough to demonstrate weak protein interactions. Our preliminary studies by isothermal titration calorimetry also failed to determine the interactions between ABD fusion proteins with serum albumin. Surface plasmon resonance assay has been widely used for the detection of interaction between ABD and its binding targets (Ahmad *et al.*, 2012; Dennis *et al.*, 2002; Jonsson *et al.*, 2008; Makrides *et al.*, 1996; Walker *et al.*, 2010). While we may refer to this method for the detection of protein interactions in the future, we have to admit that the interaction between ADC-ABD and albumin in this project is too weak to meet our expectation, and this may partially account for the undesirable results of our *in vivo* experiments.

Our *in vivo* experiments have shown that both ADC-ABD and BCA-ABD can slightly prolong the arginine depleting effect than their native counterparts in mice (Figure 5.7 A and Figure 5.12 A). These results,

however, are far from satisfactory, as BCA-ABD only maintains the plasma arginine below detection levels for ~24 h. The result is even worse for ADC-ABD, as it can only maintain the plasma arginine below detection level for 2 h. As both ADC and BCA are large proteins, they may hinder the interaction between ABD and albumin if the ABD locates too close to them. In fact, the linker between BCA and ABD is only of 11 amino acid residues in length, and the linker between ADC and ABD is even shorter. We suggest that the length of the linker sequence be increased in the future to make the ABD portion more protruding to the environment. In this way, the binding between ABD fusion proteins and albumin may be stronger.

Another reason that accounts for the undesirable performance of ADC-ABD *in vivo* lies in the fact that ADC requires additional cofactors in the surrounding environment to function optimally. It has been reported that the *in vivo* activity of the PLP-dependent methioninase is remarkably prolonged by the simultaneously administration of PLP via a subcutaneously implanted osmotic mini-pump (Sun *et al.*, 2003; Yang, Sun *et al.*, 2004). These published results on methioninase will be useful references for us to improve the *in vivo* performance of ADC and ADC-ABD in the future.

To conclude, our current ABD fusion strategy is only partially successful. The enymze portion of the fusion protein seems to function well, as ADC-ABD and BHA are found to retain the activity of ADC and BCA, respectively. On the other hand, the ABD portion of the fusion protein may not be fully functional, especially in the case of ADC-ABD. We suggest the fusion protein constructs be carefully redesigned in the future.

6.5 The possible anti-cancer effect of ADC *in vivo*

Apart from further investigations of ADC-ABD, the native form of ADC can also be tested in tumor xenograft mice models in the future. This proposal is mainly based on the fact that native forms of asparaginase originate from *E. coli* and *Erwinia chrysanthemi* have already been clinically available for years (Pasut *et al.*, 2008). These two forms of asparaginase do not present antigenic cross-reactivity, and hence patients that have developed antibodies against one form of asparaginase can be switched to the treatment of another form (Pasut *et al.*, 2008). Despite the development of antibodies against asparaginase which have been observed in a small population of patients as well as the relatively frequent injection rate (every 2-5 days), native forms of asparaginase are still a fine choice for the treatment of leukemia at present (Narta *et al.*, 2007; Pieters *et al.*, 2011).

In addition, compared to pegylated BCA, native form of BCA shows similar inhibitory effect in mice xenografts of human lung cancer, and slightly lower yet significant inhibitory effect in mice xenografts of human colorectal cancer (Leung and Lo, 2013). Therefore, it is possible that not only ADC-ABD but also native ADC can be used as a competent alternative to ADI and arginase for anti-cancer therapies in the future.

Chapter 7

Conclusions

In this project, a slightly modified, recombinant version of *E. coli* biosynthetic ADC tagged with 6 histidine residues has been successfully expressed and purified. The protein yield is around 110 mg per 1 L of shake flask culture medium. The specific activity of ADC is 28.9 ± 2.7 units/mg at 37 ℃, pH 8.0, and remains relatively stable for at least 6 months when stored at 4 ℃ in darkness.

We have demonstrated the inhibitory effect of ADC in ten cell lines of different human cancer types, including liver (HepG2), lung (A549), cervix (HeLa), melanoma (A375), pancreatic (BxPC-3, PANC-1), and colorectal cancer (HCT116, LoVo, COLO 205, SW1116), regardless of the cellular ASS protein levels. The IC_{50} values of ADC in these cell lines range from 3.8 to 38.1 μg/ml. On the other hand, we have observed that the non-tumorous HFF-1 cell line is relatively resistant to ADC. A comparison study have shown that although being less potent, ADC is of higher efficacy than ADI and BCA in three of the four cancer cell lines tested, namely HCT116, BxPC-3, and PANC-1. We have also shown that ADC is much more effective than BCA in the ADI-resistant HeLa cells.

Mechanism studies using HCT116 cell line as a model has revealed that ADC is a much stronger apoptosis inducer than BCA. The apoptosis induced by ADC in HCT116 cells follows the mitochondrial pathway, and

is caspase-3-dependent. This mitochondria- and caspase-3-dependent characteristic, however, is not observed in ADC-induced apoptotic LoVo cells. Beside apoptosis, ADC also results in cell cycle arrest at S and/or G_2/M phases in HCT116 and LoVo cells. Autophagy, on the contrary, has not been detected in ADC-treated HCT116 and LoVo cells, indicating this event may either be absent or too transient to exert much influence on these two cell lines. Preliminary studies on the cell signaling pathways suggests ADC may upregulate the PI3K/Akt pathway and downregulate the Ras/MEK/ERK pathway in HCT116 cells. Drug combination studies indicates that doxorubicin and LY294002 may be suitable combination agents for ADC in future anti-cancer studies, as their combinations with ADC in HCT116 cells show synergistic effects at high doses. Contrarily, ADC is antagonistic with both HCQ and verapamil in HCT116 cells.

To extend the circulating half-life and to eliminate the immunogenicity of ADC, the fusion protein ADC-ABD has been prepared and studied. ADC-ABD is readily expressed and purified, and almost fully retains the specific activity and stability of ADC. When tested in three colorectal cancer cell lines, ADC-ABD is of slightly lower efficacy but much greater potency than ADC. Unfortunately, ADC-ABD failed to prolong the arginine-depleting effect at a significant level in mice. Yet further studies on the BCA-ABD fusion protein, namely BHA, have proved the feasibility of ABD fusion strategy by decreasing serum arginine to an undetectable level for a much longer period (24 h) than that when using native BCA (2 h). We propose two major solutions for the improvement of the *in vivo* performance

of ADC-ABD, including the elongation of the linker sequence in the protein construct as well as the application of an osmotic pump with supplemental cofactors in mice.

To sum up, our results suggest that ADC is a promising selective anti-cancer drug candidate due to its simple production process, high protein yield, satisfactory stability, as well as the broad anti-cancer spectrum with comparable or even advantageous efficacy over ADI and BCA. Therefore, ADC is worthy to be more deeply investigated in the future.

Chapter 8

Suggestions for future studies

Suggestions for the future studies of ADC are discussed here on the aspects of protein preparation, selection of modeling tumor cell lines, mechanism studies, drug safety, the possible strategies for extending the half-life of ADC, and *in vivo* anti-cancer studies.

As mentioned, the purity of ADC after a single-step affinity chromatographic purification is satisfactory yet can be further improved. Additional purification steps can be introduced in the future to refine the purity of ADC. Apart from storing ADC in liquid form at 4 ℃, methods such as lyophilization which dehydrates materials may have a chance to further prolong the storage period of ADC while making ADC a more portable form.

We have demonstrated the broad anti-cancer spectrum of ADC in cell lines of various human cancer types, and have shown that ADC has higher efficacy than ADI and BCA in several ASS-positive cancer cell lines, including HCT116, BxPC-3, PANC-1, and HeLa. Future experiments should be focused on these cell lines and the corresponding cancer types to further elucidate the advantages of ADC over ADI and BCA. We have also identified that BxPC-3 is relatively more sensitive to agmatine than the other cell lines tested. We suggest a more thoroughly screening for agmatine-sensitive cancer cell lines and cancer types in the future, as ADC

may be more effective in these cancers. In this way, ADC may be used as a personalized therapeutic agent in the future for cancer treatment.

Future mechanism studies of ADC will be focused on two main issues. First, a tumor cell line with high levels of both ASS and OTC activities should be used to testify our hypothesis that ADC may be more effective against ASS and OTC double positive cancers compared to ADI and BCA. Besides, we would like to further explore the effects of ADC on the cell signaling molecules upstream and downstream of both Akt and ERK. We would like to specifically examine the impact of ADC on mTOR, as mTOR has been reported to be regulated by amino acids (Demetriades *et al.*, 2014; Kapahi *et al.*, 2010; Menon *et al.*, 2014; Tato *et al.*, 2011; Tsun *et al.*, 2013). The results of these mechanism studies may provide some guidance on the selection of potential combination drugs for ADC in the future.

Insufficient experiments have been conducted regarding the safety of ADC in this project due to the limitation of experimental materials. Therefore in the future, ADC should be tested in more non-tumorous cell lines as well as in animal models to testify if it is truly safe for therapeutic use as expected.

Future phamacodynamic studies of ADC and its derivatives should be conducted in BALB/c mice as this mice species is more commonly used than ICR mice. To improve the arginine-depleting activity of ADC, we may follow the previous examples of methioninase (Sun *et al.*, 2003; Yang, Sun *et al.*, 2004) by implanting an osmotic pump subcutaneously in mice to provide sufficient cofactors for the enzyme to function properly. Regarding

the improvement of the circulating half-life of ADC, we plan to redesign the construct of ADC-ABD by elongating the linker sequence between ADC and ABD. Methods with higher sensitivity for the detection of the interaction between ADC-ABD and albumin, such as surface plasmon resonance, should also be involved. Besides, as there are various types of PEG molecules which can conjugate to different amino acid residues, we can also re-explore the strategy of pegylation by testing alternate types of PEGs. For example, PEG that can be specifically conjugated to the polyhistidine tag as described by Cong *et al.* (2012) may be a suitable candidate for the modification of ADC.

Apart from the modified versions of ADC, anti-cancer effect of the native form of ADC can also be tested in mice tumor xenografts in the future.

Appendices

A

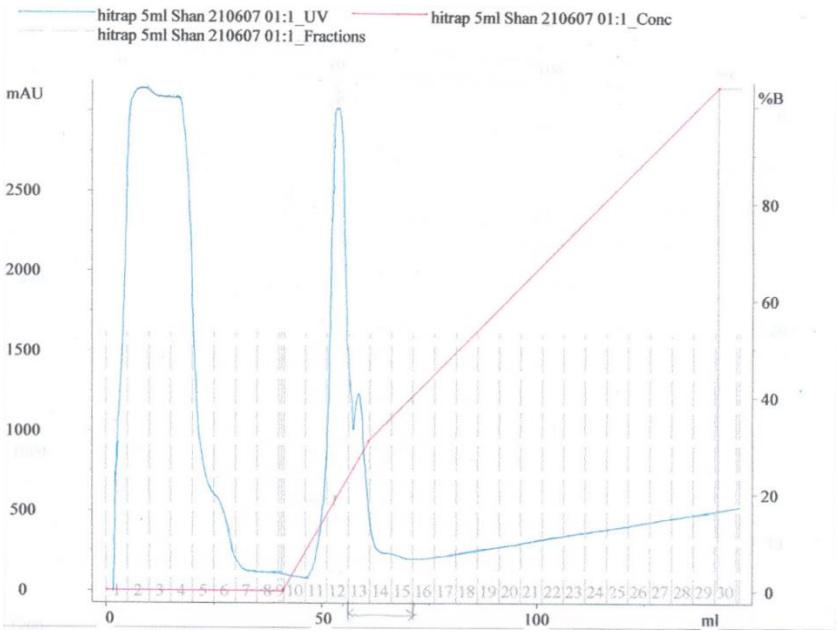

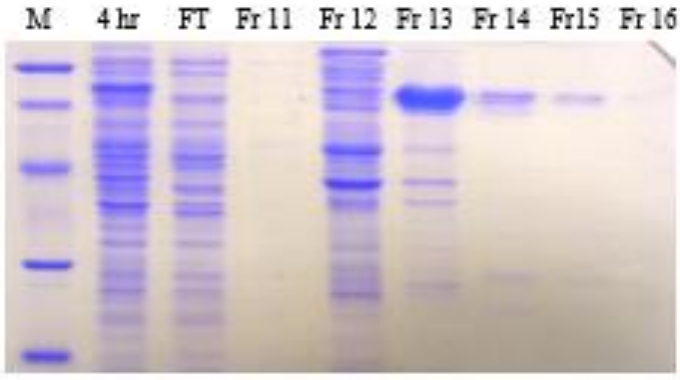

B

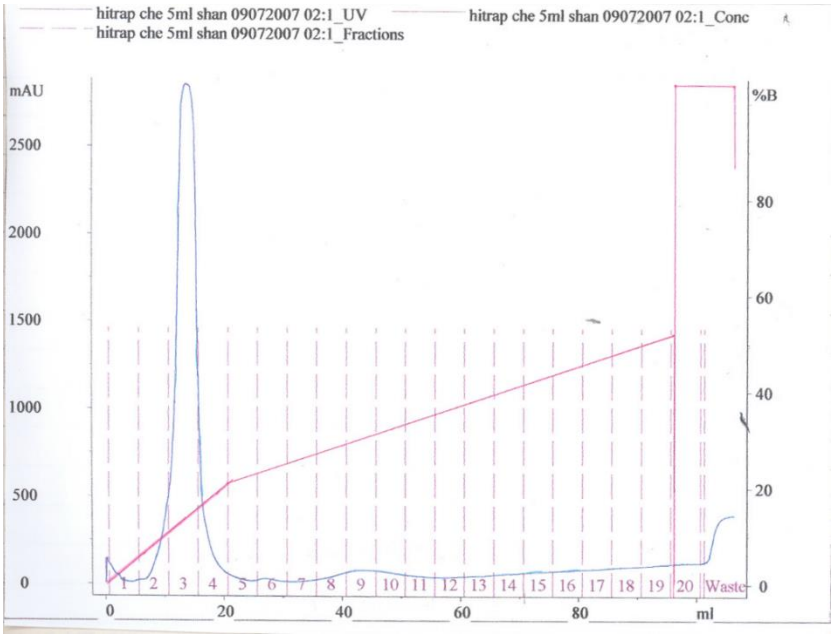
hitrap che 5ml shan 09072007 02:1_UV
hitrap che 5ml shan 09072007 02:1_Conc
hitrap che 5ml shan 09072007 02:1_Fractions
mAU
%B
2500
2000
1500
1000
500
0
80
60
40
20
1 2 3 4 5 6 7 8 9 10 11 12 13 14 15 16 17 18 19 20 Waste
0 20 40 60 80 ml

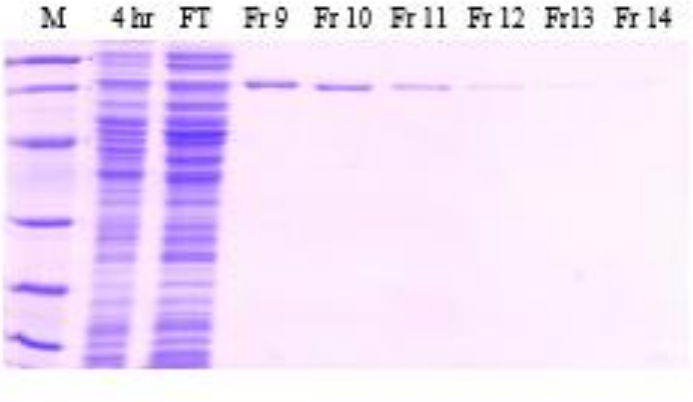
M
4 hr
FT
Fr 9
Fr 10
Fr 11
Fr 12
Fr13
Fr 14

C

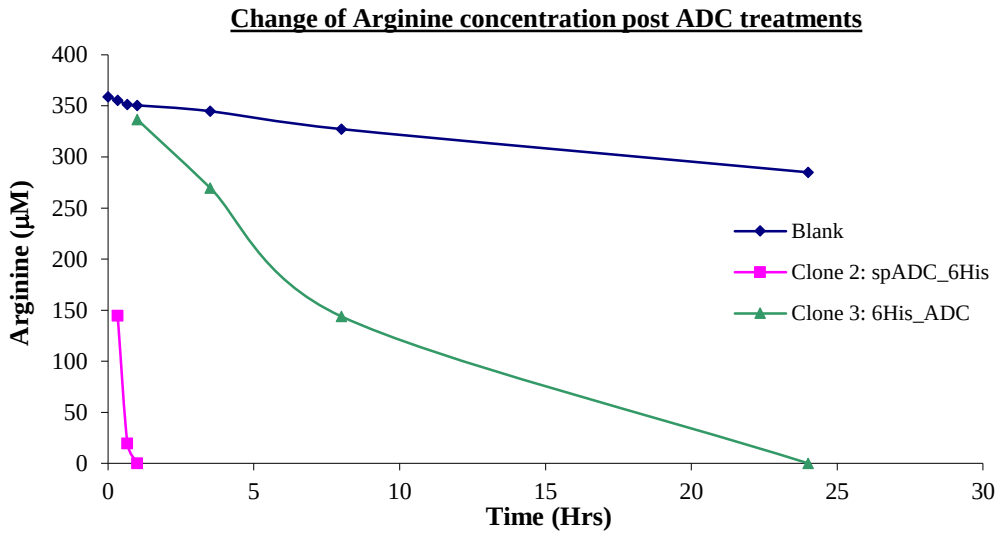
Change of Arginine concentration post ADC treatments
Arginine (µM)
400
350
300
250
200
150
100
50
0
0 5 10 15 20 25 30
Time (Hrs)
Blank
Clone 2: spADC_6His
Clone 3: 6His_ADC

App Figure 1: Elution profile, SDS-PAGE analysis, and activity of ADC with 6x histidine tag at different positions. (A) Purification of ADC with 6x histidine tag at its C-terminus; (B) Purification of ADC with 6x histidine tag at its N-terminus; (C) Activity assay of both types of ADC. Proteins were expressed in *E. coli* cells and were purified by a single step of nickel-charged 5 ml HiTrap^{TM} chelating HP column chromatography. mAU, milli absorption unit; 100% B = 0.5 M imidazole. M, SDS-PAGE molecular weight standards, low range (Bio-Rad); 4hr, total protein after 4 h of IPTG induction; FT, flow through; Fr, eluted fractions from the column. Activity assay of ADC was performed by amino acid analyzer (Hitachi 8800) to detect the arginine content in cell culture medium. Results are provided by Ms. Sandra Y. S. Siu.

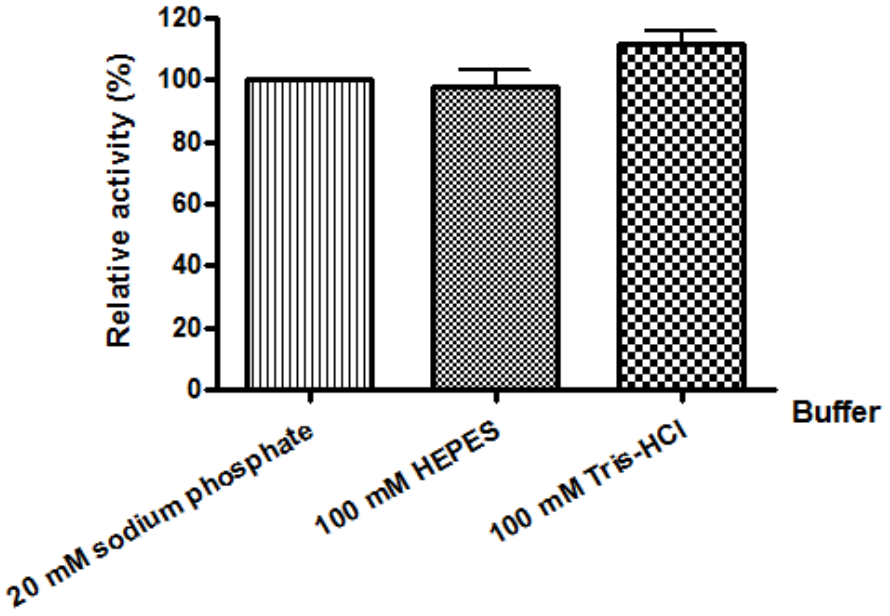

App Figure 2: Effect of buffer on the activity of ADC-ABD at 37 ℃, pH 8.0. Data are expressed as percentage of specific activity of ADC-ABD measured in 20 mM sodium phosphate buffer (pH 8.0) and are mean ± SD of a single experiment performed in triplicate. All buffers were supplemented with 1 mM $MgCl_2$ and 0.1 mM PLP.

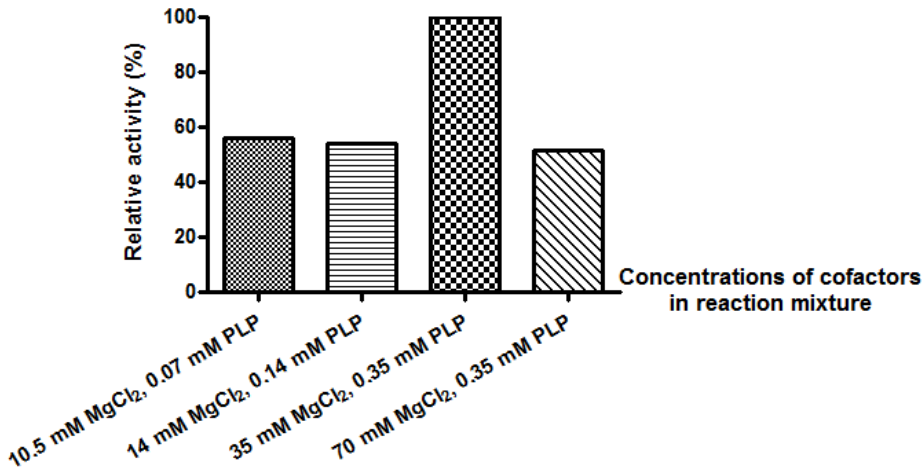

App Figure 3: Effects of $MgCl_2$ and PLP on the activity of ADC in *E. coli* cell lysate. Data are expressed as percentage of enzyme activity at 35 mM $MgCl_2$, 0.35 mM PLP. Each point represents a single measurement. All ADC-catalyzed reactions were performed in 100 mM HEPES buffer at 37 ℃.

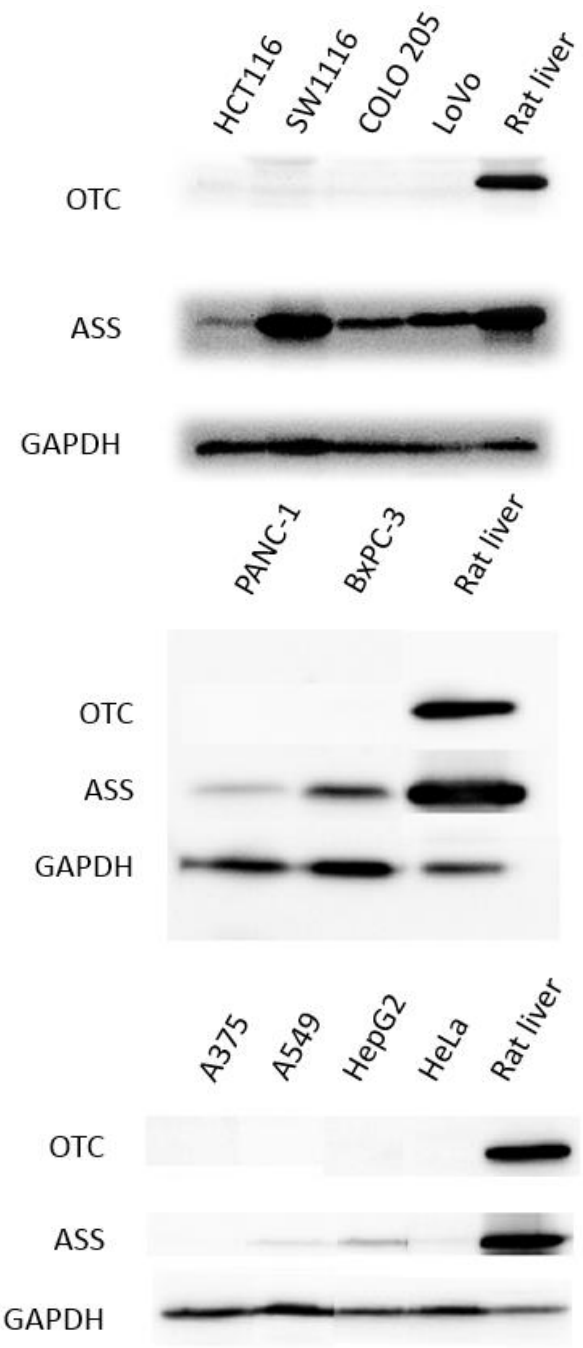

App Figure 4: Immunoblot analysis showing the expression of OTC and ASS proteins in the ten cancer cell lines used in this project. Rat liver is used as positive control. Results are provided by Dr. Ryan H. Y. Chow.

A

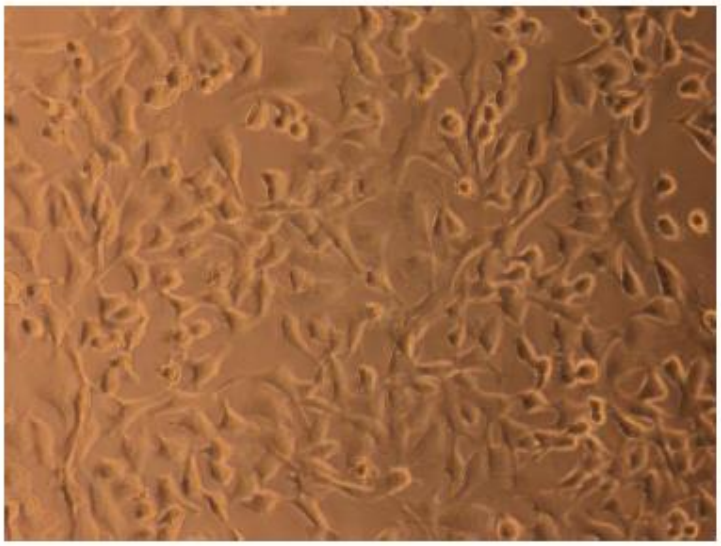

B

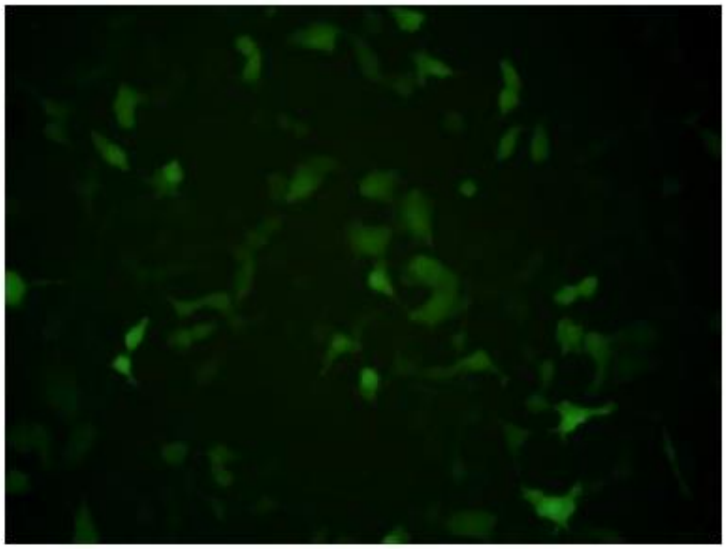

App Figure 5: The infection of adenoviruses encoding GFP into HeLa cells. Photos were taken under (A) normal light, and (B) fluorescent light. 5×10^3 HeLa cells in a volume of 100 µl of culture medium were seeded to each well of a 96-well plate and incubated overnight allowing for cell adhesion to the plate. On the next day, the culture medium was replaced by medium with adenoviruses encoding GFP at an MOI of 100 and incubated overnight prior to the observation under a fluorescent microscope.

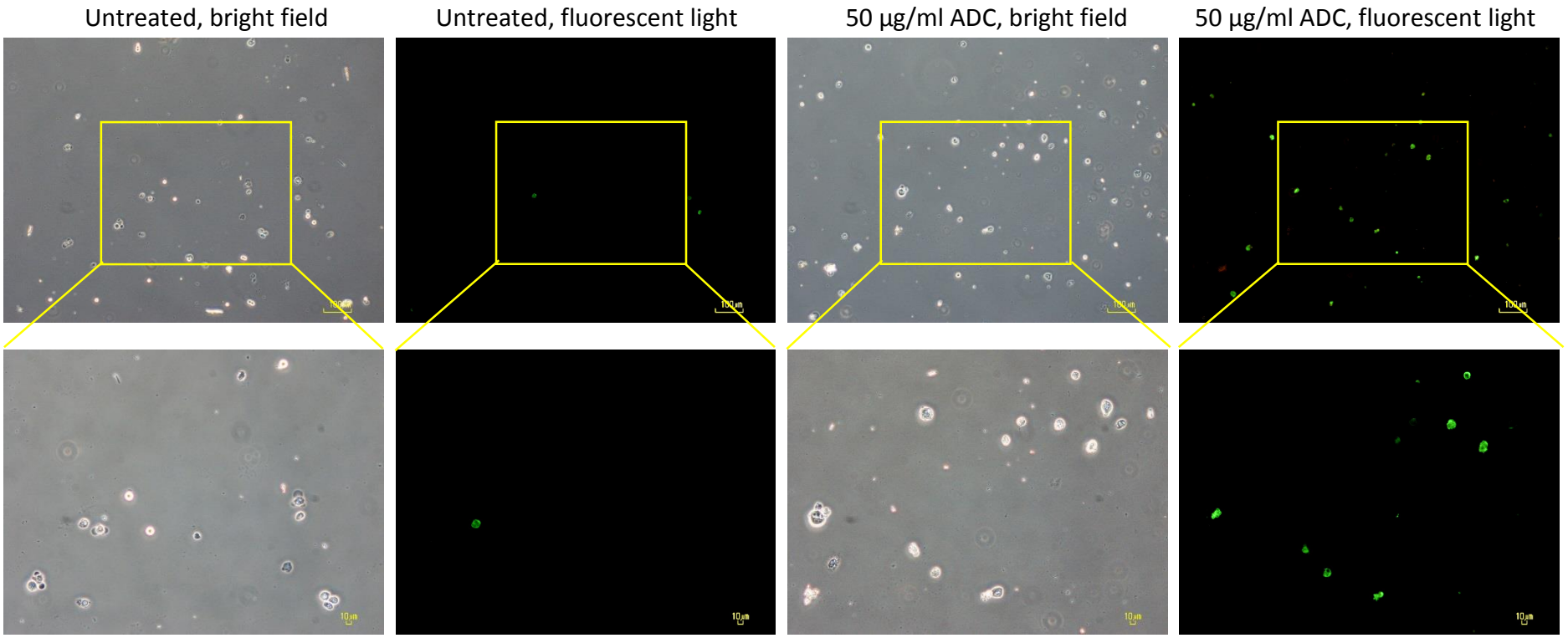

App Figure 6: Micrographs and fluorescent micrographs of HCT116 cells upon 72 h of ADC treatment. Cells were grown in complete medium with cofactors (1 mM $MgCl_2$, 0.1 mM PLP) in the absence or presence of 50 µg/ml ADC. Cells were stained with annxin V-FITC prior to the observation under a fluorescent microscope. Scale bar, 100 µm (top row), 10 µm (bottom row).

A

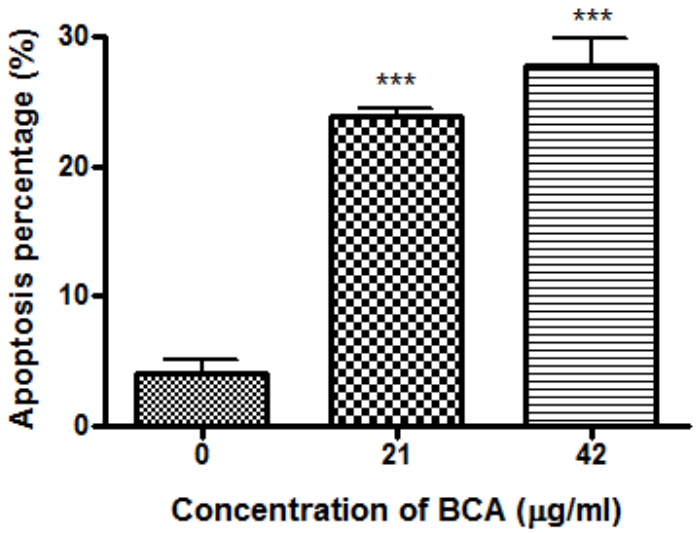

B

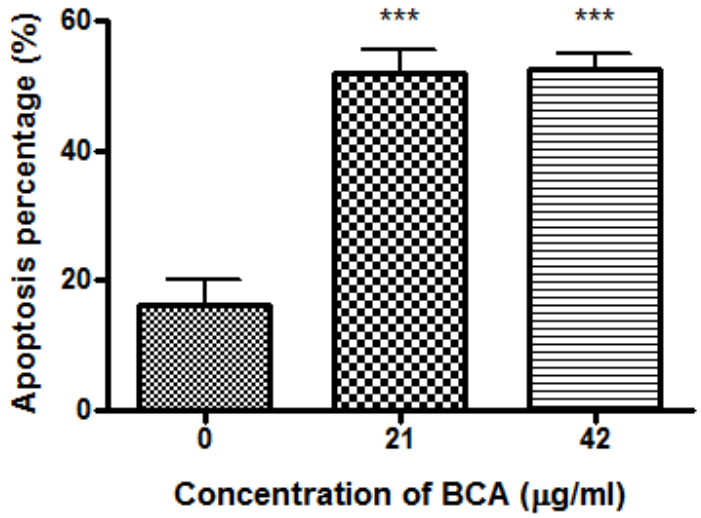

App Figure 7: BCA induces apoptosis in (A) HCT116 and (B) LoVo cells in dose-dependent manners. Bar graphs show the mean ± SEM of the apoptosis percentage after 72 h of treatment with different concentrations of BCA (n = 3). ***, $P < 0.001$ (versus 0 µg/ml control).

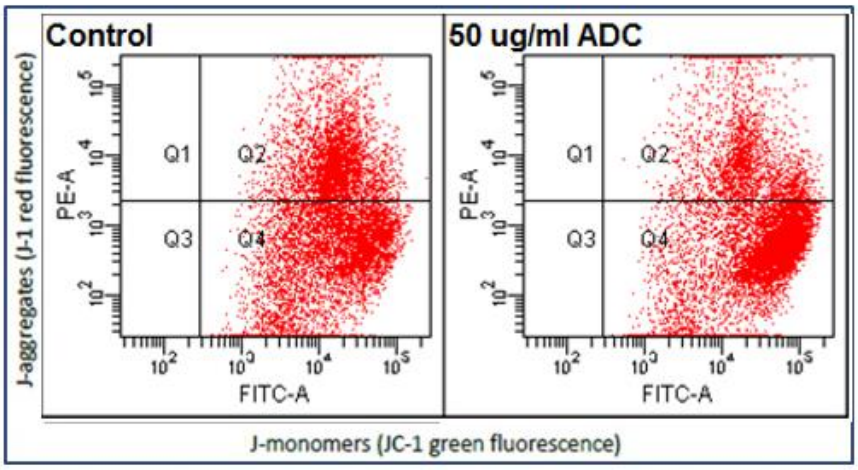

App Figure 8: A preliminary experimental trial showing the change in MOMP in ADC-treated LoVo cells using JC-1 dye and flow cytometry. Cells were grown for 72 h prior to analysis.

A

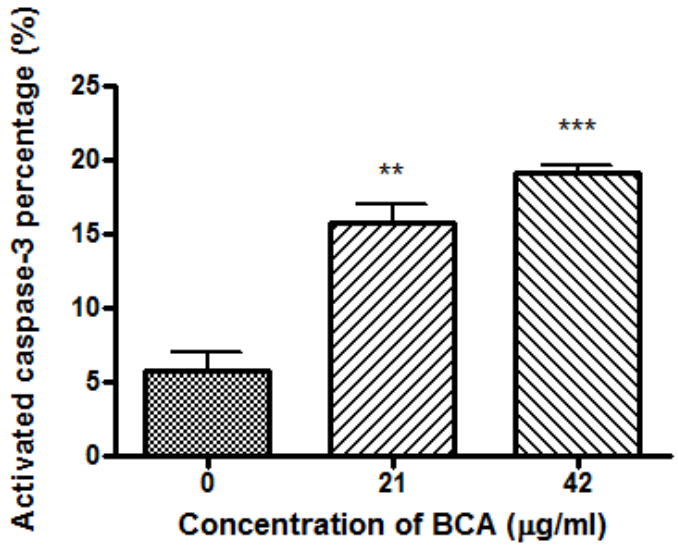

B

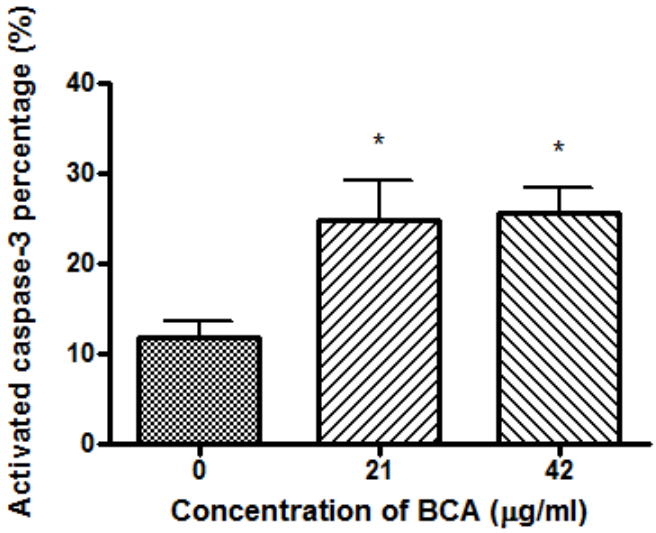

App Figure 9: FITC-DEVD-FMK staining and flow cytometry results showing the percentage of (A) HCT116 and (B) LoVo cell population with active caspase-3 upon BCA treatment. Data are expressed as mean ± SEM of three individual experiments. *, $P < 0.05$; **, $P < 0.01$; ***, $P < 0.001$ (versus 0 µg/ml control).

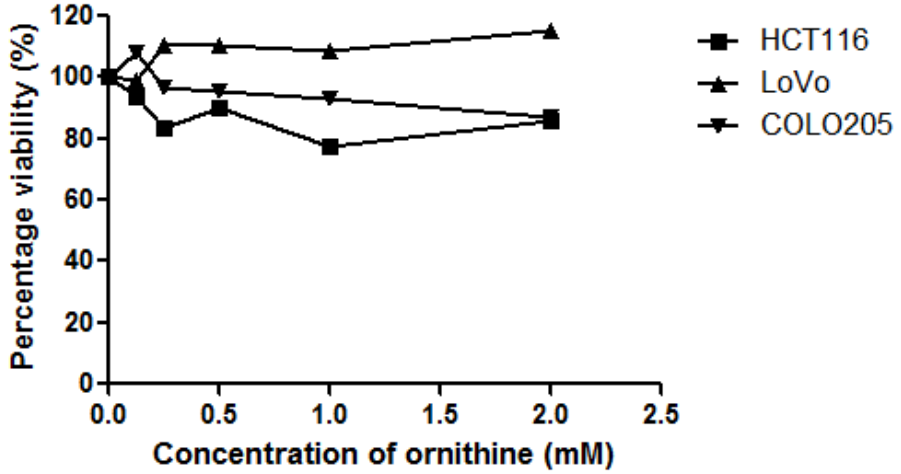

App Figure 10: Preliminary dose-response curves showing the effect of ornithine in HCT116, LoVo, and COLO 205 cell lines. Cells were incubated with different concentrations of ornithine for 72 h prior to MTT assay. Data are expressed as percentage of control treatment (0 μg/ml ADC) and are the mean ± SEM of one experiment performed in triplicate.

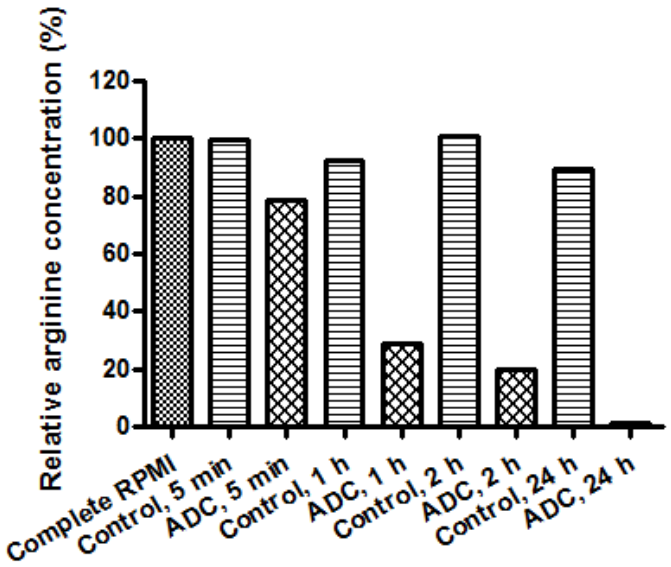

App Figure 11: Arginine level in HCT116 cell culture medium with ADC. HCT116 cells was cultured in complete RPMI medium with or without 50 μg/ml ADC. Medium samples were collected at 5 min, 1 h, 2 h, and 24 h post ADC treatment, then centrifuged to remove the suspended cells, and boiled for 10 min to inactivate ADC prior to analysis. The amount of arginine in each sample is determined by DAMO assay with excessive BCA and is expressed as percentage of the arginine content in complete RPMI (1.15 mM according to the manufacturer). Each bar represents a single measurement.

A

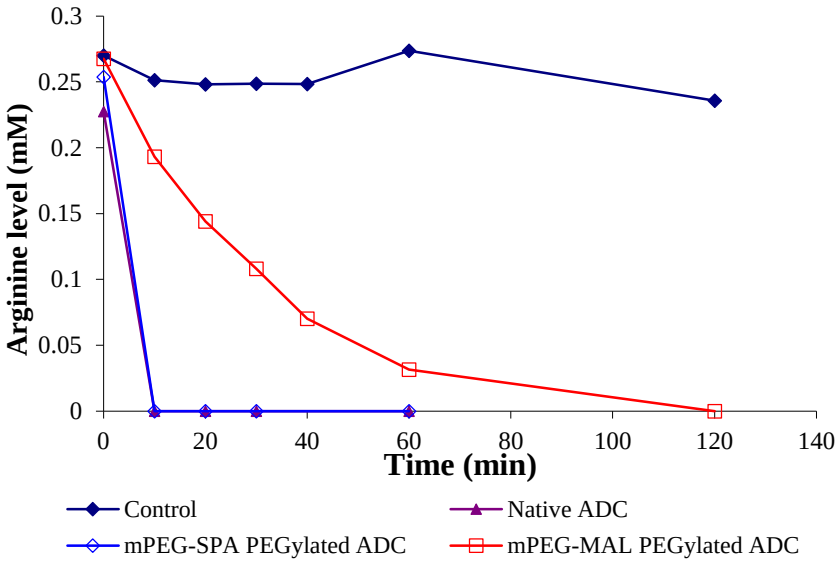
0.3
0.25
0.2
0.15
0.1
0.05
0
Arginine level (mM)
0
20
40
60
80
100
120
140
Time (min)
Control
Native ADC
mPEG-SPA PEGylated ADC
mPEG-MAL PEGylated ADC

B

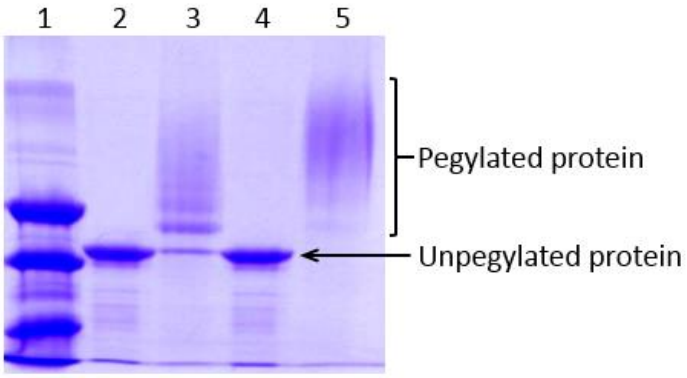
1
2
3
4
5
Pegylated protein
Unpegylated protein

C

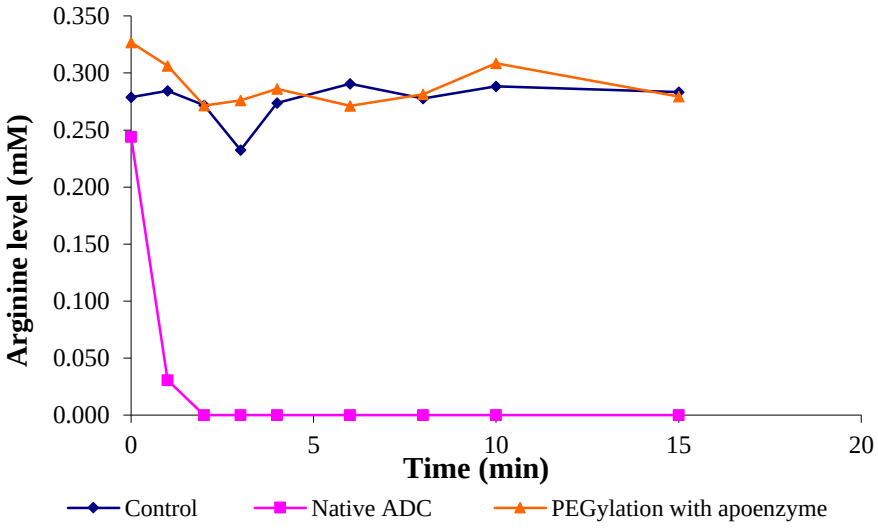
0.350
0.300
0.250
0.200
0.150
0.100
0.050
0.000
Arginine level (mM)
0
5
10
15
20
Time (min)
Control
Native ADC
PEGylation with apoenzyme

App Figure 12: The effect of pegylation on the catalytic activity of ADC. (A) The effect of pegylation of the activity of ADC holoenzyme (formulation contains 5 mM $MgSO_4$, 0.1 mM PLP). mPEG-SPA (5 kDa) was added to ADC at a molar ratio of 20:1 in buffer containing 20 mM sodium phosphate, 0.5 M NaCl at pH 7.4, and the mixture was then incubated at room temperature for overnight with stirring, while mPEG-MAL (20 kDa) was added to tris(2-carboxyethyl) phosphine (TCEP)-reduced ADC (reduction performed by incubating of ADC with excessive TCEP for 5 h at room temperature with stirring) at the same molar ratio, and the mixture was then incubated at 4 ℃ for overnight. The activity of ADC was reflected by measuring the arginine level in cell culture medium through an amino acid analyzer (BioChrom). Control: no enzyme was added; (B) SDS-PAGE gel showing the pegylation efficiency of mPEG-SPA with ADC holoenzyme and apoenzyme (without supplementation of cofactors). The molar ration of mPEG-SPA and ADC is 40:1. Lane 1, marker; lane 2, ADC holoenzyme before pegylation; lane 3, ADC holoenzyme after pegylation; lane 4, ADC apoenzyme before pegylation; lane 5, ADC apoenzyme after pegylation. (C) The effect of pegylation on the activity of ADC apoenzyme. Results are provided by Mr. Angus C. L. Chan.

App Table 1: Cell cycle distribution of HCT116 after 72 h of treatment with BCA, as measured by PI staining and flow cytometry. Data are shown as mean ± SD (n = 3). One-way ANOVA reveals significant effects of BCA on S and G_2/M phase subpopulations. *Post hoc* Dunnett's test of treatment versus control: **, $P < 0.01$.

BCA (μg/ml)	G_0/G_1 (%)	S (%)	G_2/M (%)
0	72.0 ± 0.92	18.2 ± 1.17	9.8 ± 0.25
21	19.3 ± 2.32	41.1 ± 4.49**	39.6 ± 2.93**
42	17.6 ± 2.60	53.0 ± 5.46**	29.2 ± 3.02**

App Table 2: Cell cycle redistribution of LoVo cells after 72 h of treatment with BCA, as measured by PI staining and flow cytometry. Data are shown as mean ± SD (n = 3). One-way ANOVA reveals significant effects of ADC on S phase subpopulation. *Post hoc* Dunnett's test of treatment versus control: **, $P < 0.01$.

BCA (μg/ml)	G_0/G_1 (%)	S (%)	G_2/M (%)
0	48.4 ± 0.46	38.5 ± 1.20	13.1 ± 1.61
21	36.8 ± 1.45	48.9 ± 1.67**	14.3 ± 3.10
42	34.2 ± 0.55	58.9 ± 2.20**	6.9 ± 2.65

References

Abercrombie, M. (1979). Contact inhibition and malignancy. *Nature, 281*(5729), 259-262.

Abuchowski, A., van Es, T., Palczuk, N. C., & Davis, F. F. (1977). Alteration of immunological properties of bovine serum albumin by covalent attachment of polyethylene glycol. *J Biol Chem, 252*(11), 3578-3581.

Agrawal, V., Woo, J. H., Mauldin, J. P., Jo, C., Stone, E. M., Georgiou, G., & Frankel, A. E. (2012). Cytotoxicity of human recombinant arginase I (co)-PEG5000 in the presence of supplemental L-citrulline is dependent on decreased argininosuccinate synthetase expression in human cells. *Anti-Cancer Drugs, 23*(1), 51-64.

Ahmad, J. N., Li, J., Biedermannova, L., Kuchar, M., Sipova, H., Semeradtova, A., Cerny, J., Petrokova, H., Mikulecky, P., Polinek, J., Stanek, O., Vondrasek, J., Homola, J., Maly, J., Osicka, R., Sebo, P., & Maly, P. (2012). Novel high-affinity binders of human interferon gamma derived from albumin-binding domain of protein G. *Proteins, 80*(3), 774-789.

Aida, Y., & Pabst, M. J. (1990). Removal of endotoxin from protein solutions by phase separation using triton X-114. *J Immunol Methods, 132*(2), 191-195.

Akerstrom, B., Nielsen, E., & Bjorck, L. (1987). Definition of igg-binding and albumin-binding regions of streptococcal protein-G. *J Biol Chem, 262*(28), 13388-13391.

Al-Lazikani, B., Banerji, U., & Workman, P. (2012). Combinatorial drug therapy for cancer in the post-genomic era. *Nat Biotechnol, 30*(7), 679-692.

Amaravadi, R. K., Lippincott-Schwartz, J., Yin, X. M., Weiss, W. A., Takebe, N., Timmer, W., DiPaola, R. S., Lotze, M. T., & White, E. (2011). Principles and current strategies for targeting autophagy for cancer treatment. *Clin Cancer Res, 17*(4), 654-666.

Amaravadi, R. K., & Thompson, C. B. (2007). The roles of therapy-induced autophagy and necrosis in cancer treatment. *Clin Cancer Res, 13*(24), 7271-7279.

Andersen, J. T., Pehrson, R., Tolmachev, V., Daba, M. B., Abrahmsén, L., & Ekblad, C. (2011). Extending half-life by indirect targeting of the neonatal fc receptor (FcRn) using a minimal albumin binding domain. *J Biol Chem, 286*(7), 5234-5241.

Andrell, J., Hicks, M. G., Palmer, T., Carpenter, E. P., Iwata, S., & Maher, M. J. (2009). Crystal structure of the acid-induced arginine decarboxylase from escherichia coli: Reversible decamer assembly controls enzyme activity RID B-2239-2012. *Biochemistry, 48*(18), 3915-3927.

Apel, A., Herr, I., Schwarz, H., Rodemann, H. P., & Mayer, A. (2008). Blocked autophagy sensitizes resistant carcinoma cells to radiation therapy. *Cancer Res, 68*(5), 1485-1494.

Armstrong, G. T., Liu, W., Leisenring, W., Yasui, Y., Hammond, S., Bhatia, S., Neglia, J. P., Stovall, M., Srivastava, D., & Robison, L. L. (2011). Occurrence of multiple subsequent neoplasms in long-term survivors of childhood cancer: A report from the childhood cancer survivor study. *J Clin Oncol, 29*(22), 3056-3064.

Armstrong, J. K., Hempel, G., Koling, S., Chan, L. S., Fisher, T., Meiselman, H. J., & Garratty, G. (2007). Antibody against poly(ethylene glycol) adversely affects PEG-asparaginase therapy in acute lymphoblastic leukemia patients. *Cancer, 110*(1), 103-111.

Ascierto, P., Scala, S., Castello, G., Daponte, A., Simeone, E., Ottaiano, A., Beneduce, G., DeRosa, V., Izzo, F., Melucci, M., Ensor, C., Prestayko, A., Holtsberg, F., Bomalaski, J., Clark, M., Savaraj, N., Fenn, L., & Logan, T. (2005). Pegylated arginine deiminase treatment of patients with metastatic melanoma: Results from phase I and II studies. *J Clin Oncol, 23*(30), 7660-7668.

Asselin, B. L., Whitin, J. C., Coppola, D. J., Rupp, I. P., Sallan, S. E., & Cohen, H. J. (1993). Comparative pharmacokinetic studies of three asparaginase preparations. *J Clin Oncol, 11*(9), 1780-1786.

Bach, S. J., & Simon-Reuss, I. (1953). Arginase, antimitotic agent in tissue culture. *Biochim Biophys Acta, 11*(0), 396-402.

Baddiley, J., & Gale, E. F. (1945). Codecarboxylase function of 'pyridoxal phosphate'. *Nature, 155*, 727-728.

Bae, S., Ma, K., Kim, T. H., Lee, E. S., Oh, K. T., Park, E. S., Lee, K. C., & Youn, Y. S. (2012). Doxorubicin-loaded human serum albumin nanoparticles surface-modified with TNF-related apoptosis-inducing ligand and transferrin for targeting multiple tumor types. *Biomaterials, 33*(5), 1536-1546.

Baehrecke, E. H. (2005). Autophagy: Dual roles in life and death? *Nat Rev Mol Cell Biol, 6*(6), 505-510.

Bailon, P., Palleroni, A., Schaffer, C. A., Spence, C. L., Fung, W. J., Porter, J. E., Ehrlich, G. K., Pan, W., Xu, Z. X., Modi, M. W., Farid, A., Berthold, W., & Graves, M. (2001). Rational design of a potent, long-lasting form of interferon: A 40 kDa branched polyethylene glycol-

conjugated interferon alpha-2a for the treatment of hepatitis C. *Bioconjug Chem, 12*(2), 195-202.

Balan, V. (2006). Albumin-interferon-alpha in the treatment of chronic hepatitis C. *Future Virol, 1*(3), 269-278.

Bentzen, S. M. (2006). Preventing or reducing late side effects of radiation therapy: Radiobiology meets molecular pathology. *Nat Rev Cancer, 6*(9), 702-713.

Bewley, M. C., Jeffrey, P. D., Patchett, M. L., Kanyo, Z. F., & Baker, E. N. (1999). Crystal structures of bacillus caldovelox arginase in complex with substrate and inhibitors reveal new insights into activation, inhibition and catalysis in the arginase superfamily. *Structure, 7*(4), 435-448.

Bio-Cancer Treatment International Limited; Chinese University of Hong Kong; The University of Hong Kong. (2014a). *A phase II trial of PEG-BCT-100 as the second-line therapy following sorafenib in patients with advanced hepatocellular carcinoma.* In: ClinicalTrials.gov [Internet]. Bethesda (MD): National Library of Medicine (US). [cited 2014 Jul 31]. Available from: https://clinicaltrials.gov/ct2/show/NCT02089763 NLM Identifier: NCT02089763.

Bio-Cancer Treatment International Limited; The University of Hong Kong. (2014b). *A study of the safety and efficacy of recombinant human arginase 1 (PEG-BCT-100) combined with capecitabine and oxaliplatin in patients with locally advanced or metastatic hepatocellular carcinoma.* In: ClinicalTrials.gov [Internet]. Bethesda (MD): National Library of Medicine (US). [cited 2014 Jul 31]. Available from: https://clinicaltrials.gov/ct2/show/NCT02089633 NLM Identifier: NCT02089633.

Birecka, H., Bitonti, A. J., & McCann, P. P. (1985). Activities of arginine and ornithine decarboxylases in various plant species. *Plant Physiol, 79*(2), 515-519.

Black Jr., O., & Chang, B. K. (1982). Ornithine decarboxylase enzyme activity in human and hamster pancreatic tumor cell lines. *Cancer Lett, 17*(1), 87-93.

Blagosklonny, M. V. (2006). Cell senescence: Hypertrophic arrest beyond the restriction point. *J Cell Physiol, 209*(3), 592-597.

Blagosklonny, M. V. (2011). Cell cycle arrest is not senescence. *Aging, 3*(2), 94-101.

Blethen, S. L., Boeker, E. A., & Snell, E. E. (1968). Argenine decarboxylase from escherichia coli. I. purification and specificity for substrates and coenzyme. *J Biol Chem, 243*(8), 1671-1677.

Bordier, C. (1981). Phase separation of integral membrane proteins in triton X-114 solution. *J Biol Chem, 256*(4), 1604-1607.

Bouchereau, A., Aziz, A., Larher, F., & Martin-Tanguy, J. (1999). Polyamines and environmental challenges: Recent development. *Plant Sci, 140*(2), 103-125.

Bowles, T. L., Kim, R., Galante, J., Parsons, C. M., Virudachalam, S., Kung, H. J., & Bold, R. J. (2008). Pancreatic cancer cell lines deficient in argininosuccinate synthetase are sensitive to arginine deprivation by arginine deiminase. *Int J Cancer, 123*(8), 1950-1955.

Boya, P., Gonzalez-Polo, R. A., Casares, N., Perfettini, J. L., Dessen, P., Larochette, N., Metivier, D., Meley, D., Souquere, S., Yoshimori, T., Pierron, G., Codogno, P., & Kroemer, G. (2005). Inhibition of macroautophagy triggers apoptosis. *Mol Cell Biol, 25*(3), 1025-1040.

Bratton, D. L., Fadok, V. A., Richter, D. A., Kailey, J. M., Guthrie, L. A., & Henson, P. M. (1997). Appearance of phosphatidylserine on apoptotic cells requires calcium-mediated nonspecific flip-flop and is enhanced by loss of the aminophospholipid translocase. *J Biol Chem, 272*(42), 26159-26165.

Brekke, O. H., & Sandlie, I. (2003). Therapeutic antibodies for human diseases at the dawn of the twenty-first century. *Nat Rev Drug Discov, 2*(1), 52-62.

Brown, J. M., & Giaccia, A. J. (1998). The unique physiology of solid tumors: Opportunities (and problems) for cancer therapy. *Cancer Res, 58*(7), 1408-1416.

Buch, J., & Boyle, S. (1985). Biosynthetic arginine decarboxylase in escherichia-coli is synthesized as a precursor and located in the cell-envelope. *J Bacteriol, 163*(2), 522-527.

Bulgheroni, E., Citterio, P., Croce, F., Lo Cicero, M., Vigano, O., Soster, F., Chou, T. C., Galli, M., & Rusconi, S. (2004). Analysis of protease inhibitor combinations in vitro: Activity of lopinavir, amprenavir and tipranavir against HIV type 1 wild-type and drug-resistant isolates. *J Antimicrob Chemother, 53*(3), 464-468.

Burrell, M., Hanfrey, C. C., Murray, E. J., Stanley-Wall, N. R., & Michael, A. J. (2010). Evolution and multiplicity of arginine decarboxylases in polyamine biosynthesis and essential role in bacillus subtilis biofilm formation. *J Biol Chem, 285*(50), 39224-39238.

Cagnol, S., & Chambard, J. C. (2010). ERK and cell death: Mechanisms of ERK-induced cell death--apoptosis, autophagy and senescence. *FEBS J, 277*(1), 2-21.

Capdeville, R., Buchdunger, E., Zimmermann, J., & Matter, A. (2002). Glivec (STI571, imatinib), a rationally developed, targeted anticancer drug. *Nat Rev Drug Discov, 1*(7), 493-502.

Carter, P., Presta, L., Gorman, C. M., Ridgway, J. B., Henner, D., Wong, W. L., Rowland, A. M, Kotts, C., Carver, M.E., & Shepard, H. M. (1992). Humanization of an anti-p185HER2 antibody for human cancer therapy. *Proc Natl Acad Sci USA, 89*(10), 4285-4289.

Carvajal, N., Orellana, M. S., Salas, M., Enríquez, P., Alarcón, R., Uribe, E., & López, V. (2004). Kinetic studies and site-directed mutagenesis of escherichia coli agmatinase. a role for Glu274 in binding and correct positioning of the substrate guanidinium group. *Arch Biochem Biophys, 430*(2), 185-190.

Carvalho, C., Santos, R. X., Cardoso, S., Correia, S., Oliveira, P. J., Santos, M. S., & Moreira, P. I. (2009). Doxorubicin: The good, the bad and the ugly effect. *Curr Med Chem, 16*(25), 3267-3285.

Cassidy, J., Clarke, S., Diaz-Rubio, E., Scheithauer, W., Figer, A., Wong, R., Koski, S., Rittweger, K., Gilberg, F., & Saltz, L. (2011). XELOX vs FOLFOX-4 as first-line therapy for metastatic colorectal cancer: NO16966 updated results. *Br J Cancer, 105*(1), 58-64.

Chang, B. D., Broude, E. V., Fang, J., Kalinichenko, T. V., Abdryashitov, R., Poole, J. C., & Roninson, I. B. (2000). p21Waf1/Cip1/Sdi1-induced growth arrest is associated with depletion of mitosis-control proteins and leads to abnormal mitosis and endoreduplication in recovering cells. *Oncogene, 19*(17), 2165-2170.

Chen, W., Chen, M., & Barak, L. S. (2010). Development of small molecules targeting the wnt pathway for the treatment of colon cancer: A high-throughput screening approach. *Am J Physiol Gastrointest Liver Physiol, 299*(2), G293-300.

Chen, W., Zheng, R., Zhang, S., Zhao, P., Li, G., Wu, L., & He, J. (2013). The incidences and mortalities of major cancers in china, 2009. *Chin J Cancer, 32*(3), 106-112.

Chen, Z., Romaguera, J., Wang, M., Fayad, L., Kwak, L. W., & McCarty, N. (2012). Verapamil synergistically enhances cytotoxicity of bortezomib in mantle cell lymphoma via induction of reactive oxygen species production. *Br J Haematol, 159*(2), 243-246.

Cheng, P. N., Lam, T., Lam, W., Tsui, S., Cheng, A. W., Lo, W., & Leung, Y. (2007). Pegylated recombinant human arginase (rhArg-peg5,000mw) inhibits the in vitro and in vivo proliferation of human hepatocellular carcinoma through arginine depletion. *Cancer Res, 67*(1), 309-317.

Cheung, N. K., Chau, I. Y., & Coccia, P. F. (1986). Antibody response to escherichia coli L-asparaginase. prognostic significance and clinical utility of antibody measurement. *Am J Pediatr Hematol Oncol, 8*(2), 99-104.

Chinnaiyan, A. M. (1999). The apoptosome: Heart and soul of the cell death machine. *Neoplasia, 1*(1), 5-15.

Chou, T. C. (2010). Drug combination studies and their synergy quantification using the chou-talalay method. *Cancer Res, 70*(2), 440-446.

Chou, T. C., & Talalay, P. (1984). Quantitative analysis of dose-effect relationships: The combined effects of multiple drugs or enzyme inhibitors. *Adv Enzyme Regul, 22*, 27-55.

Coiffier, B., Lepage, E., Briere, J., Herbrecht, R., Tilly, H., Bouabdallah, R., Morel, P., Van Den Neste, E., Salles, G., Gaulard, P., Reyes, F., Lederlin, P., & Gisselbrecht, C. (2002). CHOP chemotherapy plus

rituximab compared with CHOP alone in elderly patients with diffuse large-B-cell lymphoma. *N Engl J Med, 346*(4), 235-242.

Collado, M., Blasco, M. A., & Serrano, M. (2007). Cellular senescence in cancer and aging. *Cell, 130*(2), 223-233.

Cong, Y., Pawlisz, E., Bryant, P., Balan, S., Laurine, E., Tommasi, R., Singh, R., Dubey, S., Peciak, K., Bird, M., Sivasankar, A., Swierkosz, J., Muroni, M., Heidelberger, S., Farys, M., Khayrzad, F., Edwards, J., Badescu, G., Hodgson, I., Heise, C., Somavarapu, S., Liddell, J., Powell, K., Zloh, M., Choi, J. W., Godwin, A., & Brocchini, S. (2012). Site-specific PEGylation at histidine tags. *Bioconjug Chem, 23*(2), 248-263.

Corbett, T., Griswold, D., Roberts, B., Peckham, J., & Schabel, F. (1977). Evaluation of single agents and combinations of chemotherapeutic-agents in mouse colon carcinomas. *Cancer, 40*(5), 2660-2680.

Cory, S., & Adams, J. M. (2002). The Bcl2 family: Regulators of the cellular life-or-death switch. *Nat Rev Cancer, 2*(9), 647-656.

Crenn, P., Coudray–Lucas, C., Thuillier, F., Cynober, L., & Messing, B. (2000). Postabsorptive plasma citrulline concentration is a marker of absorptive enterocyte mass and intestinal failure in humans. *Gastroenterology, 119*(6), 1496-1505.

Cufi, S., Vazquez-Martin, A., Oliveras-Ferraros, C., Corominas-Faja, B., Cuyas, E., Lopez-Bonet, E., Martin-Castillo, B., Joven, J., & Menendez, J. A. (2013). The anti-malarial chloroquine overcomes primary resistance and restores sensitivity to trastuzumab in HER2-positive breast cancer. *Sci Rep, 3*, 2469.

Dallmann, K., Junker, H., Balabanov, S., Zimmermann, U., Giebel, J., & Walther, R. (2004). Human agmatinase is diminished in the clear cell type of renal cell carcinoma. *Int J Cancer, 108*(3), 342-347.

Das, K., Butler, G. H., Kwiatkowski, V., Clark, A. D.,Jr, Yadav, P., & Arnold, E. (2004). Crystal structures of arginine deiminase with covalent reaction intermediates; implications for catalytic mechanism. *Structure, 12*(4), 657-667.

Degenhardt, K., Mathew, R., Beaudoin, B., Bray, K., Anderson, D., Chen, G., Mukherjee, C., Shi, Y., Gelinas, C., Fan, Y., Nelson, D. A., Jin, S., & White, E. (2006). Autophagy promotes tumor cell survival and restricts necrosis, inflammation, and tumorigenesis. *Cancer Cell, 10*(1), 51-64.

Delage, B., Fennell, D. A., Nicholson, L., McNeish, I., Lemoine, N. R., Crook, T., & Szlosarek, P. W. (2010). Arginine deprivation and argininosuccinate synthetase expression in the treatment of cancer. *Int J Cancer, 126*(12), 2762-2772.

DeLisser, H. M., Keirns, C. C., Clinton, E. A., & Margolis, M. L. (2009). "The air got to it:" exploring a belief about surgery for lung cancer. *J Natl Med Assoc, 101*(8), 765-771.

Demetriades, C., Doumpas, N., & Teleman, A. A. (2014). Regulation of TORC1 in response to amino acid starvation via lysosomal recruitment of TSC2. *Cell, 156*(4), 786-799.

Deng, D., Xu, C., Sun, P., Wu, J., Yan, C., Hu, M., & Yan, N. (2014). Crystal structure of the human glucose transporter GLUT1. *Nature, 510*(7503), 121-125.

Deng, W., Jiang, X., Mei, Y., Sun, J., Ma, R., Liu, X., Sun, H., Tian, H., & Sun, X. (2008). Role of ornithine decarboxylase in breast cancer. *Acta Bioch Bioph Sin, 40*(3), 235-243.

Dennis, M. S., Zhang, M., Meng, Y. G., Kadkhodayan, M., Kirchhofer, D., Combs, D., & Damico, L. A. (2002). Albumin binding as a general

strategy for improving the pharmacokinetics of proteins. *J Biol Chem, 277*(38), 35035-35043.

DeSantis, C. E., Lin, C. C., Mariotto, A. B., Siegel, R. L., Stein, K. D., Kramer, J. L., Alteri, R., Robbins, A. S., & Jemal, A. (2014). Cancer treatment and survivorship statistics, 2014. *CA-Cancer J Clin, 64*(4), 252-271.

DeVita, V. T.,Jr, Young, R. C., & Canellos, G. P. (1975). Combination versus single agent chemotherapy: A review of the basis for selection of drug treatment of cancer. *Cancer, 35*(1), 98-110.

Dimri, G. P., Lee, X., Basile, G., Acosta, M., Scott, G., Roskelley, C., Medrano, E. E., Linskens, M., Rubelj, I., & Pereira-Smith, O. (1995). A biomarker that identifies senescent human cells in culture and in aging skin in vivo. *Proc Natl Acad Sci USA, 92*(20), 9363-9367.

Dinndorf, P. A., Gootenberg, J., Cohen, M. H., Keegan, P., & Pazdur, R. (2007). FDA drug approval summary: Pegaspargase (oncaspar) for the first-line treatment of children with acute lymphoblastic leukemia (ALL). *Oncologist, 12*(8), 991-998.

DiPaola, R. S. (2002). To arrest or not to G2-M cell-cycle arrest : Commentary re: A. K. tyagi et al., silibinin strongly synergizes human prostate carcinoma DU145 cells to doxorubicin-induced growth inhibition, G2-M arrest, and apoptosis. clin. cancer res., 8: 3512–3519, 2002. *Clin Cancer Res, 8*(11), 3311-3314.

Dobbelstein, M., & Moll, U. (2014). Targeting tumour-supportive cellular machineries in anticancer drug development. *Nat Rev Drug Discov, 13*(3), 179-196.

Durando, X., Farges, M. C., Buc, E., Abrial, C., Petorin-Lesens, C., Gillet, B., Vasson, M. P., Pezet, D., Chollet, P., & Thivat, E. (2010). Dietary methionine restriction with FOLFOX regimen as first line therapy of

metastatic colorectal cancer: A feasibility study. *Oncology, 78*(3-4), 205-209.

Elmore, S. (2007). Apoptosis: A review of programmed cell death. *Toxicol Pathol, 35*(4), 495-516.

El-Sayed, A. S., Shouman, S. A., & Nassrat, H. M. (2012). Pharmacokinetics, immunogenicity and anticancer efficiency of aspergillus flavipes l-methioninase. *Enzyme Microb Technol, 51*(4), 200-210.

Enari, M., Sakahira, H., Yokoyama, H., Okawa, K., Iwamatsu, A., & Nagata, S. (1998). A caspase-activated DNase that degrades DNA during apoptosis, and its inhibitor ICAD. *Nature, 391*(6662), 43-50.

Ensor, C., Holtsberg, F., Bomalaski, J., & Clark, M. (2002). Pegylated arginine deiminase (ADI-SS PEG(20,000) (mw)) inhibits human melanomas and hepatocellular carcinomas in vitro and in vivo. *Cancer Res, 62*(19), 5443-5450.

Etzel, M. (2004). Manufacture and use of dairy protein fractions. *J Nutr, 134*(4), 996S-1002S.

Faivre, S., Kroemer, G., & Raymond, E. (2006). Current development of mTOR inhibitors as anticancer agents. *Nat Rev Drug Discov, 5*(8), 671-688.

Forouhar, F., Lew, S., Seetharaman, J., Xiao, R., Acton, T. B., Montelione, G. T., & Tong, L. (2010). Structures of bacterial biosynthetic arginine decarboxylases. *Acta Crystallogr Sect F Struct Biol Cryst Commun, 66*, 1562-1566.

Fotakis, G., & Timbrell, J. A. (2006). In vitro cytotoxicity assays: Comparison of LDH, neutral red, MTT and protein assay in hepatoma

cell lines following exposure to cadmium chloride. *Toxicol Lett, 160*(2), 171-177.

Gale, E. F. (1940). The production of amines by bacteria: the decarboxylation of amino-acids by strains of Bacterium coli. *Biochem J, 34*(3), 392-413.

Ganapathy, V., Thangaraju, M., & Prasad, P. D. (2009). Nutrient transporters in cancer: Relevance to warburg hypothesis and beyond. *Pharmacol Ther, 121*(1), 29-40.

Gerber, D. E. (2008). Targeted therapies: A new generation of cancer treatments. *Am Fam Physician, 77*(3), 311-319.

Gerner, E. W., & Meyskens, F. L.,Jr. (2004). Polyamines and cancer: Old molecules, new understanding. *Nat Rev Cancer, 4*(10), 781-792.

Gewirtz, D. A. (2009). Autophagy, senescence and tumor dormancy in cancer therapy. *Autophagy, 5*(8), 1232-1234.

Gilman, A., & Philips, F. S. (1946). The biological actions and therapeutic applications of the B-chloroethyl amines and sulfides. *Science, 103*(2675), 409-436.

Gioux, S., Choi, H. S., & Frangioni, J. V. (2010). Image-guided surgery using invisible near-infrared light: Fundamentals of clinical translation. *Mol Imaging, 9*(5), 237-255.

Glazer, E. S., Kaluarachchi, W. D., Massey, K. L., Zhu, C., & Curley, S. A. (2010). Bioengineered arginase I increases caspase-3 expression of hepatocellular and pancreatic carcinoma cells despite induction of argininosuccinate synthetase-1. *Surgery, 148*(2), 310-318.

Goldberg, R. M., Sargent, D. J., Morton, R. F., Fuchs, C. S., Ramanathan, R. K., Williamson, S. K., Findlay, B. P., Pitot, H. C., & Alberts, S. R. (2004). A randomized controlled trial of fluorouracil plus leucovorin,

irinotecan, and oxaliplatin combinations in patients with previously untreated metastatic colorectal cancer. *J Clin Oncol, 22*(1), 23-30.

Goldberg, S. B., Supko, J. G., Neal, J. W., Muzikansky, A., Digumarthy, S., Fidias, P., Temel, J. S., Heist, R. S., Shaw, A. T., McCarthy, P. O., Lynch, T. J., Sharma, S., Settleman, J. E., & Sequist, L. V. (2012). A phase I study of erlotinib and hydroxychloroquine in advanced non-small-cell lung cancer. *J Thorac Oncol, 7*(10), 1602-1608.

Goldschmidt, M. C., & Lockhart, B. M. (1971a). Rapid methods for determining decarboxylase activity: Arginine decarboxylase. *Appl Microbiol, 22*(3), 350-357.

Goldschmidt, M. C., & Lockhart, B. M. (1971b). Simplified rapid procedure for determination of agmatine and other guanidino-containing compounds. *Anal Chem, 43*(11), 1475-1479.

Gong, H., Zolzer, F., von Recklinghausen, G., Havers, W., & Schweigerer, L. (2000). Arginine deiminase inhibits proliferation of human leukemia cells more potently than asparaginase by inducing cell cycle arrest and apoptosis. *Leukemia, 14*(5), 826-829.

Gong, H., Zolzer, F., von Recklinghausen, G., Rossler, J., Breit, S., Havers, W., Fotsis, T., & Schweigerer, L. (1999). Arginine deiminase inhibits cell proliferation by arresting cell cycle and inducing apoptosis. *Biochem Biophys Res Commun, 261*(1), 10-14.

Goodman, L. S., & Wintrobe, M. M. (1946). Nitrogen mustard therapy; use of methyl-bis (beta-chloroethyl) amine hydrochloride and tris (beta-chloroethyl) amine hydrochloride for hodgkin's disease, lymphosarcoma, leukemia and certain allied and miscellaneous disorders. *J Am Med Assoc, 132*, 126-132.

Graham, D. E., Xu, H., & White, R. H. (2002). Methanococcus jannaschii uses a pyruvoyl-dependent arginine decarboxylase in polyamine biosynthesis. *J Biol Chem, 277*(26), 23500-23507.

Greenhalgh, D. G. (1998). The role of apoptosis in wound healing. *Int J Biochem Cell Biol, 30*(9), 1019-1030.

Gunja, N., Roberts, D., McCoubrie, D., Lamberth, P., Jan, A., Simes, D. C., Hackett, P., & Buckley, N. A. (2009). Survival after massive hydroxychloroquine overdose. *Anaesth Intensive Care, 37*(1), 130-133.

Guo, H. Y., Herrera, H., Groce, A., & Hoffman, R. M. (1993). Expression of the biochemical defect of methionine dependence in fresh patient tumors in primary histoculture. *Cancer Res, 53*(11), 2479-2483.

Guo, H. Y., Lishko, V., Herrera, H., Groce, A., Kubota, T., & Hoffman, R. (1993). Therapeutic tumor-specific cell-cycle block induced by methionine starvation in-vivo. *Cancer Res, 53*(23), 5676-5679.

Haines, R. J., Pendleton, L. C., & Eichler, D. C. (2011). Argininosuccinate synthase: At the center of arginine metabolism. *Int J Biochem Mol Biol, 2*(1), 8-23.

Hanahan, D., & Weinberg, R. A. (2000). The hallmarks of cancer. *Cell, 100*(1), 57-70.

Hartwell, L. H., & Weinert, T. A. (1989). Checkpoints: Controls that ensure the order of cell cycle events. *Science, 246*(4930), 629-634.

He, C., & Klionsky, D. J. (2009). Regulation mechanisms and signaling pathways of autophagy. *Annu Rev Genet, 43*, 67-93.

Heinen, A., Bruss, M., Bonisch, H., Gothert, M., & Molderings, G. J. (2003). Pharmacological characteristics of the specific transporter for the endogenous cell growth inhibitor agmatine in six tumor cell lines. *Int J Colorectal Dis, 18*(4), 314-319.

Holtsberg, F. W., Ensor, C. M., Steiner, M. R., Bomalaski, J. S., & Clark, M. A. (2002). Poly(ethylene glycol) (PEG) conjugated arginine deiminase: Effects of PEG formulations on its pharmacological properties. *J Control Release, 80*(1-3), 259-271.

Hong Kong Cancer Registry, Hospital Authority. (2013). Leading cancer sites in Hong Kong in 2001. Retrieved from http://www3.ha.org.hk/cancereg/statistics.html#cancerfacts

Hopp, J., Hornig, N., Zettlitz, K. A., Schwarz, A., Fuss, N., Mueller, D., & Kontermann, R. E. (2010). The effects of affinity and valency of an albumin-binding domain (ABD) on the half-life of a single-chain diabody-ABD fusion protein. *Protein Eng Des Sel, 23*(11), 827-834.

Hyung, J. A., Kyoung, H. K., Lee, J., Ha, J., Hyung, H. L., Kim, D., Yoon, H., Kwon, A., & Se, W. S. (2004). Crystal structure of agmatinase reveals structural conservation and inhibition mechanism of the ureohydrolase superfamily. *J Biol Chem, 279*(48), 50505-50513.

Ikemoto, M., Tabata, M., & Murachi, T. (1989). Purification and properties of human erythrocyte arginase. *Ann Clin Biochem, 26*, 547-553.

Imai, K., & Takaoka, A. (2006). Comparing antibody and small-molecule therapies for cancer. *Nat Rev Cancer, 6*(9), 714-727.

Inouye, M., & Halegoua, S. (1980). Secretion and membrane localization of proteins in escherichia-coli. *CRC Crit Rev Biochem, 7*(4), 339-371.

Isome, M., Lortie, M. J., Murakami, Y., Parisi, E., Matsufuji, S., & Satriano, J. (2007). The antiproliferative effects of agmatine correlate with the rate of cellular proliferation. *Am J Physiol Cell Physiol, 293*(2), C705-11.

Izzo, F., Marra, P., Beneduce, G., Castello, G., Vallone, P., De Rosa, V., Cremona, F., Ensor, C., Holtsberg, F. Bomalaski, J., Clark, M., Ng, C.,

& Curley, S. (2004). Pegylated arginine deiminase treatment of patients with unresectable hepatocellular carcinoma: Results from phase I/II studies. *J Clin Oncol, 22*(10), 1815-1822.

Janku, F., McConkey, D. J., Hong, D. S., & Kurzrock, R. (2011). Autophagy as a target for anticancer therapy. *Nat Rev Clin Oncol, 8*(9), 528-539.

Jemal, A., Bray, F., Center, M. M., Ferlay, J., Ward, E., & Forman, D. (2011). Global cancer statistics. *CA-Cancer J Clin, 61*(2), 69-90.

Jonsson, A., Dogan, J., Herne, N., Abrahmsen, L., & Nygren, P. (2008). Engineering of a femtomolar affinity binding protein to human serum albumin. *Protein Eng Des Sel, 21*(8), 515-527.

Kanagasabapathy A. S., & Kumari, S. (2000). Urea - diacetyl monoxime method. *Guidelines on standard operating procedures for clinical chemistry* (pp. 21-24). New Delhi, India: World Health Organization, Regional Office for South-East Asia.

Kang, S. W., Kang, H., Park, I. S., Choi, S. H., Shin, K. H., Chun, Y. S., Chun, B. G., & Min, B. H. (2000). Cytoprotective effect of arginine deiminase on taxol-induced apoptosis in DU145 human prostate cancer cells. *Mol Cells, 10*(3), 331-337.

Kapahi, P., Chen, D., Rogers, A. N., Katewa, S. D., Li, P. W., Thomas, E. L., & Kockel, L. (2010). With TOR, less is more: A key role for the conserved nutrient-sensing TOR pathway in aging. *Cell Metab, 11*(6), 453-465.

Kelly, M. P., Jungbluth, A. A., Wu, B., Bomalaski, J., Old, L. J., & Ritter, G. (2012). Arginine deiminase PEG20 inhibits growth of small cell lung cancers lacking expression of argininosuccinate synthetase. *Br J Cancer, 106*(2), 324-332.

Kerr, J. F., Winterford, C. M., & Harmon, B. V. (1994). Apoptosis. Its significance in cancer and cancer therapy. *Cancer, 73*(8), 2013-2026.

Kerr, J. F., Wyllie, A. H., & Currie, A. R. (1972). Apoptosis: A basic biological phenomenon with wide-ranging implications in tissue kinetics. *Br J Cancer, 26*(4), 239-257.

Kim, J. E., Kim, S. Y., Lee, K. W., & Lee, H. J. (2009). Arginine deiminase originating from lactococcus lactis ssp. lactis american type culture collection (ATCC) 7962 induces G1-phase cell-cycle arrest and apoptosis in SNU-1 stomach adenocarcinoma cells. *Br J Nutr, 102*(10), 1469-1476.

Kim, R. H., Bold, R. J., & Kung, H. (2009). ADI, autophagy and apoptosis metabolic stress as a therapeutic option for prostate cancer. *Autophagy, 5*(4), 567-568.

Kim, R. H., Coates, J. M., Bowles, T. L., McNerney, G. P., Sutcliffe, J., Jung, J. U., Gandour-Edwards, R., Chuan, F. Y., Bold, R. J., & Kung, H. J. (2009). Arginine deiminase as a novel therapy for prostate cancer induces autophagy and caspase-independent apoptosis. *Cancer Res, 69*(2), 700-708.

Kimura, T., Takabatake, Y., Takahashi, A., & Isaka, Y. (2013). Chloroquine in cancer therapy: A double-edged sword of autophagy. *Cancer Res, 73*(1), 3-7.

Kiriyama, Y., Kubota, M., Takimoto, T., Kitoh, T., Tanizawa, A., Akiyama, Y., & Mikawa, H. (1989). Biochemical characterization of U937 cells resistant to L-asparaginase: The role of asparagine synthetase. *Leukemia, 3*(4), 294-297.

Knop, K., Hoogenboom, R., Fischer, D., & Schubert, U. S. (2010). Poly(ethylene glycol) in drug delivery: Pros and cons as well as potential alternatives. *Angew Chem Int Ed Engl, 49*(36), 6288-6308.

Kroemer, G., Galluzzi, L., Vandenabeele, P., Abrams, J., Alnemri, E. S., Baehrecke, E. H., Blagosklonny, M. V., El-Deiry, W. S., Golstein, P., Green, D. R., Hengartner, M., Knight, R. A., Kumar, S., Lipton, S. A., Malorni, W., Nunez, G., Peter, M. E., Tschopp, J., Yuan, J., Piacentini, M., Zhivotovsky, B., Melino, G., & Nomenclature Committee on Cell Death 2009. (2009). Classification of cell death: Recommendations of the nomenclature committee on cell death 2009. *Cell Death Differ, 16*(1), 3-11.

Kroemer, G., Marino, G., & Levine, B. (2010). Autophagy and the integrated stress response. *Mol Cell, 40*(2), 280-293.

Kubetzko, S., Sarkar, C. A., & Pluckthun, A. (2005). Protein PEGylation decreases observed target association rates via a dual blocking mechanism. *Mol Pharmacol, 68*(5), 1439-1454.

Kudou, D., Misaki, S., Yamashita, M., Tamura, T., Takakura, T., Yoshioka, T., Yagi, S., Hoffman, R. M., Takimoto, A., Nobuyoshi Esaki, N., & Inagaki, K. (2007). Structure of the antitumour enzyme l-methionine γ-lyase from pseudomonas putida at 1.8 Å resolution. *J Biochem, 141*(4), 535-544.

Lam, T. L., Wong, G. K. Y., Chong, H. C., Cheng, P. N. M., Choi, S. C., Chow, T. L., Kwok, S. Y., Poon, R. T. P., Wheatley, D. N., Lo, W. H., & Leung, Y. C. (2009). Recombinant human arginase inhibits proliferation of human hepatocellular carcinoma by inducing cell cycle arrest. *Cancer Lett, 277*(1), 91-100.

Lam, T. L., Wong, G. K. Y., Chow, H. Y., Chong, H. C., Chow, T. L., Kwok, S. Y., Cheng, P. N., Wheatley, D. N., Lo, W. H., & Leung, Y. C. (2011). Recombinant human arginase inhibits the in vitro and in vivo proliferation of human melanoma by inducing cell cycle arrest and apoptosis. *Pigment Cell Melanoma Res, 24*(2), 366-376.

Leung, Y. C., & Lo, W. H. (2013). Site-directed pegylation of arginases and the used thereof as anti-cancer and anti-viral agents. US Patent 8507245 B2.

Levine, B., & Klionsky, D. J. (2004). Development by self-digestion: Molecular mechanisms and biological functions of autophagy. *Dev Cell, 6*(4), 463-477.

Levine, B., & Kroemer, G. (2008). Autophagy in the pathogenesis of disease. *Cell, 132*(1), 27-42.

Li, G., Regunathan, S., Barrow, C., Eshraghi, J., Cooper, R., & Reis, D. (1994). Agmatine - an endogenous clonidine-displacing substance in the brain. *Science, 263*(5149), 966-969.

Li, M. C., Hertz, R., & Bergenstal, D. M. (1958). Therapy of choriocarcinoma and related trophoblastic tumors with folic acid and purine antagonists. *N Engl J Med, 259*(2), 66-74.

Liu, N., Huang, H., Liu, S., Li, X., Yang, C., Dou, Q. P., & Liu, J. (2014). Calcium channel blocker verapamil accelerates gambogic acid-induced cytotoxicity via enhancing proteasome inhibition and ROS generation. *Toxicol In Vitro, 28*(3), 419-425.

Lu, Z., & Xu, S. (2006). ERK1/2 MAP kinases in cell survival and apoptosis. *IUBMB Life, 58*(11), 621-631.

Maemondo, M., Inoue, A., Kobayashi, K., Sugawara, S., Oizumi, S., Isobe, H., Gemma, A., Harada, M., Yoshizawa, H., Kinoshita, I., Fujita, Y., Okinaga, S., Hirano, H., Yoshimori, K., Harada, T., Ogura, T., Ando, M., Miyazawa, H., Tanaka, T., Saijo, Y., Hagiwara, K., Morita, S., & Nukiwa, T. (2010). Gefitinib or chemotherapy for Non–Small-cell lung cancer with mutated EGFR. *N Engl J Med, 362*(25), 2380-2388.

Maiuri, M. C., Zalckvar, E., Kimchi, A., & Kroemer, G. (2007). Self-eating and self-killing: Crosstalk between autophagy and apoptosis. *Nat Rev Mol Cell Biol, 8*(9), 741-752.

Majno, G., & Joris, I. (1995). Apoptosis, oncosis, and necrosis. an overview of cell death. *Am J Pathol, 146*(1), 3-15.

Makrides, S., Nygren, P., Andrews, B., Ford, P., Evans, K., Hayman, E., Adari, H., Levin, J., Uhlen, M., & Toth, C. (1996). Extended in vivo half-life of human soluble complement receptor type 1 fused to a serum albumin-binding receptor. *J Pharmacol Exp Ther, 277*(1), 534-542.

Manca, A., Sini, M. C., Izzo, F., Ascierto, P. A., Tatangelo, F., Botti, G., Gentilcore, G., Capone, M., Mozzillo, N., Rozzo, C., Cossu, A., Tanda, F., & Palmieri, G. (2011). Induction of arginosuccinate synthetase (ASS) expression affects the antiproliferative activity of arginine deiminase (ADI) in melanoma cells. *Oncol Rep, 25*(6), 1495-1502.

Mari, M., Tooze, S. A., & Reggiori, F. (2011). The puzzling origin of the autophagosomal membrane. *F1000 Biol Rep, 3*, 25-25.

Marino, G., Niso-Santano, M., Baehrecke, E. H., & Kroemer, G. (2014). Self-consumption: The interplay of autophagy and apoptosis. *Nat Rev Mol Cell Biol, 15*(2), 81-94.

Masetti, R., & Pession, A. (2009). First-line treatment of acute lymphoblastic leukemia with pegasparaginase. *Biologics, 3*, 359-368.

Masgrau, C., Altabella, T., Farras, R., Flores, D., Thompson, A. J., Besford, R. T., & Tiburcio, A. F. (1997). Inducible overexpression of oat arginine decarboxylase in transgenic tobacco plants. *Plant J, 11*(3), 465-473.

Mayeur, C., Veuillet, G., Michaud, M., Raul, F., Blottiere, H., & Blachier, F. (2005). Effects of agmatine accumulation in human colon carcinoma

cells on polyamine metabolism, DNA synthesis and the cell cycle RID C-6120-2011. *BBA-Mol Cell Res, 1745*(1), 111-123.

McTavish, D., & Sorkin, E. M. (1989). Verapamil. an updated review of its pharmacodynamic and pharmacokinetic properties, and therapeutic use in hypertension. *Drugs, 38*(1), 19-76.

Meister, S., Frey, B., Lang, V. R., Gaipl, U. S., Schett, G., Schlotzer-Schrehardt, U., & Voll, R. E. (2010). Calcium channel blocker verapamil enhances endoplasmic reticulum stress and cell death induced by proteasome inhibition in myeloma cells. *Neoplasia, 12*(7), 550-561.

Menon, S., Dibble, C. C., Talbott, G., Hoxhaj, G., Valvezan, A. J., Takahashi, H., Cantley, L. C., & Manning, B. D. (2014). Spatial control of the TSC complex integrates insulin and nutrient regulation of mTORC1 at the lysosome. *Cell, 156*(4), 771-785.

Meric-Bernstam, F., & Gonzalez-Angulo, A. M. (2009). Targeting the mTOR signaling network for cancer therapy. *J Clin Oncol, 27*(13), 2278-2287.

Mian, A., & Lee, B. (2002). Urea-cycle disorders as a paradigm for inborn errors of hepatocyte metabolism. *Trends Mol Med, 8*(12), 583-589.

Michaloglou, C., Vredeveld, L. C., Soengas, M. S., Denoyelle, C., Kuilman, T., van der Horst, C. M., Majoor, D. M., Shay, J. W., Mooi, W. J., & Peeper, D. S. (2005). BRAFE600-associated senescence-like cell cycle arrest of human naevi. *Nature, 436*(7051), 720-724.

Mizushima, N. (2007). Autophagy: Process and function. *Gene Dev, 21*(22), 2861-2873.

Mizushima, N., Levine, B., Cuervo, A. M., & Klionsky, D. J. (2008). Autophagy fights disease through cellular self-digestion. *Nature, 451*(7182), 1069-1075.

Mohan, R. R., Challa, A., Gupta, S., Bostwick, D. G., Ahmad, N., Agarwal, R., Marengo, S. R., Amini, S. B., Paras, F, MacLennan, G. T., Resnick, M. I., & Mukhtar, H. (1999). Overexpression of ornithine decarboxylase in prostate cancer and prostatic fluid in humans. *Clin Cancer Res, 5*(1), 143-147.

Molderings, G. J., & Haenisch, B. (2012). Agmatine (decarboxylated L-arginine): Physiological role and therapeutic potential. *Pharmacol Ther, 133*(3), 351-365.

Molderings, G. J., Heinen, A., Menzel, S., Lubbecke, F., Homann, J., & Gothert, M. (2003). Gastrointestinal uptake of agmatine: Distribution in tissues and organs and pathophysiologic relevance. *Ann N Y Acad Sci, 1009*, 44-51.

Molderings, G. J., Kribben, B., Heinen, A., Schroder, D., Bruss, M., & Gothert, M. (2004). Intestinal tumor and agmatine (decarboxylated arginine): Low content in colon carcinoma tissue specimens and inhibitory effect on tumor cell proliferation in vitro. *Cancer, 101*(4), 858-868.

Moore, R. C., & Boyle, S. M. (1990). Nucleotide sequence and analysis of the speA gene encoding biosynthetic arginine decarboxylase in escherichia coli. *J Bacteriol, 172*(8), 4631-4640.

Morris, D. R., & Pardee, A. B. (1966). Multiple pathways of putrescine biosynthesis in escherichia coli. *J Biol Chem, 241*(13), 3129-3135.

Morris, S. (2002). Regulation of enzymes of the urea cycle and arginine metabolism. *Annu Rev Nutr, 22*, 87-105.

Morrissey, J., McCracken, R., Ishidoya, S., & Klahr, S. (1995). Partial cloning and characterization of an arginine decarboxylase in the kidney. *Kidney Int, 47*(5), 1458-1461.

Morrow, K., Hernandez, C. P., Raber, P., Del Valle, L., Wilk, A. M., Majumdar, S., Wyczechowska, D., Reiss, K., & Rodriguez, P. C. (2013). Anti-leukemic mechanisms of pegylated arginase I in acute lymphoblastic T-cell leukemia. *Leukemia, 27*(3), 569-577.

Mosmann, T. (1983). Rapid colorimetric assay for cellular growth and survival: Application to proliferation and cytotoxicity assays. *J Immunol Methods, 65*(1-2), 55-63.

Mouradov, D., Sloggett, C., Jorissen, R. N., Love, C. G., Li, S., Burgess, A. W., Arango, D., Strausberg, R. L., Buchanan, D., Wormald, S., O'Connor, L., Wilding, J. L., Bicknell, D., Tomlinson, I. P., Bodmer, W. F., Mariadason, J. M., & Sieber, O. M. (2014). Colorectal cancer cell lines are representative models of the main molecular subtypes of primary cancer. *Cancer Res, 74*(12), 3238-3247.

Muller, D., Karle, A., Meissburger, B., Hofig, I., Stork, R., & Kontermann, R. E. (2007). Improved pharmacokinetics of recombinant bispecific antibody molecules by fusion to human serum albumin. *J Biol Chem, 282*(17), 12650-12660.

Nakamura, K., Sasaki, T., Ohga, S., Yoshitake, T., Terashima, K., Asai, K., Matsumoto, K., Shioyama, Y., & Honda, H. (2014). Recent advances in radiation oncology: Intensity-modulated radiotherapy, a clinical perspective. *International J Clin Oncol*, in press. Epub ahead of print retrieved July 3, 2014, doi:10.1007/s10147-014-0718-y

Nardella, C., Clohessy, J. G., Alimonti, A., & Pandolfi, P. P. (2011). Pro-senescence therapy for cancer treatment. *Nat Rev Cancer, 11*(7), 503-511.

Ngwa, W., Kumar, R., Sridhar, S., Korideck, H., Zygmanski, P., Cormack, R. A., Berbeco, R., & Makrigiorgos, G. M. (2014). Targeted radiotherapy with gold nanoparticles: Current status and future perspectives. *Nanomedicine (Lond), 9*(7), 1063-1082.

Ni, Y., Schwaneberg, U., & Sun, Z. (2008). Arginine deiminase, a potential anti-tumor drug. *Cancer Lett, 261*(1), 1-11.

Nijhawan, D., Honarpour, N., & Wang, X. (2000). Apoptosis in neural development and disease. *Annu Rev Neurosci, 23*, 73-87.

Nishio, Y., Kakizoe, T., Ohtani, M., Sato, S., Sugimura, T., & Fukushima, S. (1986). L-isoleucine and L-leucine - tumor promoters of bladder-cancer in rats. *Science, 231*(4740), 843-845.

Noh, E. J., Kang, S. W., Shin, Y. J., Kim, D. C., Park, I. S., Kim, M. Y., Chun, B. G., & Min, B. H. (2002). Characterization of mycoplasma arginine deiminase expressed in E. coli and its inhibitory regulation of nitric oxide synthesis. *Mol Cells, 13*(1), 137-143.

Nygren, P., Uhlen, M., Flodby, P., Andersson, R., & Wigzell, H. (1991). In vivo stabilization of a human recombinant Cd4 derivative by fusion to a serum-albumin-binding receptor. In R. M. Chanock, H. S. Ginsberg, F. Brown & R. A. Lerner (Eds.), *Vaccines* (pp. 363-368). New York: Cold Spring Harbor Laboratory Press.

Ohsumi, Y. (2014). Historical landmarks of autophagy research. *Cell Res, 24*(1), 9-23.

O'Leary, M. H. (1992). Chapter 6: Catalytic strategies in enzymic caboxylation and decarboxylation. In D. S. Sigman (Ed.), *The enzymes* (3rd ed., pp. 235-270). San Diego: Academic Press.

Olson, A. L., & Pessin, J. E. (1996). Structure, function, and regulation of the mammalian facilitative glucose transporter gene family. *Annu Rev Nutr, 16*, 235-256.

Osborn, B., Sekut, L., Corcoran, M., Poortman, C., Sturm, B., Chen, G., Mather, D., Lin, H., & Parry, T. (2002). Albutropin: A growth hormone-albumin fusion with improved pharmacokinetics and pharmacodynamics in rats and monkeys. *Eur J Pharmacol, 456*(1-3), 149-158.

Panosyan, E. H., Seibel, N. L., Martin-Aragon, S., Gaynon, P. S., Avramis, I. A., Sather, H., Franklin, J., Nachman, J., Ettinger, L. J., La, M., Steinherz, P., Cohen, L. J., Siegel, S. E., Avramis, V. I., & Children's Cancer Group Study CCG-1961. (2004). Asparaginase antibody and asparaginase activity in children with higher-risk acute lymphoblastic leukemia: Children's cancer group study CCG-1961. *J Pediatr Hematol Oncol, 26*(4), 217-226.

Pardee, A. B. (1974). A restriction point for control of normal animal cell proliferation. *Proc Natl Acad Sci USA, 71*(4), 1286-1290.

Pasut, G., Sergi, M., & Veronese, F. M. (2008). Anti-cancer PEG-enzymes: 30 years old, but still a current approach. *Adv Drug Deliv Rev, 60*(1), 69-78.

Pasut, G., & Veronese, F. M. (2009). PEG conjugates in clinical development or use as anticancer agents: An overview. *Adv Drug Deliv Rev, 61*(13), 1177-1188.

Patchett, M., Daniel, R., & Morgan, H. (1991). Characterization of arginase from the extreme thermophile bacillus-caldovelox. *Biochim Biophys Acta, 1077*(3), 291-298.

Pattingre, S., Bauvy, C., & Codogno, P. (2003). Amino acids interfere with the ERK1/2-dependent control of macroautophagy by controlling the

activation of raf-1 in human colon cancer HT-29 cells. *J Biol Chem, 278*(19), 16667-16674.

Pattingre, S., Espert, L., Biard-Piechaczyk, M., & Codogno, P. (2008). Regulation of macroautophagy by mTOR and beclin 1 complexes. *Biochimie, 90*(2), 313-323.

Peters, T.,Jr. (1985). Serum albumin. *Adv Protein Chem, 37*, 161-245.

Philip, R., Campbell, E., & Wheatley, D. (2003). Arginine deprivation, growth inhibition and tumour cell death: 2. enzymatic degradation of arginine in normal and malignant cell cultures (vol 88, pg 613, 2003). *Br J Cancer, 89*(1), 222.

Pietenpol, J. A., & Stewart, Z. A. (2002). Cell cycle checkpoint signaling: Cell cycle arrest versus apoptosis. *Toxicology, 181-182*, 475-481.

Pieters, R., Hunger, S. P., Boos, J., Rizzari, C., Silverman, L., Baruchel, A., Goekbuget, N., Schrappe, M., & Pui, C. H. (2011). L-asparaginase treatment in acute lymphoblastic leukemia: A focus on erwinia asparaginase. *Cancer, 117*(2), 238-249.

Piletz, J. E., May, P. J., Wang, G., & Zhu, H. (2003). Agmatine crosses the blood-brain barrier. *Ann N Y Acad Sci, 1009*, 64-74.

Polaris Group. (2011a). *A randomized, double-blind, multi-center phase 3 study of ADI-PEG 20 plus best supportive care (BSC) versus placebo plus BSC in subjects with advanced hepatocellular carcinoma (HCC) who have failed prior systemic therapy.* In: ClinicalTrials.gov [Internet]. Bethesda (MD): National Library of Medicine (US). [cited 2014 Jul 29]. Available from: https://clinicaltrials.gov/ct2/show/NCT01287585 NLM Identifier: NCT01287585.

Polaris Group. (2011b). *Phase 1 trial of ADI PEG 20 plus docetaxel in advance. solid tumors with emphasis on castration resistant prostate cancer (CRPC) and advanced non-small cell lung cancer (NSCLC).* In: ClinicalTrials.gov [Internet]. Bethesda (MD): National Library of Medicine (US). [cited 2014 Jul 29]. Available from: https://clinicaltrials.gov/ct2/show/NCT01497925 NLM Identifier: NCT01497925.

Polaris Group. (2013a). *Phase 1 trial of ADI-PEG20 plus doxorubicin in patients with HER2 negative metastatic breast cancer or advanced solid tumor.* In: ClinicalTrials.gov [Internet]. Bethesda (MD): National Library of Medicine (US). [cited 2014 Jul 22]. Available from: http://clinicaltrials.gov/show/NCT01948843 NLM Identifier: NCT01948843.

Polaris Group. (2013b). *Phase 2 study of ADI-PEG20 in acute myeloid leukemia.* In: ClinicalTrials.gov [Internet]. Bethesda (MD): National Library of Medicine (US). [cited 2014 Jul 29]. Available from: https://clinicaltrials.gov/ct2/show/NCT01910012 NLM Identifier: NCT01910012.

Polaris Group. (2013c). *Phase 2 study of ADI-PEG20 in non-Hodgkin's lymphoma subjects who have failed prior systemic therapy.* In: ClinicalTrials.gov [Internet]. Bethesda (MD): National Library of Medicine (US). [cited 2014 Jul 29]. Available from: https://clinicaltrials.gov/ct2/show/NCT01910025 NLM Identifier: NCT01910025.

Polaris Group. (2014). *A phase 1 study of ADI PEG20 plus sorafenib in subjects with advanced hepatocellular carcinoma (HCC).* In: ClinicalTrials.gov [Internet]. Bethesda (MD): National Library of Medicine (US). [cited 2014 Jul 29]. Available from: https://clinicaltrials.gov/ct2/show/NCT02101593 NLM Identifier: NCT02101593.

Poon, R. Y., Jiang, W., Toyoshima, H., & Hunter, T. (1996). Cyclin-dependent kinases are inactivated by a combination of p21 and thr-14/Tyr-15 phosphorylation after UV-induced DNA damage. *J Biol Chem, 271*(22), 13283-13291.

Prager, M. D., & Bachynsky, N. (1968a). Asparagine synthetase in asparaginase resistant and susceptible mouse lymphomas. *Biochem Biophys Res Commun, 31*(1), 43-47.

Prager, M. D., & Bachynsky, N. (1968b). Asparagine synthetase in normal and malignant tissues: Correlation with tumor sensitivity to asparaginase. *Arch Biochem Biophys, 127*(1), 645-654.

Qiu, F., Chen, Y. R., Liu, X., Chu, C. Y., Shen, L. J., Xu, J., Gaur, S., Forman, H. J., Zhang, H., Zheng, S., Yen, Y., Huang, J., Kung, H. J., & Ann, D. K. (2014). Arginine starvation impairs mitochondrial respiratory function in ASS1-deficient breast cancer cells. *Sci Signal, 7*(319), ra31.

Raasch, W., Regunathan, S., Li, G., & Reis, D. J. (1995). Agmatine, the bacterial amine, is widely distributed in mammalian tissues. *Life Sci, 56*(26), 2319-2330.

Regunathan, S., & Reis, D. J. (2000). Characterization of arginine decarboxylase in rat brain and liver. *J Neurochem, 74*(5), 2201-2208.

Reis, D. J., & Regunathan, S. (1998). Agmatine: A novel neurotransmitter? *Adv Pharmacol, 42*, 645-649.

Renehan, A. G., Booth, C., & Potten, C. S. (2001). What is apoptosis, and why is it important? *BMJ, 322*(7301), 1536-1538.

Renshaw, J., Taylor, K. R., Bishop, R., Valenti, M., De Haven Brandon, A., Gowan, S., Eccles, S. A., Ruddle, R. R., Johnson, L. D., Raynaud, F. I., Selfe, J. L., Thway, K., Pietsch, T., Pearson, A. D. & Shipley, J. (2013).

Dual blockade of the PI3K/AKT/mTOR (AZD8055) and RAS/MEK/ERK (AZD6244) pathways synergistically inhibits rhabdomyosarcoma cell growth in vitro and in vivo. *Clin Cancer Res, 19*(21), 5940-5951.

Ringborg, U., Bergqvist, D., Brorsson, B., Cavallin-Stahl, E., Ceberg, J., Einhorn, N., Frodin, J. E., Jarhult, J., Lamnevik, G., Lindholm, C., Littbrand, B, Norlund, A., Nylen, U., Rosen, M., Svensson, H., & Moller, T. R. (2003). The swedish council on technology assessment in health care (SBU) systematic overview of radiotherapy for cancer including a prospective survey of radiotherapy practice in sweden 2001--summary and conclusions. *Acta Oncol, 42*(5-6), 357-365.

Roberts, M. J., Bentley, M. D., & Harris, J. M. (2002). Chemistry for peptide and protein PEGylation. *Adv Drug Deliv Rev, 54*(4), 459-476.

Roy, M., & Ghosh, B. (1996). Polyamines, both common and uncommon, under heat stress in rice (oryza sativa) callus. *Physiol Plantarum, 98*(1), 196-200.

Saelens, X., Festjens, N., Vande Walle, L., van Gurp, M., van Loo, G., & Vandenabeele, P. (2004). Toxic proteins released from mitochondria in cell death. *Oncogene, 23*(16), 2861-2874.

Sagor, G. H., Berberich, T., Takahashi, Y., Niitsu, M., & Kusano, T. (2013). The polyamine spermine protects arabidopsis from heat stress-induced damage by increasing expression of heat shock-related genes. *Transgenic Res, 22*(3), 595-605.

Saini, K. S., Loi, S., de Azambuja, E., Metzger-Filho, O., Saini, M. L., Ignatiadis, M., Dancey, J. E., & Piccart-Gebhart, M. J. (2013). Targeting the PI3K/AKT/mTOR and Raf/MEK/ERK pathways in the treatment of breast cancer. *Cancer Treat Rev, 39*(8), 935-946.

Salas, M., López, V., Uribe, E., & Carvajal, N. (2004). Studies on the interaction of escherichia coli agmatinase with manganese ions: Structural and kinetic studies of the H126N and H151N variants. *J Inorg Biochem, 98*(6), 1032-1036.

Sand, K. M. K., Bern, M., Nilsen, J., Noordzij, H. T., Sandlie, I., & Andersen, J. T. (2015). Unraveling the interaction between FcRn and albumin: opportunities for design of albumin-based therapeutics. *Front Immunol, 5*, 1-21.

Satishchandran, C., & Boyle, S. M. (1986). Purification and properties of agmatine ureohydrolyase, a putrescine biosynthetic enzyme in escherichia-coli. *J Bacteriology, 165*(3), 843-848.

Satriano, J., Matsufuji, S., Murakami, Y., Lortie, M. J., Schwartz, D., Kelly, C. J., Hayashi, S., & Blantz, R. C. (1998). Agmatine suppresses proliferation by frameshift induction of antizyme and attenuation of cellular polyamine levels. *J Biol Chem, 273*(25), 15313-15316.

Savaraj, N., You, M., Wu, C., Wangpaichitr, M., Kuo, M. T., & Feun, L. G. (2010). Arginine deprivation, autophagy, apoptosis (AAA) for the treatment of melanoma. *Curr Mol Med, 10*(4), 405-412.

Savariar, E. N., Felsen, C. N., Nashi, N., Jiang, T., Ellies, L. G., Steinbach, P., Tsien, R. Y. & Nguyen, Q. T. (2013). Real-time in vivo molecular detection of primary tumors and metastases with ratiometric activatable cell-penetrating peptides. *Cancer Res, 73*(2), 855-864.

Savoca, K., Davis, F., Vanes, T., Mccoy, J., & Palczuk, N. (1984). Cancer-therapy with chemically modified enzymes. 2. The therapeutic effectiveness of arginase, and arginase modified by the covalent attachment of polyethylene-glycol, on the taper liver-tumor and the L5178y murine leukemia. *Cancer Biochem Biophys, 7*(3), 261-268.

Schmitt, C. A. (2003). Senescence, apoptosis and therapy--cutting the lifelines of cancer. *Nat Rev Cancer, 3*(4), 286-295.

Schuler, M., & Green, D. R. (2001). Mechanisms of p53-dependent apoptosis. *Biochem Soc T, 29*(Pt 6), 684-688.

Scott, L., Lamb, J., Smith, S., & Wheatley, D. N. (2000). Single amino acid (arginine) deprivation: Rapid and selective death of cultured transformed and malignant cells. *Br J Cancer, 83*(6), 800-810.

Serrano, M., Lin, A. W., McCurrach, M. E., Beach, D., & Lowe, S. W. (1997). Oncogenic ras provokes premature cell senescence associated with accumulation of p53 and p16INK4a. *Cell, 88*(5), 593-602.

Sheen, J., Zoncu, R., Kim, D., & Sabatini, D. M. (2011). Defective regulation of autophagy upon leucine deprivation reveals a targetable liability of human melanoma cells in vitro and in vivo. *Cancer Cell, 19*(5), 613-628.

Shen, L., Lin, W., Beloussow, K., & Shen, W. (2003). Resistance to the anti-proliferative activity of recombinant arginine deiminase in cell culture correlates with the endogenous enzyme, argininosuccinate synthetase. *Cancer Lett, 191*(2), 165-170.

Shi, Y., HogenEsch, H., Regnier, F. E., & Hem, S. L. (2001). Detoxification of endotoxin by aluminum hydroxide adjuvant. *Vaccine, 19*(13-14), 1747-1752.

Shimizu, T., Tolcher, A. W., Papadopoulos, K. P., Beeram, M., Rasco, D. W., Smith, L. S., Gunn, S., Smetzer, L., Mays, T. A., Kaiser, B., Wick, M. J., Alvarez, C., Cavazos, A., Mangold, G. L., & Patnaik, A. (2012). The clinical effect of the dual-targeting strategy involving PI3K/AKT/mTOR and RAS/MEK/ERK pathways in patients with advanced cancer. *Clin Cancer Res, 18*(8), 2316-2325.

Simpson, W. G. (1985). The calcium channel blocker verapamil and cancer chemotherapy. *Cell Calcium, 6*(6), 449-467.

Singh, G., Akcakanat, A., Sharma, C., Luyimbazi, D., Naff, K. A., & Meric-Bernstam, F. (2011). The effect of leucine restriction on Akt/mTOR signaling in breast cancer cell lines in vitro and in vivo. *Nutr Cancer, 63*(2), 264-271.

Slamon, D. J., Leyland-Jones, B., Shak, S., Fuchs, H., Paton, V., Bajamonde, A., Fleming, T., Eiermann, W., Wolter, J., Pegram, M., Baselga, J., & Norton, L. (2001). Use of chemotherapy plus a monoclonal antibody against HER2 for metastatic breast cancer that overexpresses HER2. *N Engl J Med, 344*(11), 783-792.

Smith, E. R., & Klein-Schwartz, W. (2005). Are 1-2 dangerous? Chloroquine and hydroxychloroquine exposure in toddlers. *J Emerg Med, 28*(4), 437-443.

Sobrero, A. F., Maurel, J., Fehrenbacher, L., Scheithauer, W., Abubakr, Y. A., Lutz, M. P., Vega-Villegas, M. E., Eng, C., Steinhauer, E. U., Prausova, J., Lenz, H. J., Borg, C., Middleton, G., Kroning, H., Luppi, G., Kisker, O., Zubel, A., Langer, C., Kopit, J., & Burris, H. A.,3rd. (2008). EPIC: Phase III trial of cetuximab plus irinotecan after fluoropyrimidine and oxaliplatin failure in patients with metastatic colorectal cancer. *J Clin Oncol, 26*(14), 2311-2319.

Song, J., Zhou, C., Liu, R., Wu, X., Wu, D., Hu, X., & Ding, Y. (2010). Expression and purification of recombinant arginine decarboxylase (speA) from escherichia coli. *Mol Biol Rep, 37*(4), 1823-1829.

Stehle, G., Sinn, H., Wunder, A., Schrenk, H. H., Stewart, J. C., Hartung, G., Maier-Borst, W., & Heene, D. L. (1997). Plasma protein (albumin) catabolism by the tumor itself--implications for tumor metabolism and the genesis of cachexia. *Crit Rev Oncol Hematol, 26*(2), 77-100.

Stone, E., Chantranupong, L., Gonzalez, C., O'Neal, J., Rani, M., VanDenBerg, C., & Georgiou, G. (2012). Strategies for optimizing the serum persistence of engineered human arginase I for cancer therapy. *J Control Release, 158*(1), 171-179.

Stone, E. M., Glazer, E. S., Chantranupong, L., Cherukuri, P., Breece, R. M., Tierney, D. L., Curley, S. A., Iverson, B. L., & Georgiou, G. (2010). Replacing Mn(2+) with Co(2+) in human arginase I enhances cytotoxicity toward L-arginine auxotrophic cancer cell lines. *ACS Chem Biol, 5*(3), 333-342.

Stork, R., Muller, D., & Kontermann, R. E. (2007). A novel tri-functional antibody fusion protein with improved pharmacokinetic properties generated by fusing a bispecific single-chain diabody with an albumin-binding domain from streptococcal protein G. *Protein Eng Des Sel, 20*(11), 569-576.

Subramanian, G. M., Fiscella, M., Lamouse-Smith, A., Zeuzem, S., & McHutchison, J. G. (2007). Albinterferon alpha-2b: A genetic fusion protein for the treatment of chronic hepatitis C. *Nat Biotechnol, 25*(12), 1411-1419.

Sugimura, K., Ohno, T., Kusuyama, T., & Azuma, I. (1992). High-sensitivity of human-melanoma cell-lines to the growth inhibitory activity of mycoplasmal arginine deiminase invitro. *Melanoma Res, 2*(3), 191-196.

Sui, X., Chen, R., Wang, Z., Huang, Z., Kong, N., Zhang, M., Han, W., Lou, F., Yang, J., Zhang, Q., Wang, X., He, C., & Pan, H. (2013). Autophagy and chemotherapy resistance: A promising therapeutic target for cancer treatment. *Cell Death Dis, 4*, e838.

Sun, X., Yang, Z., Li, S., Tan, Y., Zhang, N., Wang, X., Yagi, S., Yoshioka, T., Takimoto, A., Mitsushima, K., Suginaka, A., Frenkel, E., & Hoffman, R. (2003). In vivo efficacy of recombinant methioninase is

enhanced by the combination of polyethylene glycol conjugation and pyridoxal 5 '-phosphate supplementation. *Cancer Res, 63*(23), 8377-8383.

Swain, A. L., Jaskolski, M., Housset, D., Rao, J. K., & Wlodawer, A. (1993). Crystal structure of escherichia coli L-asparaginase, an enzyme used in cancer therapy. *Proc Natl Acad Sci USA, 90*(4), 1474-1478.

Tabor, C. W., & Tabor, H. (1984). Polyamines. *Annu Rev Biochem, 53*, 749-790.

Tabor, C. W., & Tabor, H. (1985). Polyamines in microorganisms. *Microbiol Rev, 49*(1), 81-99.

Tacar, O., Sriamornsak, P., & Dass, C. R. (2013). Doxorubicin: An update on anticancer molecular action, toxicity and novel drug delivery systems. *J Pharm Pharmacol, 65*(2), 157-170.

Takaku, H., Takase, M., Abe, S., Hayashi, H., & Miyazaki, K. (1992). In vivo anti-tumor activity of arginine deiminase purified from mycoplasma arginini. *Int J Cancer, 51*(2), 244-249.

Takakura, T., Mitsushima, K., Yagi, S., Inagaki, K., Tanaka, H., Esaki, N., Soda, K., & Takimoto, A. (2004). Assay method for antitumor L-methionine gamma-lyase: Comprehensive kinetic analysis of the complex reaction with L-methionine. *Anal Biochem, 327*(2), 233-240.

Tan, Y., Xu, M., Tan, X., Tan, X., Wang, X., Saikawa, Y., Nagahama, T., Sun, X., Lenz, M., & Hoffman, R. (1997). Overexpression and large-scale production of recombinant L-methionine-alpha-deamino-gamma-mercaptomethane-lyase for novel anticancer therapy. *Protein Expr Purif, 9*(2), 233-245.

Tan, Y., Zavala, J. S., Han, Q., Xu, M., Sun, X., Tan, X., Magana, R., Geller, J., & Hoffman, R. M. (1997). Recombinant methioninase

infusion reduces the biochemical endpoint of serum methionine with minimal toxicity in high-stage cancer patients. *Anticancer Res, 17*(5B), 3857-3860.

Tanida, I., Ueno, T., & Kominami, E. (2008). LC3 and autophagy. *Methods Mol Biol, 445*, 77-88.

Tanios, R., Bekdash, A., Kassab, E., Stone, E., Georgiou, G., Frankel, A. E., & Abi-Habib, R. J. (2013). Human recombinant arginase I(co)-PEG5000 [HuArgI(co)-PEG5000]-induced arginine depletion is selectively cytotoxic to human acute myeloid leukemia cells. *Leuk Res, 37*(11), 1565-1571.

Tato, I., Bartrons, R., Ventura, F., & Rosa, J. L. (2011). Amino acids activate mammalian target of rapamycin complex 2 (mTORC2) via PI3K/Akt signaling. *J Biol Chem, 286*(8), 6128-6142.

te Poele, R. H., Okorokov, A. L., Jardine, L., Cummings, J., & Joel, S. P. (2002). DNA damage is able to induce senescence in tumor cells in vitro and in vivo. *Cancer Res, 62*(6), 1876-1883.

Topalian, S. L., Hodi, F. S., Brahmer, J. R., Gettinger, S. N., Smith, D. C., McDermott, D. F., Powderly, J. D., Carvajal, R. D., Sosman, J. A., Atkins, M. B., Leming, P. D., Spigel, D. R., Antonia, S. J., Horn, L., Drake, C. G., Pardoll, D. M., Chen, L., Sharfman, W. H., Anders, R. A., Taube, J. M., McMiller, T. L., Xu, H., Korman, A. J., Jure-Kunkel, M., Agrawal, S., McDonald, D., Kollia, G. D., Gupta, A., Wigginton, J. M., & Sznol, M. (2012). Safety, activity, and immune correlates of anti-PD-1 antibody in cancer. *N Engl J Med, 366*(26), 2443-2454.

Tournigand, C., Andre, T., Achille, E., Lledo, G., Flesh, M., Mery-Mignard, D., Quinaux, E., Couteau, C., Buyse, M., Ganem, G., Landi, B., Colin, P., Louvet, C, & de Gramont, A. (2004). FOLFIRI followed by FOLFOX6 or the reverse sequence in advanced colorectal cancer: A randomized GERCOR study. *J Clin Oncol, 22*(2), 229-237.

Tsai, W. B., Aiba, I., Lee, S. Y., Feun, L., Savaraj, N., & Kuo, M. T. (2009). Resistance to arginine deiminase treatment in melanoma cells is associated with induced argininosuccinate synthetase expression involving c-Myc/HIF-1alpha/Sp4。 *Mol Cancer Ther, 8*(12), 3223-3233.

Tsai, W. B., Aiba, I., Long, Y., Lin, H. K., Feun, L., Savaraj, N., & Kuo, M. T. (2012). Activation of Ras/PI3K/ERK pathway induces c-myc stabilization to upregulate argininosuccinate synthetase, leading to arginine deiminase resistance in melanoma cells. *Cancer Res, 72*(10), 2622-2633.

Tsui, S., Lam, W., Lam, T., Chong, H., So, P., Kwok, S., Arnold, S., Cheng, P. N., Wheatley, D. N., Lo, W., & Leung, Y. (2009). Pegylated derivatives of recombinant human arginase (rhArg1) for sustained in vivo activity in cancer therapy: Preparation, characterization and analysis of their pharmacodynamics in vivo and in vitro and action upon hepatocellular carcinoma cell (HCC) RID B-4146-2009. *Cancer Cell Int, 9*, 9.

Tsun, Z. Y., Bar-Peled, L., Chantranupong, L., Zoncu, R., Wang, T., Kim, C., Spooner, E., & Sabatini, D. M. (2013). The folliculin tumor suppressor is a GAP for the RagC/D GTPases that signal amino acid levels to mTORC1. *Mol Cell, 52*(4), 495-505.

van der Bij, G. J., Oosterling, S. J., Beelen, R. H., Meijer, S., Coffey, J. C., & van Egmond, M. (2009). The perioperative period is an underutilized window of therapeutic opportunity in patients with colorectal cancer. *Ann Surg, 249*(5), 727-734.

Vazquez-Martin, A., Oliveras-Ferraros, C., & Menendez, J. A. (2009). Autophagy facilitates the development of breast cancer resistance to the anti-HER2 monoclonal antibody trastuzumab. *PLoS One, 4*(7), e6251.

Vogel, C. L., Cobleigh, M. A., Tripathy, D., Gutheil, J. C., Harris, L. N., Fehrenbacher, L., Slamon, D. J., Murphy, M., Novotny, W. F., Burchmore, M., Shak, S., Stewart, S. J., & Press, M. (2002). Efficacy and safety of trastuzumab as a single agent in first-line treatment of HER2-overexpressing metastatic breast cancer. *J Clin Oncol, 20*(3), 719-726.

Wada, H., Imamura, I., Sako, M., Katagiri, S., Tarui, S., Nishimura, H., & Inada, Y. (1990). Antitumor enzyme: Polyethylene glycol-modified asparaginase. *Ann N Y Acad Sci, 613*, 95-108.

Walker, A., Dunlevy, G., Rycroft, D., Topley, P., Holt, L. J., Herbert, T., Davies, M., Cook, F., Holmes, S., Jespers, L., & Herring, C. (2010). Anti-serum albumin domain antibodies in the development of highly potent, efficacious and long-acting interferon. *Protein Eng Des Sel, 23*(4), 271-278.

Wang, J. F., Su, R. B., Wu, N., Xu, B., Lu, X. Q., Liu, Y., & Li, J. (2005). Inhibitory effect of agmatine on proliferation of tumor cells by modulation of polyamine metabolism. *Acta Pharmacol Sin*, *26*(5), 616-622.

Wang, P., Henning, S. M., & Heber, D. (2010). Limitations of MTT and MTS-based assays for measurement of antiproliferative activity of green tea polyphenols. *PLoS One, 5*(4), e10202.

Wang, S., Yu, H., & Wickliffe, J. K. (2011). Limitation of the MTT and XTT assays for measuring cell viability due to superoxide formation induced by nano-scale TiO2. *Toxicol In Vitro, 25*(8), 2147-2151.

Wang, X. W., & Harris, C. C. (1997). P53 tumor-suppressor gene: Clues to molecular carcinogenesis. *J Cell Physiol, 173*(2), 247-255.

Wang, Y. C., Wei, L. J., Liu, J. T., Li, S. X., & Wang, Q. S. (2012). Comparison of cancer incidence between china and the USA. *Cancer Biol Med, 9*(2), 128-132.

Watson, M., Emory, K., Piatak, R., & Malmberg, R. (1998). Arginine decarboxylase (polyamine synthesis) mutants of arabidopsis thaliana exhibit altered root growth. *Plant J, 13*(2), 231-239.

Weisberg, E., Manley, P. W., Cowan-Jacob, S. W., Hochhaus, A., & Griffin, J. D. (2007). Second generation inhibitors of BCR-ABL for the treatment of imatinib-resistant chronic myeloid leukaemia. *Nat Rev Cancer, 7*(5), 345-356.

Weyermann, J., Lochmann, D., & Zimmer, A. (2005). A practical note on the use of cytotoxicity assays. *Int J Pharm, 288*(2), 369-376.

Wheatley, D., Kilfeather, R., Stitt, A., & Campbell, E. (2005). Integrity and stability of the citrulline-arginine pathway in normal and tumour cell lines RID A-9842-2009. *Cancer Lett, 227*(2), 141-152.

Wolf, C., Bruss, M., Hanisch, B., Gothert, M., von Kugelgen, I., & Molderings, G. J. (2007). Molecular basis for the antiproliferative effect of agmatine in tumor cells of colonic, hepatic, and neuronal origin. *Mol Pharmacol, 71*(1), 276-283.

Wu, F. L., Liang, Y. F., Chang, Y. C., Yo, H. H., Wei, M. F., & Shen, L. J. (2011). RNA interference of argininosuccinate synthetase restores sensitivity to recombinant arginine deiminase (rADI) in resistant cancer cells. *J Biomed Sci, 18*, 25-0127-18-25.

Wu, W. H., & Morris, D. R. (1973a). Biosynthetic arginine decarboxylase from escherichia-coli - purification and properties. *J Biol Chem, 248*(5), 1687-1695.

Wu, W. H., & Morris, D. R. (1973b). Biosynthetic arginine decarboxylase from escherichia-coli - subunit interactions and role of magnesium ion rid G-4503-2011. *J Biol Chem, 248*(5), 1696-1699.

Wunder, A., Stehle, G., Sinn, H., Schrenk, H., Hoffbiederbeck, D., Bader, F., Friedrich, E., Peschke, P., Maierborst, W., & Heene, D. (1997). Enhanced albumin uptake by rat tumors. *Int J Oncol, 11*(3), 497-507.

Xue, W., Zender, L., Miething, C., Dickins, R. A., Hernando, E., Krizhanovsky, V., Cordon-Cardo, C., & Lowe, S. W. (2007). Senescence and tumour clearance is triggered by p53 restoration in murine liver carcinomas. *Nature, 445*(7128), 656-660.

Yang, Z., Sun, X., Li, S., Tan, Y., Wang, X., Zhang, N., Yagi, S., Takakura, T., Kobayashi, Y., Takimoto, A., Yoshioka, T., Suginaka, A., Frenkel, E. P., & Hoffman, R. M. (2004). Circulating half-life of PEGylated recombinant methioninase holoenzyme is highly dose dependent on cofactor pyridoxal-5′-phosphate. *Cancer Res, 64*(16), 5775-5778.

Yang, Z., Wang, J., Lu, Q., Xu, J., Kobayashi, Y., Takakura, T., Takimoto, A., Yoshioka, T., Lian, C., Chen, C., Zhang, D., Zhang, Y., Li, S., Sun,X., Tan, Y., Yagi, S., Frenkel, E., & Hoffman, R. (2004). PEGylation confers greatly extended half-life and attenuated immunogenicity to recombinant methioninase in primates. *Cancer Res, 64*(18), 6673-6678.

Yang, Z. J., Chee, C. E., Huang, S., & Sinicrope, F. A. (2011). The role of autophagy in cancer: Therapeutic implications. *Mol Cancer Ther, 10*(9), 1533-1541.

Yau, E. (2013, April 15). Targeted therapies for colorectal cancer. *South China Morning Post.* Retrieved from http://www.scmp.com/lifestyle/health/article/1213125/targeted-therapies-colorectal-cancer

Yoon, C. Y., Shim, Y. J., Kim, E. H., Lee, J. H., Won, N. H., Kim, J. H., Park, I. S., Yoon, D. K., & Min, B. H. (2007). Renal cell carcinoma does not express argininosuccinate synthetase and is highly sensitive to arginine deprivation via arginine deiminase. *Int J Cancer, 120*(4), 897-905.

Yoshioka, T., Wada, T., Uchida, N., Maki, H., Yoshida, H., Ide, N., Kasai, H., Hojo, K., Shono, K., Maekawa, R., Yagi, S., Hoffman, R. M., & Sugita, K. (1998). Anticancer efficacy in vivo and in vitro, synergy with 5-fluorouracil, and safety of recombinant methioninase. *Cancer Res, 58*(12), 2583-2587.

Young, L., Salomon, R., Au, W., Allan, C., Russell, P., & Dong, Q. (2006). Ornithine decarboxylase (ODC) expression pattern in human prostate tissues and ODC transgenic mice. *J Histochem Cytochem, 54*(2), 223-229.

Zhao, P., Dai, M., Chen, W., & Li, N. (2010). Cancer trends in china. *Jpn J Clin Oncol, 40*(4), 281-285.

Zheng, S., Zhang, S., Chen, K., Zhu, Y., & Dong, Q. (2012). 19 - Research on colorectal cancer in china. In X. Liu, S. Pestka & Y. Shi (Eds.), *Recent advances in cancer research and therapy* (pp. 535-595). Oxford: Elsevier.

Zhou, H. Y., & Huang, S. L. (2012). Current development of the second generation of mTOR inhibitors as anticancer agents. *Chin J Cancer, 31*(1), 8-18.

Zhu, M., Iyo, A., Piletz, J. E., & Regunathan, S. (2004). Expression of human arginine decarboxylase, the biosynthetic enzyme for agmatine. *BBA-Gen Subjects, 1670*(2), 156-164.